

A Study of the Phenylacetylene Oxidative Carbonylation Reaction in Oscillatory and Non- oscillatory Modes

Julie Parker

A thesis submitted for the degree of Doctor of Philosophy

School of Chemical Engineering and Advanced Materials

Newcastle University

April 2016

Abstract

The palladium-catalysed phenylacetylene oxidative carbonylation (PCPOC) reaction operates in both oscillatory and non-oscillatory modes. In oscillatory mode oscillations have been observed in pH, reaction heat (Q_r), redox potential and gas uptake. This work documents the steps towards understanding the process and uncovering the reaction mechanism. An extensive experimental study was undertaken involving small-scale (25 mL) experiments on the catalytic system and large-scale (450 mL) experiments on the whole reaction system.

The large-scale experiments on the whole system included studies at temperatures from 0-40 °C. The effect of increasing the concentration of water in the system by increasing the solvent volume ratio of water from 0% to 40% was also studied. Decreasing the reaction temperature is known to affect the period and amplitude of the pH oscillations but this work found that it also changes the selectivity of the reaction: the major product is dimethyl (2Z)-2-phenyl-2-butenedioate at 40 °C whereas at 0 °C the major product is 5,5-dimethoxy-3-phenyl-2(5H)-furanone. Increasing the concentration of water in the system affected product selectivity and the oscillatory pH behaviour. As the water concentration increased, pH behaviour changed: the regular shark fin waveform observed when no water was added to the system gradually became step-wise oscillatory behaviour.

The small-scale experiments uncovered the link between the mono-carbonylation of phenylacetylene and the generation of H^+ . They also showed the autocatalytic nature of the reaction between the PdI_2 catalyst and carbon monoxide as well as the involvement of water in H^+ generation.

Based on the experimental findings a tentative model was produced using BatchCAD which accounted for the key features of the observed pH behaviour. The modelling study showed the need for autocatalysis in the model producing the best fit when HI catalysed the reaction between PdI_2 , CO and H_2O .

Acknowledgements

I would like to thank my family for all of their encouragement and their belief that I would complete my PhD especially when I couldn't see it. I am thankful for Prof Allen Wright and his financial support without which this thesis wouldn't have been possible. I am particularly grateful for the help and support of Dr Katarina Novakovic who believed in me when I didn't believe in myself, supplied motivation when I had lost mine and was full of positivity when experiments weren't working and equipment wasn't cooperating. Without her I would have given up long ago.

Contents

Abstract	i
Acknowledgements	iii
Contents	v
List of Figures	ix
List of Tables	xvi
Nomenclature	xviii
Chapter 1. Introduction	1
1.1 Background	1
1.2 Research Aims	2
1.3 Thesis Structure	2
1.4 Presentations and Publications Resulting From This Thesis	3
1.4.1 Journal Papers	3
1.4.2 Conference Presentations	3
1.4.3 Poster Presentations	3
Chapter 2. Literature Review	5
2.1 Oscillatory Chemical Reactions	5
2.2 Carbonylation Reactions	20
2.3 PCPOC Reaction	24
Chapter 3. Aims and Objectives	29
3.1 Overview	29
3.2 Aim	29
3.3 Objectives	29
3.4 Summary of Objectives	32
Chapter 4. Experimental Study	33
4.1 Overview	33
4.2 Equipment	33
4.2.1 HEL MicroNOTE	33

4.2.2	HEL Simular	35
4.2.3	HEL Automate	40
4.2.4	Parallel Reaction System	41
4.2.5	Varian GCMS	43
4.2.6	Filtration	43
4.2.7	Chemicals	44
4.3	Experimental Studies of the Full PCPOC System	45
4.3.1	Effect of Temperature	45
4.3.2	Effect of Increased Water Concentration	46
4.4	Preliminary Subsystems Experiments	47
4.4.1	pH of Methanol	47
4.4.2	Solubility of Catalyst Components	48
4.4.3	Reaction of the Catalytic System with CO	50
4.4.4	Role of Water in the Catalytic System	51
4.5	Experimental Study of Catalyst Activation	52
4.5.1	Modifying Solvents	52
4.5.2	Adding CO Prior to PdI ₂	53
4.5.3	Filtered Catalyst Solution	54
4.6	Experimental Study of the PhAc/KI/MeOH/CO/Air Subsystem	56
4.7	Experimental Study of the PhAc/Catalyst/CO Subsystem	56
4.7.1	Changing the Order of Reactant Addition in Wet and Dried Methanol	57
4.7.2	CO Purging Time	58
4.7.3	Varying CO Flow Rate	59
4.7.4	Gas-Liquid Mass Transfer	60
Chapter 5.	Results and Discussion of Experiments on the Full PCPOC Reaction	63
5.1	Full PCPOC System - Effect of Temperature	64
5.1.1	pH and Turbidity	65

5.1.2	Phenylacetylene Conversion	82
5.1.3	Product Distribution	84
5.1.4	Summary	89
5.2	Full PCPOC System - Effect of Increased Water Concentration	89
5.2.1	pH	90
5.2.2	Phenylacetylene Conversion and Product Formation	98
5.2.3	Summary	101
Chapter 6.	Results and Discussion of Experiments on Subsystems of the PCPOC Reaction	103
6.1	Preliminary Subsystems Experiments	103
6.1.1	pH of Methanol	103
6.1.2	Solubility of Catalyst Components	104
6.1.3	Reaction of the Catalytic System with CO	108
6.1.4	Role of Water in the Catalytic System	110
6.2	Study of Catalyst Activation	111
6.2.1	Modifying Solvents	111
6.2.2	Adding CO Prior to PdI ₂	113
6.2.3	Filtered Catalyst Solution	114
6.2.4	Modelling Study	116
6.2.5	Summary	135
6.3	Study of the Phenylacetylene/KI/MeOH/CO/Air Subsystem	137
6.4	Study of the Phenylacetylene/Catalyst/CO Subsystem	137
6.4.1	Changing the Order of Reactant Addition in Wet and Dried Methanol	137
6.4.2	CO Purging Time	149
6.4.3	Varying CO Flow Rate	150
6.4.4	Gas-Liquid Mass Transfer	151
Chapter 7.	Conclusions and Recommendations for Future Work	153
7.1	Summary	157

7.2 Future Work	158
Appendix A - Additional Temperature Experiments	161
Initial Experiments on the Effect of Temperature on the PCPOC Reaction	161
Naphthalene as Internal Standard	162
Appendix B – GCMS Calibration	165
Calibration Using Relative Response Factors	165
Calibration Using Calibration Curves	165
Appendix C - Additional Data for the CO Purging Time Experiments	169
References	171

List of Figures

Figure 2.1. Example oscillations in fox and rabbit populations using the Lotka-Volterra model with $[\text{Rabbits}]_0 = 100$; $[\text{Foxes}]_0 = 25$; $k_1 = 0.03$; $k_2 = 0.0008$ and $k_3 = 0.05$.	6
Figure 2.2. Oscillations in iodine concentration found by Bray in 1921. ^[16]	7
Figure 2.3. A representation of the occurrence of bistability in a reaction in a CSTR. Measurement of a variable (e.g. concentration) as a control parameter (e.g. flow rate) is continuously varied gives two variable values for the same value of control parameter indicating the presence of 2 stable steady states.	9
Figure 2.4. Illustrative examples of mixed-mode oscillations.	10
Figure 2.5. A schematic representation of the development of target patterns.	11
Figure 2.6. The variation in pattern formation with increasing ferrocyanide concentration in the BSF reaction. ^[78]	12
Figure 2.7. (a) and (b) Mosaic patterns developing in the aniline- H_2SO_4 -bromate system with $[\text{H}_2\text{SO}_4] = 2.2 \text{ M}$, $[\text{NaBrO}_3] = 0.055 \text{ M}$, $[\text{aniline}] = 0.022 \text{ M}$; (c) the appearance of stripes in the 4-aminobenzenesulfonic acid- H_2SO_4 -bromate system with $[\text{H}_2\text{SO}_4] = 1.7 \text{ M}$, $[\text{NaBrO}_3] = 0.08 \text{ M}$, $[\text{4-aminobenzenesulfonic}] = 0.026 \text{ M}$. ^[79]	13
Figure 2.8. Wave patterns in the bromate-1,4-cyclohexanedione-ferroin system at 25 °C with $[\text{NaBrO}_3] = 0.1 \text{ M}$, $[\text{H}_2\text{SO}_4] = 0.2 \text{ M}$, $[\text{1,4-cyclohexanedione}] = 0.1 \text{ M}$, $[\text{KBr}] = 0.01 \text{ M}$, $[\text{ferroin}] = 0.005 \text{ M}$: (a) transverse waves observed in a thin layer between two glass plates; (b) crossing waves in a thin layer open to air. ^[85]	14
Figure 2.9. Pattern formation when water was added to the surface of acrylamide gel during polymerisation at an initial temperature of 40 °C. Gel composition: $[\text{acrylamide}] = 1.035 \text{ M}$, $[\text{N,N'-methylene-bisacrylamide}] = 4.85 \times 10^{-3} \text{ M}$, $[\text{triethanolamine}] = 0.055 \text{ M}$, $[(\text{NH}_4)_2\text{S}_2\text{O}_8] = 0.112 \text{ M}$, (a) spot formation occurs with $[\text{Na}_2\text{S}] = 3 \times 10^{-2} \text{ M}$, (b) stripe formation occurs with $[\text{Na}_2\text{S}] = 5 \times 10^{-2} \text{ M}$. ^[86]	15
Figure 2.10. Schematic representation of a one-side-fed reactor (OSFR).	16
Figure 2.11. Turing patterns observed in the thiourea-iodate-sulfite reaction generated using the experimental design method of Horvath and colleagues. ^[92]	17
Figure 2.12. Products of PhAc carbonylation identified by Chiusoli <i>et al.</i> ^[125]	21
Figure 2.13. Oscillations in pH and heater power observed in the PCPOC reaction at 20 °C. ^[3]	26
Figure 2.14. The effect of temperature on pH oscillations in the PCPOC reaction found by Novakovic <i>et al.</i> ^[134]	27

Figure 4.1. The HEL MicroNOTE system used in small-scale experiments on the PCPOC reaction.	33
Figure 4.2. Diagram of the main features of the HEL MicroNOTE system used for small scale experiments on the PCPOC reaction.	34
Figure 4.3. Jacketed reactor used with HEL MicroNOTE and a magnetic stirrer (Bibby B212 magnetic stirrer/hotplate) for small scale PCPOC experiments.	35
Figure 4.4. The HEL Simular used for large-scale experiments on the PCPOC reaction.	37
Figure 4.5. Diagram of the main features of the HEL Simular equipment setup used in the experiments on the full PCPOC reaction.	37
Figure 4.6. The HEL Automate used for experiments on the PCPOC reaction at increased pressure.	41
Figure 4.7. Diagram showing the main features of the HEL Automate.	41
Figure 4.8. Parallel reaction system used in small-scale experiments.	42
Figure 4.9. Sigma-Aldrich vacuum filtration apparatus.	43
Figure 4.10. Silica filters for filtration of PCPOC samples prior to GCMS analysis.	44
Figure 5.1. Products detected by GCMS in the PCPOC reaction: 1 , Methyl (E)-cinnamate; 2 , Methyl atropate; 3 , Dimethyl (2Z)-2-phenyl-2-butenedioate; 4 , Dimethyl (2E)-2-phenyl-2-butenedioate; 5 , 5,5-Dimethoxy-3-phenyl-2(5H)-furanone; 6 , Phenylmaleic anhydride; 7 , Phenylmaleic acid.	64
Figure 5.2. Diagram showing how the period, amplitude, duration, onset and end of pH oscillations were defined.	65
Figure 5.3. The pH recorded during the PCPOC reaction conducted at temperatures from 0-40 °C.	66
Figure 5.4. pH and heater power in the oscillatory PCPOC reaction at 40 °C.	71
Figure 5.5. Onset of pH oscillations in the PCPOC reaction at 40 °C.	72
Figure 5.6. Oscillations in pH and heater power in the PCPOC reaction at 40 °C from 1500-1600 min.	72
Figure 5.7. Methanol addition, indicated by spikes in the power curve, increases the period and amplitude of pH oscillations in the PCPOC reaction at 40 °C.	73
Figure 5.8. Turbidity and pH recorded in the oscillatory PCPOC reaction at 40 °C.	74
Figure 5.9. pH and heater power in the oscillatory PCPOC reaction at 30 °C.	74

Figure 5.10. Addition of methanol to the PCPOC reaction at 30 °C, indicated by the peak in heater power around 2470 min, leads to an increase in the period and amplitude of pH oscillations.	75
Figure 5.11. Onset of pH oscillations in the PCPOC reaction at 30 °C.	75
Figure 5.12. pH and heater power in the oscillatory PCPOC reaction at 30 °C from 2600-3000 min.	76
Figure 5.13. The changing shape of the pH oscillations in the PCPOC reaction at 30 °C.	76
Figure 5.14. Turbidity and pH recorded in the oscillatory PCPOC reaction at 30 °C.	77
Figure 5.15. Oscillations in turbidity are in phase with pH oscillations at 30 °C.	77
Figure 5.16. Oscillations in pH and heater power in the oscillatory PCPOC reaction at 20 °C.	78
Figure 5.17. The oscillations in pH and heater power are in phase in the oscillatory PCPOC reaction at 20 °C.	78
Figure 5.18. The changing shape of pH oscillations during the PCPOC reaction at 20 °C.	79
Figure 5.19. Turbidity and pH recorded in the oscillatory PCPOC reaction at 20 °C.	79
Figure 5.20. The development of oscillations in turbidity that are out of phase with pH oscillations at 20 °C.	80
Figure 5.21. pH and heater power in the oscillatory PCPOC reaction at 10 °C.	80
Figure 5.22. In phase oscillations in pH and heater power in the oscillatory PCPOC reaction at 10 °C.	81
Figure 5.23. Turbidity and pH recorded in the oscillatory PCPOC reaction at 10 °C.	81
Figure 5.24. Turbidity and pH recorded in the oscillatory PCPOC reaction at 0 °C.	82
Figure 5.25. Heater power from the oscillatory PCPOC reaction at 0 °C.	82
Figure 5.26. Phenylacetylene conversion in the oscillatory PCPOC reaction at 0-40 °C.	83
Figure 5.27. The reaction rate of the PCPOC reaction at temperatures from 0-40 °C increased once pH oscillations started.	84
Figure 5.28. Variation in product distribution as reaction temperature is increased from 0-40 °C in the oscillatory PCPOC reaction at 70% PhAc conversion for temperatures of 0 °C and 20-40 °C and 51% PhAc conversion at 10 °C.	85
Figure 5.29. Reactant and product distribution in the oscillatory PCPOC reaction at 40 °C.	86

Figure 5.30. Reactant and product distribution in the oscillatory PCPOC reaction at 30 °C.	86
Figure 5.31. Reactant and product distribution in the oscillatory PCPOC reaction at 20 °C.	87
Figure 5.32. Reactant and product distribution in the oscillatory PCPOC reaction at 10 °C.	87
Figure 5.33. Reactant and product distribution in the oscillatory PCPOC reaction at 0 °C.	88
Figure 5.34. The variation of Z-isomer and DMO concentrations with temperature.	88
Figure 5.35. Comparison of pH behaviour in the PCPOC reaction at 30 °C with solvent volume ratios of H ₂ O:MeOH from 0:100 to 40:60.	91
Figure 5.36. Oscillations in pH are accompanied by oscillations in heater power in the PCPOC reaction containing 20% water at 30 °C.	92
Figure 5.37. pH oscillations in the PCPOC reaction at 30 °C in 100% MeOH.	93
Figure 5.38. pH oscillations in the PCPOC reaction at 30 °C with a H ₂ O:MeOH solvent volume ratio of 5:95.	93
Figure 5.39. pH oscillations in the PCPOC reaction at 30 °C with a H ₂ O:MeOH solvent volume ratio of 20:80.	94
Figure 5.40. pH oscillations in the PCPOC reaction at 30 °C with a H ₂ O:MeOH solvent volume ratio of 30:70.	95
Figure 5.41. pH oscillations in the PCPOC reaction at 30 °C with a H ₂ O:MeOH solvent volume ratio of 40:60.	95
Figure 5.42. The variation in period of the pH oscillations during the PCPOC reaction with water concentrations of 0-30% at 30 °C.	97
Figure 5.43. The variation in the time taken for the pH to fall rapidly at the end of each oscillation as water content in the system is increased from 0-30%.	97
Figure 5.44. The variation in onset time and duration of pH oscillations as water concentration increased from 0-30%.	98
Figure 5.45. PhAc conversion and the percentage of known products produced in the PCPOC reaction at 30 °C as the solvent volume ratio of water is increased from 0-40%. In the case of the 0 and 40% experiments only a single run was conducted.	99
Figure 5.46. Variation in distribution of known products in the PCPOC reaction at 30 °C as the solvent volume ratio of water is increased from 0-40%. In the case of the 0 and 40% experiments only a single run was conducted.	100

Figure 6.1. pH of methanol.	104
Figure 6.2. Measurements of pH during the addition of PdI_2 to methanolic KI solution, $[\text{KI}] = 0.693 \text{ mol dm}^{-3}$.	106
Figure 6.3. Results of the initial experiments to determine the solubility of PdI_2 in $0.693 \text{ mol dm}^{-3}$ KI in methanol.	107
Figure 6.4. Solubility of PdI_2 in methanol containing 0.5-3 g KI.	108
Figure 6.5. The pH behaviour of catalyst solutions containing different amounts of PdI_2 on purging with $\text{CO} = 50 \text{ mL min}^{-1}$; $[\text{KI}] = 0.693 \text{ mol dm}^{-3}$.	109
Figure 6.6. Effect of water on the pH of the catalytic system when purging with $\text{CO} = 50 \text{ mL min}^{-1}$; solvent = 25 mL; KI = 2.053 g.	110
Figure 6.7. pH behaviour of the PdI_2/KI catalyst in water, methanol and dried methanol when purged with CO : $[\text{CO}] = 6 \text{ mL min}^{-1}$; $[\text{PdI}_2]_{\text{max}} = 2.221 \times 10^{-3} \text{ mol dm}^{-3}$; $[\text{KI}] = 0.48 \text{ mol dm}^{-3}$.	112
Figure 6.8. Comparison of pH behaviour in the catalytic system when CO is added to wet or dried methanolic KI solution: i) before PdI_2 is added; ii) after PdI_2 is added.	114
Figure 6.9. The effect of increased $[\text{KI}]$ on the pH behaviour of the catalyst solution with CO .	115
Figure 6.10. Effect of catalyst dilution on pH behaviour when purging with CO .	115
Figure 6.11. Purging dilute catalyst solution, $[\text{PdI}_2] = 4.44 \times 10^{-4} \text{ mol dm}^{-3}$, with CO flows of 6 mL min^{-1} and 50 mL min^{-1} .	116
Figure 6.12. Fitted data from Model 1 compared with the calculated $[\text{H}^+]$ from the experimental pH data for water shown in Figure 6.7.	121
Figure 6.13. Fitted data from Model 2 compared with the calculated $[\text{H}^+]$ from the experimental pH data for water shown in Figure 6.7.	122
Figure 6.14. Fitted data from Model 3 compared with the calculated $[\text{H}^+]$ from the experimental pH data for dried MeOH shown in Figure 6.7.	123
Figure 6.15. Fitted data from Model 4 compared with the calculated $[\text{H}^+]$ from the experimental pH data for filtered catalyst solution using wet MeOH shown in Figure 6.10.	125
Figure 6.16. Fitted data from Model 5: (a) no constraints; (b) constraint that $[\text{Pd}] = 0$; compared with the calculated $[\text{H}^+]$ from the experimental pH data for filtered catalyst solution using wet MeOH shown in Figure 6.10.	127

Figure 6.17. Fitted data from Model 6: (a) no constraints; (b) constraint that $[Pd] = 0$; compared with the calculated $[H^+]$ from the experimental pH data for filtered catalyst solution using wet MeOH shown in Figure 6.10. 129

Figure 6.18. Fitted data from Model 7: (a) no constraints; (b) constraint that $[Pd] = 0$; compared with the calculated $[H^+]$ from the experimental pH data for filtered catalyst solution using wet MeOH shown in Figure 6.10. 131

Figure 6.19. Fitted data from Model 8: (a) no constraints; (b) constraint that $[Pd] = 0$; compared with the calculated $[H^+]$ from the experimental pH data for filtered catalyst solution using wet MeOH shown in Figure 6.10. 133

Figure 6.20. The pH behaviour on the addition of PhAc (2 mL) to a $0.693 \text{ mol dm}^{-3}$ solution of KI in MeOH purged with $CO = 50 \text{ mL min}^{-1}$ and $air = 50 \text{ mL min}^{-1}$. 137

Figure 6.21. (a) pH recorded in Experiments 1-4 and (b) hydrogen ion concentrations calculated from adjusted pH. 141

Figure 6.22. Concentration profiles of phenylacetylene and products in Experiments 1-4: (a) Phenylacetylene (PhAc); (b) Methyl (E)-cinnamate, (MeCin), (**1**); (c) Phenylmaleic anhydride/Phenylmaleic acid, (PhMAN or PhMAc) (**6/7**); (d) Dimethyl (2Z)-2-phenyl-2-butenedioate, (Z-isomer), (**3**); (e) Dimethyl (2E)-2-phenyl-2-butenedioate, (E-isomer), (**4**); (f) 5,5-Dimethoxy-3-phenyl-2(5H)-furanone, (DMO), (**5**). Phenylacetylene added first in Experiments 1 and 3; CO added first in Experiments 2 and 4. 143

Figure 6.23. (a) pH and phenylacetylene measured in Experiment 3, (b) comparison of product **1** and H^+ concentration in Experiments 3 and 4. 144

Figure 6.24. pH and concentration profiles of phenylacetylene and products in experiments 5-6: (a) pH; (b) Phenylacetylene, (PhAc); (c) Methyl (E)-cinnamate, (MeCin), (**1**); (d) Phenylmaleic anhydride/Phenylmaleic acid, (PhMAN or PhMAc), (**6/7**); (e) Dimethyl (2Z)-2-phenyl-2-butenedioate, (Z-isomer), (**3**); (f) Dimethyl (2E)-2-phenyl-2-butenedioate, (E-isomer), (**4**). Phenylacetylene added first in Experiment 5; CO added first in Experiment 6. 146

Figure 6.25. Simulation of the trends observed in Experiments 1-4: $[PhAc] = 0.01 \text{ mol dm}^{-3}$, $CO = 10 \text{ mL min}^{-1}$, (a) Run 1 – PhAc added first, not dried; (b) Run 2 – CO added first, not dried; (c) Run 3 – PhAc added first, dried (d) Run 4 – CO added first, dried. 149

Figure 6.26. PhAc conversion in catalyst solutions that were purged with CO for 0-200 min prior to PhAc addition. 150

Figure 6.27. pH during the reaction of the catalyst system with PhAc at CO flow rates of 5, 10 and 15 mLmin ⁻¹ in the absence of air.	151
Figure 6.28. Concentration of PhAc after 30 min of purging with CO at flow rates of 5, 10 and 15 mLmin ⁻¹ .	151
Figure 6.29. Comparing the effect of increased stirring rate on the reaction of PhAc with PdI ₂ /KI/CO in the absence of air.	152
Figure A1. Oscillations in pH, heater power and turbidity observed in the PCPOC reaction at 20 °C without Np in the reactor.	162
Figure A2. Oscillations in pH during the PCPOC reaction with Np in the reactor.	163
Figure A3. A comparison of products during the PCPOC reaction with and without Naphthalene in the reactor.	163
Figure B1. Calibration curve used to calculate [PhAc].	166
Figure B2. Calibration curve used to calculate [E-isomer].	166
Figure B3. Calibration curve used to calculate [Z-isomer].	166
Figure B4. Calibration curve used to calculate [PhMAn or PhMAc].	167
Figure B5. Calibration curve used to calculate [MeCin].	167
Figure C1. PhAc conversion when catalyst solution was purged with CO for 60 min prior to PhAc addition.	169
Figure C2. PhAc conversion when catalyst solution was purged with CO for 120 min prior to PhAc addition.	169
Figure C3. PhAc conversion when catalyst solution was purged with CO for 200 min prior to PhAc addition.	170

List of Tables

Table 2.1. The variation in product distribution and phenylacetylene conversion found by Suleiman and colleagues using the Pd(OAc) ₂ -dppb- <i>p</i> -TsOH-CH ₃ CN-CO catalyst system at 110 °C, 100 psi CO, when Pd(OAc) ₂ was substituted with other Pd catalysts. ^[129]	22
Table 4.1. GC oven method used for the analysis of samples from the PCPOC reaction.	43
Table 4.2. Reagent quantities and stirring times for Experiment 3.	49
Table 4.3. Reagent quantities and vial numbers for Experiment 4.	50
Table 4.4. Reagent quantities and stirring times for Experiment 5.	50
Table 4.5. Initial quantities of reagents used to investigate the role of water in the catalytic system.	52
Table 4.6. Reaction conditions for the PhAc/Catalyst/CO subsystem experiments. ^a Expts 1-6: [PhAc] = 0.01 moldm ⁻³ ; CO flow = 10 mLmin ⁻¹ for the duration of the experiment. Expts 5,6: [H ₂ O] = 4.44 x 10 ⁻⁴ moldm ⁻³ .	57
Table 5.1. A summary of trends in the period of pH oscillations of the PCPOC reaction at temperatures of 0-40 °C compared with those found by Novakovic <i>et al</i> , 2009. ^[134] ^a Experiment was stopped before oscillations had ceased. ^b Some oscillations started at 270 min but were not sustained.	68
Table 5.2. A summary of trends in the amplitude of pH oscillations in the PCPOC reaction at temperatures of 0-40 °C compared with those found by Novakovic <i>et al</i> . ^[134]	69
Table 5.3. A summary of trends in the pH oscillations of the PCPOC reaction at 30 °C with solvent volume ratios of H ₂ O:MeOH from 0:100 to 40:60.	92
Table 5.4. The change in shape of pH oscillations as water content was increased from 0-30% in the PCPOC reaction at 30 °C.	96
Table 6.1. Concentration of PdI ₂ in the solutions from Experiment 3 used to determine the solubility of PdI ₂ in methanolic KI.	106
Table 6.2. BatchCAD settings used to model the experimental data from the experiments on the catalyst subsystem of the PCPOC reaction described in Section 4.5.	118
Table 6.3. Initial conditions used in the modelling studies.	118
Table 6.4. Reactions and reaction rates used in Model 1.	120
Table 6.5. Reactions and reaction rates used in Model 2.	122

Table 6.6. Reactions and reaction rates used in Model 3.	123
Table 6.7. Reactions and reaction rates used in Model 4.	124
Table 6.8. Rate constants for Models 5-8 estimated using the BatchCAD kinetic fitting package.	126
Table 6.9. Reactions and reaction rates used in Model 5.	126
Table 6.10. Reactions and reaction rates used in Model 6.	128
Table 6.11. Reactions and reaction rates used in Model 7.	130
Table 6.12. Reactions and reaction rates used in Model 8.	132
Table 6.13. Reactions and reaction rates used in Model 9.	134
Table 6.14. Reactions and reaction rates used in Model 10.	134
Table 6.15. Reactions and reaction rates used in Model 11.	134
Table 6.16. Reactions and reaction rates used in Model 12.	135
Table 6.17. Reactions and reaction rates used in the modelling study of the catalyst subsystem.	136
Table 6.18. Reactant and product conversion in Experiments 1-4.	139
Table 6.19. Model used in the simulation study in BatchCAD.	147
Table 7.1. Reactions and rates used to produce models that gave a good fit to the observed pH behaviour of the catalyst system; [cat] = HI, Pd(0), HPdI or Pd ₂ I ₂ .	156
Table B1. Concentration of analyte stock solutions and RRF values calculated from Equation (B1) used to calculate product and reactant concentrations in the experiments in Section 5.1. ^a RRF for DMO calculated from the last sample in the experiment at 0 °C where [DMO] = [PhAc] ₀ - [unreacted PhAc] - [Z-isomer] - [E-isomer]; [E-isomer] calculated using the calibration curve shown in Figure B2.	165

Nomenclature

List of acronyms

BZ	Belousov-Zhabotinsky
BSF	Bromate-Sulfite-Ferrocyanide
CP	Chemically Pure
CSTR	Continuous Stirred-Tank Reactor
DMO	5,5-Dimethoxy-3-phenyl-2(5H)-furanone
E-isomer	Dimethyl (2E)-2-phenyl-2-butenedioate
FKN	Field Körös Noyes
GCMS	Gas Chromatography – Mass Spectroscopy
Lactone	3-Phenyl-2(5H)-furanone
MeAt	Methyl atropate
MeCin	Methyl (E)-cinnamate
MeOH	Methanol
MFC	Mass Flow Controller
NaOAc	Sodium Acetate
Np	Naphthalene
OSFR	One-Side-Fed Reactor
PCPOC	Palladium-Catalysed Phenylacetylene Oxidative Carbonylation
PhAc	Phenylacetylene
PhMAc	(2Z)-2-Phenyl-2-butenedioic acid; phenylmaleic acid
PhMAN	3-Phenyl-2,5-furandione; phenylmaleic anhydride
RRF	Relative Response Factor
TROPP	Tropylidene Phosphane
Z-isomer	Dimethyl (2Z)-2-phenyl-2-butenedioate

List of symbols

A	Reactant in the Brusselator and Gray-Scott models
A_{ht}	Heat transfer area, m^2
B	Reactant in the Brusselator and Gray-Scott models
C	Product in the Brusselator and Gray-Scott models
$C_{p(oil)}$	Specific heat capacity of oil in the jacket in reaction calorimetry, $Jkg^{-1}K^{-1}$
D	Product in the Brusselator model
E	BrO_3^-
f	Stoichiometric factor significant for the BZ reaction
k	Rate constant, $mol^{(1-n)}dm^{-3(n-1)}min^{-1}$ where n = reaction order
m_{oil}	Mass flow rate of oil through the jacket in reaction calorimetry, kgs^{-1}
P	HOB r
P_0	Baseline heater power prior to reaction, W
P_t	Heater power at time t , W
Q_r	Reaction heat, W
ΔS	Change in entropy, $JK^{-1}mol^{-1}$
T_j	Temperature of oil jacket in reaction calorimetry, $^{\circ}C$
T_r	Temperature of reactor contents in reaction calorimetry, $^{\circ}C$
ΔT_{oil}	Change in oil temperature, $^{\circ}C$
U	Heat transfer coefficient, $Wm^{-2}K^{-1}$
V	HBrO $_2$
W	Br^-
X	Intermediate in the Brusselator model
Y	Intermediate in the Brusselator model
Z	Ce $^{4+}$

Chapter 1. Introduction

1.1 Background

The oxidative carbonylation of phenylacetylene catalysed by palladium is a reaction that offers a direct pathway to the synthesis of carbonyl compounds and is therefore important to synthetic chemistry.^[1] On the surface it appears to be a straightforward reaction between phenylacetylene (PhAc), carbon monoxide (CO) and methanol (MeOH) in the presence of a palladium(II) iodide/potassium iodide (PdI₂/KI) catalyst producing a variety of products depending on the reaction conditions. In reality, the reaction is capable of exhibiting complex behaviour. This extraordinary reaction is capable of achieving oscillations in reaction heat exotherm (Q_r) and pH when operated under stirred batch conditions.^[2, 3] It is a rare example of a reaction catalysed by metal complexes that exhibits oscillatory behaviour. It is also the first oscillatory process that converts simple starting materials into relatively complex products. Other oscillatory reactions lead to the destruction of complex molecules.^[4]

The oscillatory behaviour of this reaction was first reported in 1997 by Malashkevich and colleagues who found oscillations in pH, redox potential and gas uptake.^[5] Initially the behaviour was difficult to replicate but Novakovic *et al* recently reported that, using specialist reaction calorimetry equipment, it is now possible to routinely obtain reproducible oscillations in both pH and Q_r.^[2, 3]

A number of products of this reaction are reported including: dimethyl (2Z)-2-phenyl-2-butenedioate (Z-isomer), dimethyl (2E)-2-phenyl-2-butenedioate (E-isomer), methyl atropate (MeAt), methyl (E)-cinnamate (MeCin) and 3-phenyl-2(5H)-furanone (Lactone).^[6] It has also been found that product selectivity is high when the reaction oscillates and that product formation is low until oscillations start, after which the Z-isomer is selectively formed (>90%).^[2] When the reaction does not oscillate selectivity is poor leading to a mixture of products. The ability to affect product selectivity by switching from non-oscillatory to oscillatory modes is important from the point of view of reaction engineering.

It is not known why this reaction oscillates and how the mechanism of this reaction differs when operated in oscillatory and non-oscillatory regimes although a number of ideas have been discussed.^[7-10]

1.2 Research Aims

The palladium-catalysed phenylacetylene oxidative carbonylation (PCPOC) system displays a number of interesting and important phenomena and needs to be investigated to understand and subsequently exploit the experimental observations. This work aims to do this by analysing and characterising the PCPOC reaction in both oscillatory and non-oscillatory modes. This will be achieved through a comprehensive experimental study of this reaction. The proposed work will consist of two approaches: a top-down approach investigating the behaviour of the reaction system as a whole under different conditions i.e. a range of temperatures, increased water concentration; and a bottom-up approach which will focus on dividing the reaction into a series of subsystems to be analysed separately. The results from these two approaches will be combined to elucidate the reaction network responsible for oscillations with the goal of understanding the observed behaviour of this reaction so that the knowledge gained can be applied to other systems.

1.3 Thesis Structure

Chapter 2 of this work reviews the literature and gives a brief introduction to oscillatory processes and non-linear dynamics before introducing carbonylation reactions. The PCPOC reaction is then discussed giving an overview of the work that has been done so far on this system. A more detailed discussion of the aims and objectives of this thesis is presented in Chapter 3.

Chapter 4 describes the experimental methods used in the study of the PCPOC reaction. A brief outline is given of the equipment and chemicals used followed by a more detailed description of the experiments which were conducted. Two approaches were followed: the top-down approach and the bottom-up approach. The chapter begins with the top-down approach by describing two studies conducted on the full PCPOC reaction system. The first investigates the effect of temperature on the pH oscillations and product formation in the PCPOC reaction. The second study investigates the effect increasing the concentration of water has on the pH oscillations and product formation in the PCPOC reaction. These are followed by the experiments using the bottom-up approach which begins with a set of experiments to determine the baseline pH of methanol and solubility of the catalyst components. Initial experiments on the pH behaviour of the catalyst system with CO and also with water are then presented. This is followed by a more detailed study into the activation

of the catalyst in the system. The experiments are then expanded to include phenylacetylene.

Chapter 5 presents and discusses the results of the experiments on the full PCPOC system. Chapter 6 presents and discusses the results of the experimental study of subsystems of the PCPOC reaction as well as presenting the results of two modelling studies. Conclusions based on the results are presented in Chapter 7 which also outlines possible directions for future study on the PCPOC reaction system.

1.4 Presentations and Publications Resulting From This Thesis

1.4.1 Journal Papers

Novakovic, K. and Parker, J. *Catalyst initiation in the oscillatory carbonylation reaction*. International Journal of Chemical Engineering, 2011.

Parker, J. and Novakovic, K. *Influence of water and the reactant addition sequence on palladium(II) iodide-catalysed phenylacetylene carbonylation*. Industrial & Engineering Chemistry Research, 2013. **52**(7): p. 2520-2527.

Donlon, L., Parker J. and Novakovic, K. *Oscillatory carbonylation of phenylacetylene in the absence of externally supplied oxidant*. Reaction Kinetics, Mechanisms and Catalysis, 2014. **112**(1): p. 1-13.

Parker, J. and Novakovic, K. *Autonomous reorganization of the oscillatory phase in the PdI_2 catalysed phenylacetylene carbonylation reaction*. Reaction Kinetics, Mechanisms and Catalysis, 2016: p. 1-13. doi: 10.1007/s11144-016-0979-8

1.4.2 Conference Presentations

Parker, J. and Novakovic, K. *The influence of reaction temperature on the dynamics of product formation during the oscillatory mode of the phenylacetylene oxidative carbonylation reaction*. 19th International Congress of Chemical and Process Engineering. 2010. Prague, Czech Republic.

1.4.3 Poster Presentations

Novakovic, K. and Parker, J. *Palladium(II) iodide in the oscillatory phenylacetylene carbonylation reaction*. 19th International Conference of Chemical and Process Engineering. 2010. Prague, Czech Republic.

Parker, J. and Novakovic, K. *The influence of reaction temperature on the dynamics of product formation during the oscillatory mode of the phenylacetylene oxidative carbonylation reaction*. 19th International Congress of Chemical and Process Engineering. 2010. Prague, Czech Republic.

Parker, J. and Novakovic, K. *Oscillatory phenylacetylene carbonylation reaction*. Gordon Research Conference: Oscillations & Dynamic Instabilities in Chemical Systems. 2010. Il Ciocco Hotel and Resort, Lucca (Barga), Italy

Parker, J. and Novakovic, K. *Oscillations in the concentration of phenylacetylene and its carbonylation products*. Gordon Research Conference: Oscillations & Dynamic Instabilities in Chemical Systems. 2012. Colby College, Waterville, ME.

Parker, J. and Novakovic, K. *From oscillations to step-wise pH behaviour in the palladium-catalysed oxidative carbonylation reaction by increasing water concentration*. Gordon Research Conference: Oscillations and Dynamic Instabilities in Chemical Systems. 2014. PGA Catalunya Business and Convention Centre, Girona, Spain.

Parker, J. and Novakovic, K. *From small molecule to macromolecule oscillatory chemical reactions*. ChemEngDayUK 2015. University of Sheffield, Sheffield, UK.

Chapter 2. Literature Review

The behaviour of the oscillatory PCPOC reaction is complex and a study of this reaction system needs to bridge a number of research areas. Initially it requires a knowledge and understanding of oscillatory processes and carbonylation reactions.

2.1 Oscillatory Chemical Reactions

Oscillatory processes have been known since the 17th century when Robert Boyle first noticed that phosphorus would luminesce periodically.^[11] Other oscillatory processes have been reported since then^[12] but it was not until 1910 that a model consisting of a series of chemical reactions that would give damped oscillations was produced by Alfred Lotka.^[13] In 1920 Lotka updated this model to give a series of chemical reactions that would produce undamped oscillations and also applied them to biological systems.^[14] In 1925 he applied his equations to the analysis of predator-prey interactions. The ecologist Vito Volterra was working on similar ideas in relation to species populations.^[15] These resulted in the Lotka-Volterra model which is used to study predator-prey interactions. The model is outlined in Equations (2.1)-(2.3).



The rate expressions for this model are shown in Equation (2.4) and (2.5).

$$\frac{d[\text{Rabbits}]}{dt} = k_1 [\text{Rabbits}] - k_2 [\text{Rabbits}][\text{Foxes}] \quad (2.4)$$

$$\frac{d[\text{Foxes}]}{dt} = k_2 [\text{Rabbits}][\text{Foxes}] - k_3 [\text{Foxes}] \quad (2.5)$$

The model assumes that there is an abundant supply of grass. With an initial rabbit population of 100, an initial fox population of 25 and using arbitrary values for the rate constants with $k_1 = 0.03$, $k_2 = 0.0008$ and $k_3 = 0.05$ an example of the oscillations produced is shown in Figure 2.1.

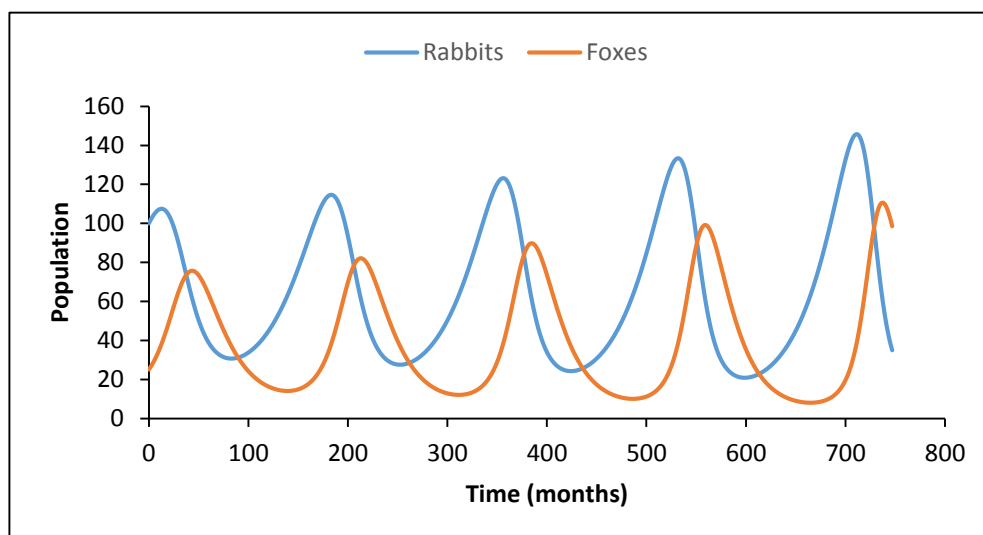


Figure 2.1. Example oscillations in fox and rabbit populations using the Lotka-Volterra model with $[\text{Rabbits}]_0 = 100$; $[\text{Foxes}]_0 = 25$; $k_1 = 0.03$; $k_2 = 0.0008$ and $k_3 = 0.05$.

No actual homogeneous chemical oscillator was known at this time. However, in 1921 the chemist William Bray was investigating the action of hydrogen peroxide as both an oxidising and reducing agent using an iodine-iodic acid couple.^[16] The hydrogen peroxide oxidises iodine to iodic acid (Equation (2.6)):



whilst simultaneously reducing iodic acid to iodine (Equation (2.7)):



The overall reaction being the decomposition of hydrogen peroxide (Equation (2.8)):



During the course of his experiments Bray noticed that under certain conditions the concentration of iodine would oscillate (Figure 2.2).^[16]

Image removed from electronic copy due to copyright issues

Figure 2.2. Oscillations in iodine concentration found by Bray in 1921.^{[16]*}

This was the first documented example of a homogeneous chemical oscillator although at first it was not accepted as such. In fact, the decomposition of hydrogen peroxide by the iodine-iodic acid couple was initially attributed to a heterogeneous impurity reaction occurring on the surface of dust particles.^[17] Further study established the conditions for the various reactions between the components in the reaction mixture and produced preliminary measurements on reaction rates.^[18, 19]

Bray's student, Herman Liebhafsky, went on to study this reaction extensively.^[20-25] Due to the complex nature of the overall reaction Liebhafsky initially identified two reactions which he could study separately. The first was the reaction in which iodate ion was reduced by hydrogen peroxide.^[21] The second was the reaction in which iodine was oxidised to iodate by hydrogen peroxide.^[20] He then went on to consider the catalytic decomposition of hydrogen peroxide by the iodine-iodide couple.^[22-24] It was only in the 1970's that the reaction, which became known as the Bray-Liebhafsky reaction, was accepted as a genuine homogeneous chemical oscillator.^[25, 26]

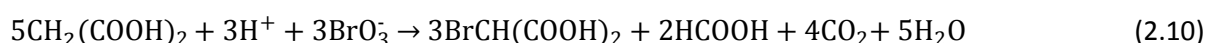
One of the main reasons many refused to accept the existence of chemical oscillations was due to the mistaken belief that chemical oscillations contradict the second law of thermodynamics, Equation (2.9), which has the condition that the change in entropy, ΔS , of a system and its surroundings increases i.e.

$$\Delta S \geq 0 \quad (2.9)$$

* Reprinted with permission from Bray, W.C. (1921) 'A periodic reaction in homogeneous solution and its relation to catalysis', *Journal of the American Chemical Society*, 43(6), 1262-1267. Copyright 1921 American Chemical Society.

However, there is no contradiction. Unlike physical oscillatory systems, a swinging pendulum for example, which passes through its equilibrium position as it swings back and forth until it comes to rest, oscillatory chemical reactions do not pass through their position of equilibrium as they oscillate. The observed oscillations e.g. changes in colour or pH, occur due to oscillations in the concentrations of intermediate species during the reaction when it is far from equilibrium.

Even the most widely studied oscillatory process, the Belousov-Zhabotinsky (BZ) reaction, was initially not accepted as such.^[27-32] This reaction was discovered by Boris Belousov in 1951 when he was studying the cerium ion-catalysed reaction of citric acid with bromate. During the course of the reaction the colour of the solution began to oscillate from colourless to yellow. Belousov thought this was due to oscillations in the concentration of free bromine. Although he realised the importance of this discovery his work was rejected for publication by several journals and it was not until 1959 that he managed to publish an article on the reaction.^[33] Anatol Zhabotinsky began to study the process several years after Belousov's initial discovery. He substituted malonic acid for the citric acid used by Belousov which made the colour change much easier to see. Zhabotinsky realised the oscillations in colour were due to oscillations in the concentration of Ce^{4+} and later showed the inhibitory role that bromide ions play in the reaction.^[34] The reaction subsequently became known as the BZ reaction and it has played a central role in the development of nonlinear chemical dynamics.^[26] The overall reaction is given in Equation (2.10).^[35]



Several other oscillating chemical reactions have also been discovered. For example, the Briggs-Rauscher reaction, which combines elements of the Bray-Liebhafsky and the BZ reactions, gives oscillations in iodine and iodide concentrations.^[36] The oxidation of 2,4-pentanedione by bromate in the presence of a manganese(II) catalyst exhibits oscillations in transmittance at 425 nm.^[37] The decomposition of sodium dithionite has shown oscillations in dithionite and hydrogen ion concentrations.^[38] Oscillations in electrode potential have been observed in the air oxidation of benzaldehyde with the oscillations being sensitive to air flow.^[39]

The initial work on oscillatory reactions, such as the BZ^[29, 40] and Bray-Liebhafsky^[16, 21, 25, 41] reactions, was conducted under batch conditions. However, under these conditions the reactions are closed systems and therefore produce transient

oscillatory behaviour as the system gradually approaches equilibrium. The introduction of the CSTR (continuous stirred-tank reactor) allowed oscillatory reactions to be conducted as open systems.^[42, 43] Under these conditions the reactions never approach equilibrium as there is a constant inflow of reactants to the reactor, with the products continually flowing out. Instead of reaching equilibrium, stable long term behaviour occurs. This may be steady state or sustained oscillatory behaviour. Using a CSTR allows the flow rates of the reactants into the reactor to be varied while monitoring parameters inside the reactor such as temperature, pH and the concentrations of various species. It was under these conditions that multistability, which generally occurs in open systems, was discovered. The simplest form of multistability is bistability (illustrated in Figure 2.3). This is when a reaction can have two stable steady states for the same values of some input parameter, e.g. flow rate of a reactant.

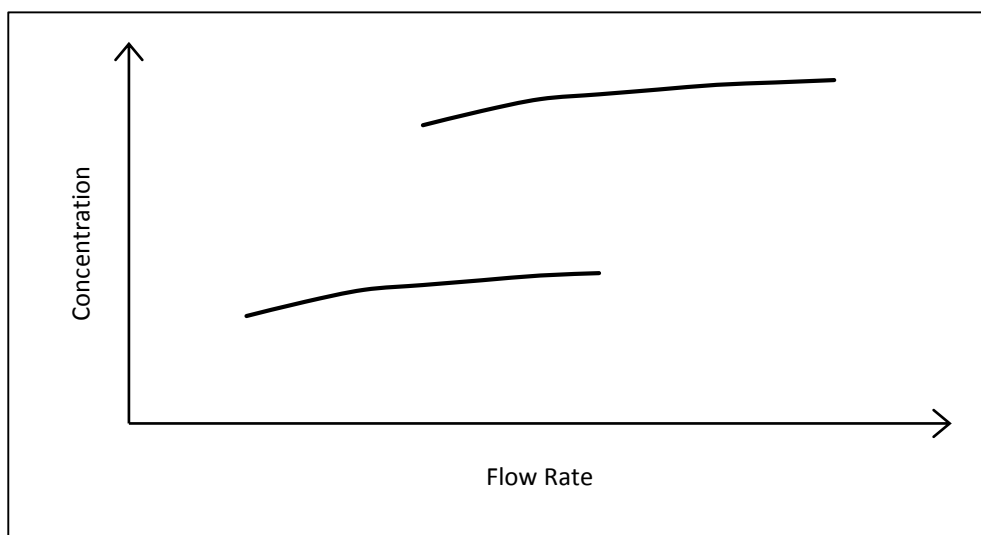


Figure 2.3. A representation of the occurrence of bistability in a reaction in a CSTR. Measurement of a variable (e.g. concentration) as a control parameter (e.g. flow rate) is continuously varied gives two variable values for the same value of control parameter indicating the presence of 2 stable steady states.

Bistability has been observed in a number of reactions including the reaction of peroxidase,^[44] the iodate oxidation of arsenous acid,^[45] and the Briggs-Rauscher reaction.^[43, 46] Tristability, the occurrence of three stable steady states under the same conditions, has been found in the chlorite-iodide-iodate-arsenite system^[47] and the chlorite-thiosulfate-iodide-iodine system.^[48] Birhythmicity, the coexistence of two stable oscillatory modes, has also been found in the chlorite-thiosulfate-iodide-iodine system^[48] as well as in the chlorite-bromate-iodide system.^[49]

The introduction of the CSTR enabled the discovery of more oscillatory systems. Several oscillatory reaction systems based on manganese have been discovered. The reaction of permanganate, hydrogen peroxide and phosphoric acid in a CSTR is an example of a halogen-free oscillatory reaction and was the first transition metal based oscillator.^[50] The minimal manganese oscillator was found to be the Guyard reaction between permanganate and Mn(II) with the addition of phosphate ion in the form of KH_2PO_4 in a CSTR.^[51] The addition of phosphate was found to be essential and its role included buffering the solution at a pH around 7 and stabilising reaction intermediates. Using this reaction as the core oscillator a number of manganese oscillators were discovered which had either permanganate and a reductant or Mn(II) and an oxidant.^[52] Doona *et al* found that they could still achieve oscillations if they replaced the phosphate with hydrogen arsenate or hydrogen orthovanadate to stabilise the intermediates. They also found that if they used phosphate or hydrogen arsenate as the stabilisers they could replace the reductant with arsenite, thiocyanate, thiourea or hydroxylamine, amongst others, and still achieve oscillations.^[52] The reduction of permanganate by hydrogen peroxide or ninhydrin has been shown to exhibit transient oscillations in a closed system and mixed-mode oscillations in a CSTR.^[53] The bromate-oxalic acid-acetone-Mn(II) system has been found to show oscillations in a CSTR.^[54] Large amplitude oscillations, two kinds of mixed mode oscillations (illustrated in Figure 2.4), quasiperiodicity and bursts of large amplitude oscillations were observed although the more complex behaviour did not occur without acetone.

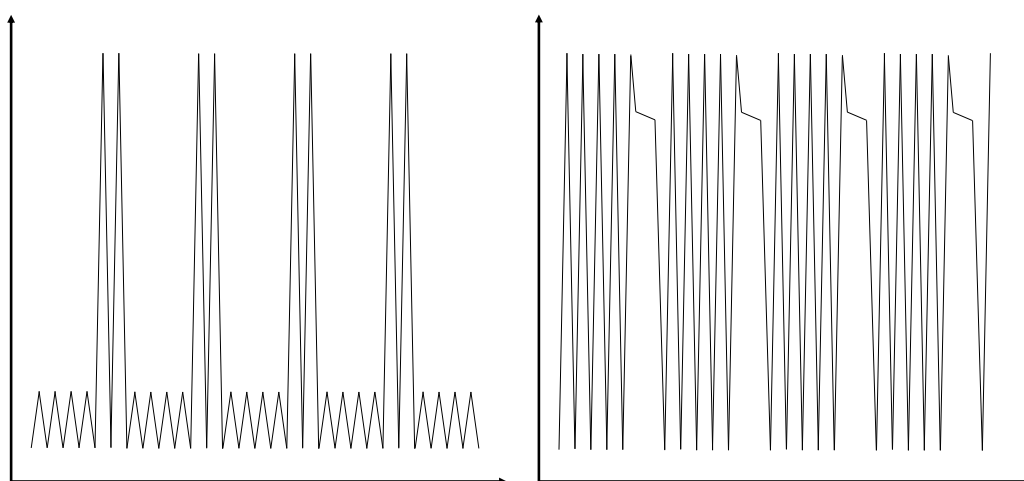


Figure 2.4. Illustrative examples of mixed-mode oscillations.

Following the discovery of the oscillatory nature of the BZ reaction under well-stirred conditions, further experimentation uncovered a number of spatiotemporal phenomena. Busse found alternating layers in the BZ reaction with a wavelength of 0.5 mm in the bromate-malonic acid-cerous ion system using ferroin as an indicator.^[55] Zaikin and Zhabotinsky performed the reaction using bromate, bromomalonic acid and ferroin as the catalyst in a petri dish at room temperature without stirring.^[40] They found the completely reduced catalyst would develop points where the catalyst oxidised. These points became circular concentration waves which propagated through the solution (target patterns), represented schematically in Figure 2.5.

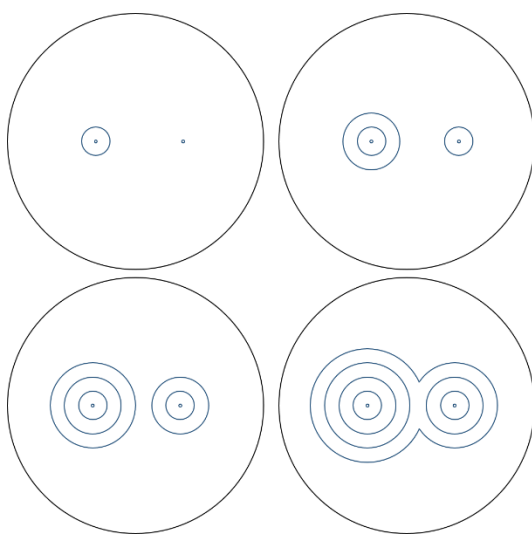


Figure 2.5. A schematic representation of the development of target patterns.

When waves collided they annihilated each other rather than generating the interference patterns observed when light or water waves collide. Winfree found spiral waves could be generated by tilting the petri dish containing the BZ reaction mixture once the circular waves had begun to propagate.^[56] If the reaction mixture was sheared rather than tilted, scroll waves were produced.^[57] Scroll rings (scroll waves in which the ends are joined) were discovered by having a stack of Millipore filters which had been impregnated with the BZ reaction mixture. When a heated filament touched the centre of the stack on the upper surface the scroll rings were generated.^[58] These wave patterns have been studied extensively.^[59-66]

The development of these patterns generated much interest as they could be used to model biological processes.^[67] For example, Turing had proposed a system of chemical reactions to produce a model of the generation of stationary patterns and

showed that they could be used to account for the tentacle patterns on *Hydra*.^[68] He also postulated that the formation of these stationary patterns in two dimensions could account for phyllotaxis, the arrangement of leaves around a stem. Glycolysis has also been shown to generate similar spatiotemporal patterns.^[69] These patterns are produced by the propagation of chemical waves as substances, often catalyst, diffuse through an unstirred reaction mixture. These reaction-diffusion systems have been widely studied to understand the processes involved in pattern formation.^[40, 70-72] Numerical studies investigating the effect of chemical and thermal convection on chemical wave propagation have been undertaken.^[73, 74] The effects of convection on wave propagation in chemicals systems, for example the iodate-arsenous acid system and the iron(II)-nitric acid system, have also been studied.^[75-77]

Pattern formation has also been found in other oscillatory reactions. For example, in the bromate-sulfite-ferrocyanide (BSF) system Molnar and Szalai found a number of pattern formations including labyrinthine, filament and Turing-type patterns as the initial concentration of ferrocyanide was increased (Figure 2.6).^[78]

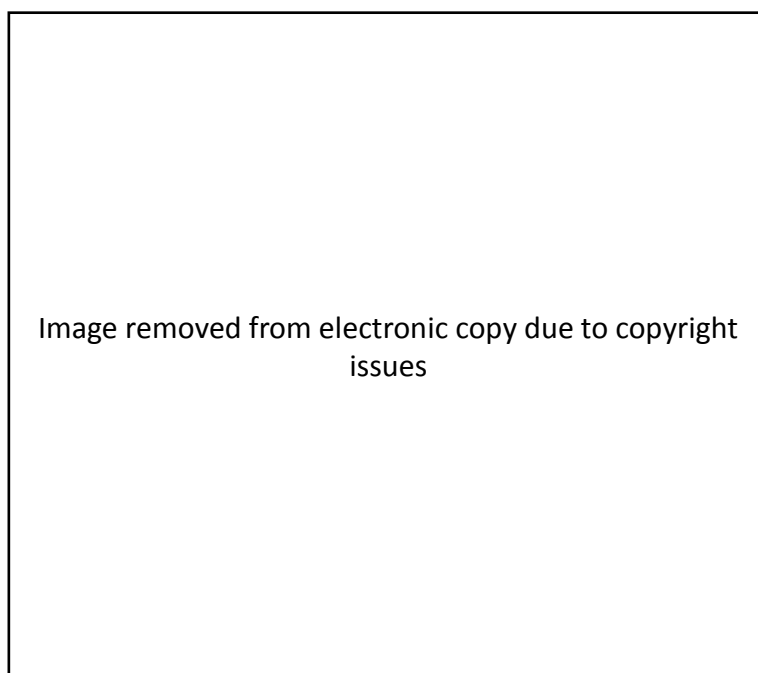


Figure 2.6. The variation in pattern formation with increasing ferrocyanide concentration in the BSF reaction.^{[78]†}

[†] Reprinted with permission from Molnár, I. and Szalai, I. (2015) 'Pattern formation in the bromate–sulfite–ferrocyanide reaction', *The Journal of Physical Chemistry A*, 119(39), 9954-9961. Copyright 2015 American Chemical Society.

In the uncatalysed reaction of aromatics with bromate and sulfuric acid Orban observed trigger waves, mosaic and striped patterns in a petri dish at 24-25 °C.^[79] The patterns observed were dependent on the chemical composition of the solution and the thickness of the solution layer in the petri dish. Figure 2.7 gives an example of the mosaic structure and the striped patterns that Orban observed.^[79]



Figure 2.7. (a) and (b) Mosaic patterns developing in the aniline-H₂SO₄-bromate system with [H₂SO₄] = 2.2 M, [NaBrO₃] = 0.055 M, [aniline] = 0.022 M; (c) the appearance of stripes in the 4-aminobenzenesulfonic acid-H₂SO₄-bromate system with [H₂SO₄] = 1.7 M, [NaBrO₃] = 0.08 M, [4-aminobenzenesulfonic] = 0.026 M.^{[79]‡}

The mosaic patterns did not form when the reaction was conducted in a closed system i.e. when the petri dish was sealed. Orban suggests the formation of the mosaic patterns, which is accompanied by precipitation, is due to oxygen from the atmosphere being mixed into the solution by convective motion in the solution.^[79] Mosaic structures have also been observed in the BZ reaction performed in thin layers.^[80]

[‡] Reprinted with permission from Orbán, M. (1980) 'Chemical oscillation during the uncatalyzed reaction of aromatic compounds with bromates. 4. Stationary and moving structures in uncatalyzed oscillatory chemical reactions', *Journal of the American Chemical Society*, 102(13), 4311-4314. Copyright 1980 American Chemical Society.

The bromate-hypophosphite-acetone-dual catalyst oscillator was developed specifically to study pattern formation.^[81] The reaction is precipitate free and produces oscillations under batch conditions. Using acetone to remove bromine prevents bubble formation and both Mn(II)-Ru(bpy)₃SO₄ and Mn(II)-ferroin were good catalysts that produced a long-lasting oscillator which could generate wave patterns for up to 7 hr.

The chlorite-iodide-malonic acid system (CIMA) exhibits trigger waves and stationary patterns.^[82, 83] The CIMA reaction has also been shown to exhibit spatial bistability.^[84] Spatial bistability occurs when a reaction can exhibit two stable pattern formations for a given range of a particular control parameter, for example substrate concentration. In the CIMA reaction the two stable patterns were stripes and hexagonal spots.^[84] The bromate-1,4-cyclohexanedione-ferroin system exhibits transverse wave and crossing wave patterns (Figure 2.8).^[85]

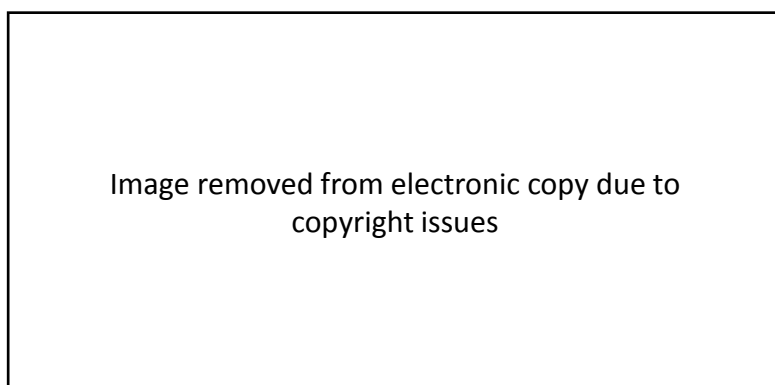


Figure 2.8. Wave patterns in the bromate-1,4-cyclohexanedione-ferroin system at 25 °C with [NaBrO₃] = 0.1 M, [H₂SO₄] = 0.2 M, [1,4-cyclohexanedione] = 0.1 M, [KBr] = 0.01 M, [ferroin] = 0.005 M: (a) transverse waves observed in a thin layer between two glass plates; (b) crossing waves in a thin layer open to air.^[85]

Pattern formation has also been observed during the polymerisation of acrylamide gel when a layer of water was added to the gel surface.^[86] Spots or stripes were formed depending on the S²⁻ concentration used in the reaction (Figure 2.9). When the S²⁻ concentration was zero there was no pattern formation.

[§] Reprinted with permission from Kurin-Csörgei, K., Zhabotinsky, A.M., Orbán, M. and Epstein, I.R. (1996) 'Bromate-1,4-cyclohexanedione-ferroin gas-free oscillating reaction. 1. Basic features and crossing wave patterns in a reaction-diffusion system without gel', *The Journal of Physical Chemistry*, 100(13), 5393-5397. Copyright 1996 American Chemical Society.

Image removed from electronic copy due to copyright issues

Figure 2.9. Pattern formation when water was added to the surface of acrylamide gel during polymerisation at an initial temperature of 40 °C. Gel composition: [acrylamide] = 1.035 M, [*N,N'*-methylene-bisacrylamide] = 4.85×10^{-3} M, [triethanolamine] = 0.055 M, [(NH₄)₂S₂O₈] = 0.112 M, (a) spot formation occurs with [Na₂S] = 3×10^{-2} M, (b) stripe formation occurs with [Na₂S] = 5×10^{-2} M.^{[86]**}

Most of the initial studies on pattern formation in the oscillatory reactions were conducted in batch conditions which result in transient patterns that decay as the reaction mixture gradually approaches equilibrium. There is also the disadvantage that convective currents^[79] and bubble formation can be a problem.^[87] Conducting the experiments in gel helps to ensure the reaction is not affected by convective motion or bubbles. Castets and coworkers conducted the CIMA reaction in a polyacrylamide hydrogel and were the first to observe Turing patterns during the reaction.^[83] Turing patterns are caused by stationary waves in reaction-diffusion systems producing stationary patterns e.g. spots or stripes.^[68] Turing patterns have also been found in the CIMA reaction in gel-free conditions by using a capillary tube reactor containing the starch-based thiodene iodine indicator.^[88] More recently, Turing-type patterns have been found in the bromate-sulfite-ferrocyanide (BSF) system when the reaction was conducted in an open one-side-fed reactor (OSFR, Figure 2.10).^[78]

** Reprinted with permission from Orbán, M., Kurin-Csörgei, K., Zhabotinsky, A.M. and Epstein, I.R. (1999) 'Pattern formation during polymerization of acrylamide in the presence of sulfide ions', *The Journal of Physical Chemistry B*, 103(1), 36-40. Copyright 1999 American Chemical Society.

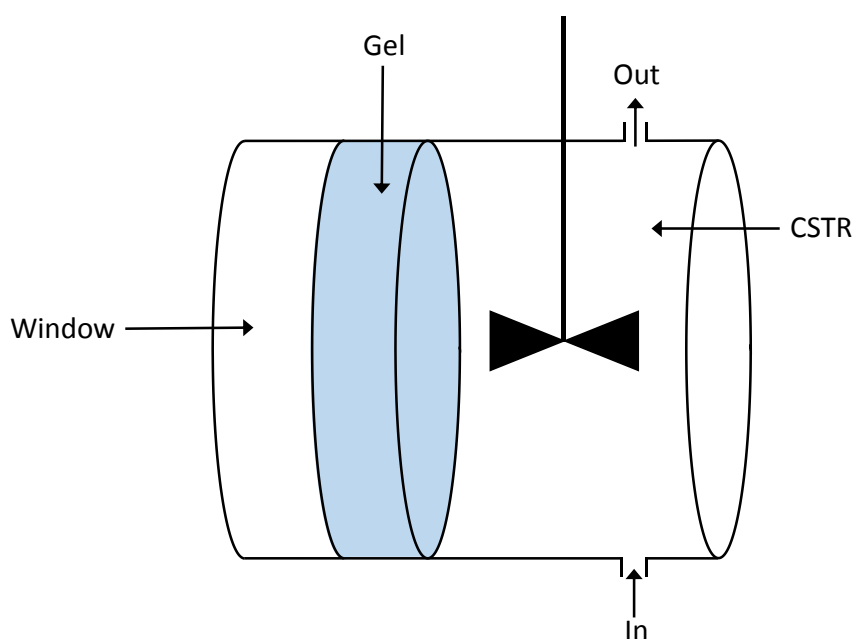


Figure 2.10. Schematic representation of a one-side-fed reactor (OSFR).

An OSFR is effectively a CSTR (continuous stirred-tank reactor) with a gel layer at one end so that one face of the gel is in contact with the contents of the CSTR. The other side of the gel is pressed against a transparent window allowing pattern formation to be viewed. The reaction occurs in both the gel layer and the CSTR but the reaction mixture in the CSTR is maintained such that the extent of the reaction in the CSTR is low.^[78] Reactants and products diffuse in and out of the gel with the gel preventing convection.^[89] The use of an OSFR allowed pH patterns including hexagonal spots and stripes to be observed in the reaction between iodate, sulfite and thiosulfate using bromocresol green as the pH indicator to visualise the patterns.^[90]

It has been shown that simple reaction-diffusion systems containing a single autocatalytic step should be able to generate Turing structures when the reaction is conducted in a continuously-fed unstirred reactor.^[91] An experimental method has been developed by Horvath and colleagues to search for reaction systems that can display Turing patterns.^[92] The 3 steps of the method are:

1. Generate spatial bistability;
2. Produce spatiotemporal oscillations by using an independent negative-feedback (inhibitory species);
3. Use a complexing agent with low mobility to induce a space-scale separation of the activatory and inhibitory processes.

An example of Turing patterns generated using this method in the thiourea-iodate-sulfite reaction by Horvath *et al* is shown in Figure 2.11.



Figure 2.11. Turing patterns observed in the thiourea-iodate-sulfite reaction generated using the experimental design method of Horvath and colleagues.^{[92]††}

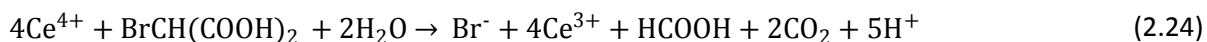
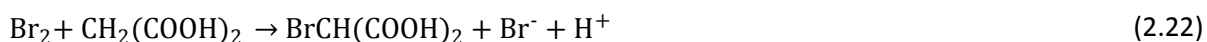
Understanding the mechanism to explain the oscillatory behaviour observed in these reactions is challenging. The first model of an oscillatory system that behaved more like real chemical systems was proposed by Prigogine and Lefever in 1968.^[93] The model consists of reactants A and B forming products C and D via intermediates X and Y. The rate constants of each step are k_4 - k_7 . This model later became known as the “Brusselator” and is shown in Equations (2.11)-(2.14).^[94]



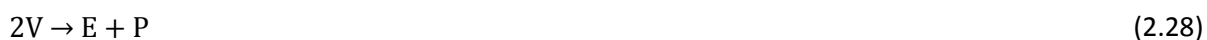
Following the discovery of the oscillatory BZ reaction Field, Körös and Noyes conducted an extensive experimental study on the reaction which enabled them to produce a detailed mechanism, the FKN model, that explained the behaviour of the BZ reaction. The mechanism is shown in Equations (2.15)-(2.24).^[28, 95]



†† From Horváth, J., Szalai, I. and De Kepper, P. (2009) [‘An experimental design method leading to chemical Turing patterns’](#), *Science*, 324(5928), 772-775. Reprinted with permission from AAAS.



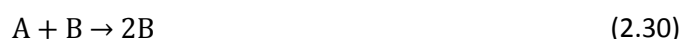
They were able to apply this mechanism to explain the pattern formation observed in early experiments.^[70] They later modified the FKN mechanism to yield the five step Oregonator model that still maintained many of the major features of the BZ reaction.^[96] This was achieved by realising that the FKN model consisted of 2 overall processes: the reduction of bromate ion by bromide, Equations (2.15)-(2.17) and (2.22), and the production of $\text{BrO}_2\cdot$, Equations (2.18)-(2.20). The Oregonator model, summarised by Noyes in 1990 is shown in Equations (2.25)-(2.29).^[97]



$\text{E} \equiv \text{BrO}_3^-$; $\text{V} \equiv \text{HBrO}_2$; $\text{W} \equiv \text{Br}^-$; $\text{Z} \equiv 2\text{Ce}^{4+}$; $\text{P} \equiv \text{HOBr}$; $f \equiv$ stoichiometric factor significant for the BZ reaction.

The Oregonator model has since been modified further to account for some of the more complex behaviour observed in the BZ reaction. For example, Showalter and colleagues used a reversible Oregonator model to simulate the chaotic behaviour in the BZ reaction observed by Schmitz and colleagues.^[98, 99] Nagy-Ungvarai and colleagues extended the Oregonator, again including some reversibility, to model differences in the velocity of trigger waves in the BZ reaction.^[100, 101] The Oregonator model has also been modified to investigate the effect of temperature on oscillation period and amplitude in the BZ reaction.^[102]

With the introduction of CSTRs to study oscillatory reactions Gray and Scott showed that even simple autocatalytic reactions such as those shown in Equations (2.30) and (2.31) could display a range of behaviour including isolas and mushrooms in plots of conversion against residence time.^[103]





The cubic autocatalytic reaction in Equation (2.31) was able to display multistability, hysteresis and sustained oscillatory behaviour.^[104, 105] The model by Gray and Scott has been used as a basis to model reaction-diffusion systems.^[106, 107]

As the understanding of the mechanisms of oscillatory reactions increased it became possible to design oscillatory reaction systems. The chlorite-arsenite-iodate system is an example of a specifically designed homogeneous oscillator.^[108] De Kepper and coworkers suggested that for oscillations to occur a reaction system should be far from equilibrium, have some sort of feedback which is often in the form of autocatalysis and exhibit bistability.^[108] They supplied the first condition by operating in a CSTR. The autocatalytic reaction of arsenite and iodate was found to be bistable^[109] to which they added chlorite to fulfil the second and third conditions and induce oscillations.^[108] The success of this process led to the discovery of several oscillatory reactions, many based on halogens. An example of a halogen free oscillatory reaction is the reaction of sulfide with hydrogen peroxide in a CSTR.^[110] The reaction of sodium chlorite, sodium sulfite and sulfuric acid in a CSTR has been found to exhibit a range of dynamic behaviour including bistability and aperiodic oscillations.^[111] In the same study, the reaction was also conducted under batch conditions and damped oscillations were observed.

Oscillations in pH have been found in the Bray-Liebhafsky reaction but were limited to the first hour of the experiment and were very small, <0.025 pH units.^[41] The BZ reaction has also been reported to exhibit small-amplitude pH oscillations (<0.03 pH units) when the reaction was conducted without sulfuric acid using Ce(NO₃)₃ or MnSO₄ as catalyst although no pH oscillations were observed when the catalyst was ferroin or Ru(bpy)₃.^[112] The pH oscillations in both cases are not central to the processes behind the primary oscillatory behaviour.

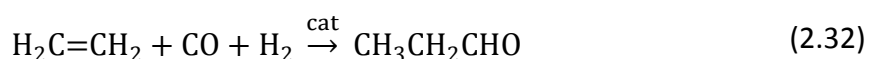
Many oscillatory reactions have oscillations in pH but “pH oscillators” are reactions that exhibit pH oscillations with an amplitude spanning several pH units when the reaction is conducted in unbuffered solution. In the presence of buffer, the oscillations cease and the reaction proceeds monotonically.^[101, 113] A number of pH oscillators have been identified^[101] including the sulfide-hydrogen peroxide system,^[110] the iodate-sulfite-ferrocyanide system,^[114] and the oxidation of hydroxylamine by periodate,^[115] amongst others. Generally they are aqueous redox

reactions involving one oxidant and one or two reductants.^[101] In the one reductant systems the reductant can be oxidised via two pathways: one which consumes H⁺ and one which generates H⁺. In the two reductant system the reductants are oxidised by separate pathways. One of the reductants will generate H⁺ in the process whilst the oxidation of the other reductant occurs via a pathway which consumes H⁺. All of these pH oscillators occur only under flow conditions although progress has been made to produce pH oscillators that operate in closed systems.^[116] The reactions tested were the iodate-sulfite-ferrocyanide system,^[114] the bromate-sulfite-ferrocyanide system^[117] and the bromate-sulfite-Mn(II) system.^[118] Reaction in a closed system was achieved by impregnating a gel with SO₃²⁻ ion (in the form of Na₂SO₃) which was situated at the bottom of a batch reactor allowing the slow dissolution of the SO₃²⁻ ion into the reactor effectively forming a semi-batch process.

All of these reactions occur in aqueous conditions and many do not show oscillations in batch conditions. One of the more recent discoveries, the study of which is the focus of this work, was reported by Malashkevich *et al* who recorded oscillations in pH, redox potential and gas uptake in the palladium-catalysed phenylacetylene oxidative carbonylation (PCPOC) reaction.^[5]

2.2 Carbonylation Reactions

The PCPOC reaction comes from the family of carbonylation reactions which are important in both synthetic and industrial chemistry. They are C-C bond forming reactions that can directly synthesise carbonyl compounds by the addition of carbon monoxide to an organic substrate as shown in Equation (2.32).^[119]



A number of different organic substrates can be employed. For example Heck carbonylation produces aldehydes, esters or carboxylic or keto acids and amides from aryl and vinyl halides.^[120-122] The PCPOC reaction is an example of Reppe carbonylation which utilises alkene and alkyne substrates.^[123] A number of transition metal compounds are able to catalyse carbonylation reactions including compounds based on Co, Pd, Pt, Ni, Rh, and Ru. Palladium and rhodium are most frequently employed as they can be used under milder conditions.^[124]

The products of alkyne carbonylation are dependent on the conditions and the catalyst used. The reaction can proceed in an oxidative or reductive manner with the

products formed resulting from mono- or di- carbonylation. Chiusoli *et al* reported a number of products, shown in Figure 2.12, from the carbonylation of phenylacetylene in methanol.^[125]

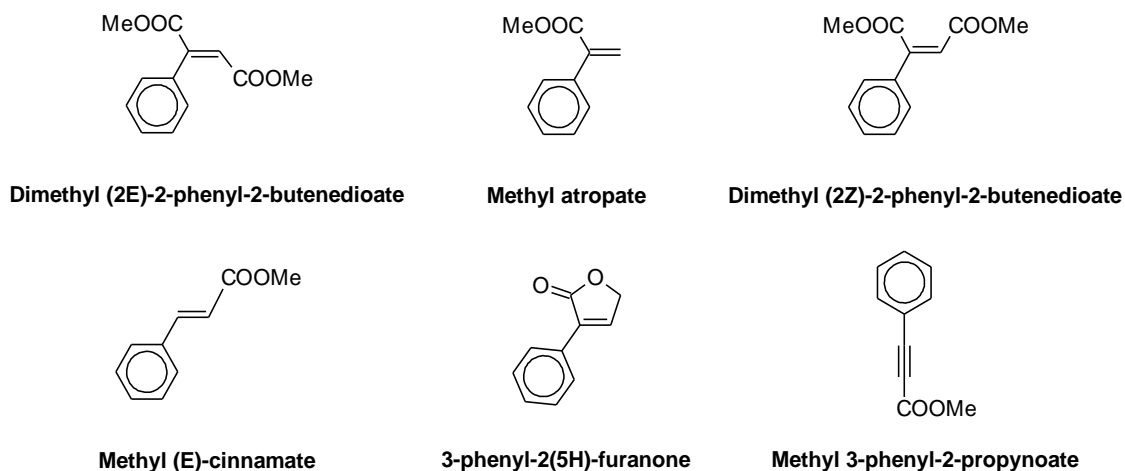


Figure 2.12. Products of PhAc carbonylation identified by Chiusoli *et al*.^[125]

They used a PdCl₂-thiourea catalyst at room temperature and atmospheric pressure of CO. They obtained dimethyl (2E)-2-phenyl-2-butenedioate (from oxidative carbonylation) and the lactone, 3-phenyl-2(5H)-furanone, (from reductive carbonylation) as the two main products.

Tsuji and colleagues reported alkynylcarboxylate products from the carbonylation of terminal acetylenes when they used a PdCl₂ catalyst in combination with CuCl₂. Experiments were conducted at room temperature in methanol in the presence of NaOAc with a CO pressure slightly above atmospheric pressure. With phenylacetylene they obtained a 74% yield of methyl 3-phenyl-2-propynoate (Figure 2.12) in 2 hours. However when no base was present a mixture of unsaturated diesters was obtained.^[126] Bettuci *et al* also produced alkynylcarboxylate esters from terminal alkynes.^[127] They used Pd(II)-TROPP complexes as catalysts in the presence of *p*-benzoquinone at a higher temperature and CO pressure (70 °C and 7-28 bar respectively) than Tsuji and colleagues. With phenylacetylene they observed phenylacetylene conversions of 93-95% selectively forming methyl 3-phenyl-2-propynoate with 100% selectivity (Figure 2.12).^[127] In the absence of *p*-benzoquinone phenylacetylene conversion was only 2-3% and they obtained a mixture of MeAt (75%) and MeCin (25%).

Drent *et al* achieved 99% selectivity to methylmethacrylate (from monocarbonylation) when carbonylating propyne in methanol at 60-80 °C with a CO pressure of 60 bar.

They used a Pd(II) species with a 2-pyridylphosphine ligand in both batch and continuous (CSTR) experiments. Similar results were obtained when other terminal alkynes were used.^[128] Suleiman *et al* found that using a Pd(OAc)₂-dppb-*p*-TsOH-CH₃CN-CO catalyst system also gave monocarbonylation products with phenylacetylene but at 110 °C and 100 psi CO.^[129] Methyl (E)-cinnamate (Figure 2.12) was the major product (88%) and methyl atropate (12%) was also formed. They compared other palladium catalysts and found the selectivity varied from 12-100% MeAt and phenylacetylene conversion ranged from 4-99% depending on the catalyst used (Table 2.1).

Table 2.1. The variation in product distribution and phenylacetylene conversion found by Suleiman and colleagues using the Pd(OAc)₂-dppb-*p*-TsOH-CH₃CN-CO catalyst system at 110 °C, 100 psi CO, when Pd(OAc)₂ was substituted with other Pd catalysts.^[129]

Catalyst	PhAc Conversion (%)	Product Distribution (%)	
		MeCin	MeAt
Pd(OAc) ₂	99	88	12
PdCl ₂	27	75	25
PdCl ₂ (PPh ₃) ₂	7	0	100
Pd(PhCN) ₂ Cl ₂	4	0	100
Pd(CN) ₂	22	65	35
PdSO ₄	99	38	62
Pd-C (5%)	97	87	13

Gabriele and co-workers found that dicarbonylation products resulted from the carbonylation of terminal alkynes using PdI₂/KI as catalyst in methanol at 25-80 °C and a CO pressure of 20 atm.^[130] They achieved alkyne conversions of 72-100% and dicarbonylated product yields of 68-100% depending on the amount of catalyst added and the reaction temperature. The products consisted of a mixture of Z-diester, the dimethoxylactone, E-isomer, and the diacid depending on the alkyne substrate.^[130] The Z-diester was the major product except when the experiments were conducted with phenylacetylene at 25 °C and 40 °C. At 25 °C, 36 % Z-isomer and 45 % DMO (5,5-Dimethoxy-3-phenyl-2(5H)-furanone) were obtained and at 40 °C, 42 % Z-isomer and 44 % DMO were produced.^[130] This change in selectivity may not be purely due to the change in reaction temperature as they also reduced the catalyst loading when they reduced the temperature. The effect of changing the catalyst loading was evident from experiments they conducted at 60 °C in which the

catalyst loading was increased from 1000 to 3000 mol substrate/mol catalyst. They found the yield of DMO reduced from 37% to 21% whilst the yield of Z-isomer remained at 46%.^[130] When a similar methodology using the same PdI₂/KI catalytic system was applied to functionalised alkynes e.g. alkynyl alcohols, functionalised heterocyclic compounds were produced.^[1]

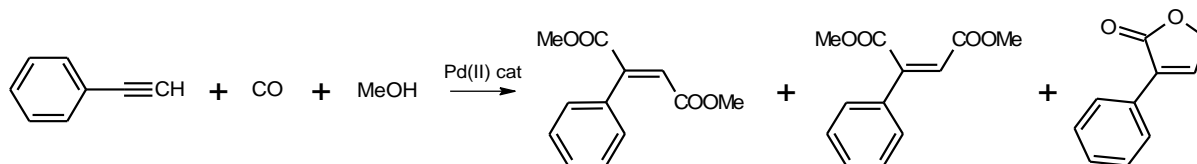
Alkyne carbonylation can also proceed in aqueous conditions. For example, in aqueous dioxane the main product of PhAc carbonylation is phenylmaleic anhydride when the reaction is carried out at 60-80 °C with PdI₂/KI as catalyst using a mixture of CO/air/CO₂ in the ratio 4:1:10 under pressure (60 atm at 25 °C).^[119] This is in line with earlier results reported by Zargarian and Alper who also reported increased formation of anhydrides in the presence of a higher concentration of water.^[131]

The carbonylation of alkynes by electrochemical means has also been achieved. Under these conditions the catalyst is regenerated at the anode rather than requiring the addition of a reoxidant (e.g. CuCl₂) to the system. For example, in 1993 Hartstock *et al* reported using a palladium(II) chloride catalyst at 50 °C and 1 atm CO with several terminal alkynes giving predominantly unsaturated *cis*-diesters.^[132] In contrast, alkynylcarboxylate products were reported by Chiarotto and Carelli when using palladium(II) complexes with triphosphine ligands as catalyst.^[133] Their experiments were conducted under mild conditions (room temperature; CO = 1 atm) but included the presence of a base (NaOAc or NEt₃).^[133] The results of Chiarotto and Carelli only gave yields of 45-57% which are lower than the 74% reported by Tsuji *et al* who also reported alkynylcarboxylate products but using a PdCl₂ catalyst with CuCl₂ as the reoxidant.^[126]

It is evident from the large number of possible products of alkyne carbonylation reactions just how important reaction conditions are for this process. One factor that has not been considered in the reactions mentioned above is the presence or absence of oscillations. In none of these cases were parameters followed that have been reported to exhibit oscillatory behaviour. The palladium-catalysed phenylacetylene oxidative carbonylation reaction, which has been shown to exhibit oscillations, is therefore worthy of investigation to understand the effect that oscillatory behaviour has on phenylacetylene conversion, selectivity and product distribution of the reaction.

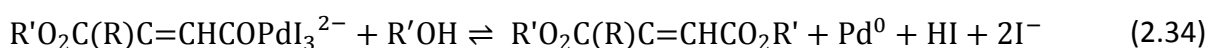
2.3 PCPOC Reaction

The carbonylation of phenylacetylene results in a number of products. Using a Pd(II) catalyst Chiusoli and colleagues found the reaction generated several products including those in Scheme 1 depending on reaction conditions.^[125]



Scheme 1.

Malashkevich and colleagues first reported oscillations in the PCPOC reaction in 1997 when they were investigating oxidative alkyne carbonylation which had previously been described by Gabriele and co-workers in 1994.^[5, 130] Gabriele and colleagues reacted terminal alkynes in alcohols at 25-80 °C under pressures of CO from 15-25 atm and air from 6-10 atm using PdI_2 and an excess of KI as catalyst. Gabriele *et al* noted a mixture of products which were dependent on the organic substrate although they only mentioned the dicarbonylated products.^[130] With phenylacetylene they obtained dimethyl (2Z)-2-phenyl-2-butenedioate, dimethyl (2E)-2-phenyl-2-butenedioate, (2Z)-2-phenyl-2-butenedioic acid and DMO. They did not report any oscillations as they were not looking for them, however they did propose a reaction scheme the main features of which are shown in Equations (2.33)-(2.35).^[130]

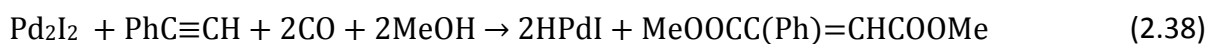


Gabrielle and colleagues identified the catalytic species involved in the reaction as PdI_4^{2-} . The PdI_4^{2-} reacts with the alcohol, CO and alkyne to form an organopalladium species which goes on to react with more alcohol to give the dicarbonylation products producing HI in the process.^[130]

When Malashkevich *et al* reported the oscillatory carbonylation of phenylacetylene they noted the products of the reaction as predominantly Z-isomer (dimethyl (2Z)-2-phenyl-2-butenedioate), with small amounts of DMO and E-isomer (dimethyl (2E)-2-phenyl-2-butenedioate) but no mention of any acid.^[5] They used the same catalytic

system as *Gabriele et al*^[130] i.e. PdI₂-KI-O₂-MeOH, but added NaOAc. Malashkevich and colleagues conducted all experiments at 40 °C and atmospheric pressure of CO and O₂ using a gas burette.^[5] With the addition of a platinum electrode and a glass pH electrode they were able to measure oscillations in pH and redox potential in the reaction that lasted for 3.5 h.

The mechanism of palladium-catalysed oxidative carbonylation is not fully understood at present although several theories have been put forward.^[7, 8] Malashkevich *et al* originally suggested a mechanism for the oscillatory PCPOC reaction consisting of 6 steps shown in Equations (2.36)-(2.41).^[5]



Later studies by Gorodskii and colleagues give a mechanism consisting of 7 steps. The first four steps are the same reactions as those in Equations (2.36)-(2.39) but instead of the reactions in Equations (2.40) and (2.41) they postulate the reactions in Equations (2.42)-(2.44).^[9]



The mechanisms are similar with regards to product formation: the first step in both mechanisms forms HPdI which reacts to generate the catalytic species (Pd₂I₂). This is then involved in product formation. There are, however, differences in the way in which each mechanism accounts for regeneration of the PdI₂. Malashkevich proposes a reaction between HPdI, O₂ and HI yielding palladium(II) iodide and water,^[5] Equation (2.40), whereas Gorodskii proposes a reaction between HPdI and O₂ only,^[9] Equation (2.42). This also produces PdI₂ as well as Pd(0) and hydrogen peroxide (which, as demonstrated by Bray, can act as both an oxidant and a reductant^[16]). Gorodskii's mechanism then has an additional step involving Pd(0) and

I_2 , Equation (2.43), which does not appear in the mechanism proposed by Malashkevich. Neither mechanism features autocatalysis.

More recently, the PCPOC reaction has been studied at Newcastle University by Novakovic and colleagues using specialist reaction calorimetry equipment. Initial findings showed that, as well as producing oscillations in pH, the system also produces oscillations in heater power and hence reaction heat, Q_r , (Figure 2.13).^[3] The study was conducted using power compensation calorimetry. This involves using an electric heater in the reaction vessel to maintain a constant reaction temperature by responding to changes in the system whilst an external oil jacket is maintained at a constant but lower temperature. If the reaction produces heat i.e. is exothermic, then the power to the electric heater is reduced by an amount sufficient to maintain a constant reaction temperature. If the reaction takes in heat i.e. is endothermic, then the power to the electric heater increases accordingly. Any changes in the heater power are therefore directly related to the reaction heat, Q_r . The oscillations in heater power are therefore a direct measurement of oscillations in Q_r .

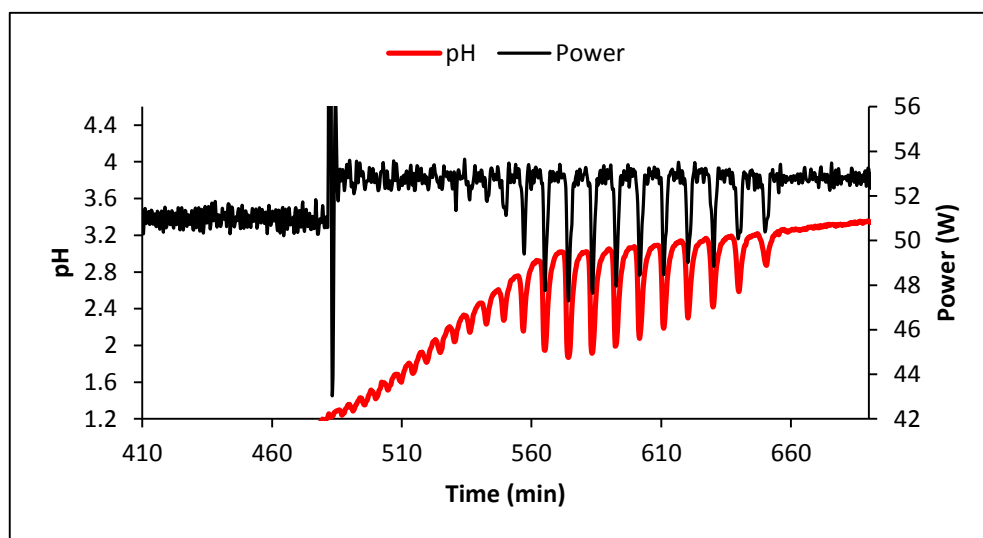


Figure 2.13. Oscillations in pH and heater power observed in the PCPOC reaction at 20 °C.^[3]

Novakovic *et al* also noted that temperature has an effect on the pH oscillations.^[134] As Figure 2.14 shows, the period and amplitude of the pH oscillations increases as the reaction temperature decreases. The maximum period of the oscillations is 182 min at 10 °C but only 12 min at 40 °C with the maximum amplitude of the pH oscillations being 3.1 pH units at 10 °C which reduces to 0.6 pH units at 40 °C.

Image removed from electronic copy due to copyright issues

Figure 2.14. The effect of temperature on pH oscillations in the PCPOC reaction found by Novakovic *et al.*^{[134]††}

Novakovic *et al* also documented that the presence or absence of oscillations affected the selectivity of the reaction.^[2] They noted that in a non-oscillatory regime the main products were Z-isomer, methyl (E)-cinnamate (MeCin) and methyl atropate (MeAt). In contrast, when the experiment was conducted in an oscillatory regime Z-isomer was the major product with only trace amounts of methyl atropate detected. What has not been considered is how these two effects combine i.e. how the dynamics of product formation are affected when the reaction is conducted at different temperatures in oscillatory mode.

The scope for work on this reaction is vast. This thesis will initially focus on understanding the behaviour of the reaction and work towards producing a model which accounts for the observed behaviour. To do this an extensive experimental study is needed to gain an insight into the behaviour of all of the species in this system to determine the reaction mechanism. As this system is complex consisting of 7 species, two of which are gases, the methodology that will be used here is a combination of two approaches. The first is based on that followed by Field, Korös and Noyes when they were developing the FKN mechanism of the BZ reaction. It

†† Adapted from Novakovic, K., Mukherjee, A., Willis, M.J., Wright, A.R. and Scott, S.K. (2009) '[The influence of reaction temperature on the oscillatory behaviour in the palladium-catalysed phenylacetylene oxidative carbonylation reaction.](#)', *Physical Chemistry Chemical Physics*, 9044-9049, with permission of the PCCP Owner Societies.

involves breaking the system down into smaller subsystems for study. This will allow the interactions of the components of the catalyst system to be better understood. Combining this with information gathered as additional components are included along with information from the behaviour of the full reaction will help to elucidate the reaction network responsible for the oscillatory behaviour in the PCPOC reaction.^[26]

The second follows a process summarised by Epstein and Pojman as a series of steps to construct a mechanism for a complex reaction system.^[26] The steps are:

1. Gather relevant experimental data.
2. Identify the stoichiometry of the overall reaction and the main component processes.
3. List the plausible species involved in the reaction – reactants, products and intermediates.
4. Gather thermodynamic data on the species.
5. Consider the possible elementary steps that make up the main processes of the reaction and gather relevant kinetic data for those steps.
6. Use known rate constants and estimate unknowns
7. Combine the thermodynamically plausible steps with kinetic data to produce a tentative mechanism to describe the qualitative behaviour of the system.
8. Use numerical methods to simulate the experimental results.
9. Test the mechanism against new experimental data and continually refine and improve it.

As this study into the PCPOC reaction is in its early stages step 1 is the main focus of this work.

Chapter 3. Aims and Objectives

3.1 Overview

To understand the processes responsible for the occurrence of oscillations in pH and reaction heat (Q_r) in the PCPOC reaction an in depth understanding of the reaction network is required. This understanding can only be gained through an extensive experimental study of the system. This chapter describes the aims and objectives of the experiments conducted in this study of the PCPOC reaction.

3.2 Aim

The aim of this thesis is to determine the main features of the reaction network that are responsible for producing oscillations in pH and reaction heat (Q_r) in the PCPOC reaction system. The PCPOC reaction is a complex reaction involving 7 species (PhAc, CO, MeOH, PdI_2 , KI, O_2 and NaOAc). Uncovering the reaction network underlying the oscillations in pH and Q_r is, therefore, a complex task. The experimental study designed to complete this task consists of two approaches: a top-down approach investigating the behaviour of the reaction system as a whole under different conditions e.g. different reaction temperatures, reagent concentrations; and a bottom-up approach which divides the reaction system into a series of subsystems to be studied separately. The information gained from the results of both of these approaches will be combined to produce initial models for the reaction network responsible for oscillations.

3.3 Objectives

In order to determine the underlying reactions responsible for the oscillations in pH and Q_r a number of objectives have been identified:

- *Objective 1* is to establish the reproducibility of the experiments conducted by Novakovic and colleagues and extend those experiments. The top-down approach, involving all components of the PCPOC system, will be used to achieve this based on the previous experiments conducted by Novakovic *et al.*^[2, 3, 134] The experiments will be conducted on a large scale (450 mL) using a reaction calorimeter following the experimental procedure reported to achieve oscillatory behaviour to allow direct comparison of the new results with those collected previously.^[134] The previous experiments focused on the

effect of reaction temperature on the pH behaviour of the PCPOC reaction. Those experiments will be repeated however the temperature range will be extended down to 0 °C to see if the observed trends continue as the temperature is reduced further.

- *Objective 2* is to monitor the turbidity (a measure of clarity of the solution due to suspended particles) of the reaction mixture continuously to gain possible insights into the behaviour of the catalyst during the reaction.
- *Objective 3* is to follow product formation in the reaction system. Previous experiments did not follow the product formation during the reaction so it is not known if product formation is affected by changes in reaction temperature. Product formation will, therefore, be followed by taking samples of the reaction mixture throughout the experiments at 0-40 °C and analysing them by GCMS.
- *Objective 4* is to look into how increasing the concentration of water affects the system. Malashkevich and colleagues mentioned adding 2 mmol of water to their reaction mixture to maintain the water level in the reaction mixture constant at approximately 0.2 molL⁻¹.^[5] The reason for this is not clear and further studies of how an increased concentration of water in the system affects pH behaviour and products are considered beneficial.
- *Objective 5* is to establish baseline parameters for the components of the catalyst system, in particular the solubility of PdI₂. Novakovic and colleagues noted that the granularity of PdI₂ may have affected the pH behaviour in the PCPOC reaction preventing them from reproducing the two sets of pH oscillations they had originally obtained at 40 °C. They observed that using a finely powdered form of PdI₂ the pH changed from 3.6-0.35 but did not oscillate.^[3] This would suggest that the PdI₂ does not dissolve readily at the start of the experiment. A series of small-scale experiments to determine the solubility of PdI₂ in methanol and methanolic KI and how it affects pH behaviour in the PCPOC reaction will therefore be conducted.
- *Objective 6* is to discover which reactions of the catalyst system are responsible for which aspects of the observed pH behaviour in the full PCPOC reaction system. This will be achieved by using the bottom-up approach. The PCPOC reaction will be broken down into a series of subsystems for

investigation using small-scale experiments (25-250 mL) in which pH and temperature will be monitored. The experiments will focus on the reactions of the catalyst system ($\text{PdI}_2/\text{KI}/\text{MeOH}$) with CO.

- *Objective 7* is to use the experimental information obtained from the experiments on the catalyst system in combination with the kinetic fitting and simulation software BatchCAD to produce a tentative model of the reactions of the catalyst system with CO. This will involve identifying from the literature possible reactions between combinations of PdI_2 , KI, MeOH and CO and seeing which reactions fit the experimental observations.
- *Objective 8* is to determine the effect combining PhAc with the $\text{PdI}_2/\text{KI}/\text{MeOH}$ subsystem has on pH behaviour when the system is purged with CO. This will help to determine if the reaction between the catalyst system and PhAc plays a role in the observed pH oscillations. These experiments will also be conducted on a small scale. As PhAc carbonylation can produce a number of products depending on reaction conditions, product formation will be monitored during these experiments to help determine which product-forming reactions are linked to oscillatory pH behaviour.
- *Objective 9* is to improve the model produced in Objective 7 to include PhAc using the experimental data obtained from Objective 8. Again this will be accomplished with the aid of the BatchCAD kinetic fitting and simulation package. The intention is to produce a model that will not only simulate the pH behaviour of the small-scale experiments on the catalyst subsystem but will also account for the observed product formation when PhAc is added.
- *Objective 10* of the work in this thesis is to perform exploratory studies into the gas-liquid mass transfer limitations of the PCPOC reaction. Mass transfer limitations were noted by Novakovic and colleagues when they found that reducing the stirrer speed in the large-scale experiments on the full PCPOC reaction system produced changes in the oscillatory pH behaviour.^[3] They found that reducing the agitation speed from 550 rpm to 400 rpm in otherwise identical experiments produced fewer oscillations. This is in contrast to the work by Malashkevich and colleagues who found that changing the stirring speed from 300 to 600 rpm had no effect on the magnitude, period or shape of

the oscillations.^[5] These contrasting findings may be due to the differences in scale of the two studies. In an effort to gain insight into any gas-liquid mass transfer limitations experiments will be conducted on a small scale (50 mL) using the same conditions as in the experiments in Objective 8 but the reaction mixture will be purged with CO at flow rates of 5-15 mLmin⁻¹. Further experiments will be conducted using the Automate high pressure reactor at higher pressure (approx. 5 bar) at low and high stirring speeds. Monitoring PhAc during both sets of experiments should highlight any differences in gas-liquid mass transfer.

3.4 Summary of Objectives

1. Reproduce and extend the previous work by Novakovic and colleagues;^[3, 134]
2. Monitor the turbidity of the full PCPOC reaction system;
3. Follow product formation in the full PCPOC reaction system;
4. Consider the effect increased concentration of water has on the system;
5. Establish baseline parameters for the main components of the catalyst system e.g. PdI₂ solubility;
6. Establish which components react resulting in changes in pH when PhAc is absent from the reaction mixture;
7. Use the experimental data from Objective 6 to produce a tentative model to account for the observed pH behaviour;
8. Establish the effect on pH of adding PhAc to subsystems identified in Objective 6;
9. Extend the model from Objective 7 to include PhAc using the experimental data obtained from Objective 8;
10. Investigate mass-transfer limitations of the PCPOC reaction.

Chapter 4. Experimental Study

4.1 Overview

To achieve the objectives outlined in Chapter 3 requires an extensive experimental study. The equipment and experimental methods used to conduct the experimental study are described in this chapter. The experiments are divided into two sections: large scale experiments on the full PCPOC reaction system and small scale experiments on subsystems of the PCPOC reaction system.

4.2 Equipment

The equipment used to conduct the experiments were an HEL MicroNOTE system, a HEL Simular reaction calorimeter, an HEL Automate high pressure reactor and a parallel reactor system. A Varian Saturn 2200 GCMS was used for sample analysis. This section describes each of these pieces of equipment.

4.2.1 HEL MicroNOTE

HEL MicroNOTE (Figure 4.1) is a data logging system that can be used to record pH and temperature over prolonged periods of time. The system is customisable allowing additional equipment such as circulators, stirrers and dosing pumps to be added as necessary.

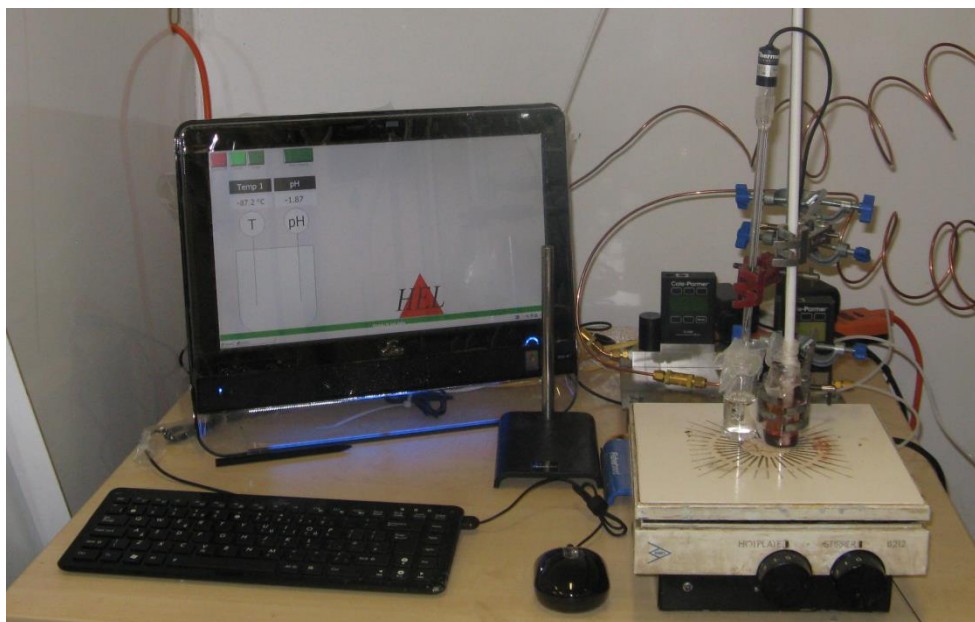


Figure 4.1. The HEL MicroNOTE system used in small-scale experiments on the PCPOC reaction.

The system used for this study consists of a touchscreen PC with HEL WinISO data logging software installed, connected to a Pt100 temperature probe and a combined pH electrode. Stirring is currently provided by a Bibby B212 magnetic stirrer/hotplate. This is an inefficient method of stirring but the presence of the pH electrode and Pt100 temperature probe in the reactor act as baffles which help to improve mixing in the reactor. The main components of the system are shown in Figure 4.2.

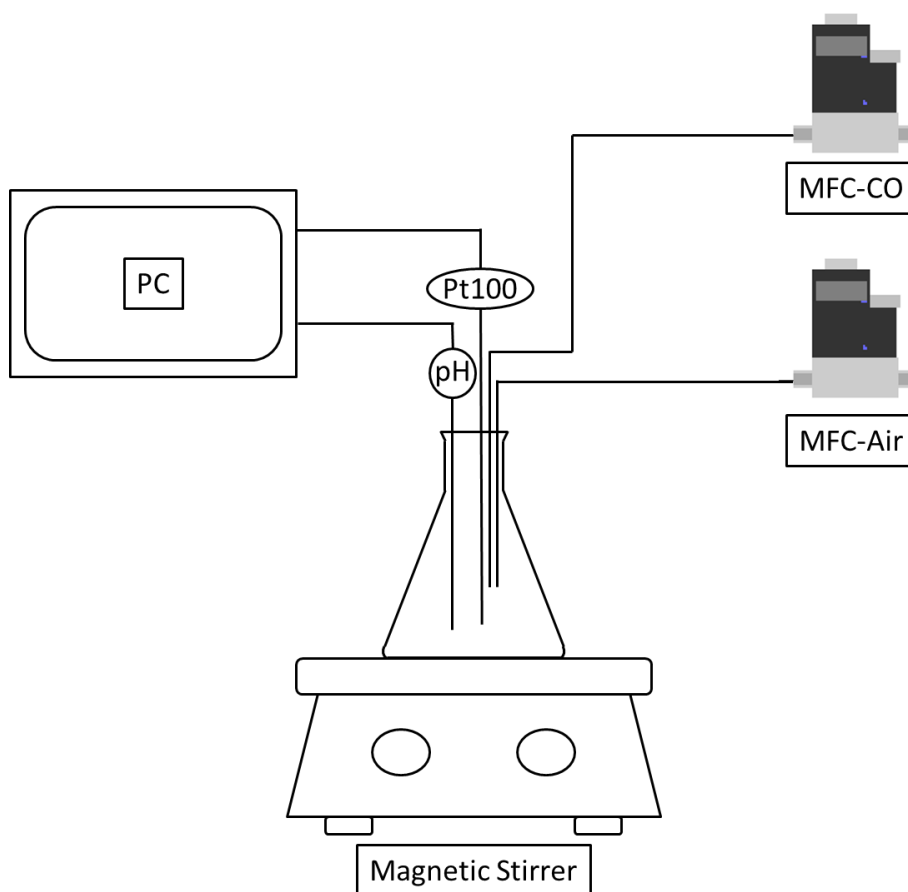


Figure 4.2. Diagram of the main features of the HEL MicroNOTE system used for small scale experiments on the PCPOC reaction.

The HEL MicroNOTE system is used in conjunction with two Cole-Parmer 16 Series mass flow controllers (MFCs) which are calibrated for use with any one of 29 different gases/gas mixtures: air; argon; methane; carbon monoxide; carbon dioxide; ethane; hydrogen; helium; nitrogen; nitrous oxide; neon; oxygen; propane; normal-butane; acetylene; ethylene; iso-butane; krypton; xenon; sulphur hexafluoride; 75% argon/25% carbon dioxide; 90% argon/10% carbon dioxide; 92% argon/8% carbon dioxide; 98% argon/2% carbon dioxide; 75% carbon dioxide/25% argon; 75% argon/25% helium; 75% helium/25% argon; 90% helium/7.5% argon/2.5% carbon dioxide; 90% argon/8% carbon dioxide/2% oxygen; 95% argon/5% methane; The mass flow controllers offer

flow rates of 2-200 mLmin⁻¹. One mass flow controller is currently used specifically for controlling CO flow whilst the other controls the flow of air to the reaction vessel. PTFE tubing with an internal diameter of 1.58 mm and outer diameter of 3.18 mm delivers the gases to the reaction vessel without the aid of a sparger. The reaction vessel can be any suitable vessel depending on the requirements of the experiment being conducted. These include 25 mL vials, conical flasks (100-250 mL) and a 100 mL jacketed reactor that was produced in-house to allow improved temperature control (Figure 4.3).

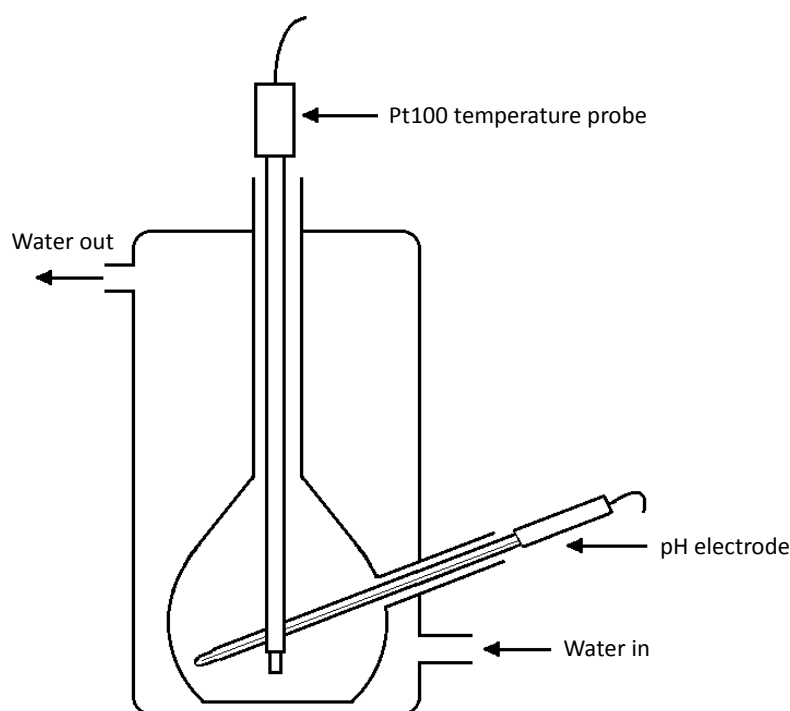


Figure 4.3. Jacketed reactor used with HEL MicroNOTE and a magnetic stirrer (Bibby B212 magnetic stirrer/hotplate) for small scale PCPOC experiments.

4.2.2 *HEL Simular*

The HEL Simular (Figure 4.4) is a reaction calorimeter that has the ability to record heat flow data whilst performing chemical reactions. It consists of a 1 L double-jacketed glass reactor. The outer jacket is a vacuum jacket and the inner jacket is an oil jacket. Reactor temperature is monitored by a Pt100 temperature probe while internal heating is provided by a 150 W internal heater. The oil jacket temperature is controlled by a Julabo FP50-HD circulator with a working temperature range of -50-200 °C. The reactor is fitted with a Russell combined pH electrode which has the reference electrode and measuring electrode combined in a single unit. There is also an HEL turbidity probe which measures relative turbidity by reflectance. The reactor

has a Brooks Smart series 5850S mass flow controller which can dose gases with flow rates from 0.003-30 Lmin⁻¹. This is currently used to dose CO which is delivered to the reactor via PTFE tubing with an internal diameter of 1.58 mm and outer diameter of 3.18 mm without the aid of a sparger. There is an independent Cole-Parmer 16 Series mass flow controller which is calibrated for use with any one of 29 different gases (as listed in Section 4.2.1) with flow rates ranging from 5–500 mLmin⁻¹. This is currently used to control air flow with the air being delivered to the reactor using Tygon 2075 tubing with an internal diameter of 4.8 mm and outer diameter of 7.9 mm also without the aid of a sparger. A Gala 1601 ProMinent gamma/ L Solenoid Dosing pump allows liquids to be automatically added to the reactor. It is a diaphragm pump which can dose liquids at a maximum rate of 1.1 Lh⁻¹ at a 100% stroke rate. The feed for the pump sits on an Oxford F series top pan balance and liquids are dosed by weight. The reactor also has a Harvard Pump 11 single syringe pump fitted with a 50 mL syringe allowing the dosing of liquids with flow rates from 0.0973–1576 mLh⁻¹. The syringe pump doses liquids by volume and allows more accurate dosing of small volumes of liquid. There is a solid dosing unit which sits on another Oxford F series top pan balance allowing the automatic addition of solid reagents to the reactor by weight. The HEL Simular also has the facility to be programmed to take up to 999 samples automatically using an automatic sampling unit although only 6 samples can be taken before the sample vials need to be emptied. The installed WinISO software allows the HEL Simular to run completely unaided once it is set up. All data are automatically saved via the data logging software. The data can then be viewed later in the proprietary HEL IQ software or can be transferred to other software e.g. Windows Excel for analysis. The main components of the HEL Simular setup used to study the PCPOC reaction are shown in Figure 4.5.

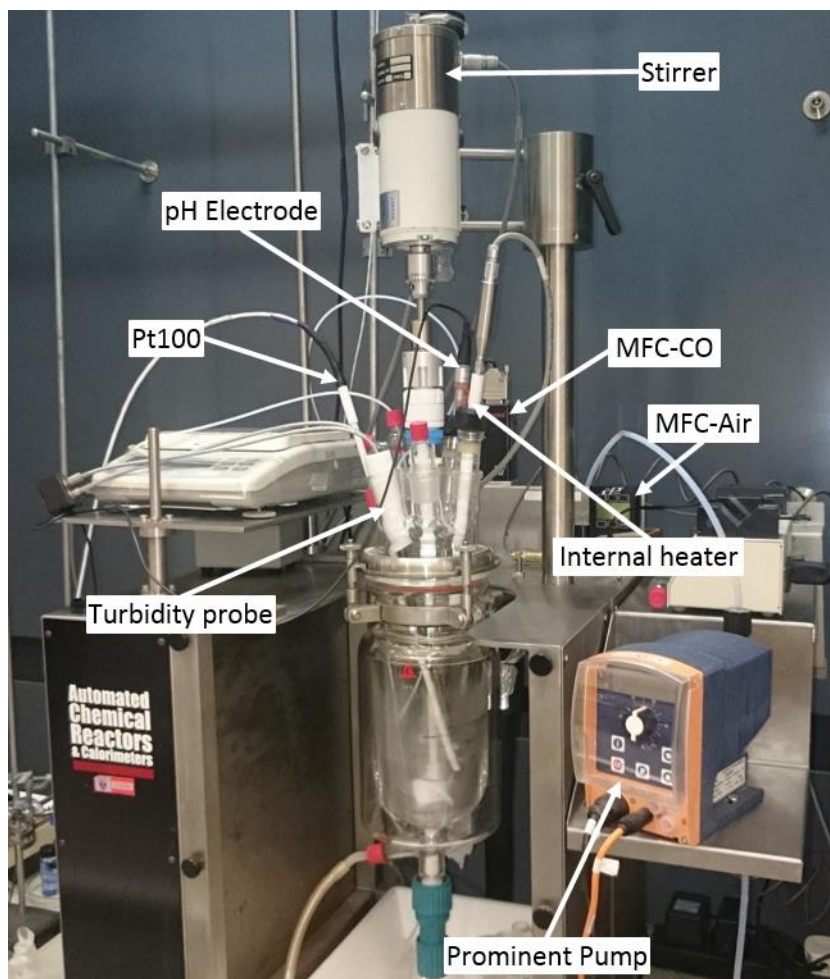


Figure 4.4. The HEL Simular used for large-scale experiments on the PCPOC reaction.

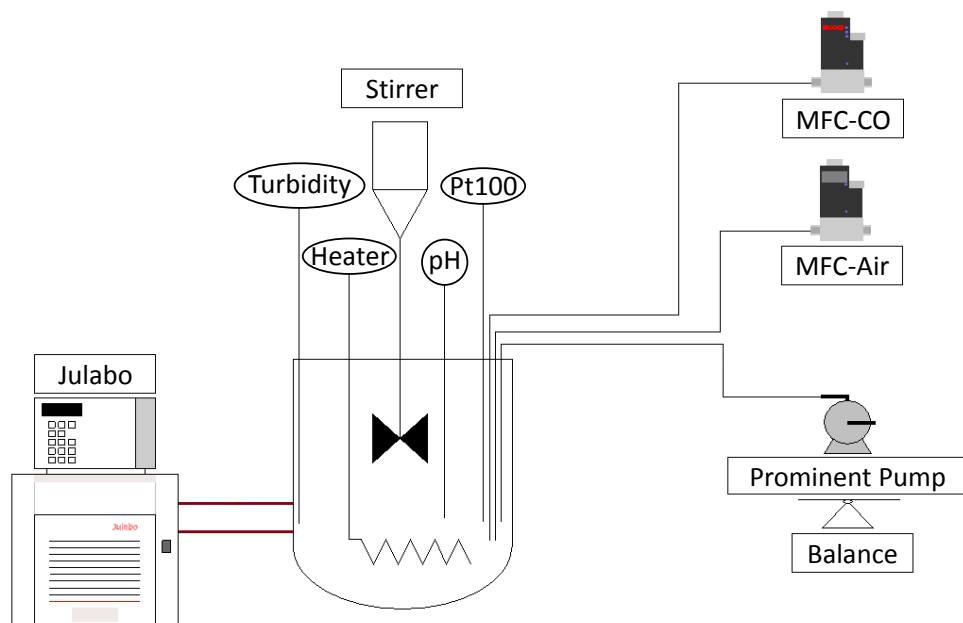


Figure 4.5. Diagram of the main features of the HEL Simular equipment setup used in the experiments on the full PCPOC reaction.

The HEL Simular reaction calorimeter can be used as a standard laboratory reactor or it can be run in several different modes to obtain calorimetry data depending on requirements.

Calorimetry is the measurement of energy changes that occur during physical or chemical processes, for example when a substance dissolves in solution, when chemicals react or when substances change state e.g. ice melting. In its simplest form calorimetry can be performed using a lidded vessel with a thermometer to measure any change in temperature during a process. Dedicated reaction calorimeters allow precise control of reaction temperatures whilst measuring other parameters to produce calorimetry data on chemical reactions by performing a heat balance on the reactor. The HEL Simular reaction calorimeter can perform heat balance, heat flow and power compensation calorimetry.

Heat Balance Calorimetry: the reactor temperature is controlled by the temperature of the oil in the oil jacket of the reactor. The technique uses low oil flow rates. As the temperature in the reactor changes during the course of a reaction the inlet temperature of the oil is changed accordingly to maintain approximately isothermal conditions within the reactor. The change in oil temperature therefore reflects the heat absorbed/released by the reaction (Q_r) according to Equation (4.1) where m_{oil} is the mass flow rate of oil through the reactor jacket and $C_{p(oil)}$ is the specific heat capacity of the oil. This relationship only applies to isothermal conditions.

$$Q_r = m_{oil} \cdot C_{p(oil)} \cdot \Delta T_{oil} \quad (4.1)$$

From Equation (4.1) it is evident that it is not necessary to know the heat transfer characteristics of the reactor in heat balance calorimetry. It is, however, necessary to perform calibration steps prior to the onset of the reaction and once the reaction is complete to determine the heat capacity of the oil. Heat balance calorimetry can also be performed under non-isothermal conditions but this requires an accumulation term to be added to Equation (4.1).

Heat Flow Calorimetry: the principles behind heat flow calorimetry are similar to those used in heat balance calorimetry. Again the reactor temperature is controlled by the oil jacket temperature. However, high oil flow rates are used to maintain a uniform oil jacket temperature. In this instance, the change in Q_r is related to the difference

between the oil jacket temperature, T_j , and the reaction temperature, T_r , by Equation (4.2) under isothermal conditions.

$$Q_r = UA_{ht}(T_r - T_j) \quad (4.2)$$

In Equation (4.2) U = heat transfer coefficient ($Wm^{-2}K^{-1}$) and A_{ht} = heat transfer area (m^2). The parameter UA_{ht} needs to be determined by experiment, hence, as with heat balance calorimetry, heat flow calorimetry requires additional calibration steps to ultimately determine Q_r . Heat flow calorimetry is best suited to situations in which the heat transfer coefficient and heat transfer area do not change during the course of the reaction.

Power Compensation Calorimetry: in power compensation calorimetry a constant reactor temperature is maintained by an internal electrical heater (compensation heater) that is situated in the reactor. The oil jacket temperature is maintained constant at a lower temperature than the required reaction temperature. The temperature difference between the oil jacket and the required reaction temperature (the compensation drop) is determined by the expected reaction exotherm of the reaction being studied. The internal heater supplies heat to the reactor to bring the reactor contents to the required reaction temperature. Under isothermal conditions when no reaction is occurring inside the reactor a continuous and constant input of power to the heater is supplied. When the reaction occurs, the power to the internal heater is increased or decreased as necessary to maintain a constant reactor temperature. The change in the power delivered to the internal heater is therefore a direct measure of the reaction heat via the relationship in Equation (4.3) where P_0 is the baseline heater power and P_t is the heater power at time t .

$$Q_r = P_t - P_0 \quad (4.3)$$

As a result, calibration steps are not required and so experiments are shorter. There is also the advantage that the response of the internal heater to changes in the reaction temperature are rapid compared to the response of the circulating oil used to perform heat balance and heat flow calorimetry. For these reasons power compensation calorimetry was used in the study of the full PCPOC reaction in this work.

4.2.3 *HEL Automate*

The HEL Automate, Figure 4.6, was used to conduct all experiments requiring increased CO pressure. It comprises of a 100 mL Parr series 4560 fixed head reactor made from T316 stainless steel. The reactor has a flat, PTFE gasket which fits into a recess in the reactor head. This provides a good seal once the accompanying splitting cover clamp fitted with six cap screws is put in place and the screws are tightened. Stirring is provided by a Parr AC1120HC6 magnetic stirrer drive attached to a 1.38 in, four-blade impeller which is fitted to the reactor allowing stirring speeds up to 1200 rpm. The reactor is fitted with a gas inlet valve and a liquid sampling unit. Liquid dosing is provided by a Knauer Wellchrom K-120 HPLC pump fitted with a 10 mL pump head. Heating is provided by a 400 W external heating mantle which enables reactor temperatures up to 320 °C to be achieved if the reactor is well-insulated. The mantle temperature is monitored by a Type J thermocouple. Reactor temperature is also measured using a Type J thermocouple which sits inside a protective well in the reactor to protect it from physical damage and corrosion. The reactor is fitted with an analogue pressure gauge (0-140 bar) and a Gems Sensors and Controls 2200 series pressure transducer (0-250 bar). The equipment uses HEL's WinISO software for data-logging and control. The main features of the Automate are shown in Figure 4.7.

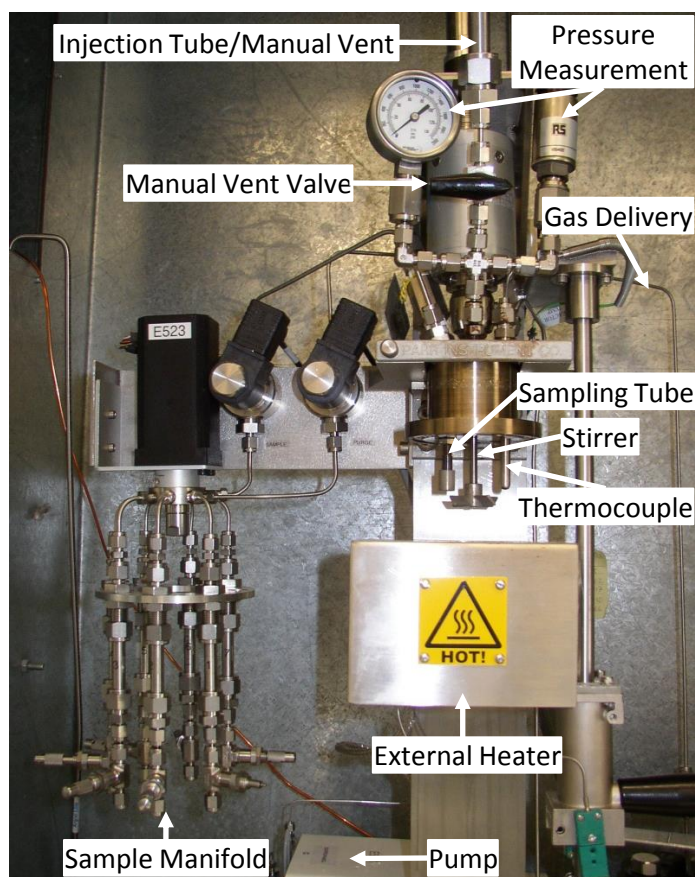


Figure 4.6. The HEL Automate used for experiments on the PCPOC reaction at increased pressure.

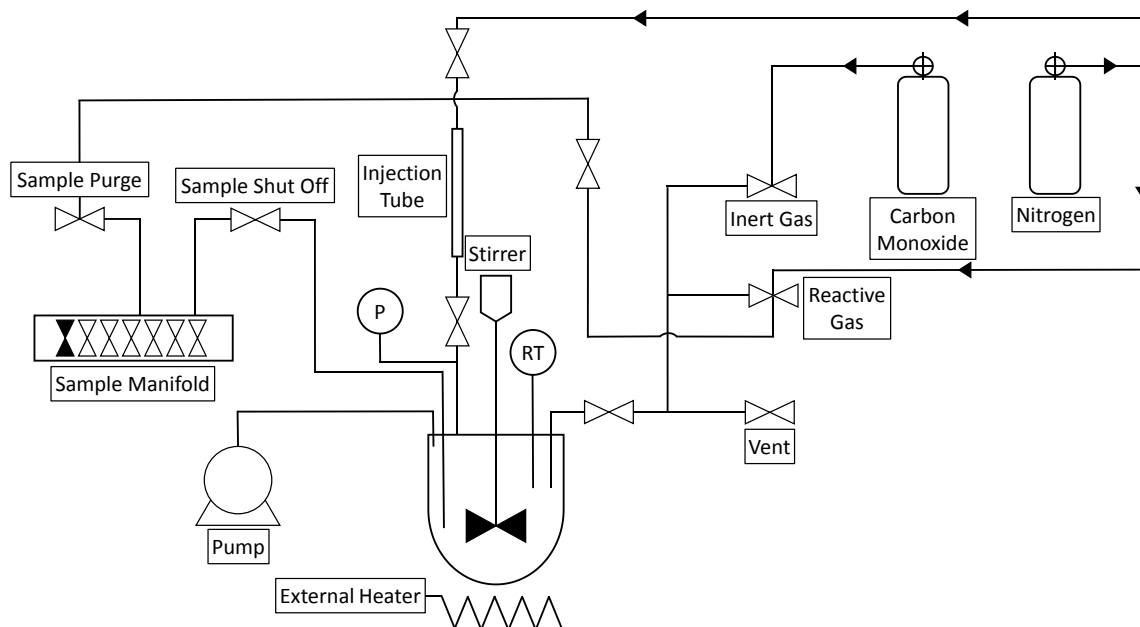


Figure 4.7. Diagram showing the main features of the HEL Automate.

4.2.4 Parallel Reaction System

A parallel reaction system was created which allows pH and temperature to be recorded in up to 6 reactors simultaneously (see Figure 4.8). The system consists of

an EA Instruments 6-channel pH and temperature monitoring unit connected to a laptop for datalogging. The unit is fitted with six Pt100 temperature probes and 6 Hanna Instruments HI-1331B glass combination pH electrodes. Twelve Omega FMA-2600 Series mass flow controllers which are calibrated for use with any one of 29 different gases/gas mixtures, similar to those used with the HEL MicroNOTE system (see Section 4.2.1), deliver gases - 6 MFCs deliver CO, 6 MFCs deliver air. The MFCs offer flow rates of up to 100 mLmin⁻¹. PTFE tubing with an internal diameter of 1.58 mm and outer diameter of 3.18 mm delivers the gases to the reaction vessel without the aid of spargers. Conical flasks (100 mL) are used as the reaction vessels. The flasks are placed in a Clifton NE4-22HT circulating water bath fitted with a Nickel-Electro DC2-300 immersion dip cooler allowing temperatures of 5-99 °C to be achieved. The contents of the flasks are stirred using a 2mag MIXdrive 15 HT multi-position stirrer submerged in the water bath. The stirrer is connected to a control unit which offers stirring speeds from 100-1600 rpm.

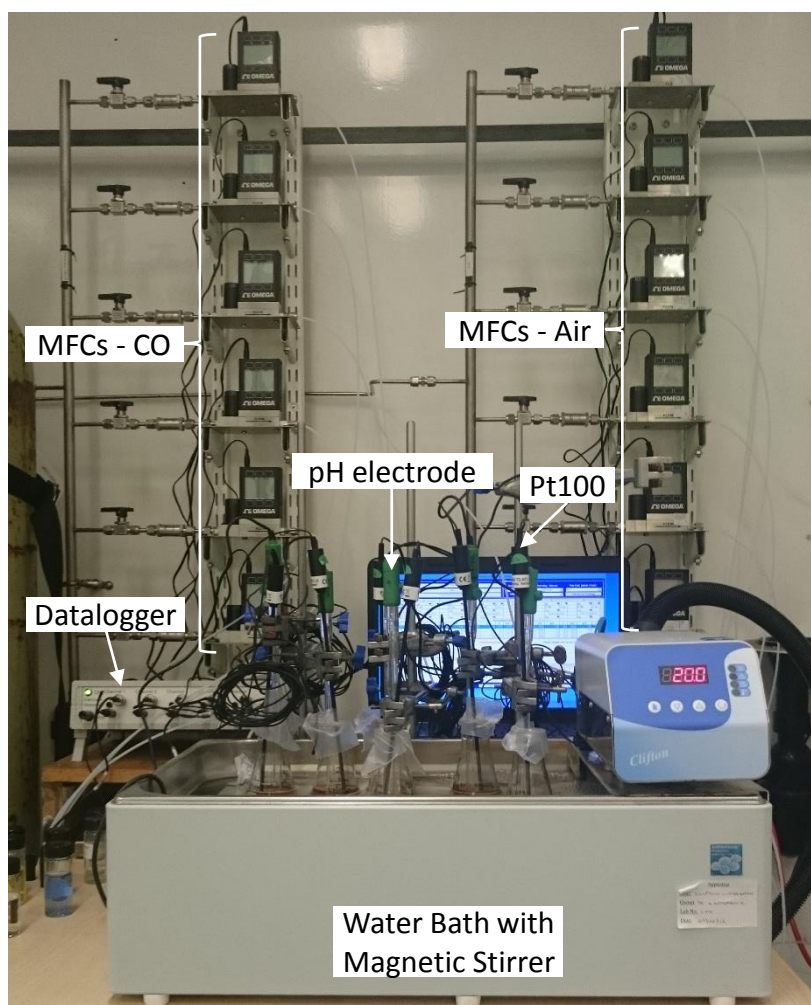


Figure 4.8. Parallel reaction system used in small-scale experiments.

4.2.5 Varian GCMS

GC analysis was carried out using a Varian Saturn 2200 GCMS fitted with a Varian VF-5ms capillary column (30 m x 0.25 mm, 0.25 μm) and a CombiPAL autosampler. Unless otherwise stated the GC method used for all analysis consisted of: a 1 μL split injection; injector temperature 150 $^{\circ}\text{C}$; split ratio 20; helium carrier gas flow rate 1 mLmin^{-1} ; initial oven temperature 100 $^{\circ}\text{C}$ and then as set out in Table 4.1.

Table 4.1. GC oven method used for the analysis of samples from the PCPOC reaction.

Temp ($^{\circ}\text{C}$)	Rate ($^{\circ}\text{C/min}$)	Hold (min)	Total (min)
100		3.00	3.00
120	20	5.00	9.00
140	20	5.00	15.00
160	30	5.00	20.67
180	20	5.00	26.67
195	20	5.00	35.42

Details of the preparation of calibration samples and examples of calibration curves are given in Appendix B.

4.2.6 Filtration

For experiments using filtered catalyst solution, the catalyst solution was prepared and then filtered under vacuum using a vacuum filtration apparatus from Sigma-Aldrich (Figure 4.9). The filtration unit was used in conjunction with a 47 mm Millipore Fluoropore PTFE membrane filter with a pore size of 0.02 μm .

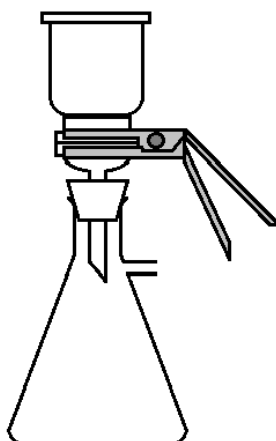


Figure 4.9. Sigma-Aldrich vacuum filtration apparatus.

When required, samples of the PCPOC reaction mixture were filtered over silica using filters as shown in Figure 4.10. The silica filter was prepared by placing a small piece of cotton wool into a 150 mm glass Pasteur pipette and adding Silica 60A to an approximate depth of 2 cm. The top of the pipette was then filled with the solution to be filtered. Compressed air was used to gently push the solution through the bed of silica. The resulting filtrate was collected in a vial for subsequent GCMS analysis.

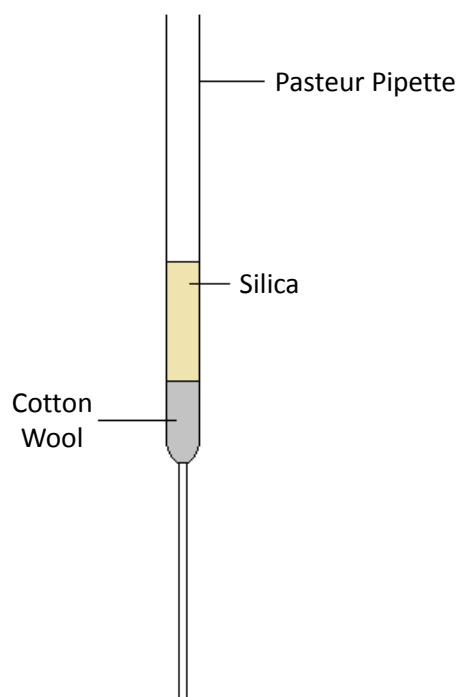


Figure 4.10. Silica filters for filtration of PCPOC samples prior to GCMS analysis.

4.2.7 Chemicals

Palladium(II) iodide (PdI_2), phenylacetylene (PhAc), potassium iodide (KI), Chromasolv[®] HPLC grade (99.9%, <0.03% H_2O content) methanol, sodium acetate (NaOAc), naphthalene (Np), phenylmaleic acid (PhMAc), phenylmaleic anhydride (PhMAAn), methyl cinnamate (MeCin) and 3 Å molecular sieves were purchased from Sigma-Aldrich. Cylinders of air, CP (chemically pure) grade carbon monoxide (CO) and oxygen-free nitrogen (N_2) were purchased from BOC.

The pH electrodes from each piece of equipment were calibrated before each experiment with aqueous pH buffers purchased from Fisher Scientific: pH 2 (glycine), pH 7 (phosphate) and pH 10 (borate). Silica 60A, particle size 60-200 micron, used in the preparation of the filters for sample filtration was also purchased from Fisher Scientific.

4.3 Experimental Studies of the Full PCPOC System

Experimental studies of the full PCPOC reaction in which all reaction components were present investigated two scenarios: 1) the effect of temperature; 2) the effect of increased water concentration; on the oscillatory behaviour of the PCPOC reaction.

4.3.1 Effect of Temperature

The period and amplitude of oscillations in the PCPOC reaction have been shown to be temperature dependent when the reaction temperature is varied from 10-40 °C – lower temperatures produce oscillations with a larger period and amplitude.^[134] However, the accompanying effect on PhAc consumption and product formation has not been investigated. To see how PhAc consumption and product distribution are affected by changing the reaction temperature a study of the PCPOC reaction in oscillatory mode over the temperature range 0-40 °C was conducted using the HEL Simular reaction calorimeter (Section 4.2.2) to precisely control the reaction temperature.

Initial experiments followed the procedure used by Novakovic *et al* with reaction temperatures of 10 °C and 20 °C.^[134] The experimental procedure and pH results of these experiments are in Appendix A. The change in reaction temperature from 10 °C to 20 °C affected the rate of methanol evaporation during the experiment which impacted on the molar concentrations of reactants and products in the reaction vessel. This meant a direct comparison of reactant and product concentrations between experiments was not possible. Using a standard inside the reactor during the reaction would solve this problem. Naphthalene (Np) had already been selected as a good internal standard for the GCMS analysis as it has a phenyl group and, under the GCMS analysis conditions used, is well resolved from all product and reactant peaks. A small scale test experiment was conducted to assess naphthalene as a suitable candidate to be used inside the reactor i.e. to ensure that it did not interfere with the reaction (see Appendix A).

Once naphthalene was proven to be a suitable internal standard the experiments at 10 and 20 °C were repeated with Np in the reaction mixture and additional experiments at 0, 30 and 40 °C were conducted. The updated procedure was as follows: methanol (400 mL) was added to the HEL Simular reactor and heated to the required reaction temperature (0-40 °C) while stirring at 250 rpm after which the palladium(II) iodide (434 mg) was added. After stirring at 250 rpm for 35 min, 113 mg

of NaOAc and 37.392 g of KI were added along with 30 mL of methanol to wash down any solid remaining on the reactor walls. The stirrer speed was increased to 350 rpm to aid the dissolution of the KI. After a further 10 min, 1.154 g of Np was added followed by 20 mL of methanol. Five minutes after adding Np the stirrer speed was returned to 250 rpm and purging with CO (50 mLmin^{-1}) and air (50 mLmin^{-1}) commenced. Phenylacetylene (6.2 mL) was added to the reactor 20 min after purging began. Temperature, pH and turbidity were monitored throughout and additional methanol was added as necessary to compensate for evaporative loss of the solvent. An initial sample was taken 2-3 min after PhAc was added and further samples were taken periodically throughout the reaction. All samples were filtered over silica (as in Section 4.2.6) and diluted 1:9 with methanol before analysis by GCMS.

4.3.2 Effect of Increased Water Concentration

During the experiments in Section 4.3.1 it was observed that the addition of HPLC grade methanol to the PCPOC reaction during oscillations caused the period and amplitude of the oscillations to increase. It was also observed that the addition of HPLC grade methanol to the PCPOC reaction mixture prior to the onset of pH oscillations could initiate oscillatory behaviour. Perturbation studies by Mukherjee^[135] found that the addition of HPLC grade methanol to the PCPOC reaction system when large sustained oscillations were present caused a slight increase in the period of the oscillations. However, when anhydrous methanol was used as both reactant and solvent the PCPOC reaction did not exhibit any meaningful pH oscillations. These observations suggest that the $<0.03\%$ water in the HPLC grade methanol used in the experiments can affect the oscillations. The experiments in this section were conducted to investigate these observations by increasing the amount of water in the PCPOC reaction system and assessing how the pH oscillations and product distribution of the PCPOC reaction were affected. Experiments were conducted using the HEL Simular reaction calorimeter (Section 4.2.2) at a reaction temperature of 30°C with deionised water concentrations of 0, 5, 10, 20, 30 and 40% by volume. The solvent (400 mL of the required composition of methanol and deionised water) was added to the HEL Simular reactor and heated to 30°C while stirring at 250 rpm. The palladium(II) iodide (434 mg) was then added. After stirring at 250 rpm for 35 min, 114 mg of NaOAc and 37.392 g of KI were added along with 30 mL of the required methanol/water mixture to wash any solids remaining on the reactor walls

into solution. The stirrer speed was increased to 350 rpm to aid the dissolution of the KI. After 10 min, 1.154 g of naphthalene was added followed by a further 20 mL of solvent of the required methanol/water composition. Five minutes after adding the naphthalene the stirrer speed was returned to 250 rpm and purging with CO (50 mLmin⁻¹) and air (50 mLmin⁻¹) commenced. Phenylacetylene (6.2 mL) was added 20 min after purging with CO and air began. Temperature and pH were monitored throughout and additional solvent of the required methanol/water composition was added as necessary to compensate for evaporative loss of the solvent. An initial sample was taken 2-3 min after PhAc was added and further samples were taken periodically throughout the reaction. All samples were filtered over silica, as in Section 4.2.6, and diluted (200 μ L of sample, 1800 μ L methanol) before analysis by GCMS.

4.4 Preliminary Subsystems Experiments

In order to understand the underlying processes responsible for the oscillatory pH behaviour in the PCPOC system including the observations from Section 4.3, the full PCPOC reaction was reduced to a number of subsystems to be studied individually to uncover the behaviour and reactions of the various components in the system. Initial experiments were performed to establish baseline pH measurements of the catalyst components as well as conducting preliminary investigations on the catalyst system concentrating on three areas:

- the solubility of catalyst components;
- the reaction of the catalytic system with CO;
- the role of water in the catalytic system.

4.4.1 pH of Methanol

The baseline pH of the HPLC grade methanol used in all experiments was established by placing a 500 mL conical flask containing 250 mL of the aforementioned methanol on a stirrer/hotplate. The pH electrode from the HEL Simular system was calibrated using aqueous buffers (pH 2 and 10) and placed in the flask along with the Pt100 temperature probe. The top of the flask was closed using blue roll and the flask contents were set to stir for over 24 h, monitoring pH and temperature throughout.

4.4.2 Solubility of Catalyst Components

The experiments in this section investigated the solubility of the catalyst components PdI_2 and KI in methanol. The following five experiments were conducted:

- Experiment 1: solubility of PdI_2 in MeOH;
- Experiment 2: solubility of KI in MeOH;
- Experiment 3: solubility of PdI_2 in methanolic KI;
- Experiment 4: detailed study of the solubility of PdI_2 in methanolic KI;
- Experiment 5: extended study of the solubility of PdI_2 in methanolic KI.

Experiment 1: The solubility of PdI_2 was studied first. An experiment was set up using a 250 mL conical flask containing 150 mL of HPLC grade methanol and 8 mg of PdI_2 at room temperature. The mixture was placed on a magnetic stirrer/hotplate and was stirred at room temperature (21.4°C) while being visually inspected at regular intervals to see if the PdI_2 had dissolved. The pH electrode and Pt100 temperature probe from the HEL Simular (Figure 4.4) were used to record pH and solution temperature. After 70 min the PdI_2 did not appear to be dissolving at room temperature so the hotplate was switched on and the flask was heated to try to increase the solubility of PdI_2 . The temperature was gradually increased over a period of 3 h until the methanol began to boil while continuing to visually inspect the flask to see if the PdI_2 had dissolved.

Experiment 2: The solubility of KI in methanol is reported to be 1 g in 7.4 mL of methanol at 25°C .^[136] This was tested by adding 6.233 g of KI to 50 mL of methanol in a 100 mL conical flask, sealing it with parafilm and leaving it to stir overnight at room temperature (21.4°C). The solubility was assessed visually by inspecting the flask to ensure all the KI had dissolved. This gives a maximum concentration of $7.51 \times 10^{-1} \text{ mol dm}^{-3}$ KI in methanol at a temperature of 21.4°C .

Experiment 3: The solubility of PdI_2 in methanolic KI solution was studied by adding a known amount of PdI_2 to a prepared solution of KI in methanol. A methanolic KI solution was prepared in which the KI concentration was $0.693 \text{ mol dm}^{-3}$ - this concentration is just below the maximum solubility of KI in methanol ($0.751 \text{ mol dm}^{-3}$) found in Section 4.4.2, Experiment 2. The KI solution was prepared by weighing 57.516 g of KI into a 500 mL volumetric flask. The flask was topped up to the mark with HPLC grade methanol and the mixture was stirred until the KI was fully dissolved.

A portion of this solution (150 mL) was transferred to a 500 mL conical flask to which the required amount of PdI_2 was added as per Table 4.2, Flask 1.

Table 4.2. Reagent quantities and stirring times for Experiment 3.

		Flask Number			
		1	2	3	4
Reagent	KI-MeOH/mL	150	150	150	0
	PdI_2 /mg	93	82	18	12
	KI/g	0	0	0	5.7
	MeOH/mL	0	0	0	50
Stirring Time (min)		200	105	300	>120

The pH electrode and Pt100 from the HEL Simular were put in place in the flask to monitor pH and temperature. The solution was stirred for at least 105 min at room temperature to dissolve the PdI_2 whilst regularly being visually inspected to see if the PdI_2 had dissolved. As the PdI_2 did not fully dissolve the experiment was repeated with reduced amounts of PdI_2 (Table 4.2, Flasks 2 and 3). As the PdI_2 still did not fully dissolve the order of addition of the PdI_2 and KI to the methanol was changed to see if this affected the solubility of the palladium salt. To do this the palladium iodide and KI were added to 50 mL of methanol in a 100 mL conical flask at the same time and the solution was left to stir for several hours (Table 4.2, Flask 4). Each of the solutions was filtered under vacuum using the equipment in Figure 4.9 (Section 4.2.6) and a pre-weighed Whatman 0.45 μm cellulose nitrate membrane filter. The filter was dried and weighed to measure the amount of PdI_2 remaining on the filter and hence determine the concentration of PdI_2 in the solutions.

Experiment 4: This larger solubility study involved varying the amounts of KI (from 0.5-3.0 g) and PdI_2 (from 5-45 mg) added to 25 mL of HPLC grade methanol in a 25 mL glass vial. A total of 30 vials were prepared and numbered as per Table 4.3.

Table 4.3. Reagent quantities and vial numbers for Experiment 4.

		Amount of KI/g					
		0.5	1.0	1.5	2.0	2.5	3.0
Amount of Pdl ₂ /mg	5	1	21	26	11	16	6
	15	2	22	27	12	17	7
	25	3	23	28	13	18	8
	35	4	24	29	14	19	9
	45	5	25	30	15	20	10

The vials were sealed and stirred for 2 hours before they were filtered under vacuum using a Sigma-Aldrich vacuum filtration unit (Figure 4.9) fitted with a pre-weighed Millipore Fluoropore 0.2 µm FG PTFE membrane filter. The filter was left to dry and was reweighed to determine the amount of Pdl₂ in each of the solutions.

Experiment 5: The results of Experiment 4 implied the need to further investigate the solubility of Pdl₂ in methanolic KI solution. To do this, 2 vials were set up as per Table 4.4. Their contents were stirred for the required time after which the contents were filtered as in Experiment 4 to determine the amount of Pdl₂ in each of the solutions.

Table 4.4. Reagent quantities and stirring times for Experiment 5.

		Vial Number	
		1	2
Reagent	MeOH/mL	25	25
	KI/g	2	2
	Pdl ₂ /mg	50	500
Stirring Time (days)		6	84

4.4.3 Reaction of the Catalytic System with CO

Preliminary experiments were carried out using the filtrates from Flasks 1-3, Experiment 3 (containing 70 mg, 48 mg and 3 mg Pdl₂ respectively after filtration) described in Section 4.4.2, to see how the pH of each of them behaved when purged with CO. The required flask of solution was placed on the Bibby B212 magnetic stirrer/hotplate. The Pt100, turbidity probe and pH electrode from the HEL Similar

system (Section 4.2.2) were placed in the flask along with the PTFE tubing bringing CO to the flask from the Brooks mass flow controller. The solution was stirred for 20 min and then purged with CO at 50 mLmin⁻¹ for several hours. Temperature and pH were recorded throughout and the same procedure was followed for each solution.

4.4.4 Role of Water in the Catalytic System

As the experiments in Section 4.3 had shown that water affects the pH oscillations, experiments were conducted to investigate the effects more closely. Initially, the effect of water on the catalytic system was investigated by comparing the pH behaviour of catalyst solution prepared using standard HPLC grade methanol (99.9%) with the pH behaviour of catalyst solution prepared using dried methanol upon purging with CO. The dried methanol was prepared by placing 500 mL of the standard HPLC grade methanol into a glass bottle containing a layer of 3 Å molecular sieves sufficient to cover the base of the bottle. This was left to dry for 2 days before use. Two 25 mL glass vials were set up each containing the same amounts of PdI₂, KI and either standard HPLC grade (wet) methanol or dried methanol (Table 4.5). The contents of both vials were stirred for 3 hours then each was filtered under vacuum using the equipment described in Section 4.2.6. The solutions were retained and topped up with 25 mL of the appropriate methanol before being purged with CO as described in Section 4.4.3. A third vial was set up with a reduced quantity of PdI₂ to clarify the results of the experiment conducted in Section 4.4.3 which suggested that the initial pH drop may be related to PdI₂ concentration. After stirring the mixture for 3 h it, too, was filtered and the remaining solution was topped up with wet methanol and purged with CO.

Table 4.5. Initial quantities of reagents used to investigate the role of water in the catalytic system.

		Vial Number		
		1	2	3
Initial Reagents	Dried MeOH/mL	25	0	0
	Wet MeOH/mL	0	25	25
	KI/g	2.05	2.05	2.05
	PdI ₂ /g	25	25	7

4.5 Experimental Study of Catalyst Activation

To begin extracting the reaction network for the PCPOC reaction a series of experiments to investigate the initial reactions of the catalyst was carried out using the HEL MicroNOTE system (Section 4.2.1) for measurement of temperature and pH. These experiments focused on the interactions of PdI₂, KI and methanol with CO. All experiments were carried out in 25 mL vials at room temperature on a magnetic stirrer/hotplate.

4.5.1 Modifying Solvents

The preliminary experiments in Section 4.4.4 gave an overview of the effect water has on the catalyst system in the PCPOC reaction. To obtain more detailed information on the effect of water on the catalyst system when purging with CO a set of experiments were conducted using methanol, dried methanol and water as solvents. The concentration of the catalyst (PdI₂, KI) was the same as in the oscillatory experiments performed by Novakovic *et al*^[2, 134] and was kept constant with the total volume and CO flow scaled down.

Methanol: The initial experiment acted as a baseline using all chemicals as purchased without further manipulation. A stock solution of KI in methanol was prepared by adding 8 g KI to 100 mL of standard methanol in a 100 mL bottle. The mixture was stirred on a magnetic stirrer for 5 h until all of the KI had dissolved. A 25 mL aliquot of the KI stock solution was transferred to a 25 mL vial. The pH electrode and Pt100 from the HEL MicroNOTE (Section 4.2.1) were put in place in the vial and the solution was stirred on a magnetic stirrer for 12 min while monitoring pH and temperature. The PdI₂ (24 mg) was added and the solution was stirred for a further

83 min after which the solution was purged with carbon monoxide at 6 mLmin⁻¹ for 5 h while monitoring pH and temperature.

Water: This experiment was performed as for methanol but using 25 mL of deionised water instead of methanol. Purging with CO began approximately 1 h after PdI₂ was added.

Dry Methanol: This experiment used methanol which had been dried using 3 Å molecular sieves. A stock solution of KI in dried methanol was prepared by adding 8 g KI and 4.672 g of molecular sieves to 100 mL of methanol in a 100 mL bottle. The solution was stirred overnight. A 25 mL aliquot of the stock solution was transferred to a 25 mL vial containing 1 g of new molecular sieves. The solution was stirred for 13 min while monitoring pH and temperature before adding 24 mg PdI₂. The solution was then stirred for 1 h after which the solution was purged with CO at 6 mLmin⁻¹ for 3 h while continuing to record pH and temperature.

4.5.2 Adding CO Prior to PdI₂

The experiments in Section 4.5.1 added PdI₂ to the reactor prior to purging with CO in accordance with the experiments by Novakovic *et al.*^[2, 3, 134] To assess if the order of addition of catalyst affected the pH behaviour of the catalyst components under CO purging and hence reveal alternative chemical reactions, PdI₂ was added after the methanolic KI solution had been purged with CO for approximately 1 h. The experiments were conducted in standard methanol and methanol that had been dried over 3 Å molecular sieves overnight. The HEL MicroNOTE system (Section 4.2.1) was used to record pH and temperature. The experiments were conducted as follows:

Methanol: A 25 mL aliquot of the KI stock solution used in Section 4.5.1 was transferred to a 25 mL vial. The pH electrode and Pt100 from the HEL MicroNOTE (Section 4.2.1) were put in place in the vial and the solution was stirred on a magnetic stirrer for 20 min while monitoring pH and temperature. The solution was purged with carbon monoxide at 6 mLmin⁻¹ for 73 min before PdI₂ (24 mg) was added after which the solution was stirred for a further 150 min while continuing to purge with CO and record pH and temperature.

Dry Methanol: This experiment used methanol which had been dried by using the dried KI solution from Section 4.5.1. A 25 mL aliquot of the stock solution was transferred to a 25 mL vial containing 1 g of new molecular sieves. The pH electrode

and Pt100 from the HEL MicroNOTE (Section 4.2.1) were put in place in the vial and the solution was stirred on a magnetic stirrer for 78 min while monitoring pH and temperature. The solution was purged with carbon monoxide at 6 mLmin^{-1} for 60 min before PdI_2 (24 mg) was added then the solution was stirred for a further 150 min while continuing to purge with CO and record pH and temperature.

4.5.3 Filtered Catalyst Solution

The results of Experiment 4 in Section 4.4.2, which studied the solubility of PdI_2 in methanolic KI solutions, highlighted the fact that the solubility of PdI_2 increases over time. This could have an effect on the pH behaviour of the catalyst solution when undergoing CO purging. To ensure that the initial concentration of PdI_2 in solution was constant a solution of catalyst was prepared and filtered to determine the concentration of catalyst in solution prior to use. The filtered catalyst solution was then used to investigate the pH behaviour of the solution when being purged with CO ensuring that any differences in behaviour were not due to different concentrations of catalyst in solution resulting from the difficulties in dissolving PdI_2 consistently. The aim of the experiments was to see if there is a link between PdI_2 concentration and the extent of any pH drop on purging the solution with CO. It is also known that the presence of a soluble salt can have an effect on the solubility of gases in aqueous solutions.^[137] The presence of the salt can have either a salting-in or salting-out effect whereby it increases or decreases the solubility of the dissolved gas. To see if the pH behaviour was affected by a change in KI concentration an experiment was conducted in which the concentration of KI was increased while keeping the concentration of PdI_2 constant.

The catalyst solution was prepared by pipetting 100 mL of methanol into a 100 mL glass bottle. Potassium iodide (8 g) was added along with 96 mg of palladium(II) iodide. The mixture was stirred overnight on a magnetic stirrer and the level of solution was marked on the bottle. The solution was filtered under vacuum using the Sigma vacuum filtration apparatus and a pre-weighed membrane filter (Section 4.2.6), with no rinsing of the bottle or filter to ensure the solution was not diluted. The filtrate was returned to the original, cleaned, 100 mL bottle and topped up to the mark with methanol. The membrane filter was then rinsed with methanol followed by deionised water and more methanol before being left to dry under vacuum. Once dry, the filter was weighed. To ensure the filter was dry it was re-weighed after a further

60 min to ensure its weight remained unchanged. The calculated concentration of the PdI_2 catalyst solution was $2.22 \times 10^{-3} \text{ mol dm}^{-3}$. The catalyst solution was then used in conjunction with the HEL MicroNOTE system (see Section 4.2.1) in the following experiments:

Filtered Solution Baseline: A 25 mL aliquot of the catalyst solution was pipetted into a 25 mL vial and the pH and temperature probes from the HEL MicroNOTE system were put in place before the vial was sealed with parafilm. The solution was then stirred for 20 min on a magnetic stirrer while monitoring pH and temperature to obtain a baseline. Once a suitable baseline had been obtained the solution was purged with CO (6 mL min^{-1}) for approximately 3 h monitoring temperature and pH throughout.

Filtered Solution, Increased KI: This experiment examined the effect of increasing the concentration of potassium iodide on the behaviour of the catalyst solution when purged with CO . As above, 25 mL of the standard PdI_2/KI /methanol solution was pipetted into a 25 mL vial and then an additional 1 g of KI was added. The pH and temperature probes from the HEL MicroNOTE system were put in place and the vial was sealed with parafilm. The solution was stirred for 20 min on a magnetic stirrer while monitoring pH and temperature to obtain baseline measurements and dissolve the KI. The solution was then purged with CO at 6 mL min^{-1} while continuing to monitor temperature and pH.

Filtered Solution, 1:4 Dilution: A 5 mL aliquot of the prepared PdI_2/KI /methanol solution was pipetted into a 25 mL vial along with 20 mL of methanol. The pH and temperature probes from HEL MicroNOTE were put in place before the vial was sealed with parafilm. The solution was stirred for 20 min using a magnetic stirrer while monitoring pH and temperature to obtain a baseline. The solution was then purged with CO (6 mL min^{-1}) monitoring temperature and pH throughout.

Filtered Solution, 1:24 Dilution: In this experiment 1 mL of the prepared PdI_2/KI /methanol solution was pipetted into a 25 mL vial using a 100-1000 μL pipettor while 24 mL of methanol was added using a 25 mL graduated glass pipette. The experiment was then conducted in the same manner as that for the 1:4 dilution.

Filtered Solution, 1:4 Dilution, Increased CO: This experiment looked at the effect of increasing the CO flow rate to assess if the system is gas-liquid mass transfer limited.

The same procedure was used as described for the 1:4 dilution with the CO flow increased to 50 mLmin⁻¹.

4.6 Experimental Study of the PhAc/KI/MeOH/CO/Air Subsystem

Experiments were conducted to establish the baseline pH behaviour of PhAc in methanolic KI solution when purged with CO and air in the absence of PdI₂. The experiments were conducted in standard laboratory glassware using the pH electrode and Pt100 from the HEL Simular (Section 4.2.2) for temperature and pH monitoring along with the WinISO software for datalogging.

Potassium iodide (11.507 g) was weighed into a 100 mL volumetric flask and made up almost to the mark with methanol (HPLC grade) to prepare a 0.693 moldm⁻³ solution. A stirbar was added and after stirring the solution on a magnetic stirrer/hotplate to fully dissolve the KI the stirbar was removed and the solution was topped up to the mark. The KI solution was transferred into a 150 mL conical flask along with a stirbar. The conical flask was placed on a magnetic stirrer/hotplate. After calibration with pH 2 and pH 10 buffers the pH electrode was put in the conical flask along with the Pt100 temperature probe. Temperature and pH were monitored while purging the methanol with air (50 mLmin⁻¹) and CO (50 mLmin⁻¹). After 12 min, 2 mL PhAc was added using a Fisherbrand 100-1000μL pipette to give a PhAc concentration of 0.182 moldm⁻³. The solution was left to stir for 140 min after PhAc addition whilst continuing to purge the solution with CO and air, monitoring pH and temperature throughout.

4.7 Experimental Study of the PhAc/Catalyst/CO Subsystem

The results from the preliminary experiments in Section 4.4 and the study of the catalyst subsystem in Section 4.5 (focusing on the pH behaviour of the catalyst subsystem when purging with CO) showed the significant effect trace water (from the HPLC grade methanol used in the experiments) has on the pH behaviour of the catalyst system. The experiments in this section expand on those with the addition of a further reactant: phenylacetylene (PhAc). The addition of PhAc allows PhAc conversion and product distribution to be studied under different conditions. The experiments focus on 3 scenarios:

- changing the order of reactant addition in wet and dried methanol;

- changing the length of time the catalyst solution is purged with CO prior to PhAc addition;
- conducting experiments under pressure of CO.

4.7.1 *Changing the Order of Reactant Addition in Wet and Dried Methanol*

Four experiments were performed to investigate further the influence of water (contained in the HPLC grade methanol used as both solvent and reactant) on pH behaviour during the carbonylation of PhAc as well as the effect on product formation and product distribution. The experiments also looked to uncover any differences in pH behaviour and product formation that occur when the catalyst solution is purged with CO prior to PhAc addition compared to when PhAc is added before CO purging begins. Additional experiments involving the controlled addition of water to dried catalyst solution validated the findings. The reaction conditions for the experiments are summarised in Table 4.6.

Table 4.6. Reaction conditions for the PhAc/Catalyst/CO subsystem experiments. ^aExpts 1-6: [PhAc] = 0.01 mol dm⁻³; CO flow = 10 mL min⁻¹ for the duration of the experiment. Expts 5,6: [H₂O] = 4.44 x 10⁻⁴ mol dm⁻³.

Experiment No ^a	Reactant Added First	Reactant Added Second	Dried Catalyst Solution	Water Added
1	PhAc	CO	No	No
2	CO	PhAc	No	No
3	PhAc	CO	Yes	No
4	CO	PhAc	Yes	No
5	PhAc	CO	Yes	Yes
6	CO	PhAc	Yes	Yes

All experiments were performed in a 100 mL jacketed glass reactor made in-house (Figure 4.3). Tap water was circulated through the jacket to maintain the temperature in the reactor approximately constant (18 °C). HEL MicroNote (Section 4.2.1) was used for on-line recording of reaction pH and temperature.

A stock solution of catalyst was prepared and used in all experiments. Palladium(II) iodide (1 g), potassium iodide (20 g) and HPLC grade methanol (250 ml) were stirred together for 24 h. The solution was then filtered under vacuum (Section 4.2.6) and

the amount of palladium(II) iodide remaining in the solution was determined to be 698 mg. Naphthalene (76 mg) was added as an internal standard and the solution was made up to 300 mL with methanol. The initial concentrations of PdI_2 and naphthalene were calculated to be $6.46 \times 10^{-3} \text{ mol dm}^{-3}$ and $2.0 \times 10^{-3} \text{ mol dm}^{-3}$ respectively.

In all experiments, the empty reaction vessel was purged with nitrogen before adding 50 mL of stock catalyst solution. On-line recording of pH and temperature then commenced. An all-aqueous pH meter set-up consisting of aqueous pH electrode filling solution and aqueous calibration buffers was used in all experiments. The order of reactant addition and the presence or absence of water for each experiment are given in Table 4.6. When CO was added first, the solution was purged for 3 hours before PhAc was added. In Experiments 3 and 4, the stock solution (50 mL) was dried before use for approximately 15 h using 5 g of molecular sieves (pore size 3 Å and absorption $\geq 15\%$). To confirm that any differences were due to the water content of the catalyst solution, 2 experiments (5 and 6) were conducted using dried catalyst solution (following the same procedure as for Experiments 3 and 4) with 0.4 μL water added using a 10- μL GC syringe. The amount of water added was determined based on the results of a modelling study conducted using the results of the experiments in Section 4.5 in which an initial water concentration of $3.4 \times 10^{-4} \text{ mol dm}^{-3}$ gave the best fit to the data.^[138]

Sampling Procedure: The sample vials were closed and purged with nitrogen prior to use and syringes with needles were used for sample handling to minimise contact with atmospheric oxygen and water. After transferring the sample to the vial, the sample was purged with nitrogen to remove any remaining carbon monoxide from the solution and quench the reaction. Sample analysis was carried out using the Varian Saturn 2200 GCMS (Section 4.2.4).

4.7.2 CO Purging Time

The results of the experiments in Section 4.7.1 showed a link between the addition of CO to the PdI_2 catalyst solution prior to PhAc and reduced PhAc conversion. This unexpected result was investigated by changing the length of time the catalyst solution was purged with CO prior to PhAc addition to see how this affected PhAc conversion. The experiments were conducted in the same manner as those in Section 4.7.1 but the catalyst solutions were purged with CO for 0, 4, 60, 120 and 200 min prior to PhAc addition. The stock catalyst solution used in the experiments

was prepared as in Section 4.7.1. After the solution had been filtered and topped up to 300 mL the PdI_2 concentration of the catalyst solution was determined to be $7.38 \times 10^{-3} \text{ mol dm}^{-3}$. The PdI_2 concentration was adjusted to $6.46 \times 10^{-3} \text{ mol dm}^{-3}$ (the concentration used in the experiments in Section 4.7.1) by the addition of 43 mL of $0.402 \text{ mol dm}^{-3}$ methanolic KI solution. Naphthalene (86 mg) was added to the catalyst solution as an internal standard and the solution was stirred to ensure it dissolved.

4.7.3 Varying CO Flow Rate

As two of the reactants in the PCPOC reaction are gases the gas-liquid mass transfer limitations of the PCPOC reaction were investigated. Initial experiments were conducted using the parallel reaction system described in Section 4.2.4 with CO flow rates of 5, 10 and 15 mL min^{-1} . To allow comparison of the results of these experiments with the results of Experiment 1 in Section 4.7.1, the stock catalyst solution used in the experiments was prepared as in Section 4.7.1. After the stock solution had been filtered and topped up to 300 mL the PdI_2 concentration of the catalyst solution was determined to be $7.69 \times 10^{-3} \text{ mol dm}^{-3}$. The PdI_2 concentration was adjusted to $6.46 \times 10^{-3} \text{ mol dm}^{-3}$ by the addition of 57 mL of $0.402 \text{ mol dm}^{-3}$ methanolic KI solution. Naphthalene (89 mg) was added to the catalyst solution as an internal standard and the solution was stirred to ensure it dissolved. Six parallel reactions were set up in 6 conical flasks (100 mL), 2 reactions using a CO flow rate of 5 mL min^{-1} , 2 reactions using a CO flow rate of 10 mL min^{-1} and 2 reactions using a CO flow rate of 15 mL min^{-1} . Each flask was set up following the same procedure. The flask was purged with nitrogen before use to remove oxygen. Nitrogen purging of the flask continued while adding 50 mL of catalyst solution. The flask was placed in position on the magnetic stirrer in the water bath which was set at 20°C . The pH electrode and Pt100 temperature probes were put in place and the flask contents were set to stir at 350 rpm for the duration of the experiment. The flask continued to be purged with nitrogen while 55 μL PhAc was added. The first sample from the flask (900 μL) was taken using a 1 mL plastic syringe fitted with a long stainless steel hypodermic needle (203 mm long, 18 gauge) to minimize the introduction of oxygen from the air to the flask. The sample was transferred to an 8 mL vial and the sample was purged with nitrogen. The sample was then transferred to a 2 mL GC vial and analysed by GCMS using the method outlined in Section 4.2.5. The tube supplying CO was placed in the reaction flask, purging of the flask with nitrogen ceased and

purging of the flask with CO at the required flow rate commenced. After 30 min purging with CO sample 2 was taken following the same procedure as for sample 1 (purging the sample with nitrogen before analysis removed the CO and quenched the reaction). Purging of the reaction mixture with CO continued for a further 3 h at which time sample 3 was taken. The procedure was repeated for each flask.

4.7.4 Gas-Liquid Mass Transfer

To further investigate the effect gas-liquid mass transfer may have on the system a series of experiments were conducted using the HEL Automate high pressure reactor (see Section 4.2.3) under CO pressures of approximately 5 bar with stirring rates of 188 rpm and 1036 rpm. To allow comparison of the results with Experiment 1 in Section 4.7.1 and the experiments in 4.7.3, a stock catalyst solution was prepared with the same PdI_2 concentration as used in Section 4.7.1 by following the procedure outlined in Section 4.7.2. After the stock solution had been filtered and topped up to 300 mL the PdI_2 concentration of the catalyst solution was determined to be $7.71 \times 10^{-3} \text{ mol dm}^{-3}$. The PdI_2 concentration was adjusted to $6.46 \times 10^{-3} \text{ mol dm}^{-3}$ by the addition of 58 mL of $0.402 \text{ mol dm}^{-3}$ methanolic KI solution. Naphthalene (89.6 mg) was added to the catalyst solution as an internal standard and the solution was stirred to ensure it dissolved.

The experiment was conducted as follows: the catalyst solution containing Np internal standard (80 mL) was transferred to the Automate reactor and then 88 μL PhAc was added to the catalyst solution. The solution was stirred with a glass stirring rod and a 200 μL sample was taken using a 20-200 μL pipette and transferred to a 300 μL GC vial for analysis by GCMS (Section 4.2.5). The reactor was sealed, the manual vent valve on the reactor was opened and the nitrogen flow was started to purge the headspace in the reactor with nitrogen to remove oxygen. Nitrogen purging lasted for 10 min with a pressure in the reactor of 1.7 bar throughout. After 10 min the nitrogen flow was stopped and purging with CO commenced to remove the nitrogen from the reactor headspace. This purging procedure was to mimic the reaction conditions of the experiments in Sections 4.7.1 and 4.7.3. After 10 min of purging with CO the manual vent valve was closed and the reactor was pressurised with CO to approximately 5 bar. Sample 2 was then taken. The valve to the CO supply was left open so that a constant pressure of CO was maintained throughout the experiment. Stirring commenced at 188 rpm and regular samples were taken

throughout the reaction. The experiment was allowed to run for 3.5 h while continuing to monitor pressure and reactor temperature. All samples were transferred to 300 μ L GC vials (which had been purged with nitrogen) and analysed by GCMS (Section 4.2.5). The experiment was repeated with stirring speed increased to 1036 rpm.

Chapter 5. Results and Discussion of Experiments on the Full PCPOC Reaction

Understanding the reaction network responsible for the observed phenomena during the oscillatory and non-oscillatory modes of the PCPOC reaction is a complex task requiring an exhaustive experimental study. Two approaches were used to study the behaviour of the PCPOC reaction: top down – investigating the reaction as a whole, and bottom up – investigating small subsystems of the reaction. The results of both approaches will be presented and discussed in this chapter.

The top-down approach focussed on expanding the study conducted by Novakovic *et al* which investigated the effect of reaction temperature on the oscillatory behaviour of the PCPOC reaction.^[134] The temperature range of the study was extended and the effect of reaction temperature on product distribution and PhAc conversion in the PCPOC reaction (Section 4.3.1) was investigated. Following some interesting observations from these experiments the full PCPOC system was studied with increased water concentration (Section 4.3.2) to see how this affected the pH oscillations and the product distribution during the reaction.

The bottom-up approach looked into the behaviour of subsystems of the PCPOC reaction (Sections 4.4-4.7) to gain some insight into the reaction network responsible for the oscillatory behaviour and explain the results and observations of the experiments of the full PCPOC reaction at different temperatures and with increased water concentration. The results of experiments on the following subsystems will be presented here:

- catalyst (MeOH/KI/PdI₂) with CO;
- PhAc/KI/MeOH/CO/air;
- catalyst with CO and PhAc.

The PCPOC reaction can give a number of products including mono- and di-esters, anhydrides, acids and heterocyclic compounds depending on the reaction conditions.^[6] In the experiments involving phenylacetylene, whether using the full PCPOC reaction or during the investigations of the subsystems, samples taken from the reaction mixture during experiments were analysed by GCMS using the GC

method described in Section 4.2.5. This analysis identified the products in the reactions carried out in this study as those shown in Figure 5.1.

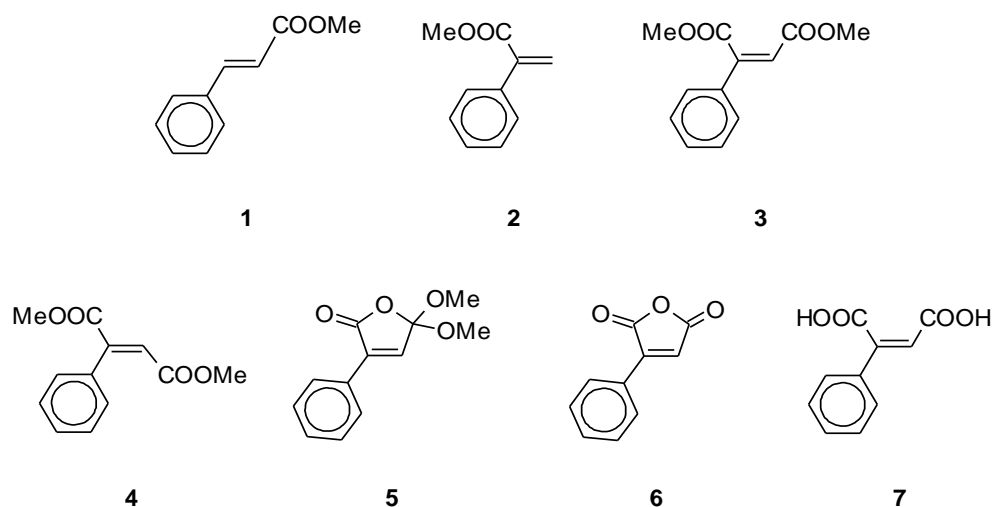


Figure 5.1. Products detected by GCMS in the PCPOC reaction: **1**, Methyl (E)-cinnamate; **2**, Methyl atropate; **3**, Dimethyl (2Z)-2-phenyl-2-butenedioate; **4**, Dimethyl (2E)-2-phenyl-2-butenedioate; **5**, 5,5-Dimethoxy-3-phenyl-2(5H)-furanone; **6**, Phenylmaleic anhydride; **7**, Phenylmaleic acid.

5.1 Full PCPOC System - Effect of Temperature

Previously, experiments at 10-40 °C showed that temperature has an effect on the period and amplitude of oscillations in the PCPOC reaction.^[134] Higher temperatures give smaller amplitude, higher frequency oscillations and as the temperature is decreased the period and amplitude of the oscillations increases. However, the corresponding effect on the conversion of phenylacetylene and the distribution of products has not been studied. This work sought to address that gap in the literature by conducting a series of experiments using the same procedure and equipment as that previously employed but over an extended temperature range in the oscillatory region i.e. 0-40 °C. However, when following product and reactant concentrations measured over long periods of time (e.g. days) in a vessel where the solution volume is affected by evaporation of the solvent it is difficult to compare concentrations from one experiment with those of another. Using naphthalene as an internal standard *in situ* overcame this difficulty. The results of the experiments show the effect of temperature on:

- pH and turbidity
- phenylacetylene conversion
- product distribution

- product formation

5.1.1 pH and Turbidity

Novakovic *et al* conducted PCPOC experiments at temperatures from 10-50 °C. They found the frequency and amplitude of the pH oscillations varies with temperature from 10-40 °C with no pH oscillations exhibited at 50 °C.^[134] The experiments in this study were conducted at temperatures of 0-40 °C using the HEL Simular reaction calorimeter (Section 4.2.2) to monitor pH, temperature and turbidity following the procedure in Section 4.3.1.^[139] The progress of the reaction was followed by GCMS analysis of samples of the reaction mixture taken periodically during the course of the reaction using the method described in Section 4.2.5. The onset and end of pH oscillations were noted along with the period, amplitude and duration of oscillations according to the designations in Figure 5.2.

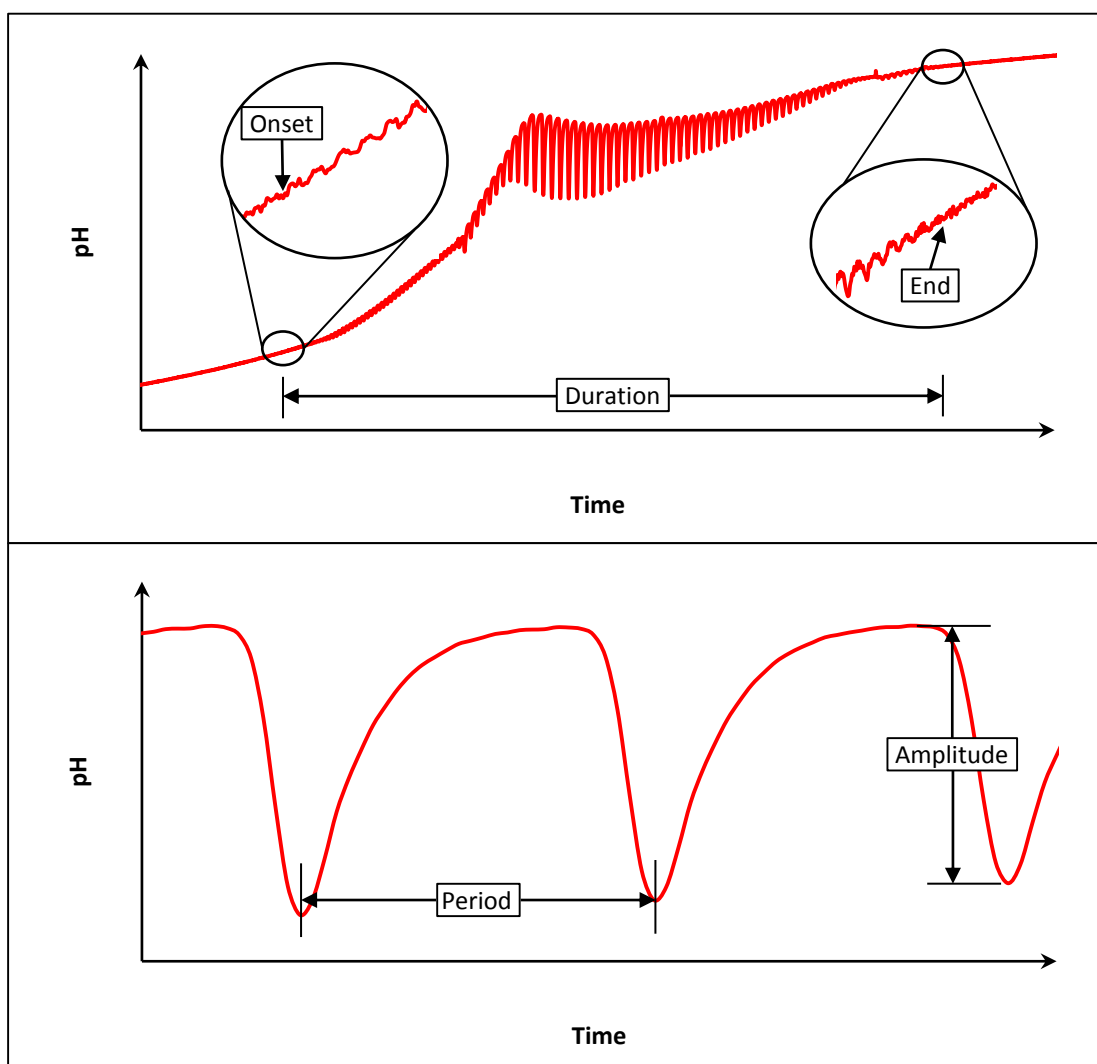


Figure 5.2. Diagram showing how the period, amplitude, duration, onset and end of pH oscillations were defined.

The pH results from the experiments are shown in Figure 5.3. It is interesting to note from Figure 5.3 that only the experiments conducted at 0 °C and 10 °C showed more than 1 set of oscillations with the exception of the experiment conducted in this study at 40 °C which showed 2 sets of oscillations. The second set of oscillations in the experiment conducted at 40 °C were short-lived and seemed to be induced by the addition of methanol to the system, which was not the case for the experiments conducted at 0 °C and 10 °C. The experiments conducted at 0 °C and 10 °C were stopped before the oscillations had ceased due to time constraints. It is likely that other sets of oscillations would have been observed if the experiments were conducted for longer as the pH of the reaction solution was still in the oscillatory region when the experiments were stopped.

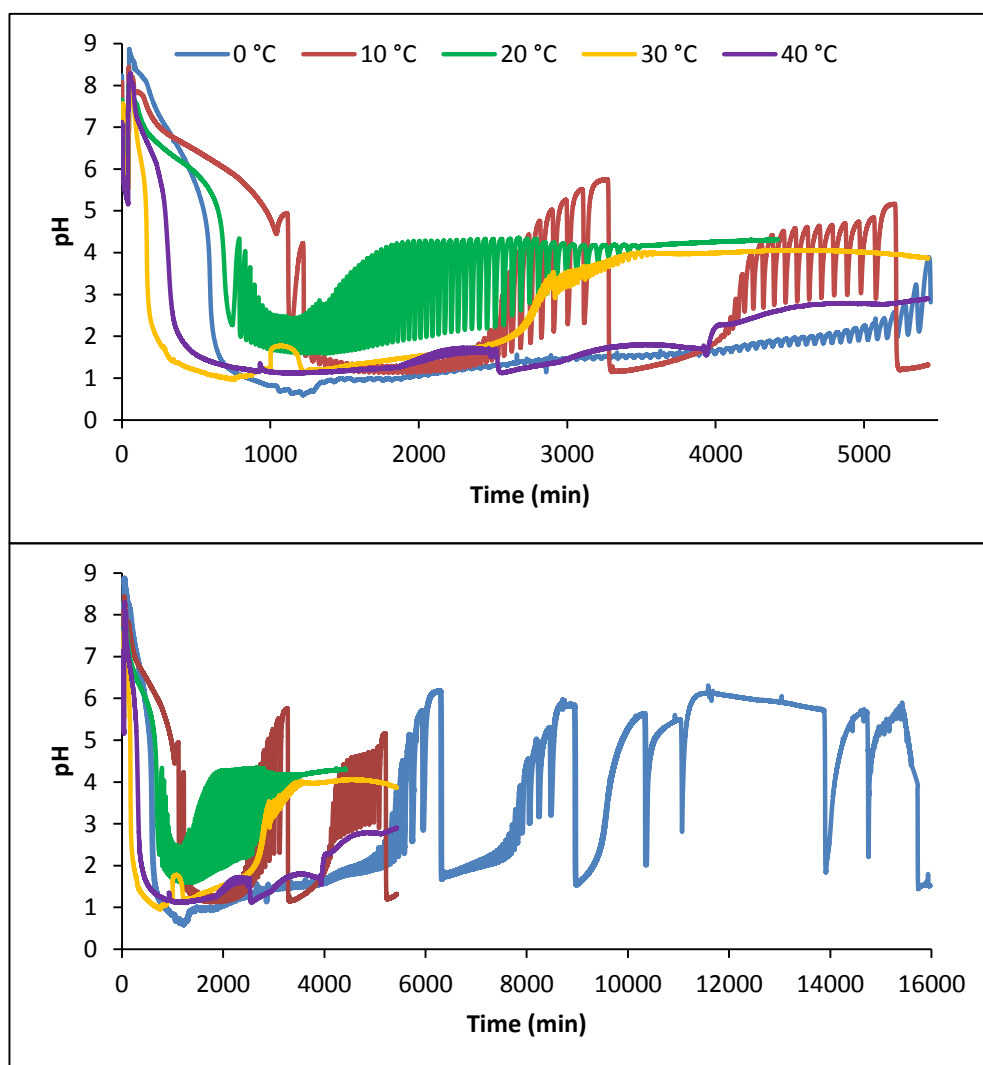


Figure 5.3. The pH recorded during the PCPOC reaction conducted at temperatures from 0-40 °C.

A comparison of trends in the period and amplitude of the pH oscillations produced by the PCPOC reaction in this study and those found by Novakovic *et al* are summarised in Table 5.1 and Table 5.2.

Table 5.1. A summary of trends in the period of pH oscillations of the PCPOC reaction at temperatures of 0-40 °C compared with those found by Novakovic *et al*, 2009.^[134] ^aExperiment was stopped before oscillations had ceased. ^bSome oscillations started at 270 min but were not sustained.

Temperature (°C)	Time of onset (min)		Duration (min)		No. of sets		Period (min)			
							This study		Novakovic	
	This study	Novakovic	This study	Novakovic	This study	Novakovic	Max	Min	Max	Min
0	990	-	16000 ^a	-	2 ^a	-	1375	47	-	-
10	1042	2030	4201 ^a	5970	2 ^a	3 ^a	189	27	182	-
20	744	2117	2737	4323	1	1	71	22	71	-
30	2421 ^b	928	1190	1452	1	1	45	6	21	-
40	1270	1115	4389	640	2	1	10	5	12	-

Table 5.2. A summary of trends in the amplitude of pH oscillations in the PCPOC reaction at temperatures of 0-40 °C compared with those found by Novakovic *et al.*^[134]

Temperature (°C)	pH at onset (pH units)		pH range (pH units)		Amplitude (pH units)			
					This study		Novakovic	
	This study	Novakovic	This study	Novakovic	Max	Min	Max	Min
0	0.82	-	0.59-6.13	-	3.61	0.04	-	-
10	4.44	3.78	1.13-5.75	2.0-6.0	4.6	0.012	3.1	-
20	2.27	3.13	1.58-4.35	2.0-4.8	2.35	0.071	2.4	-
30	1.74	1.21	1.74-4.01	1.21-3.68	0.614	0.003	0.8	-
40	1.93	1.61	1.93-3.14	1.61-3.70	0.164	0.002	0.6	-

The onset of oscillations (Table 5.1) occurs at different times in all of the experiments. Although the time of onset of the oscillations does not appear to be temperature dependent, it is interesting to note from Figure 5.3 that the pH oscillations in the experiments conducted at 0-20 °C start when the pH is falling whereas at higher temperatures the pH oscillations start when the pH has started rising. In general the duration of the pH oscillations increases as the temperature is decreased with the exception of the study conducted at 40 °C where the oscillations lasted for over 4000 min in this study compared to the 640 min in the 40 °C experiment conducted by Novakovic *et al.*^[134] This difference in duration of the pH oscillations at 40 °C was accompanied by a reduction in the maximum amplitude of the oscillations to 1/3 of that found by Novakovic and colleagues (Table 5.2).

The increase in the duration of the oscillations as the reaction temperature is reduced is likely a consequence of the reduction in reaction rate at lower temperatures. The difference in the experiments at 40 °C may be explained by problems with the granularity of PdI₂ noted by Novakovic *et al* when they had difficulties replicating the oscillatory behaviour of their previous experiments at 40 °C.^[2] If all of the PdI₂ is not in solution this may introduce mass-transfer limitations by altering the concentration of catalyst available in solution and hence affecting the dynamics of the relevant reactions in the reaction network (e.g. involving the generation and consumption of [H⁺]) thereby altering the oscillatory pH behaviour. At lower temperatures the reaction rate is slower, as expected from Arrhenius law, and therefore these mass transfer limitations may not be an issue.

In terms of the period of oscillations the results are in agreement with those found by Novakovic *et al*^[134] i.e. the period of oscillations increases as reaction temperature is decreased and this trend continues down to 0 °C. The actual values at each temperature are also very similar to those found by Novakovic *et al* (see Table 5.1).

The pH at which the oscillations start changes with temperature (see Table 5.2). It is known that the measurement of pH in aqueous solutions is temperature dependent with alkaline solutions being affected more than acidic solutions.^[140] An acidic solution with pH 1.00 at 25 °C will have a pH of 1.01 at 60 °C but 0.99 at 0 °C whereas a neutral solution with pH 7.00 at 25 °C will have a pH of 6.51 at 60 °C but 7.47 at 0 °C. In this study, for temperatures of 10-30 °C, the pH at onset of the

oscillations drops from 4.44 to 1.74. Novakovic *et al* found a similar trend (3.78 to 1.21).^[134] This trend is therefore unlikely to be solely due to the temperature dependence of pH measurement. It is notable that this trend is not followed at 0 °C or at 40 °C: at 0 °C the pH at onset of the oscillations is very low (0.82); at 40 °C the pH at onset of the oscillations is slightly higher than that at 30 °C: 1.93 in this study and a pH of 1.61 in the study by the Novakovic group.^[134]

Figure 5.4 gives the overall view of the oscillations in pH and heater power for the PCPOC reaction when conducted at 40 °C. The large spikes in the power curve correspond to the addition of methanol to the reactor to compensate for evaporative loss of the solvent. At 40 °C extra solvent was added on 6 occasions to ensure that the pH electrode was immersed in solution and to reduce the variability in solvent volume and hence reactant/product concentrations within the reactor.

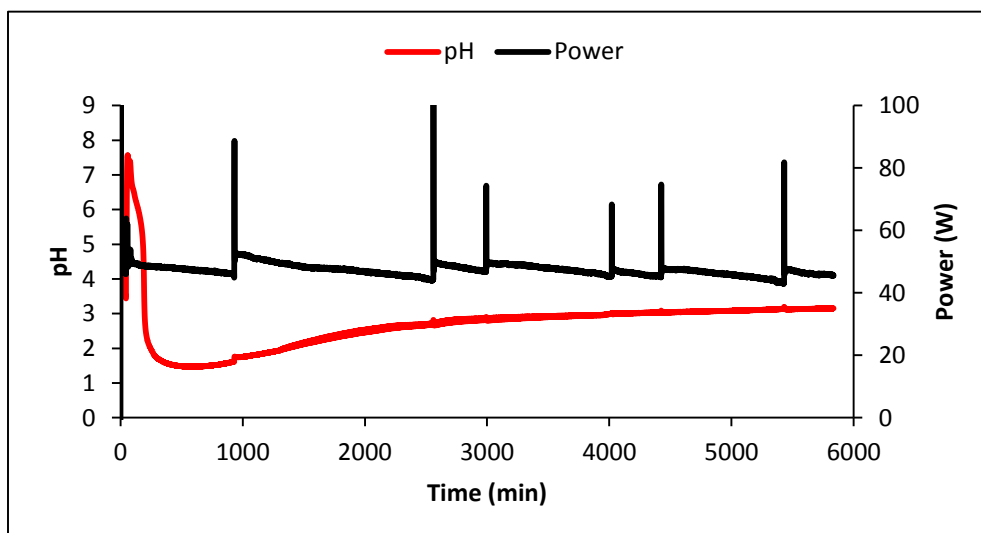


Figure 5.4. pH and heater power in the oscillatory PCPOC reaction at 40 °C.

The time of onset of oscillations at 40 °C in the Novakovic study (see Table 5.1) and in this study (Figure 5.5) is over 1000 min from the start of the experiment with the appearance of oscillations in this study occurring 183 min later than those observed by Novakovic *et al*.^[134]

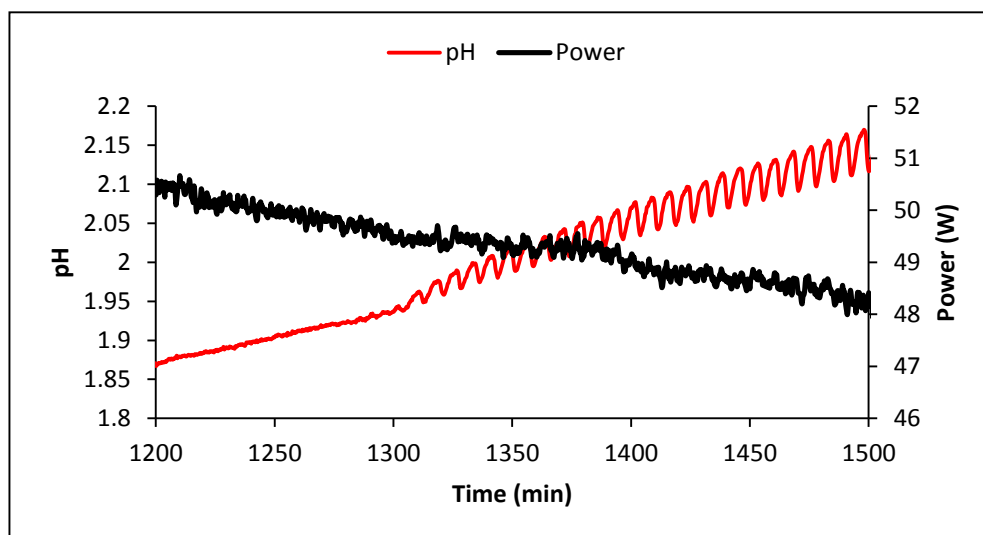


Figure 5.5. Onset of pH oscillations in the PCPOC reaction at 40 °C.

At 40 °C the maximum period of the pH oscillations was 10 min and the maximum amplitude was 0.164 pH units (Figure 5.6) which are both lower than the oscillations observed by Novakovic *et al*.^[134] at the same temperature. Novakovic *et al* also noted that the waveform of the pH oscillations was shark fin-like whereas in this study the waveform is more symmetrical (Figure 5.6).

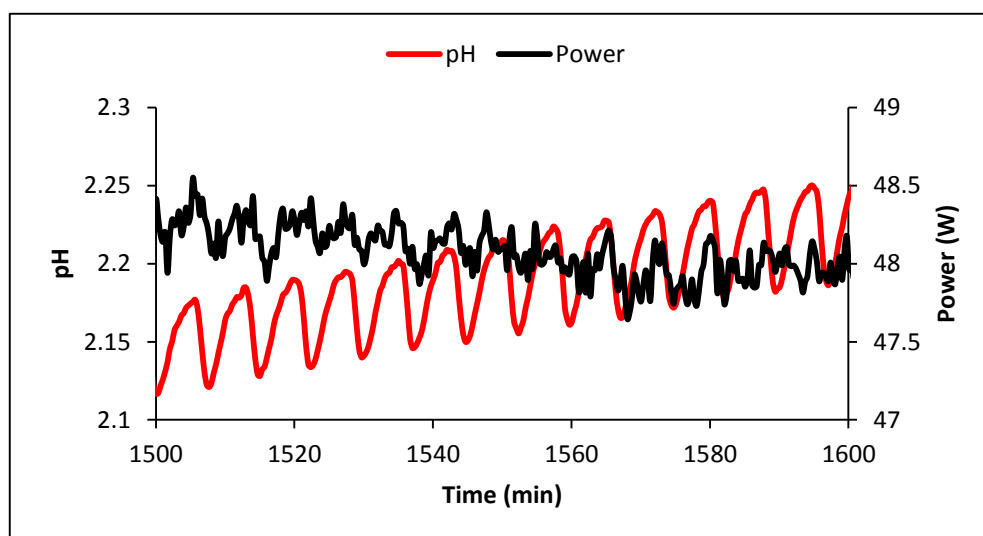


Figure 5.6. Oscillations in pH and heater power in the PCPOC reaction at 40 °C from 1500-1600 min.

An interesting observation is that the period and amplitude of the pH oscillations at 40 °C increased when methanol was added to compensate for evaporative loss of the solvent (Figure 5.7a-c). For example, the addition of methanol at 2560 min caused the amplitude of the pH oscillations to increase by 0.04 pH units (a 100% increase) and the period to increase from 7 min to 10 min (Figure 5.7a). The addition of methanol also initiated oscillations once they had ceased (Figure 5.7d). As

methanol was in huge excess already it is most likely to be trace amounts of water in the HPLC grade methanol that is responsible for these observations. This is supported by the observations of Mukherjee who found that using anhydrous methanol during perturbation studies of the PCPOC system did not result in oscillatory pH behaviour.^[135]

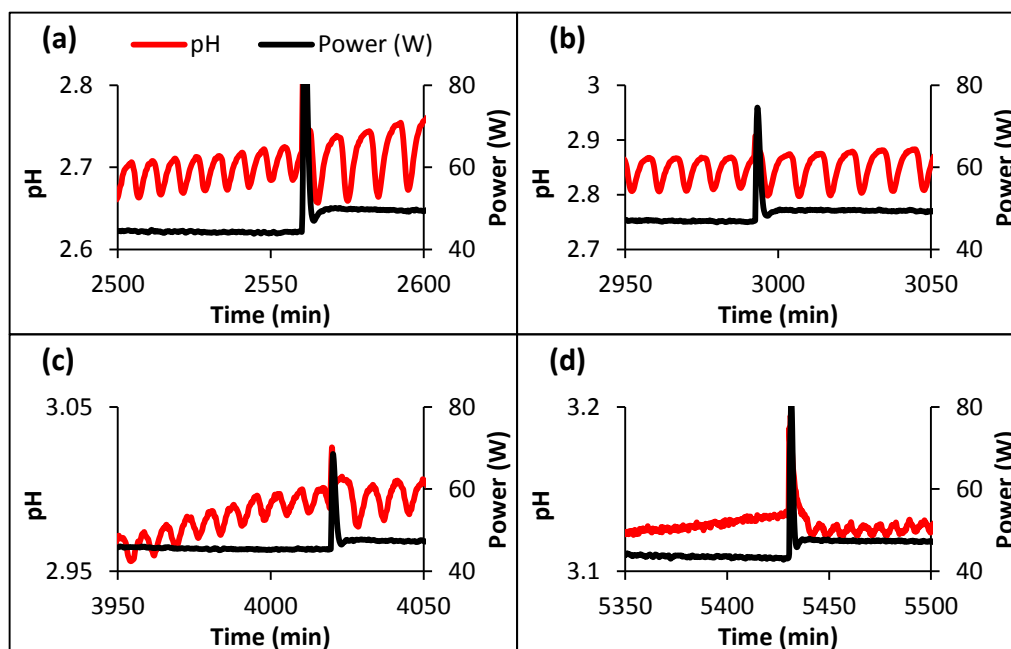


Figure 5.7. Methanol addition, indicated by spikes in the power curve, increases the period and amplitude of pH oscillations in the PCPOC reaction at 40 °C.

The relative turbidity of the reaction mixture was also recorded. Turbidity measures the clarity of a solution due to the presence of suspended particles. It can therefore detect changes in the numbers of particles in a liquid caused by precipitation. As relative turbidity is measured it is only an indication of the changes that occur during the reaction and cannot give an absolute measure of concentration. The turbidity is measured in arbitrary units with a turbidity of 0 being a clear solution with no particles. The turbidity recorded during the oscillatory PCPOC reaction at 40 °C is shown in Figure 5.8. No oscillatory behaviour was apparent in turbidity although there was a sudden drop in turbidity at 2561 min which coincided with the spike in pH and heater power that occurred when MeOH was added to the reactor (Figure 5.7a). The turbidity then rapidly fluctuated between 31 and 32 for the remainder of the reaction.

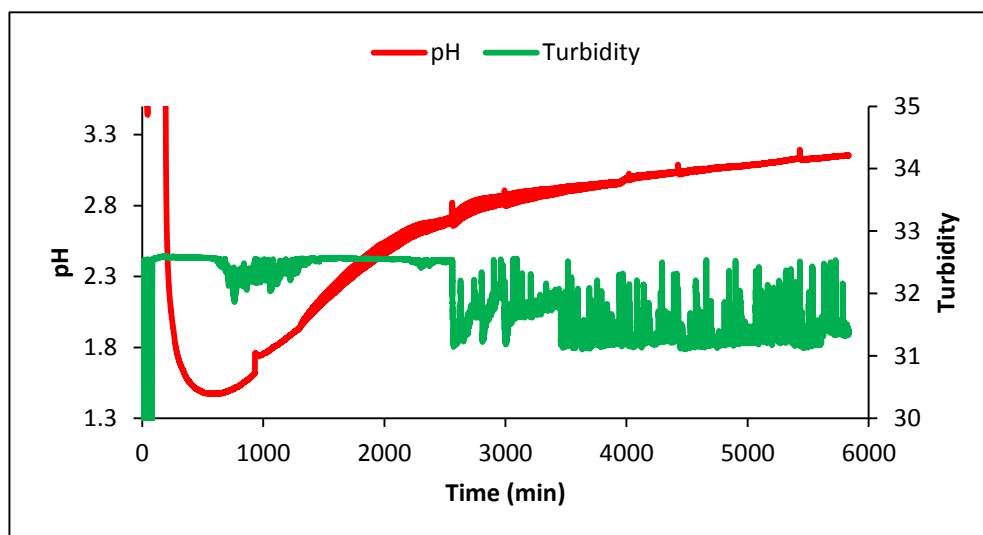


Figure 5.8. Turbidity and pH recorded in the oscillatory PCPOC reaction at 40 °C.

The pH and heater power data from the experiment conducted at 30 °C are shown in Figure 5.9. Additional methanol was only required on one occasion which is evident from the single spike in the power curve in Figure 5.9 at 2470 min.

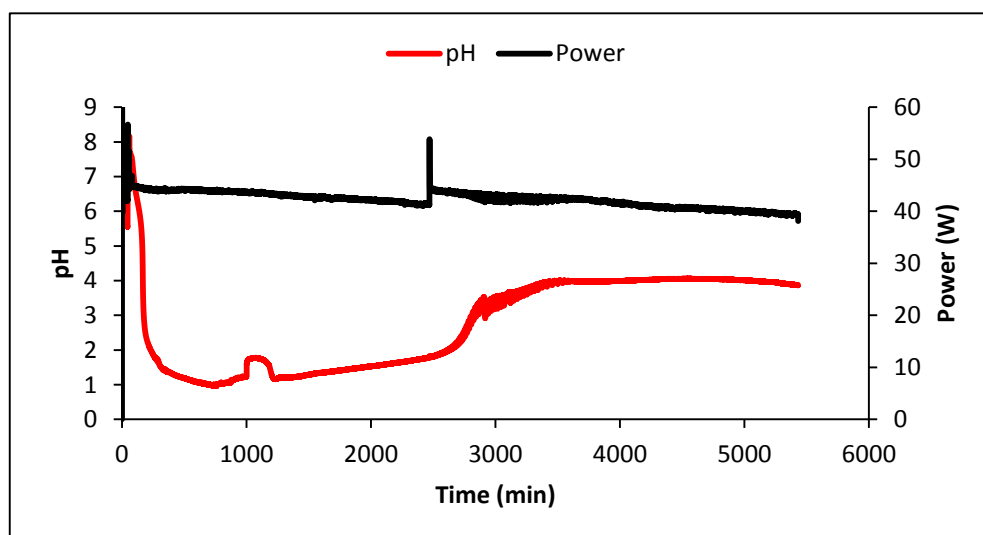


Figure 5.9. pH and heater power in the oscillatory PCPOC reaction at 30 °C.

Figure 5.10 shows the addition of methanol caused an increase in the period (from 9 min to 10 min) and amplitude (from 0.01 to 0.02 pH units) of the pH oscillations at 30 °C which are smaller than the increases seen when methanol was added to the PCPOC reaction at 40 °C (Figure 5.7).

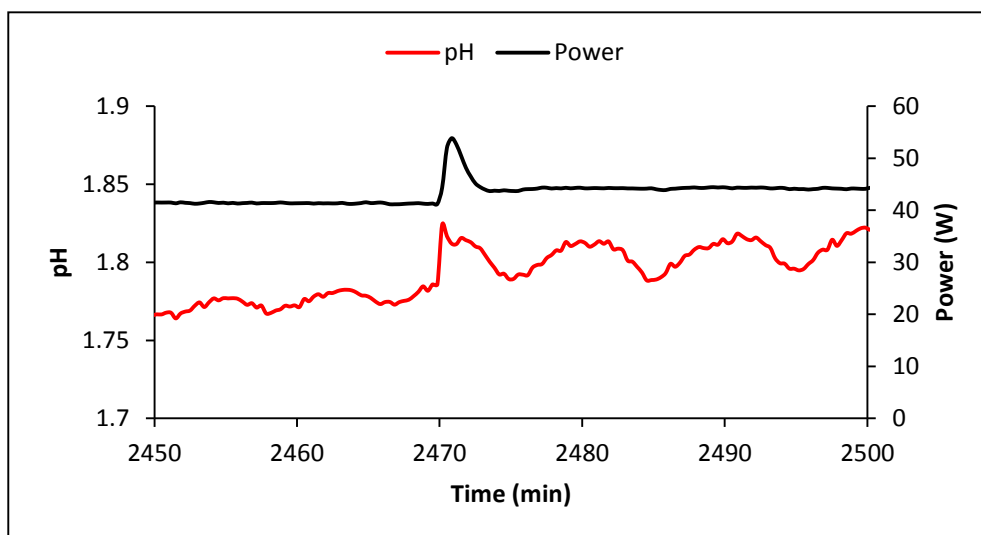


Figure 5.10. Addition of methanol to the PCPOC reaction at 30 °C, indicated by the peak in heater power around 2470 min, leads to an increase in the period and amplitude of pH oscillations.

There is an indication of the pH beginning to oscillate after 270 min (see Figure 5.11) but the oscillations were not sustained and the oscillations did not become established until 2421 min after the experiment was started.

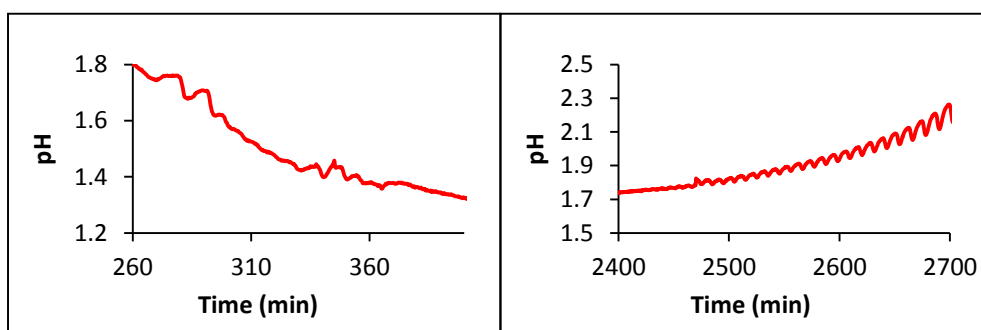


Figure 5.11. Onset of pH oscillations in the PCPOC reaction at 30 °C.

Figure 5.12 shows how the oscillations in pH increased in period and amplitude as the pH increased from 2 to 3.5 with a maximum period of 24 min in this region. The pH oscillations are accompanied by oscillations in heater power which also increase in size in phase with the pH oscillations.

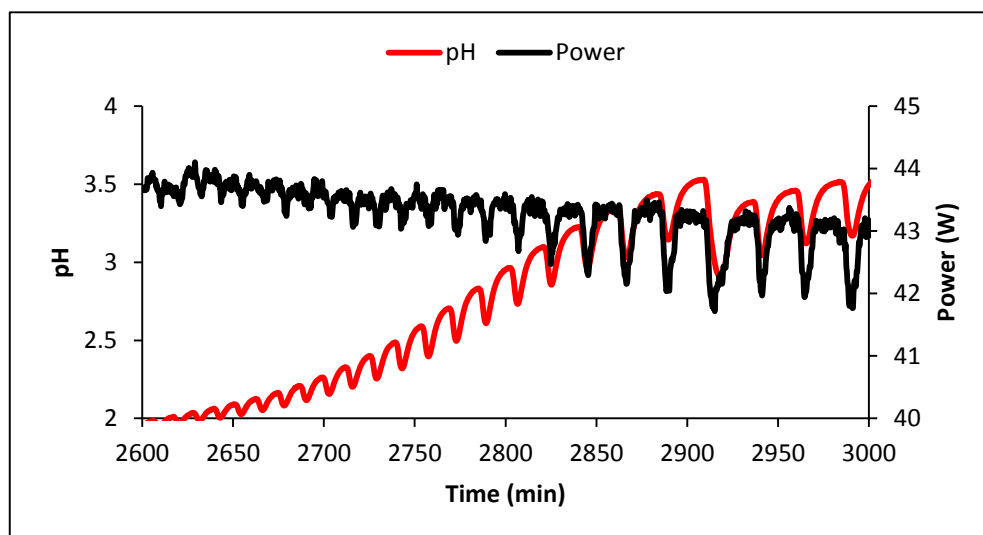


Figure 5.12. pH and heater power in the oscillatory PCPOC reaction at 30 °C from 2600-3000 min.

It is interesting to note the general shape of each oscillation is similar to that found by Novakovic *et al*^[134] initially but near the end of the experiment the shape of the oscillations changes (Figure 5.13). Instead of the relaxation oscillations which occurred for the majority of the reaction where pH increased gradually over approximately 20 min, slowing as it reached the local maximum, then dropping rapidly to the local minimum, the pH gradually increased to the local maximum over 15 min and then fell slowly in a linear fashion for 20-25 min before dropping rapidly to the local minimum.

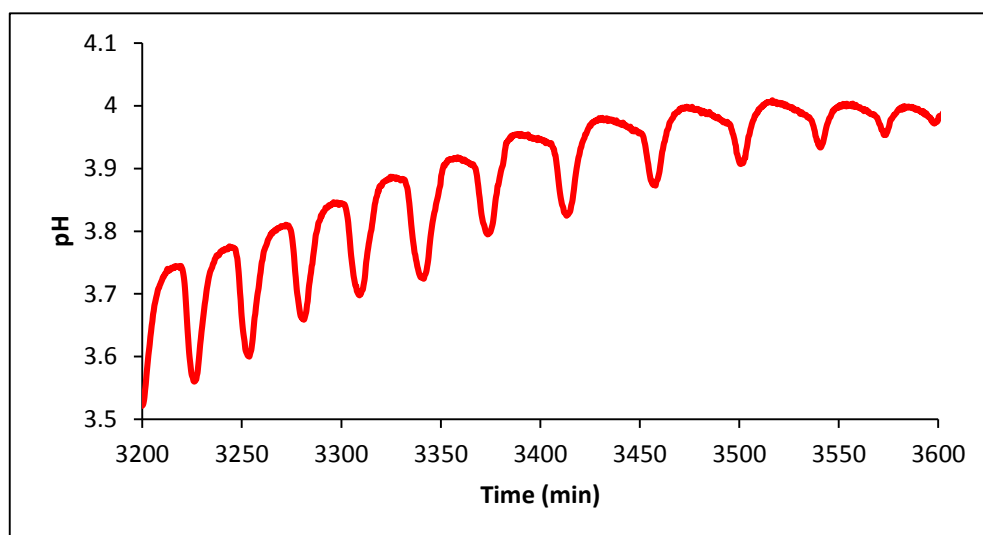


Figure 5.13. The changing shape of the pH oscillations in the PCPOC reaction at 30 °C.

The turbidity recorded in the PCPOC reaction at 30 °C is shown in Figure 5.14. Initially the turbidity was static at 32.5 until 1544 min from the start of the reaction at

which point it dropped and began to fluctuate around a value of 30 as in the experiment conducted at 40 °C.

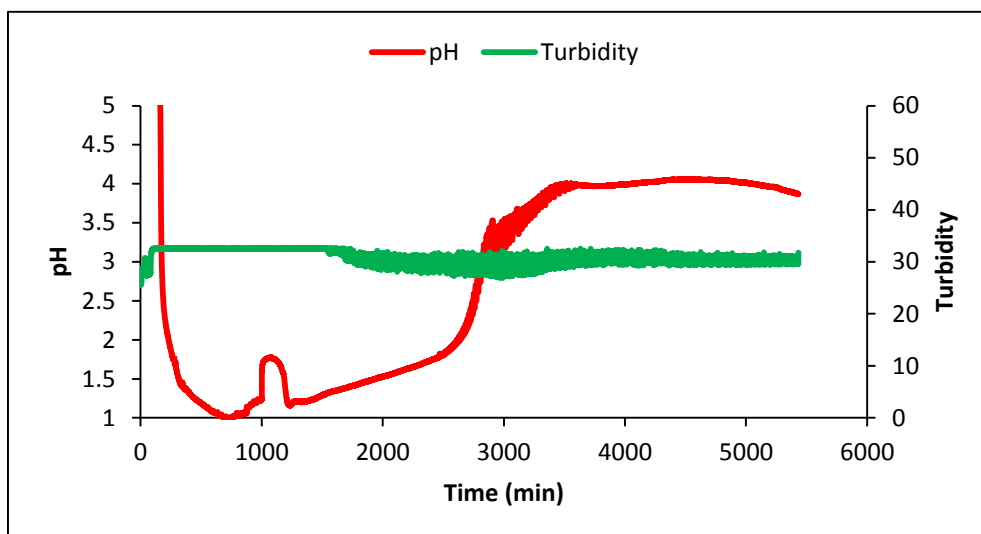


Figure 5.14. Turbidity and pH recorded in the oscillatory PCPOC reaction at 30 °C.

At approximately 2500 min the fluctuations in turbidity gradually became more regular until, by 2700 min, regular sustained oscillations were established which lasted until the pH oscillations ceased at 3600 min. The oscillations in pH and turbidity were in-phase (Figure 5.15).

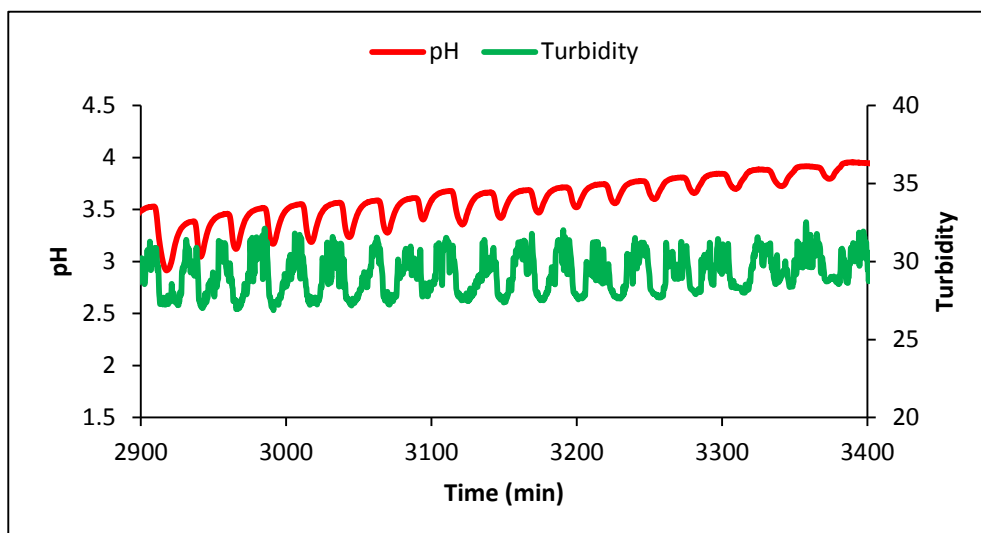


Figure 5.15. Oscillations in turbidity are in phase with pH oscillations at 30 °C.

Figure 5.16 and Figure 5.17 show the large period and amplitude of pH oscillations at 20 °C, with the period reaching a maximum of 71 min and the amplitude having a maximum value of 2.35 pH units. It is also notable that, unlike at 30 °C and 40 °C, the pH oscillations began when the pH was dropping. The dip in the power curve between 2500-3000 min is caused by frequent sampling during that period. The drop

in volume leads to a reduction in the power necessary to maintain the reaction temperature at 20 °C. The subsequent spike in power is due to the addition of methanol to top up the solvent volume in the reactor to compensate for evaporative loss.

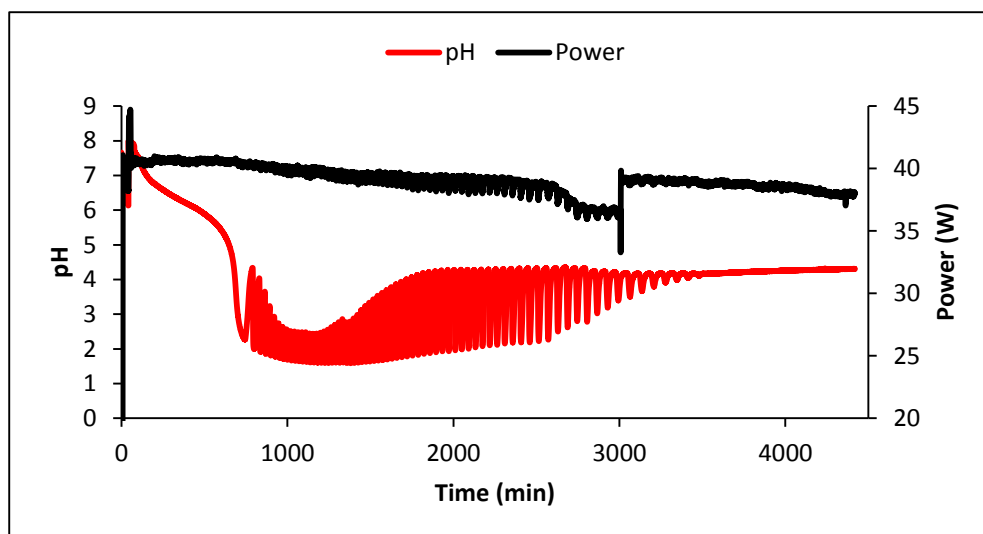


Figure 5.16. Oscillations in pH and heater power in the oscillatory PCPOC reaction at 20 °C.

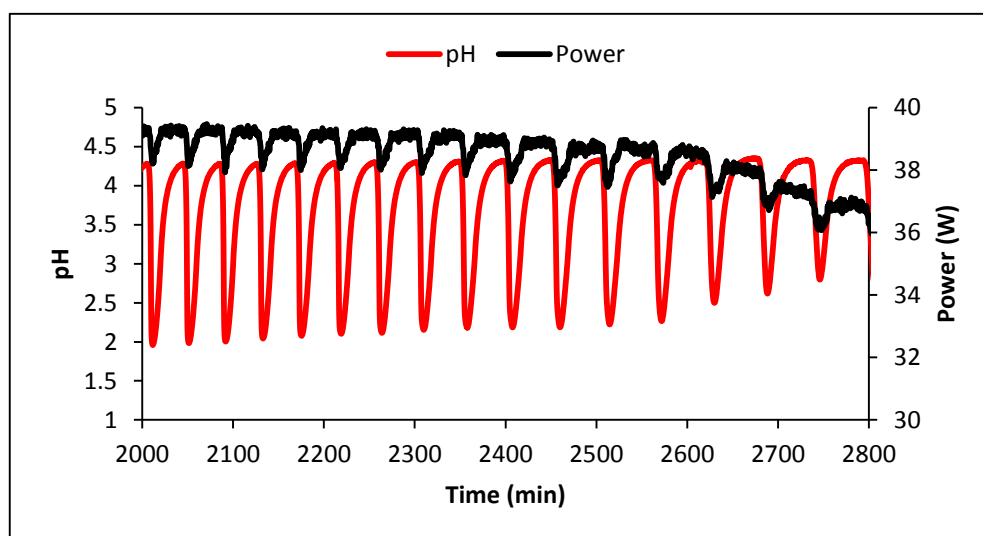


Figure 5.17. The oscillations in pH and heater power are in phase in the oscillatory PCPOC reaction at 20 °C.

The pH oscillations changed shape during the course of the reaction at 20 °C. The oscillations had a saw-tooth waveform when they started, changing to the familiar shark-fin shape once the oscillations were established and then becoming flatter and more symmetrical as they gradually ceased (Figure 5.18).

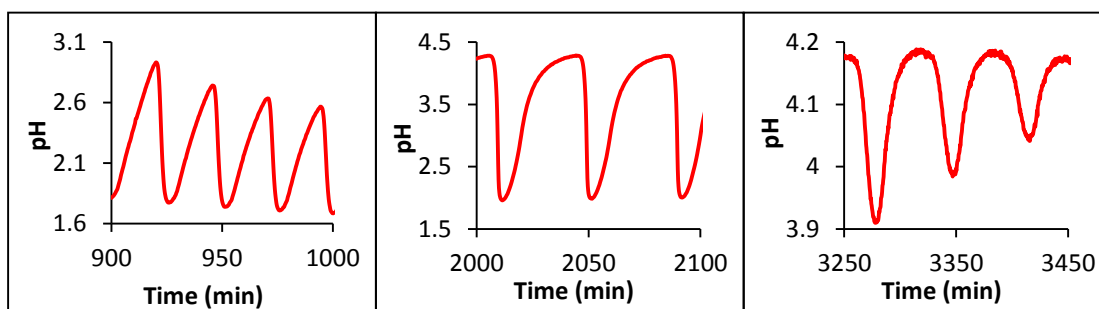


Figure 5.18. The changing shape of pH oscillations during the PCPOC reaction at 20 °C.

The turbidity recorded at 20 °C is shown in Figure 5.19. For most of the reaction the turbidity fluctuated around a value of 30 as it did in the experiment conducted at 40 °C (Figure 5.8).

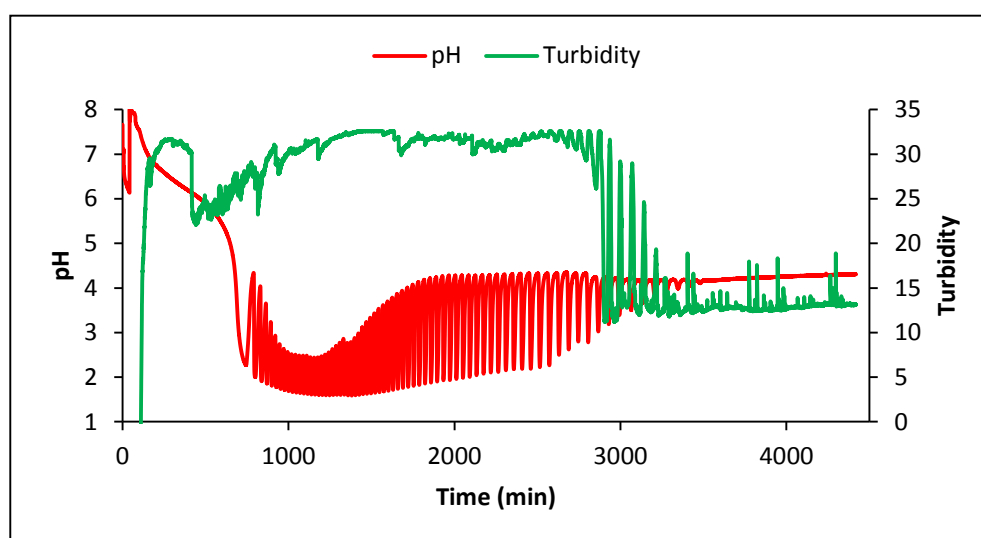


Figure 5.19. Turbidity and pH recorded in the oscillatory PCPOC reaction at 20 °C.

However, at approximately 2200 min the turbidity behaviour began to be more regular until sustained oscillations were observed. Unlike at 30 °C, the turbidity oscillations were out of phase with the pH oscillations (Figure 5.20). At 2882 min a large drop in turbidity was recorded (from 32.3 to 11.3) and oscillations continued from the lower baseline. After the shift in the baseline the largest turbidity oscillations in the PCPOC system were recorded. Subsequently, oscillations in turbidity and pH gradually ceased.

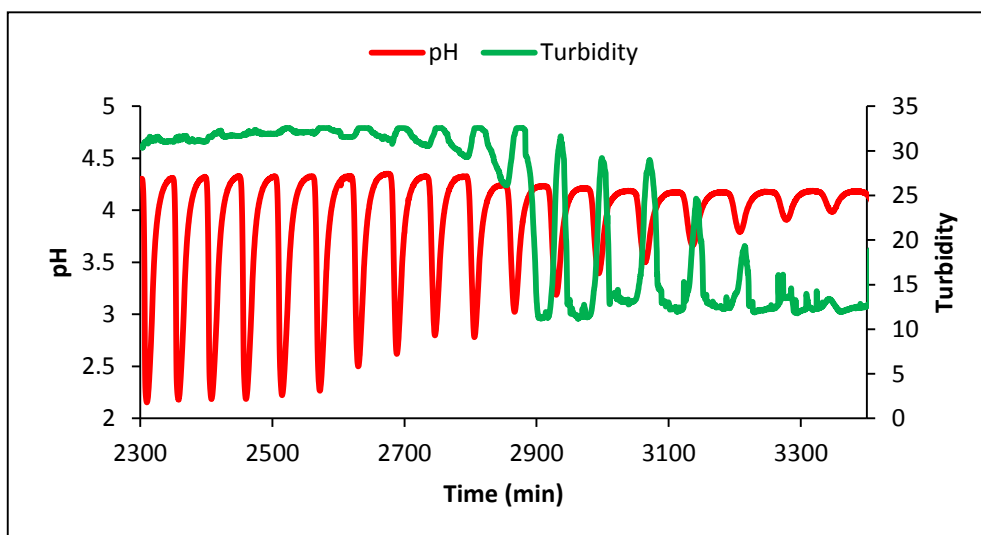


Figure 5.20. The development of oscillations in turbidity that are out of phase with pH oscillations at 20 °C.

At 10 °C there were 2 sets of pH oscillations during the experiment (Figure 5.21) although more sets of oscillations would likely have been observed if the experiment had been run longer as the pH when the experiment was stopped was still in the oscillatory region. As at 20 °C, the period and amplitude of the pH oscillations were much larger than those at 40 °C. The onset of the oscillations again occurred while the pH was still falling following the addition of PhAc.

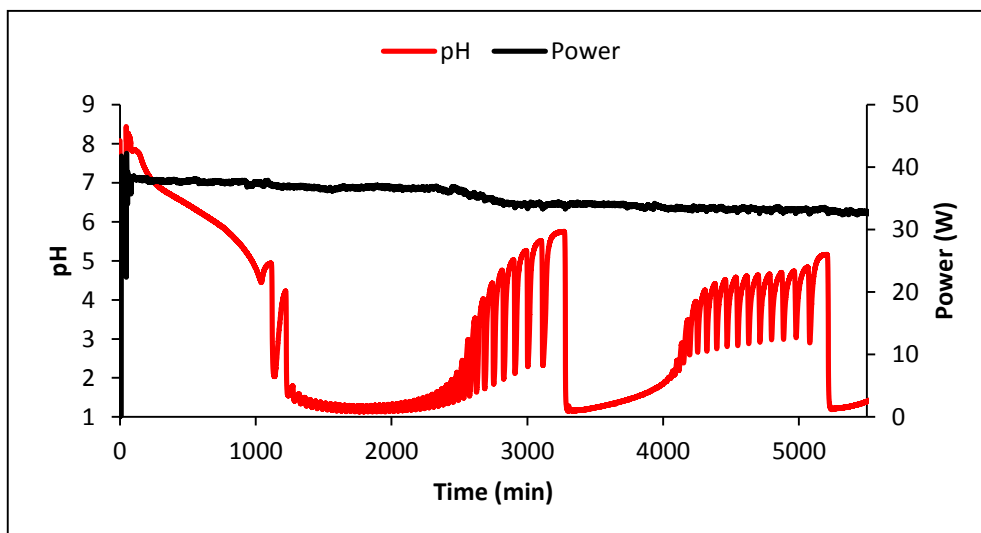


Figure 5.21. pH and heater power in the oscillatory PCPOC reaction at 10 °C.

Figure 5.22 shows the oscillations in pH and power are in phase with the period and amplitude of the power oscillations increasing as the pH oscillations increase.

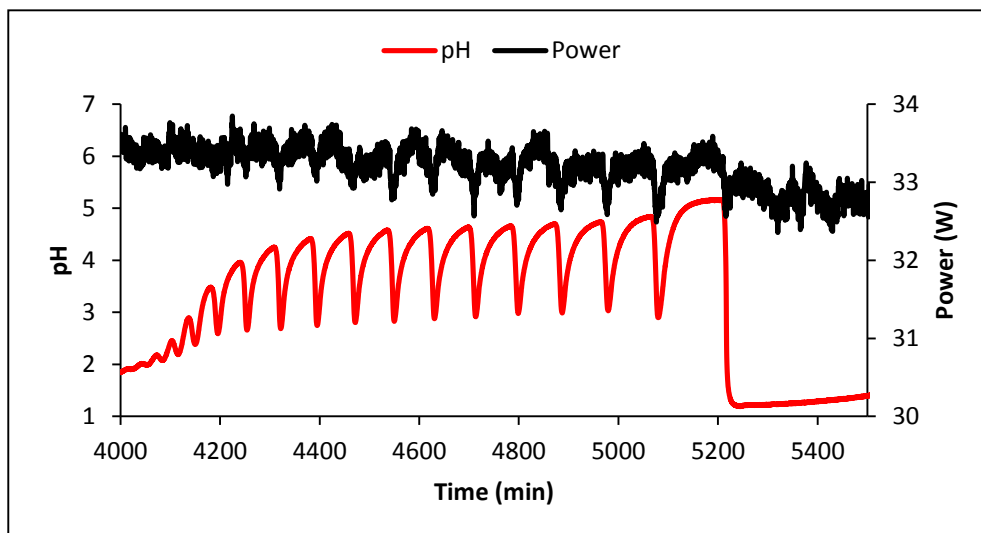


Figure 5.22. In phase oscillations in pH and heater power in the oscillatory PCPOC reaction at 10 °C.

Figure 5.23 shows the turbidity recorded during the PCPOC reaction at 10 °C. The spikes at the beginning of the reaction were due to the addition of reagents to the reactor. Afterwards, the turbidity fluctuated around a value of 30.

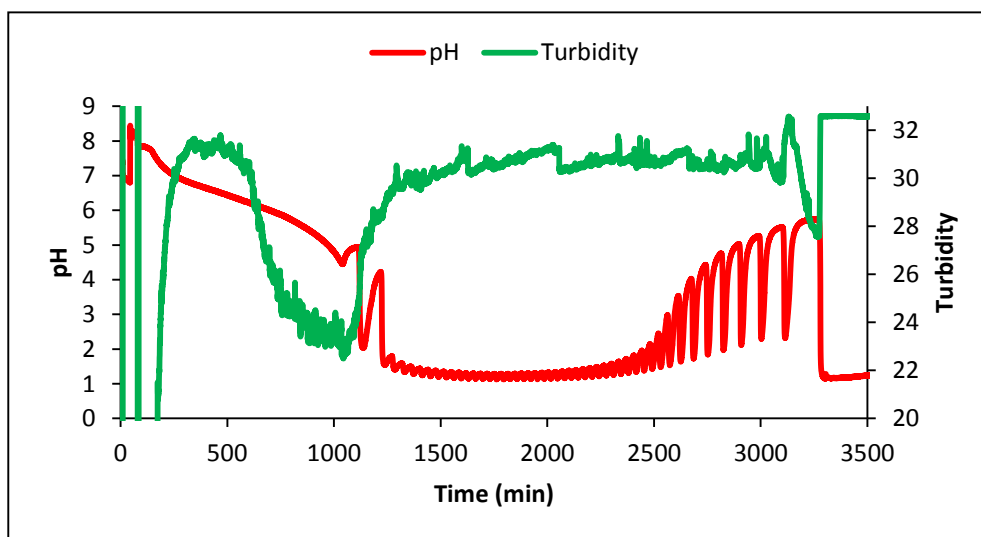


Figure 5.23. Turbidity and pH recorded in the oscillatory PCPOC reaction at 10 °C.

The largest pH oscillations occurred at 0 °C. This experiment also produced several sets of pH oscillations as shown in Figure 5.24. It is noteworthy that a drop in turbidity occurred at the same time as the final oscillation in each set which would suggest that the last pH drop coincided with a drop in the amount of precipitate which then reformed.

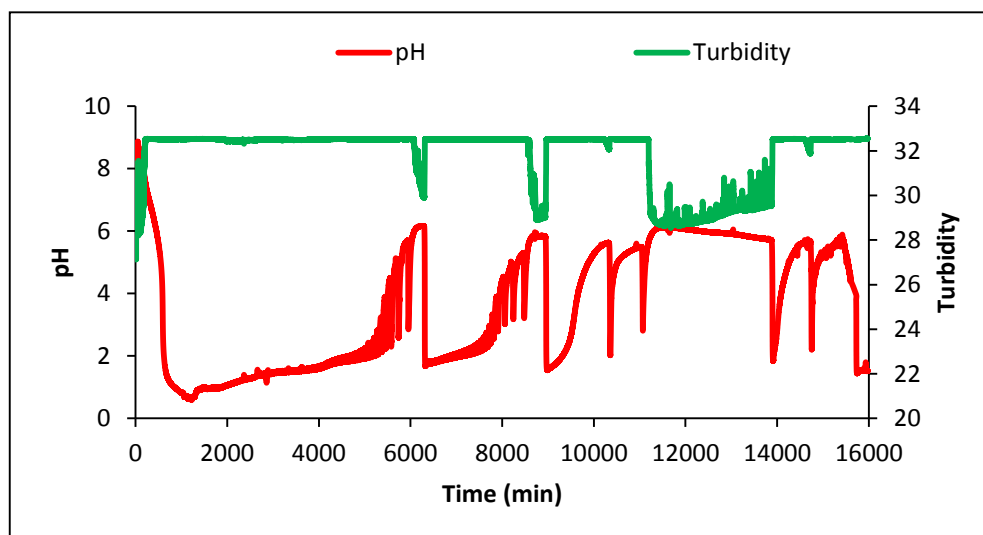


Figure 5.24. Turbidity and pH recorded in the oscillatory PCPOC reaction at 0 °C.

Figure 5.25 shows the power curve to have several large spikes. These were caused by a problem with the PC being used for datalogging. The PC would freeze after running for 2-3 days and needed to be rebooted to allow the experiment to continue. Each time the PC was rebooted a spike was produced in the heater power which was reflected in the power curve presented in Figure 5.25. Switching off the PC did not seem to affect the progress of the reaction for the first 9000 minutes. After this point it is evident from Figure 5.24 that there is a change in the oscillatory behaviour with the pH oscillations becoming irregular.

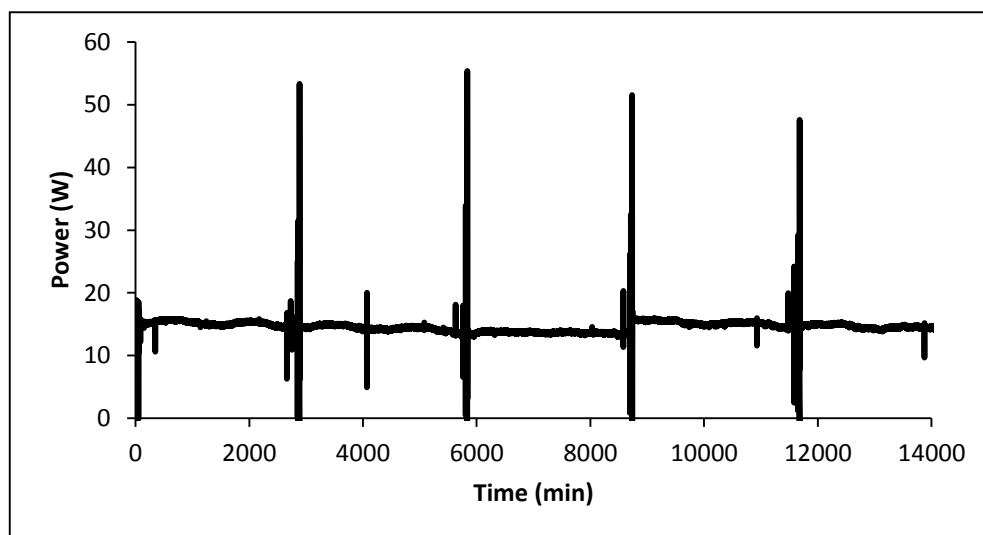


Figure 5.25. Heater power from the oscillatory PCPOC reaction at 0 °C.

5.1.2 Phenylacetylene Conversion

Monitoring changes in reactant and product concentrations is difficult when studying a reaction running for extended periods of time i.e. days, in which the solvent is

evaporating. Evaporation was reduced by working in a closed reactor but the system could not be sealed due to the constant purging of the reactor with CO and air. The evaporation of solvent affects the concentrations of reactant and products in the reactor and hence any changes are therefore difficult to quantify. To solve this problem naphthalene (Np) was added to the reaction mixture as an internal standard prior to the addition of PhAc. The Np was used as an internal standard to calculate the concentrations of reactant and products as described in Appendix B.

When the reaction temperature of the oscillatory PCPOC reaction was reduced from 40 °C to 0 °C as described in Section 4.3.1, the rate of PhAc conversion was reduced. Figure 5.26 shows that the oscillatory PCPOC reaction achieved PhAc conversions of around 90% at reaction temperatures of 20 and 30 °C but at 40 °C the conversion reduced to 80%. At 0 and 10 °C the reaction was stopped while still oscillating (even after 8 days at 0 °C) so the conversions for those experiments may not be the final values.

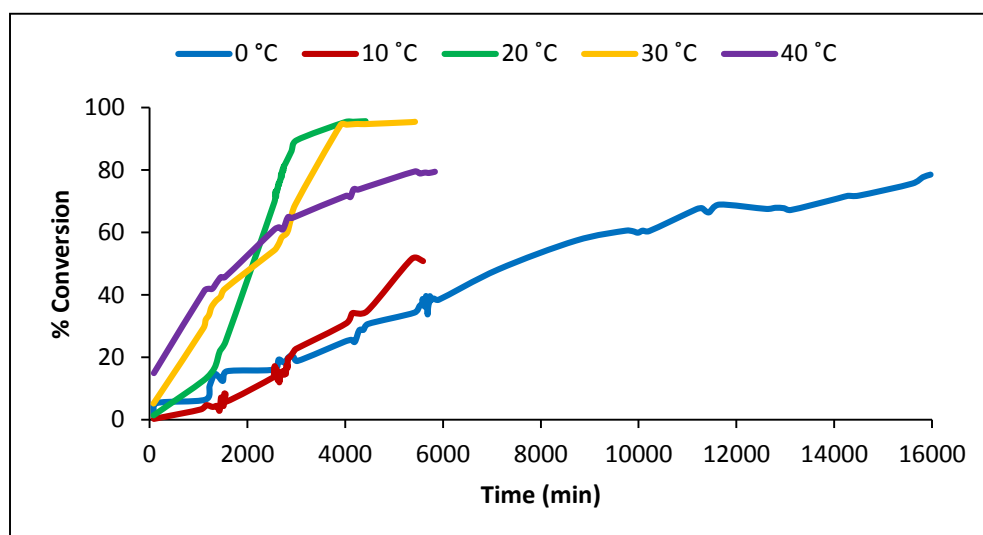


Figure 5.26. Phenylacetylene conversion in the oscillatory PCPOC reaction at 0-40 °C.

Novakovic and colleagues reported PhAc conversions of 73%^[2] and 88.5%^[6] in the oscillatory system at 40 °C although the 88.5% was at higher catalyst concentrations (10 mol%) than those used in this study (2 mol%). Gabriele and colleagues achieved conversions of 80-100% at temperatures of 25-80 °C even though they were using much lower catalyst concentrations (0.0333-0.5 mol%). The 80% conversion was achieved at 80 °C with a PhAc/catalyst molar ratio of 3000. They were, however, operating with a higher PhAc concentration (0.5 mol dm⁻³) than that used in this study (0.124 mol dm⁻³).

Novakovic and colleagues found that the reaction rate increased when the oscillations started.^[2] Figure 5.27 shows the reaction rate also increased in the experiments in this study once the oscillations started. This is most apparent for the experiments conducted at 0 and 40 °C and less obvious for the 10 °C. It was impossible to predict exactly when the reaction would start oscillating at each temperature (occasionally occurring overnight) making it difficult to coordinate the sampling times with the onset of oscillations. This would therefore need to be studied further to be able to quantify the increase.

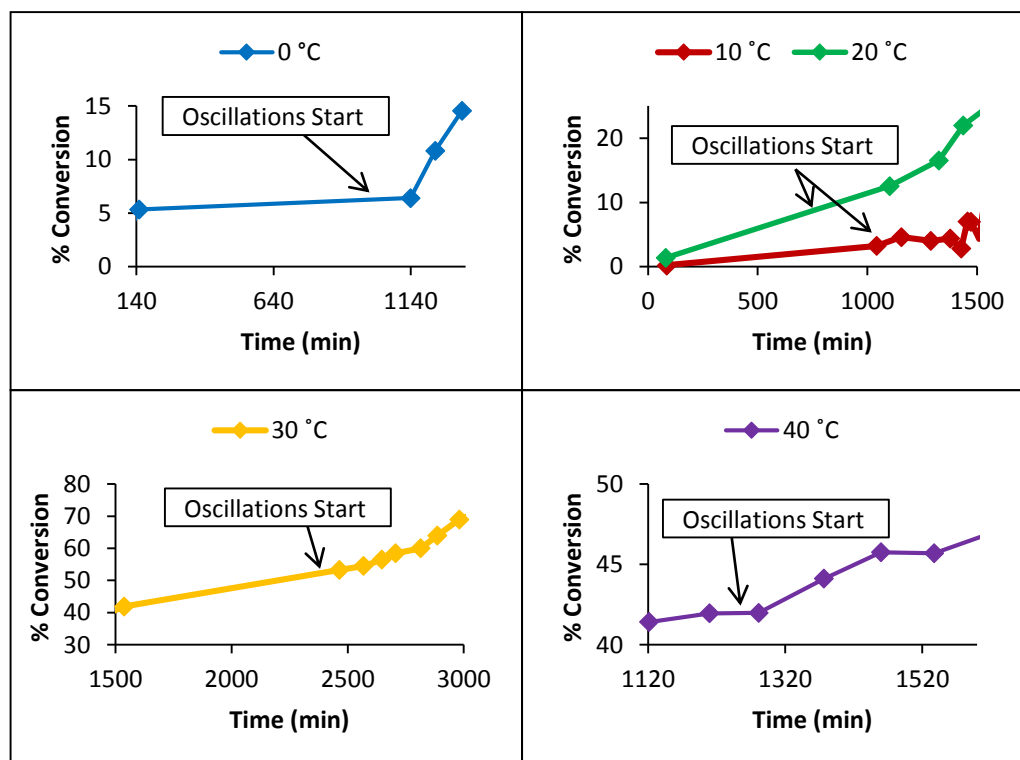


Figure 5.27. The reaction rate of the PCPOC reaction at temperatures from 0-40 °C increased once pH oscillations started.

5.1.3 Product Distribution

Novakovic and colleagues focused their study on the effect of reaction temperature on the pH oscillations in the PCPOC reaction but did not consider how temperature affected the distribution of products during the reaction. As Np was used in the reactor during the experiments it was possible to account for any changes in product concentrations caused by solvent evaporation and therefore follow the product formation during the reaction at each temperature allowing the results to be compared. However, as it could not be certain that the reactions at 0 and 10 °C had finished the product distributions were compared at a similar level of PhAc conversion rather than comparing the last sample taken in each experiment. Figure

5.28 shows how the distribution of products changes with temperature at approximately 70% conversion for the experiments conducted at 0 °C and 20-40 °C. This value of PhAc conversion was chosen as most of the experiments had results at this level of conversion except the experiment conducted at 10 °C. At 10 °C, the maximum PhAc conversion was 51% so the results for this value are shown. It is noticeable that as the temperature reduces the formation of DMO increases whilst the formation of Z-isomer decreases.^[141] Methyl atropate is only detected at 40 °C.

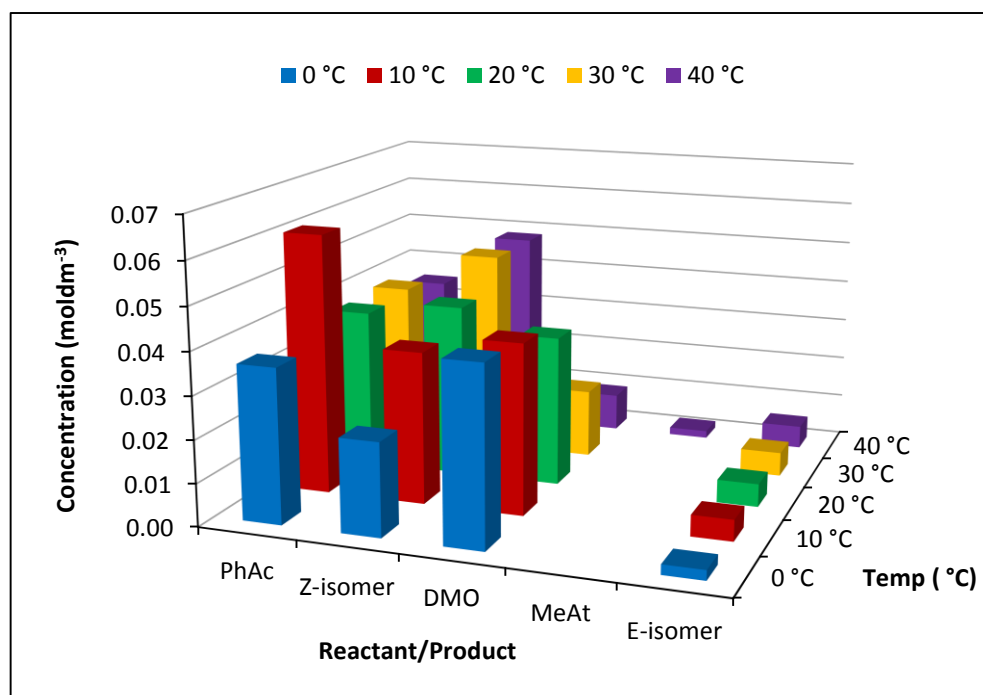


Figure 5.28. Variation in product distribution as reaction temperature is increased from 0-40 °C in the oscillatory PCPOC reaction at 70% PhAc conversion for temperatures of 0 °C and 20-40 °C and 51% PhAc conversion at 10 °C.

The results of the GCMS analysis of samples taken during the experiment conducted at 40 °C are shown in Figure 5.29. Four products were observed with the major product being the Z-isomer. The E-isomer was present at concentrations of $<0.006 \text{ mol dm}^{-3}$ with only trace amounts of MeAt detected.

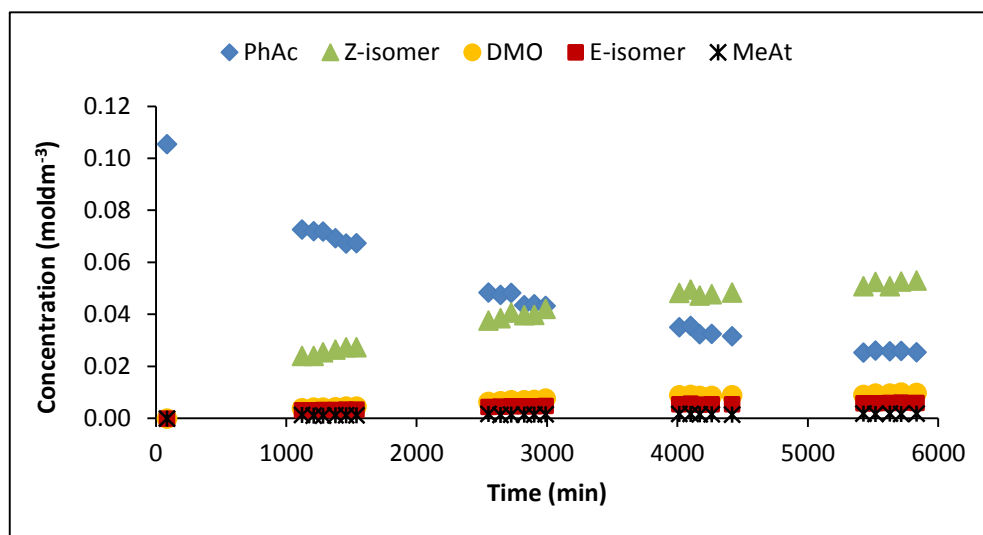


Figure 5.29. Reactant and product distribution in the oscillatory PCPOC reaction at 40 °C.

At 30 °C only 3 products were observed (Figure 5.30). Again the major product was the Z-isomer although there DMO concentration had increased. MeAt was not detected and the E-isomer was present at levels $<0.008 \text{ mol dm}^{-3}$.

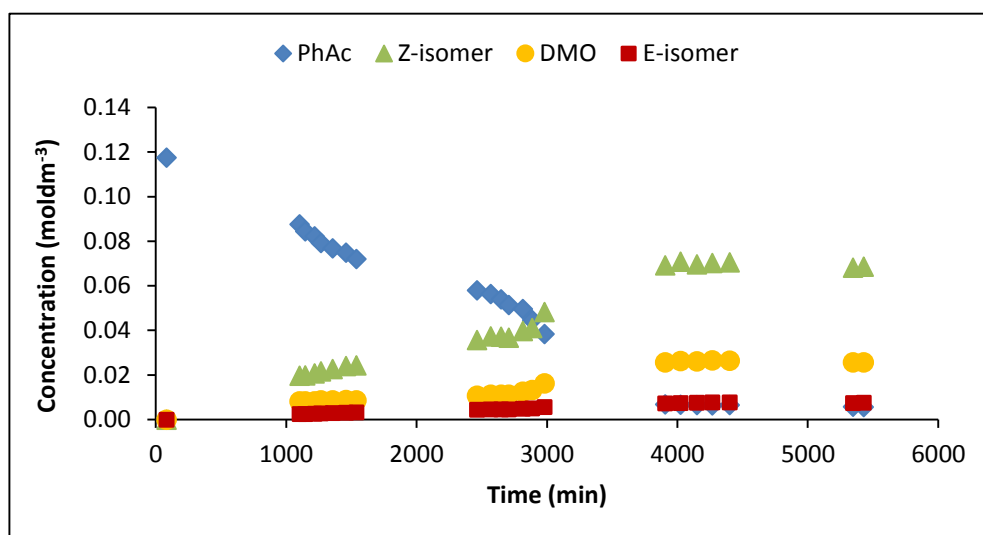


Figure 5.30. Reactant and product distribution in the oscillatory PCPOC reaction at 30 °C.

Figure 5.31 shows that at 20 °C, as at 30 °C, only 3 products were obtained. It is noticeable that as the reaction temperature decreased the formation of DMO increased although the Z-isomer was still the major product. Again E-isomer formation was low ($<0.008 \text{ mol dm}^{-3}$) and MeAt was not detected.

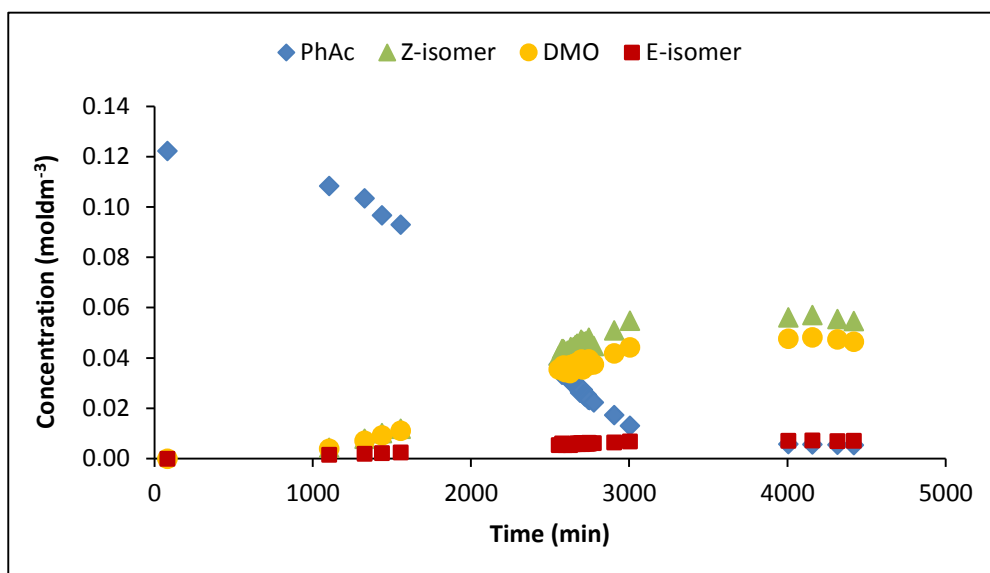


Figure 5.31. Reactant and product distribution in the oscillatory PCPOC reaction at 20 °C.

There were only 3 products detected at 10 °C (Figure 5.32). E-isomer was formed in small quantities, $<0.006\text{mol dm}^{-3}$, but DMO formation increased so that Z-isomer and DMO were formed in almost equal quantities.

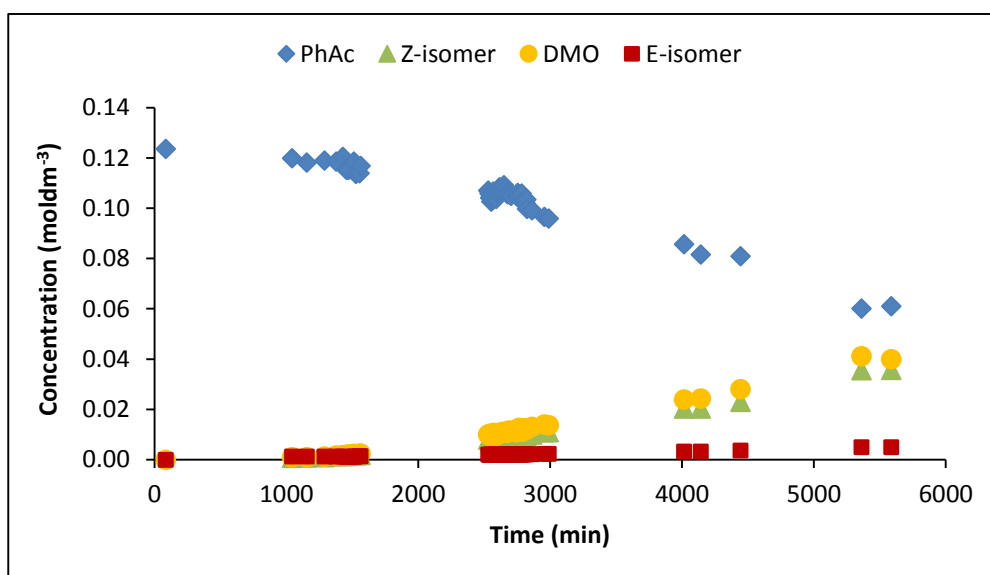


Figure 5.32. Reactant and product distribution in the oscillatory PCPOC reaction at 10 °C.

As Figure 5.33 shows a reaction temperature of 0 °C produced the same 3 products that were produced at 10-30 °C. The major product at 0 °C was DMO with the Z-isomer being formed in appreciable quantities. Again E-isomer was formed in low quantities ($<0.003\text{mol dm}^{-3}$).

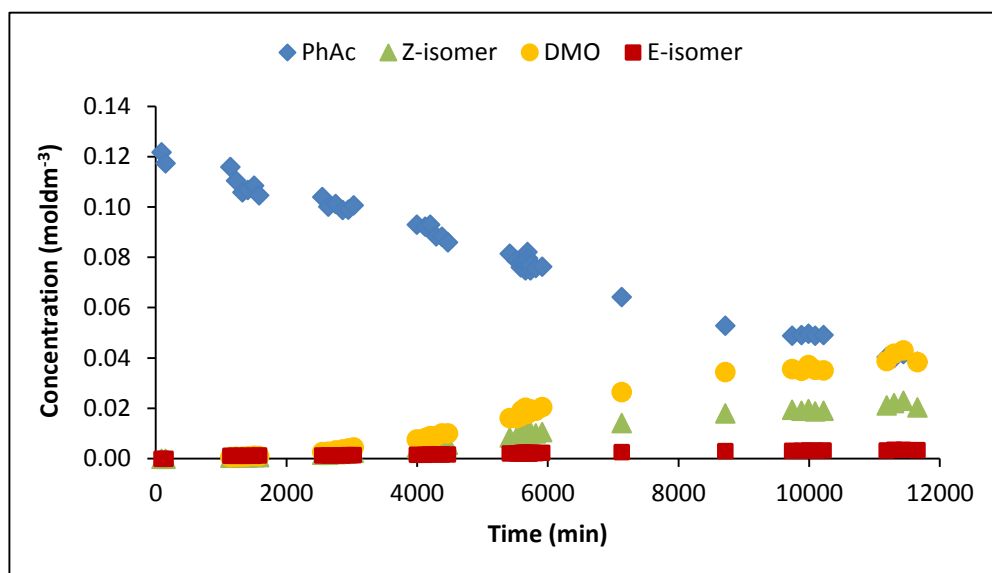


Figure 5.33. Reactant and product distribution in the oscillatory PCPOC reaction at 0 °C.

The change in selectivity is illustrated in Figure 5.34. It shows that at temperatures above 10 °C Z-isomer formation was favoured over the formation of DMO but below 10 °C DMO formation was favoured.

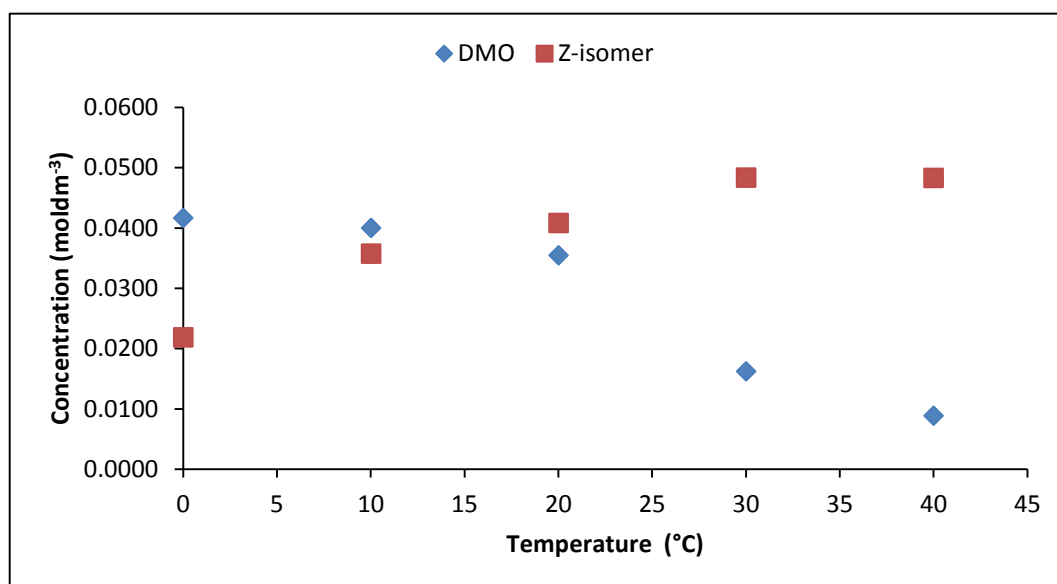


Figure 5.34. The variation of Z-isomer and DMO concentrations with temperature.

This change in selectivity appears to agree with the assertion by Gabrielle *et al*^[130] that DMO is readily transformed into Z-isomer at temperatures higher than 40 °C. Consequently, at temperatures below 40 °C the transformation occurs less readily resulting in increased DMO being detected. However, as they also suggest the Z-isomer may be formed directly from the same acyl(alkoxy)diiodopalladate intermediate that produces the DMO, it may be that the direct pathway to Z-isomer is

favoured at higher temperatures which would lead to lower DMO formation at lower temperatures.

5.1.4 Summary

The experiments on the PCPOC reaction at temperatures from 0-40 °C showed:

- the period and amplitude of the oscillations increased as the reaction temperature was reduced to 0 °C;
- the rate of reaction increased when oscillations started;
- oscillations in heater power and hence Q_r were in phase with pH oscillations;
- oscillations in turbidity were found at 20 °C and 30 °C;
- turbidity oscillations were in phase with pH oscillations at 30 °C;
- turbidity oscillations were out of phase with pH oscillations at 20 °C;
- the formation of Z-isomer was favoured at temperatures above 10 °C;
- the formation of DMO was favoured at temperatures below 10 °C;
- different shapes of the waveform of the pH oscillations occurred at lower temperatures.

5.2 Full PCPOC System - Effect of Increased Water Concentration

One of the interesting observations made during the investigations of the PCPOC reaction at temperatures from 0-40 °C was the effect on the period and amplitude of the pH oscillations of adding methanol to the reaction mixture. Without exception, the addition of methanol caused the period and amplitude of the pH oscillations to increase and even appeared to restart oscillations when they had previously ceased. The methanol is in huge excess relative to the other reactants so is unlikely to be responsible for these observations. The most likely cause is the trace water found in the HPLC methanol (stated as <0.03% by Sigma-Aldrich). Water is therefore proposed to be involved in the processes in the reaction mechanism that produce the pH oscillations. The exact concentration of water in the system is unknown but is very low compared to the concentration of the other reactants in the experiment. If the water concentration is such that it is in excess compared to the other components of the reaction i.e. the PdI_2 and PhAc, then any small increases in water concentration due to the addition of methanol would not have an appreciable effect on the system or the pH oscillations. This would then make it easier to understand how changes in the concentrations of the other reactants affect the system. A series of experiments

in which the water concentration was increased were conducted at 30 °C as this gave large pH oscillations with a reasonable period in a shorter reaction time. The ratio by volume of H₂O:MeOH was increased from 0:100 to 40:60. All experiments were carried out in the HEL Simular reaction calorimeter (Section 4.2.2) so that changes in pH and Q_r could be monitored continuously for extended periods of time allowing direct comparison to the results in Section 5.1. The experiments were conducted following the procedure in Section 4.3.2.

5.2.1 pH

In the oscillatory PCPOC reaction conducted at 30 °C the addition of PhAc to the reactor containing the rest of the catalyst components resulted in a drop in pH from 7.5 to a pH of 1. Over the following 1000 min the pH slowly increased and then oscillations began (Figure 5.35). As the amount of water in the system was increased the initial fall in pH took longer and pH did not recover (Figure 5.35). The extent of the pH drop and the final pH value was dependent on the amount of water in the system – increasing water content reduced the final pH reading. These observations are a consequence of the fact that the standard pH scale is based on measurements in water. As the amount of organic solvent in the system is increased it alters the pK_a of the acid in the system and hence alters the pH that is observed. In 100% methanol pH values can be adjusted by adding 2.3 to the observed pH measurements to get the equivalent pH value in water.^[142] However, as the solvent composition changes the amount by which the observed pH values need to be adjusted also changes.^[143] This means that under the conditions used in these experiments a direct comparison of the observed pH values is meaningless. An interesting observation from Figure 5.35 is the change in shape of the oscillations from regular oscillations when the H₂O:MeOH was 0:100 to stepwise oscillations at H₂O:MeOH of 20:80 and above until at 40:60 oscillations ceased. It is also notable that at H₂O:MeOH of 5:95 and above oscillations started as the pH was falling.

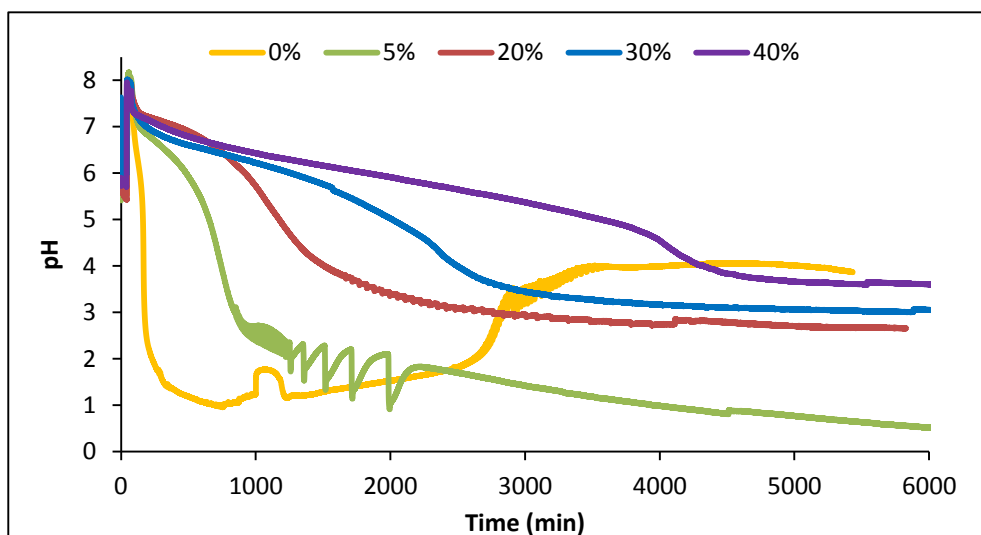


Figure 5.35. Comparison of pH behaviour in the PCPOC reaction at 30 °C with solvent volume ratios of H₂O:MeOH from 0:100 to 40:60.

The trends in the oscillations are summarised in Table 5.3. The amplitude of the oscillations decreased as the amount of water in the system increased although this may be due to the changing water content of the system affecting pH measurement rather than due to changes in the reaction. Increasing the water content of the system will also increase the [H⁺] content of the system making any small changes in [H⁺] and hence oscillations more difficult to see. Table 5.3 shows that increasing the water content of the system from 5 to 30% by volume delayed the onset of oscillations, with the change from 5% to 20% water taking 60% longer before oscillations occur whilst going from 5% to 30% takes almost 3 times longer for oscillations to start. The increase in water content also increased the duration of the oscillations from 1149 min at 5% water to 3122 min at 30% water. This suggests that the increased water content of the system slowed the reaction.

Table 5.3. A summary of trends in the pH oscillations of the PCPOC reaction at 30 °C with solvent volume ratios of H₂O:MeOH from 0:100 to 40:60.

Temperature (°C)	30				
% H ₂ O	0	5	20	30	40
pH trend at onset of oscillations	rising	falling	falling	falling	N/A
pH at onset of oscillations	1.75	2.99	4.35	4.23	N/A
Onset time of oscillations (min)	2421	845	1351	2387	N/A
Oscillations duration (min)	1190	1149	2876	3122	N/A
Max height (pH units)	0.61	1.19	0.10	0.03	N/A
Min height (pH units)	0.003	0.17	0.018	0.007	N/A
Max period (min)	45	277	190	238	N/A
Min period (min)	6	9	5	4	N/A

Oscillations in heater power, although small, were still evident and were in phase with the pH oscillations (Figure 5.36).

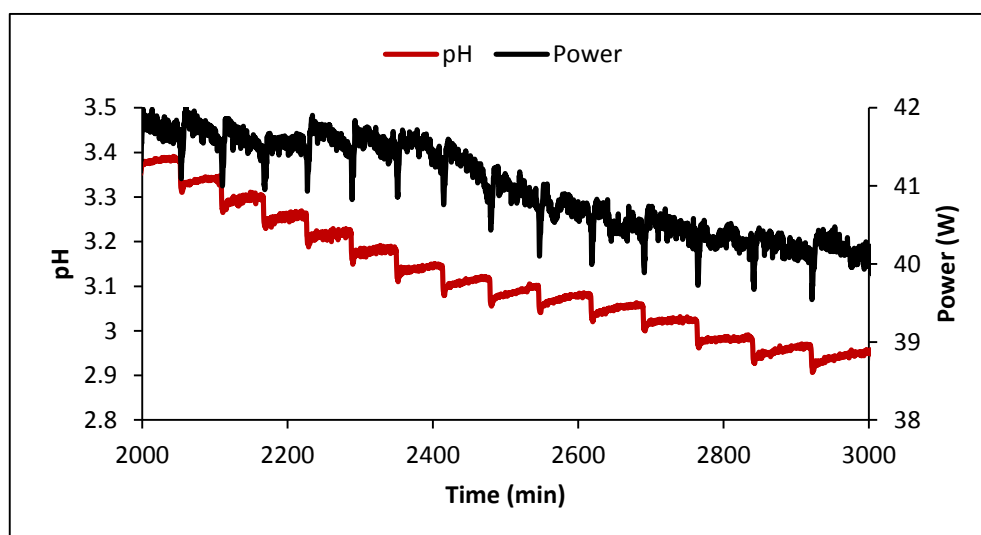


Figure 5.36. Oscillations in pH are accompanied by oscillations in heater power in the PCPOC reaction containing 20% water at 30 °C.

The pH oscillations for each solvent composition are shown in Figure 5.37-Figure 5.41. The pH oscillations in Figure 5.37 were taken as the baseline pH behaviour (100% MeOH) to which the pH behaviour in the other solvent compositions could be compared. In 100% MeOH the pH dropped rapidly after PhAc addition and then rose

slowly over the next 1700 min until it reached a pH of 1.5 after 2421 min when oscillations began (Figure 5.35). Once oscillations started the rate at which the pH rose increased and the pH oscillations gradually increased in period and amplitude (Figure 5.37). The rate of the pH increase then slowed at 2900 min until the oscillations finally stopped.

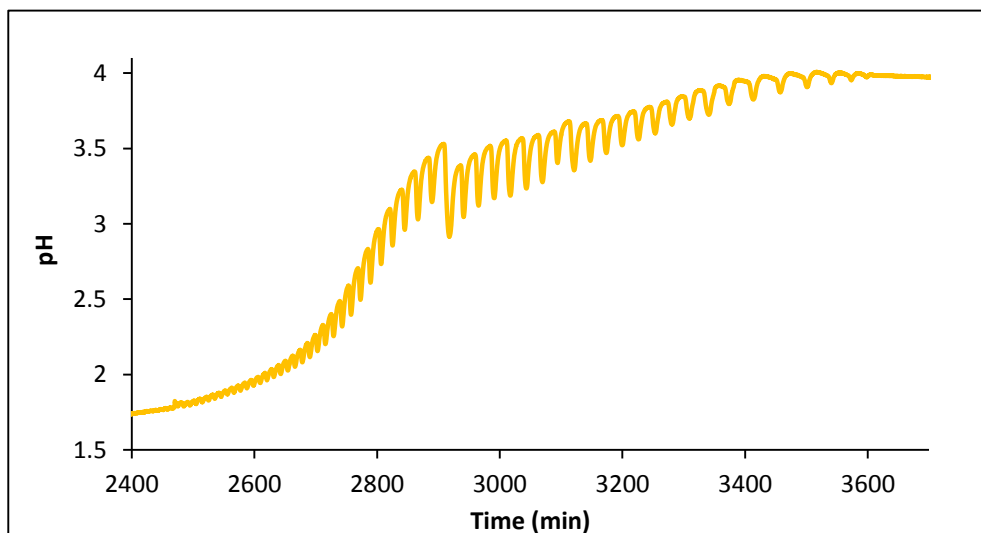


Figure 5.37. pH oscillations in the PCPOC reaction at 30 °C in 100% MeOH.

The pH oscillations for the experiment in which the H₂O:MeOH was 5:95 are shown in Figure 5.38. It shows the onset of pH oscillations occurred when the pH was falling. Initially the shape of the oscillations was similar to that occurring in the baseline experiment conducted in 100% MeOH (Figure 5.37)

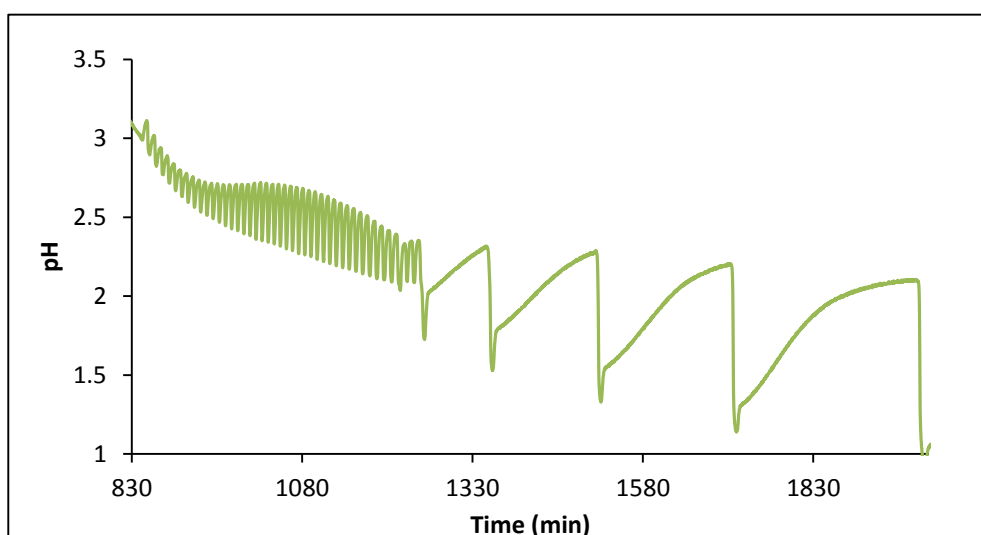


Figure 5.38. pH oscillations in the PCPOC reaction at 30 °C with a H₂O:MeOH solvent volume ratio of 5:95.

Note the switching of the oscillatory behaviour which occurred after 1245 min producing the large relaxation oscillations (Figure 5.38). This was not due to any deliberate perturbation of the system. This may mark a transition from one oscillatory state to another indicating the presence of birhythmicity.

Once the H₂O:MeOH solvent volume ratio reached 20:80 the oscillatory behaviour changed again. The oscillations still occurred when the pH was falling but the shape of the oscillations changed to more stepwise behaviour (Figure 5.39). The period and amplitude of the oscillations was much smaller than in the experiment using 100% MeOH and the experiment with the H₂O:MeOH solvent volume ratio of 5:95 (Figure 5.37 and Figure 5.38).

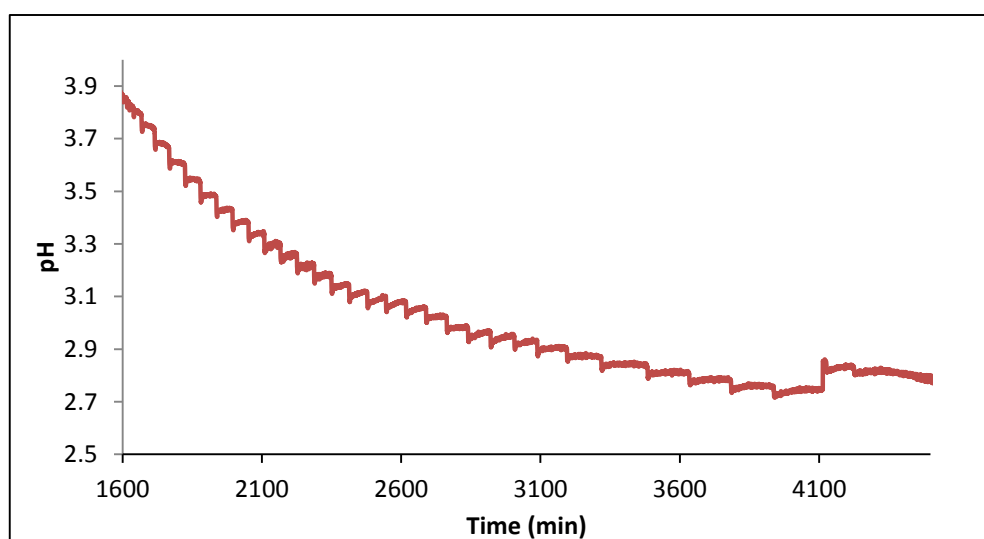


Figure 5.39. pH oscillations in the PCPOC reaction at 30 °C with a H₂O:MeOH solvent volume ratio of 20:80.

However, as the measurement of pH is affected by the composition of the solvent it is difficult to meaningfully compare the differences in amplitude of the pH oscillations between these experiments.

At a H₂O:MeOH solvent volume ratio of 30:70 the oscillatory behaviour was similar to that of the experiment in which the H₂O:MeOH solvent volume ratio was 20:80. The oscillations still occurred when the pH was falling and stepwise pH behaviour was apparent (Figure 5.40). The period and amplitude of the oscillations were reduced even further compared to the experiment using a H₂O:MeOH solvent volume ratio of 20:80 (Figure 5.39). However, as mentioned previously, as the measurement of pH is affected by the composition of the solvent it is difficult to compare the differences in amplitude of the pH oscillations between these experiments.

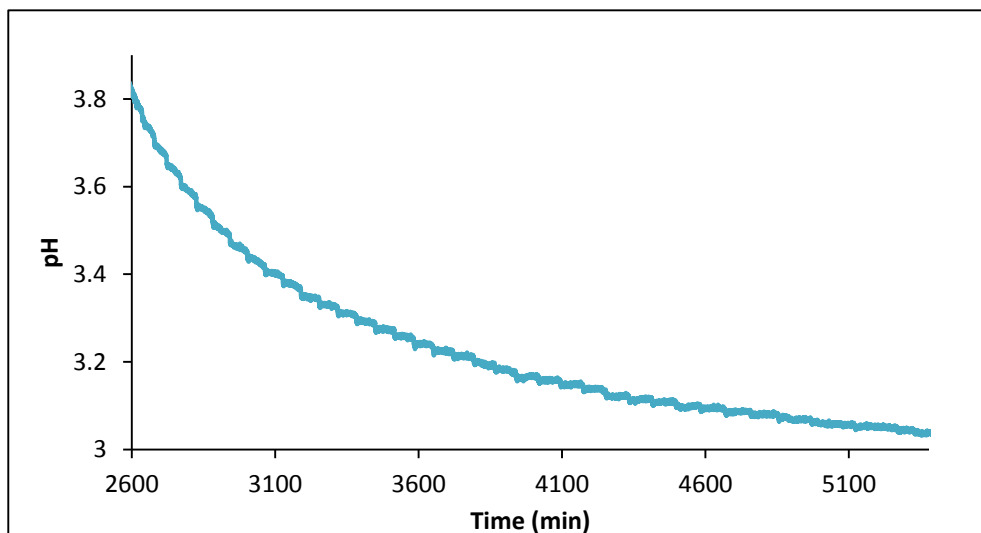


Figure 5.40. pH oscillations in the PCPOC reaction at 30 °C with a H₂O:MeOH solvent volume ratio of 30:70.

By the time a H₂O:MeOH solvent volume ratio of 40:60 was reached (Figure 5.41) pH oscillations were barely discernible. This may be due to the greater concentration of [H⁺] present in the water which could be masking the changes in [H⁺] concentrations due to the reaction.

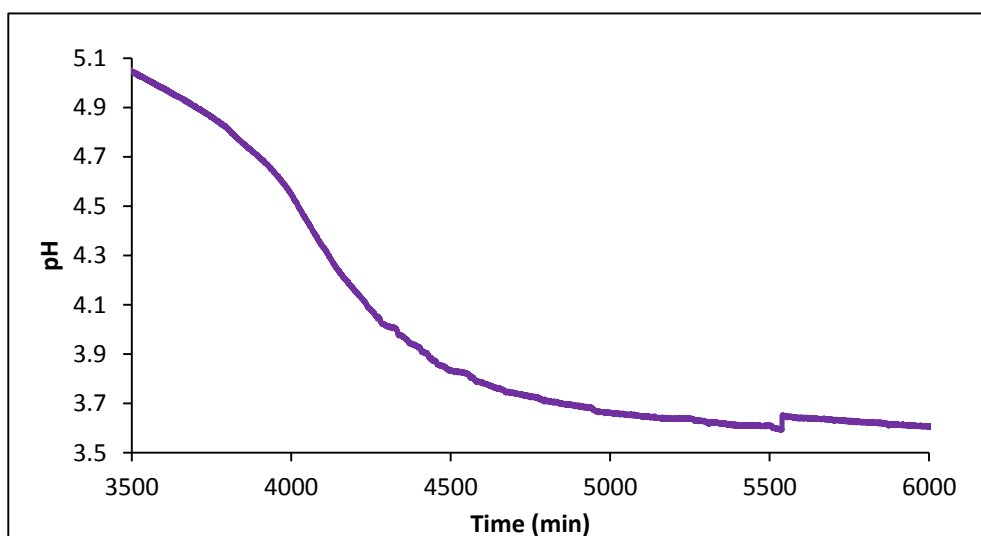
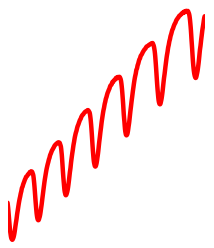
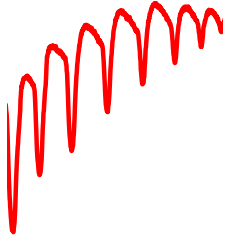

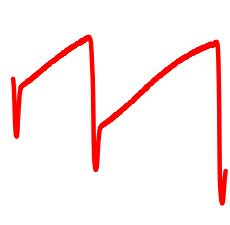
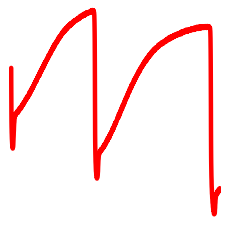



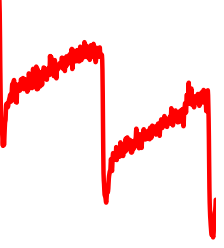




Figure 5.41. pH oscillations in the PCPOC reaction at 30 °C with a H₂O:MeOH solvent volume ratio of 40:60.

The experiments on the PCPOC reaction at temperatures from 0-40°C (Section 5.1.1) found that changing the reaction temperature produced changes in the shape of the pH oscillations. Increasing the water content of the reaction also affects the shape of the pH oscillations as shown in Table 5.4.

Table 5.4. The change in shape of pH oscillations as water content was increased from 0-30% in the PCPOC reaction at 30 °C.

%H ₂ O	Oscillation Waveforms			
0				
5				
20				
30				

As the amount of water in the system increases the oscillations become more step-like in nature. When the water content is 5% and 20% there is also a sudden change from small sinusoidal-type oscillations to large oscillations that are almost square near the end of the reaction. This is shown clearly in Figure 5.42 with the large increase in the period of oscillations between oscillations number 40 and 50, and also around oscillation number 70 when the water content is 30%. This sudden change likely reflects a switch from one stable state to another as the reaction is progressing.

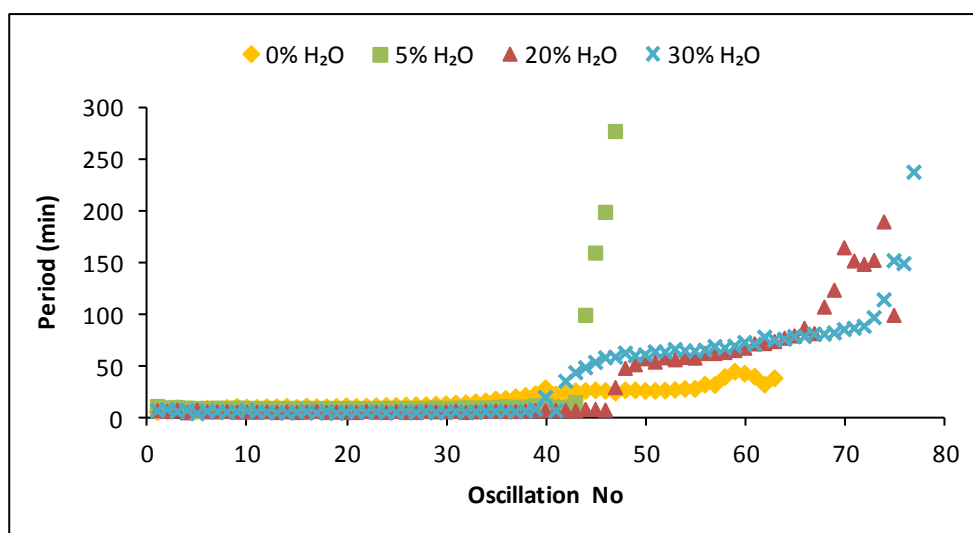


Figure 5.42. The variation in period of the pH oscillations during the PCPOC reaction with water concentrations of 0-30% at 30 °C.

As in the experiments by Novakovic and colleagues,^[134] Figure 5.43 shows the time taken for the pH to drop at the end of each oscillation stayed fairly constant at 1-5 min. The time only increased markedly during the 0% and 5% water experiments at the point in those experiments when the period and amplitude of the oscillations increased dramatically.

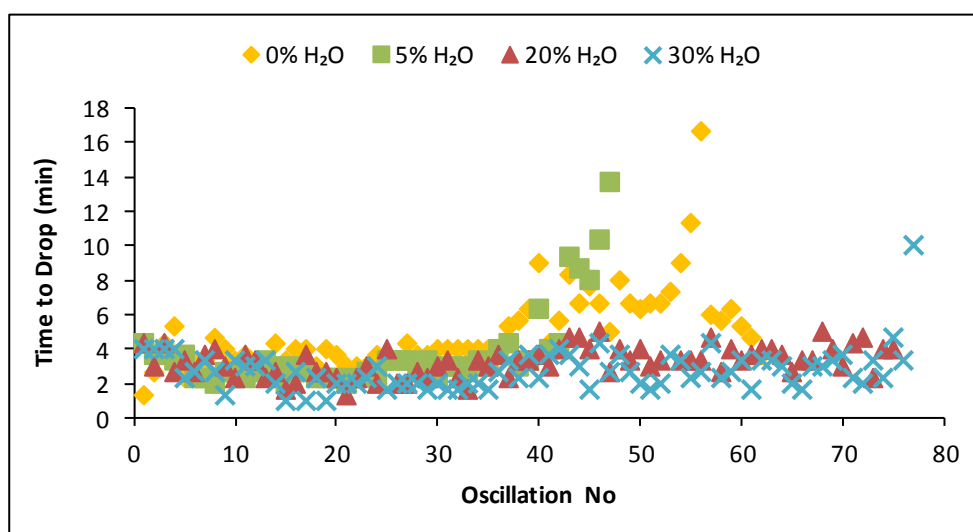


Figure 5.43. The variation in the time taken for the pH to fall rapidly at the end of each oscillation as water content in the system is increased from 0-30%.

As Figure 5.44 shows, increasing the concentration of water in the system initially reduced the time to the onset of oscillations in pH although the onset of oscillations was progressively delayed as the concentration of water increased. The duration of oscillations at 0% and 5% water were similar with the duration of oscillations increasing as the water content increases. At 40% water pH oscillations were not

observed, however the $[H^+]$ produced by the reaction may still be oscillating but it may be insignificant compared to the $[H^+]$ due to the excess water present in the system and hence the oscillations were not detected.

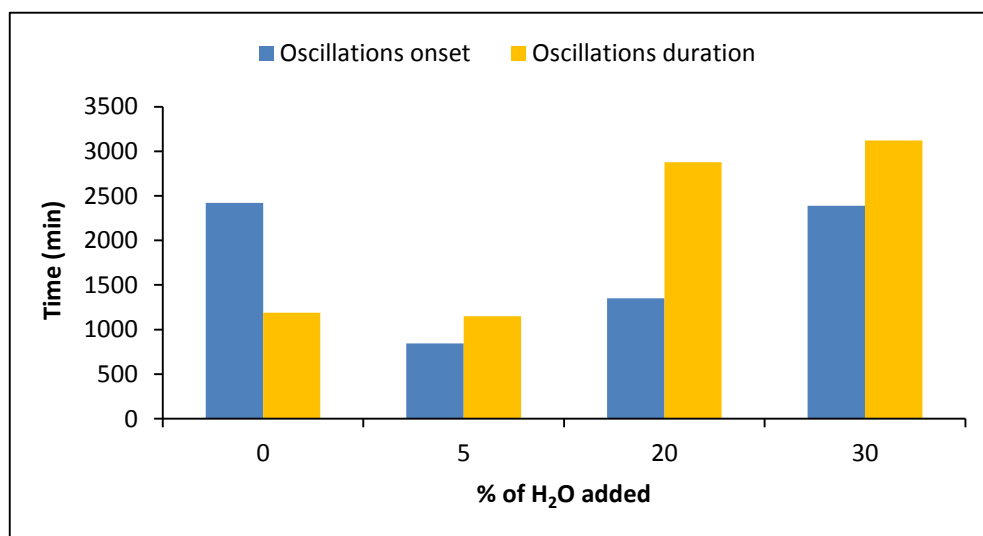


Figure 5.44. The variation in onset time and duration of pH oscillations as water concentration increased from 0-30%.

5.2.2 Phenylacetylene Conversion and Product Formation

GCMS analysis of the samples from the experiments conducted at 30 °C in which the solvent volume ratio of water was increased from 0-40% showed that PhAc conversion was consistently 95-100% (Figure 5.45). Interestingly, as the concentration of water in the system increased the product distribution changed significantly. When the PCPOC reaction was conducted at 30 °C in methanol with no water added the main products were the known products: Z-isomer, DMO and E-isomer. However, as the concentration of water in the system increased the proportion of known products decreased to around 50% of the products formed (Figure 5.45). A number of unknown products appeared with at least 7 unknown products detected by GCMS analysis when the solvent volume ratio was 40% water, although not all peaks were well separated so the number of unidentified products may be more than this.

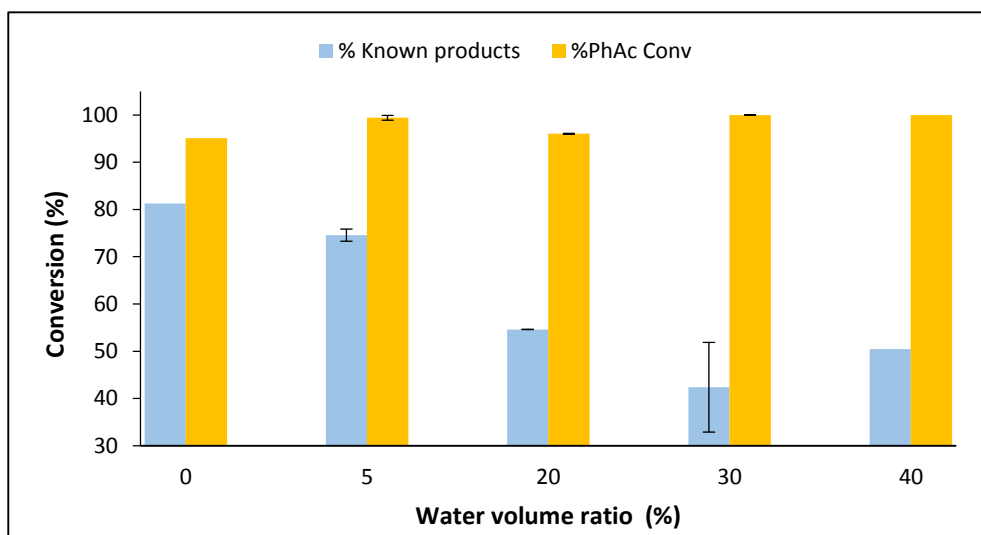


Figure 5.45. PhAc conversion and the percentage of known products produced in the PCPOC reaction at 30 °C as the solvent volume ratio of water is increased from 0-40%. In the case of the 0 and 40% experiments only a single run was conducted.

The retention times of the products varied between 4 and 25 min suggesting the products differ in mass and polarity. It is interesting to note that the mass spectra of all of the unidentified products had the base peak at m/z 105 and contained fragments with m/z of 51 and 77. This is strongly suggestive of the benzoyl ion $C_6H_5CO^+$. Further investigation is needed to identify these products. The variation in the known products with the increase in water in the system is shown in Figure 5.46. The major known product remained the Z-isomer as the concentration of water in the system increased. Increasing the water content of the system to 5% did not affect the final concentration of Z-isomer. As the concentration of water was increased further, however, the concentration of Z-isomer decreased by 1/3. There was a more dramatic reduction of 60% in the proportion of E-isomer formed as the water content increased to 5%. This fell further to a reduction of 86% in the proportion of E-isomer formed when the water content was 40%.

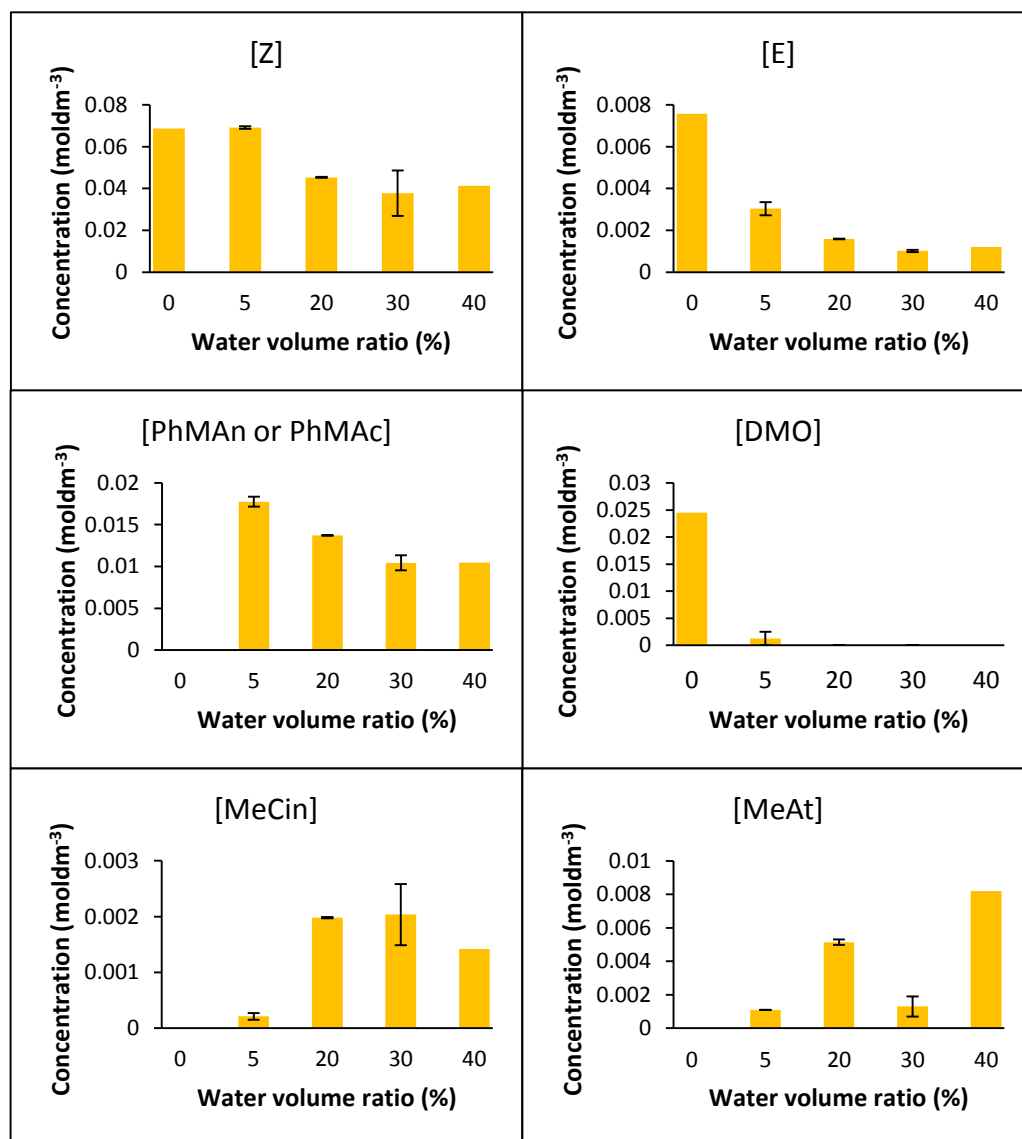


Figure 5.46. Variation in distribution of known products in the PCPOC reaction at 30 °C as the solvent volume ratio of water is increased from 0-40%. In the case of the 0 and 40% experiments only a single run was conducted.

As the water content of the system increased, the formation of DMO ceased and PhMAc or PhMAN formed. The formation of the acid/anhydride in the presence of water agrees with the findings of Gabriele *et al* who obtained maleic acids and anhydrides when the carbonylation of 1-alkynes was conducted in 1,2-dimethoxyethane/H₂O and 1,4-dioxane/H₂O mixtures respectively.^[119] The reaction is reported to occur via CO addition to the IPdCOOH species formed from the reaction of PdI₂ with CO and water. The equivalent reaction involving MeOH instead of water will be a competing reaction in the system under study here, leading to the formation of the Z- and E- diesters. The monocarbonylated products MeAt and MeCin are also detected as the concentration of water increases (Figure 5.46).

5.2.3 Summary

The experiments in this section investigated the effect on the PCPOC reaction of increasing the water concentration in the system from H₂O:MeOH solvent volume ratios of 0:100 to 40:60 at 30 °C.

It was found that increasing water concentration:

- reduces the induction period to the onset of pH oscillations from 2421 min when no water is added to 845 min with H₂O:MeOH solvent volume ratios of 5:95;
- results in a change from defined oscillations to stepwise changes in pH;
- increases the duration of pH oscillations;
- results in a number of different oscillation waveforms;
- has little effect on the time taken for pH to drop rapidly at the end of each oscillation;
- leads to increased PhMAN or PhMAc formation although this reduces as the water concentration continues to increase;
- almost completely inhibits DMO formation;
- reduces E-isomer formation;
- leads to increased formation of the monocarbonylation products MeAt and MeCin.

Chapter 6. Results and Discussion of Experiments on Subsystems of the PCPOC Reaction

The experiments on the PCPOC reaction discussed in Chapter 1 showed that reaction temperature and the concentration of water have an effect on the pH behaviour of the oscillatory PCPOC reaction. In order to determine a possible reaction network behind this oscillatory pH behaviour, the PCPOC reaction was divided into subsystems to be studied separately to understand the interactions of the different components of the reaction system. The experiments consisted of:

- preliminary experiments: to establish baseline parameters;
- experiments on the catalyst subsystem: to uncover possible reactions responsible for hydrogen ion generation;
- experiments involving PhAc without PdI_2 : to find out if hydrogen ion formation occurred without catalyst;
- experiments on the PhAc/catalyst/CO subsystem: to find out how the addition of PhAc affected the pH behaviour of the catalyst and investigate mass transfer limitations.

6.1 Preliminary Subsystems Experiments

To study the subsystems of the PCPOC reaction it is necessary to establish some baseline parameters by measuring the pH of methanol, and determining the solubility of the catalyst components. It was particularly necessary to clear up some discrepancies from the literature involving the solubility of the PdI_2 catalyst. Malashkevich and colleagues reported dissolving PdI_2 , KI and NaOAc in methanol with vigorous stirring for 15 min.^[5] However, Novakovic *et al* reported problems with the granularity of PdI_2 affecting the reproducibility of oscillations.^[2] If the PdI_2 dissolved easily granularity would not be a problem. Therefore an experimental study was needed to establish the solubility of PdI_2 and confirm that of KI.

6.1.1 pH of Methanol

The pH in organic liquids is subject to drift caused by dehydration of the membrane of the pH electrode.^[144] An experiment described in Section 4.4.1 was conducted at room temperature to see how a pH electrode behaved when exposed to methanol for an extended period of time. It also gave a baseline pH reading for the HPLC grade methanol which was to be used in subsequent experiments. As can be seen from

Figure 6.1, initially (time zero) pH dropped sharply when stirring commenced due to the dissolution of CO₂ from the atmosphere. This was followed by a slower decrease over the first 100 min which coincided with a rise in temperature. The pH was otherwise stable at 6.9 for over 16 h so pH drift was not an issue under these conditions.

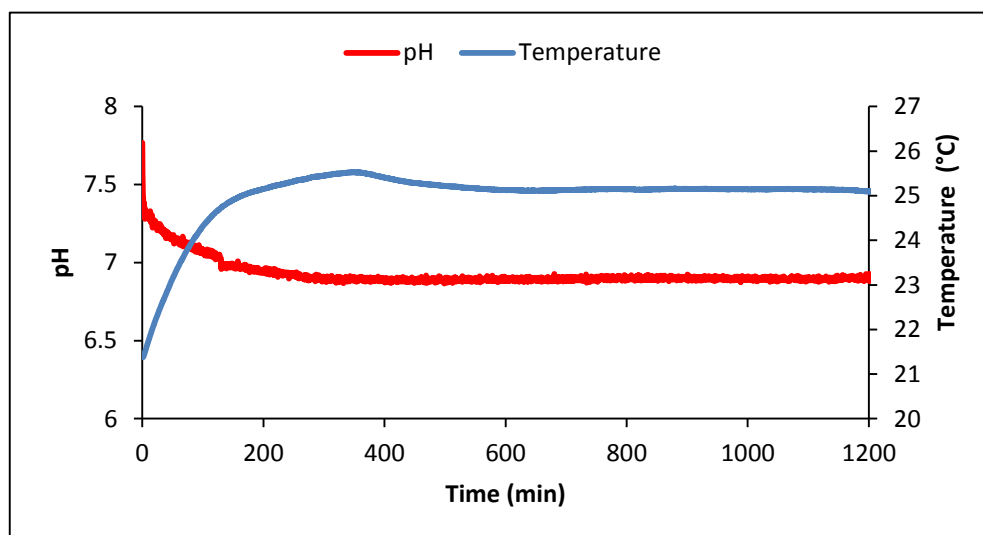


Figure 6.1. pH of methanol.

6.1.2 Solubility of Catalyst Components

Malashkevich *et al* described dissolving PdI₂ in methanol with KI by rapidly stirring for 15 min.^[5] However, this was contradicted by Novakovic *et al* who found that the granularity of the PdI₂ affected its solubility.^[2] Systematic experiments (described in Section 4.4.2) were therefore conducted to independently assess the solubility of the catalyst components.

Experiment 1, described in Section 4.4.2, involved stirring PdI₂ in methanol for 4 h. Even with heating, the bulk of the solid PdI₂ remained in the reaction flask. This confirmed that PdI₂ is insoluble in methanol alone thus necessitating the addition of KI to aid PdI₂ solubility.

Following this, *Experiment 2* (described in Section 4.4.2) determined the solubility of KI in methanol to be 1 g in 8 mL of methanol at 21.4 °C which is in good agreement with the 1g in 7.5 mL reported by Larson and Hunt at 25 °C, although they purified the methanol prior to use in their experiments.^[136] Subsequent experiments were intended to determine the solubility of PdI₂ in a concentrated solution of KI in methanol. A solution of approximately 0.7 moldm⁻³ KI in methanol was, therefore,

prepared (the actual concentration being $0.693 \text{ mol dm}^{-3}$) to ensure all KI remained in solution.

Experiment 3 (see Section 4.4.2) was intended to estimate the solubility of PdI_2 in $0.693 \text{ mol dm}^{-3}$ methanolic KI. PdI_2 was to be gradually added in small amounts to 150 mL of the KI solution while stirring until the PdI_2 no longer dissolved. As Novakovic *et al* added 430 mg PdI_2 to 450 mL of methanol to which 37.39 g of KI was subsequently added^[134] a smaller amount (93 mg) of PdI_2 was initially added to the 150 mL of KI solution with the intention of gradually adding more as it dissolved. On addition of PdI_2 the colour of the solution immediately changed from colourless to dark red-brown indicating the dissolution of PdI_2 . However, after stirring for 200 min visual inspection of the flask revealed that the PdI_2 had not completely dissolved as some black powder remained at the bottom of the flask. Assuming the possibility that the maximum solubility of PdI_2 had been exceeded the experiment was repeated, this time adding only 82 mg of PdI_2 to 150 mL of KI solution. The same colour change was observed and the solution was left to stir for 1 h 45 min after which visual inspection of the solution again found black PdI_2 particles remaining at the bottom of the flask. To ensure that the maximum solubility of PdI_2 in methanolic KI was not exceeded the experiment was repeated adding a much smaller amount (18 mg) of PdI_2 to 150 mL of methanolic KI. The same colour change was noted as in the previous experiments but even though the solution was left to stir for 5 h black PdI_2 still remained in the flask. As Malaskevich *et al* added KI and PdI_2 to methanol at the same time rather than preparing a KI solution first,^[5] this procedure was employed for a subsequent experiment in which 12 mg of PdI_2 and 5.7 mg KI were added to 50 mL of methanol. Again the PdI_2 was not completely soluble in the solution although the colour changed from colourless to red-brown. The pH of each of the solutions was recorded during the experiments and is shown in Figure 6.2. The pH of the KI/MeOH solution was recorded for at least 20 min prior to addition of the PdI_2 . The dips in the pH curves for the solutions in which 93 mg and 82 mg PdI_2 were added to KI/MeOH were caused by the removal of the pH electrode from the KI/MeOH to add the PdI_2 . The second dip in the pH curve for the 82 mg PdI_2 experiment occurred when the pH electrode was removed to inspect the flask to see if the PdI_2 had dissolved. The addition of the PdI_2 had no effect on the pH of the solutions indicating that there was no reaction generating H^+ when PdI_2 was added.

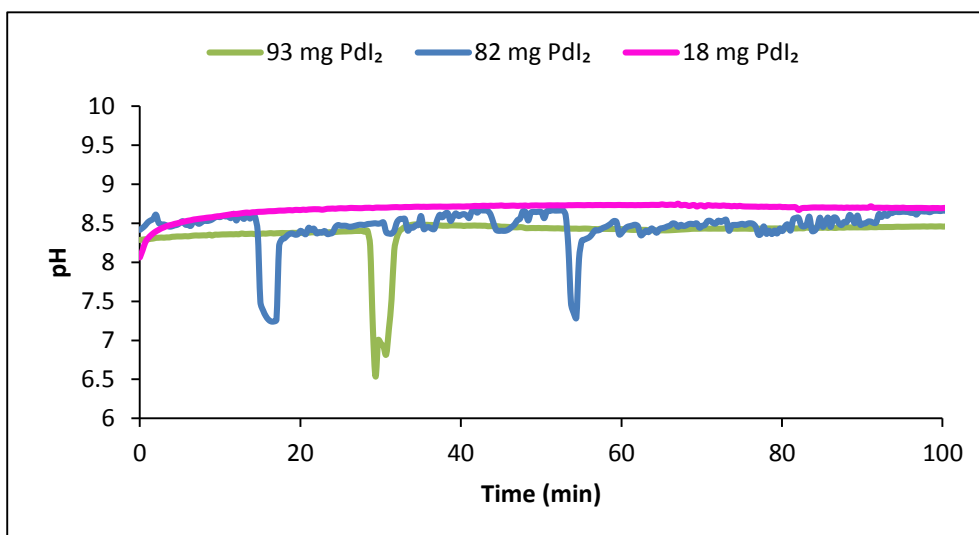


Figure 6.2. Measurements of pH during the addition of PdI_2 to methanolic KI solution, $[\text{KI}] = 0.693 \text{ mol dm}^{-3}$.

Each of the solutions was filtered under vacuum as described in Section 4.2.6 to determine the amount of palladium iodide that had not dissolved and hence the concentrations of the remaining solutions (Table 6.1).

Table 6.1. Concentration of PdI_2 in the solutions from Experiment 3 used to determine the solubility of PdI_2 in methanolic KI.

	PdI_2 Added (mg)			
	12	18	82	93
Mass of PdI_2 on filter (mg)	6	15	34	23
Mass of PdI_2 in solution (mg)	6	3	48	70
Solution volume (mL)	50	150	150	150
Solution concentration (mol dm^{-3})	3.33×10^{-4}	2.78×10^{-4}	8.88×10^{-4}	1.30×10^{-3}

It was found that PdI_2 did not fully dissolve in methanolic KI in any of the experiments conducted here, even after 5 h of stirring. Full dissolution of PdI_2 was not achievable in 15 min as suggested by Malashkevich *et al.*^[5] In fact, instead of giving a definitive value for the solubility of PdI_2 in a $0.693 \text{ mol dm}^{-3}$ solution of KI in methanol the results (Figure 6.3) imply that more PdI_2 dissolves as more PdI_2 is added to the solution.

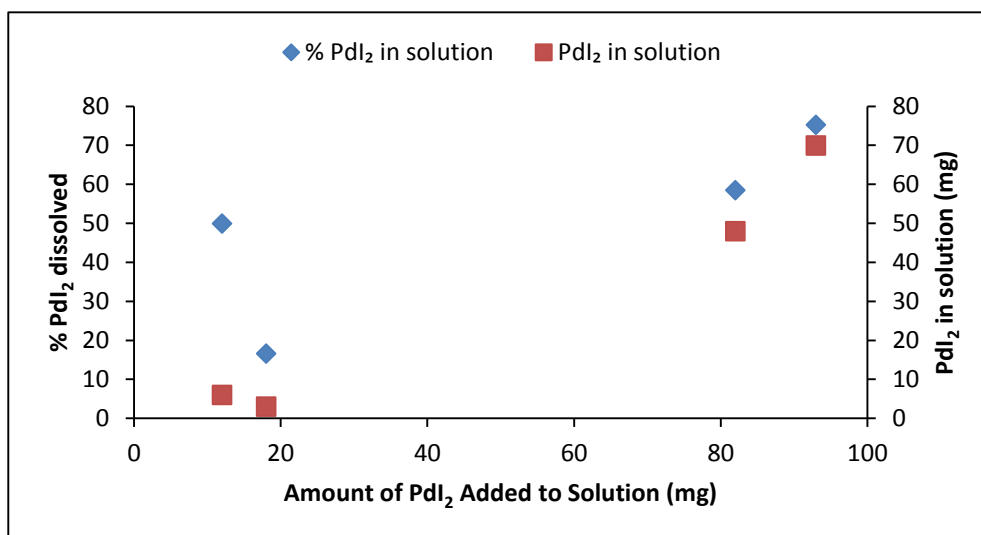


Figure 6.3. Results of the initial experiments to determine the solubility of Pdl₂ in 0.693 moldm⁻³ KI in methanol.

This unusual behaviour has been reported in aqueous solutions of Pdl₂ which required 6-12 days equilibration time before stable solubilities were obtained.^[145] As the solubility of Pdl₂ was not successfully determined from Experiment 3 a larger solubility study was conducted.

Experiment 4 (described in Section 4.4.2) was a larger solubility study in which 5-45 mg Pdl₂ were added to methanol containing 0.5-3 g KI with each solution being stirred for 2 h. After 2 h, the solutions were filtered under vacuum so the amount of Pdl₂ that had dissolved could be determined. The results of the experiment are plotted in Figure 6.4. They show that the maximum solubility of Pdl₂ occurred in the solutions containing 2.5 g of KI in 25 mL of methanol i.e. 0.602 moldm⁻³ and at 3.0 g of KI in 25 mL of methanol i.e. 0.722 moldm⁻³, the solubility of Pdl₂ decreased.

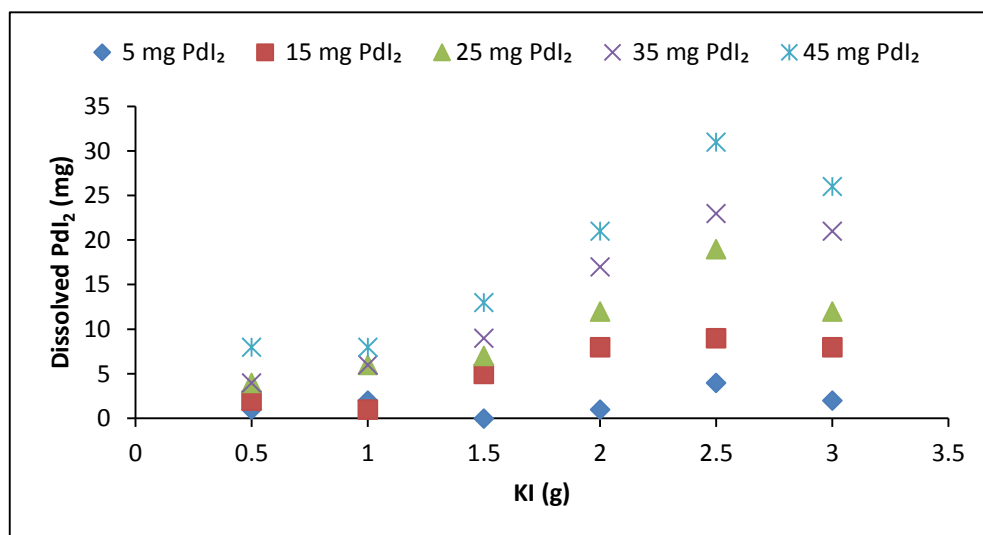


Figure 6.4. Solubility of PdI₂ in methanol containing 0.5-3 g KI.

Experiment 5 (described in Section 4.4.2) looked into the effect of stirring time on the solubility of PdI₂ in a 0.482 moldm⁻³ solution of KI in methanol. Two vials were set up. Vial 1 contained 50 mg PdI₂ in KI solution; vial 2 contained 500 mg PdI₂ in KI solution. After 6 days of stirring, the solutions were filtered under vacuum to determine the PdI₂ concentrations of each solution. Vial 1, which had been stirred for 6 days, had 46 mg of PdI₂ in solution, a concentration of 5.11×10^{-3} moldm⁻³. In contrast vial 2, which had been left for 12 weeks, had 433 mg of PdI₂ in solution, a concentration of 4.81×10^{-2} moldm⁻³. This shows that the solubility of PdI₂ in methanolic potassium iodide solution is dependent on the rate of solubility and can take several weeks for the maximum solubility to be reached. When combined with the results of the other solubility studies it is apparent that the final concentration of PdI₂ in solution for any initial amount of PdI₂ added varies depending on the length of time the solution is stirred and the amount of KI added. This means care must be taken when preparing the catalyst solution to ensure consistency between experiments. Based on this information PdI₂ solutions in methanolic KI were prepared and filtered under vacuum using 0.2 μ m PTFE membrane filters as described in Section 4.2.6 in order to determine the amount of PdI₂ that had dissolved and hence determine the concentration of PdI₂ in the solution.

6.1.3 Reaction of the Catalytic System with CO

The preliminary experiments in this section were designed to acquire insight into the catalytic processes behind the pH oscillations in the PCPOC reaction. The first step was to see how the pH of the catalyst solution behaved when it was purged with CO

in order to find out if reactions with the catalyst were responsible for the drop in pH observed in the PCPOC reaction. The solutions from Experiment 3 described in Section 4.4.2 and discussed in Section 6.1.2 which were intended to determine the solubility of PdI_2 in methanolic KI were purged with CO and their pH was measured to see how it was affected by CO addition. The results (Figure 6.5) show that solutions prepared with the same concentration of potassium iodide but different concentrations of PdI_2 all exhibited two drops in pH when purged with CO.

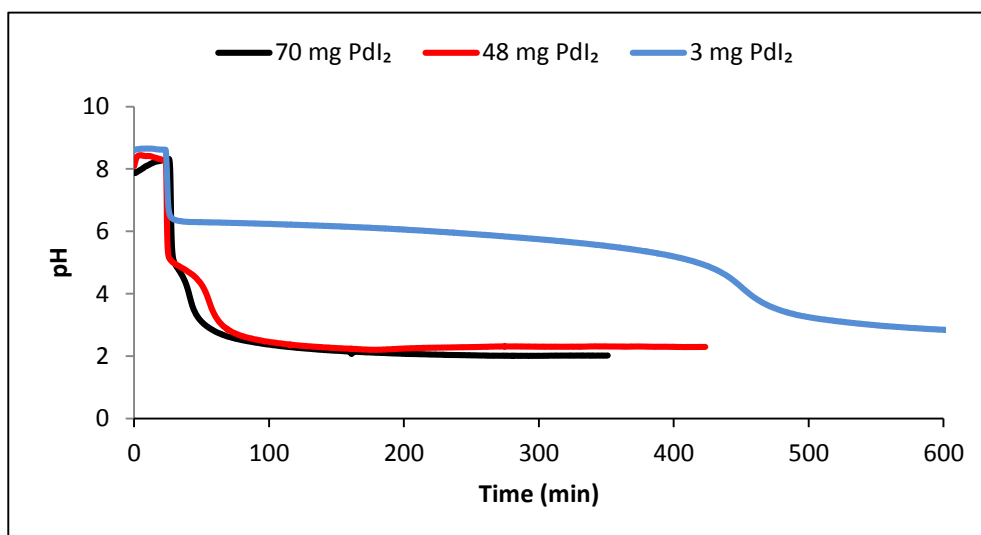


Figure 6.5. The pH behaviour of catalyst solutions containing different amounts of PdI_2 on purging with $\text{CO} = 50 \text{ mLmin}^{-1}$; $[\text{KI}] = 0.693 \text{ mol dm}^{-3}$.

The first pH drop was rapid and it appears it may be dependent on the concentration of PdI_2 in the solutions i.e. the production of H^+ is a function of PdI_2 . However, although the amount of PdI_2 added to the solutions was known, the molar concentrations of the PdI_2 in the solutions was unknown. This was because the final volumes of the solutions following vacuum filtration were not measured as the solutions were not initially intended to be used for experiments. The second pH drop was much slower and the length of the plateau between the pH falls was different for each of the solutions. The plateau was shortest for the solution containing the most PdI_2 and longest for the solution containing the least PdI_2 . This implies that CO is involved in a reaction producing H^+ ions, indicated by the falls in pH, and the reaction producing H^+ ions is dependent on PdI_2 concentration. Gabriele and colleagues suggest a reaction between PdI_2 , MeOH and CO occurs.^[1] This reaction could account for the observed pH behaviour and is given in Equation (6.1).



The shape of the plateau suggests the generation of HI is an autocatalytic process. The results of this experiment suggested the need to investigate the relationship between PdI_2 concentration and the pH behaviour on purging with CO more carefully to see if the extent of the pH drop is dependent on PdI_2 concentration.

6.1.4 Role of Water in the Catalytic System

Malashkevich *et al* mentioned the addition of 2 mmol of water in experiments on the PCPOC system to maintain a constant water concentration.^[5] To understand why this was necessary, experiments were conducted using two different catalyst solutions. Both solutions were prepared using the same amounts of KI and PdI_2 . The first was prepared from standard HPLC methanol without further manipulation, referred to as wet MeOH. The second catalyst solution was prepared using methanol that had been dried over 3 Å molecular sieves, referred to as dried MeOH. Both solutions were purged with CO to see if the pH behaviour and hence the reactions that were occurring in the catalyst solution were affected by the amount of water present in the solutions. An additional experiment was conducted using wet MeOH with a reduced amount of PdI_2 to confirm the results of the experiment discussed in Section 6.1.3 which suggested the extent of the initial drop in pH on CO purging was dependent on PdI_2 concentration. As Figure 6.6 shows, each of the experiments exhibited the same initial fall in pH indicating that the extent of the initial pH drop was independent of the concentration of water and the concentration of PdI_2 .

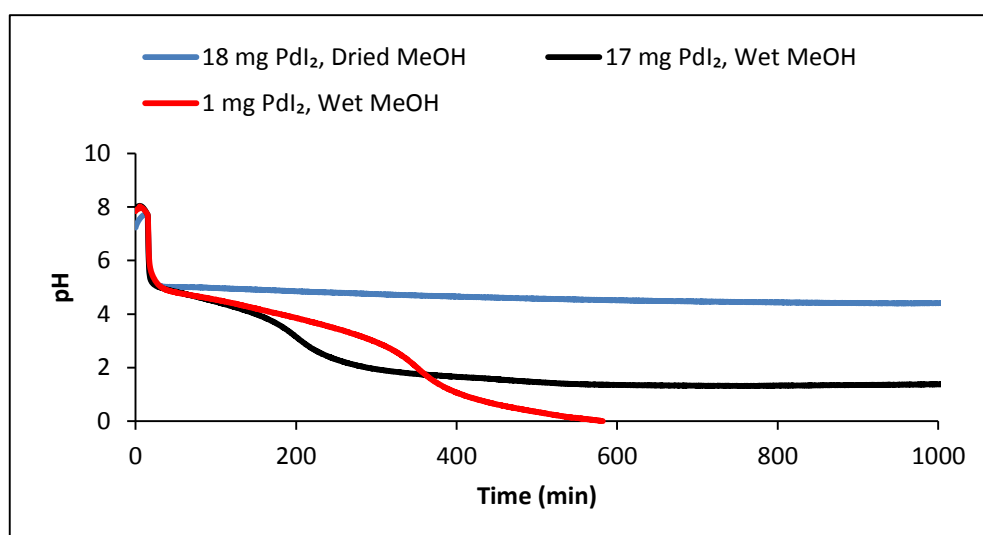


Figure 6.6. Effect of water on the pH of the catalytic system when purging with CO = 50 mLmin⁻¹; solvent = 25 mL; KI = 2.053 g.

The results support the presence of the reaction given in Equation (6.1). However, the experiment conducted in dried methanol did not show any further pH fall in contrast to the two experiments which involved wet methanol. This suggests that the reaction responsible for the second pH drop requires the presence of water. Furthermore, the length of time for the second pH fall to occur in the wet experiments was longer in the experiment with the lower concentration of PdI_2 suggesting that the second reaction is also dependent on PdI_2 concentration. Malashkevich *et al* and Gorodskii *et al* both postulate the existence of a reaction between PdI_2 , CO and water.^[4, 5, 9] This reaction could account for the observed pH behaviour and is shown in Equation (6.2).



Alternatively, Chiusoli *et al* and Gabriele *et al* suggest a reaction analogous to Equation (6.1) in which an organopalladium species is formed (Equation (6.3)).^[119, 146]



6.2 Study of Catalyst Activation

The aim of this work is ultimately to understand the behaviour of the PCPOC reaction in oscillatory and non-oscillatory modes by elucidating the reaction network. The initial experiments have shown that MeOH, CO, PdI_2 and H_2O all have a role to play in the generation of H^+ and the observed pH behaviour in the catalytic system of the PCPOC reaction. A more detailed experimental study on the catalyst system was conducted to investigate the relationship between each of the catalyst components and the observed pH behaviour.^[138]

6.2.1 Modifying Solvents

The experiments discussed in Section 6.1.3 showed that purging PdI_2 solutions in methanolic KI with CO produced a drop in pH. The results of the experiments discussed in Section 6.1.4 showed that the presence of water in the catalyst system during CO purging leads to a second drop in pH that does not occur when water is absent. The drop in pH is consistent with a chemical reaction that produces hydrogen ions on CO addition. To study this further under more controlled conditions, a series of experiments were conducted in methanol, dried methanol and water as described in Section 4.5.1. Figure 6.7 shows that an initial pH drop occurs in all three of the

solvents. However, in water and methanol that had not been dried the pH continues to fall. This suggests a second reaction occurs involving PdI_2 , water and CO. These results agree with those found in Sections 6.1.3 and 6.1.4.

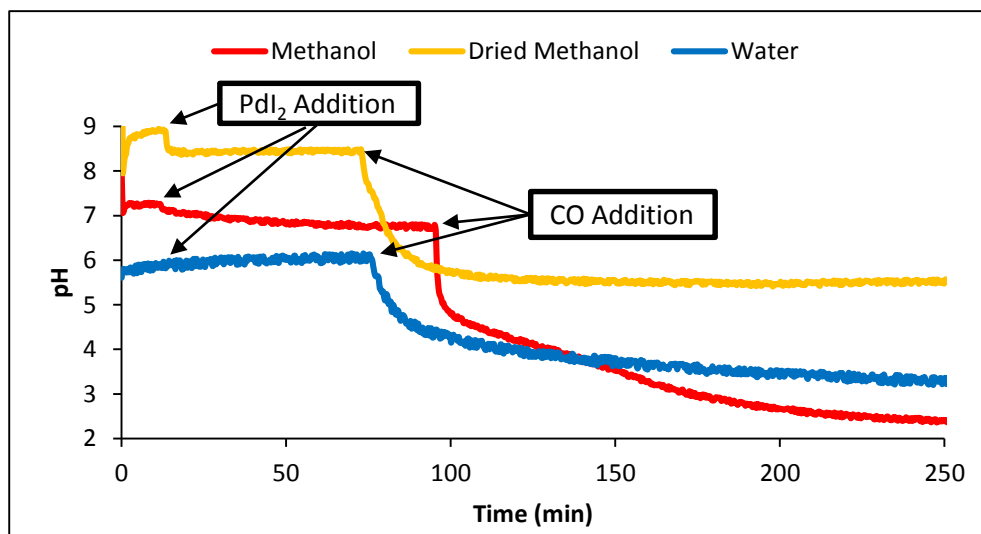


Figure 6.7. pH behaviour of the PdI_2/KI catalyst in water, methanol and dried methanol when purged with CO: $[\text{CO}] = 6 \text{ mLmin}^{-1}$; $[\text{PdI}_2]_{\text{max}} = 2.221 \times 10^{-3} \text{ mol dm}^{-3}$; $[\text{KI}] = 0.48 \text{ mol dm}^{-3}$.

This suggests that PdI_2 , CO and MeOH are reacting according to Equation (6.1) with PdI_2 , CO and water reacting possibly according to Equation (6.2) or (6.3). The colour of the methanolic solutions was dark red-brown and remained so throughout the experiment. The aqueous solution was brown initially but over the course of the experiment it became colourless and a black precipitate was observed. No precipitate was observed in either of the experiments using methanolic solutions. This suggests a reaction leading to the production of $\text{Pd}(0)$. As the precipitate is not observed in the methanolic solutions it could suggest there is a second process which consumes $\text{Pd}(0)$. These observations would be consistent with the decomposition of HPdI (formed by the reaction of PdI_2 , CO and H_2O (Equation (6.1)) or the decomposition of IPdCOOH formed by the reaction in Equation (6.3)).^[1, 9, 119] These reactions are shown in Equations (6.4) and (6.5).



The occurrence of the reactions in Equations (6.4) and (6.5) may account for the second pH drop that is seen in the experiment with wet methanol and in water but not observed when dry methanol is used. The amount of PdI_2 added to each of the solutions was the same and yet the pH of the dried methanolic solution does not fall

as far as the pH of the wet methanolic solution. This implies that HI generation is not as great when the reaction occurs in dried conditions. As the amount of PdI_2 is the same in each experiment this difference in pH drop is most likely due to the way in which PdI_2 reacts. If PdI_2 reacts according to Equation (6.2) producing HPdI (or according to Equation (6.3) producing IPdCOOH which then decomposes to HPdI , as in Equation (6.4)) followed by the decomposition of HPdI (producing HI), then the overall process will generate twice as much HI as the equivalent reaction with methanol (Equation (6.6)).



It may also be the case that the reaction of PdI_2 , CO and MeOH is limited in some way, for example if the process is reversible. The lack of a precipitate in the methanolic experiments may be due to a reaction which consumes it. Gorodskii and colleagues suggest the active catalytic species is a Pd(I) complex.^[4] They suggest a suitable reaction for its formation is that shown in Equation (6.7).



6.2.2 Adding CO Prior to PdI_2

The experiments by Novakovic *et al* added PdI_2 to methanol in the reaction vessel along with KI prior to the onset of CO purging.^[2, 3, 134] In order to see any differences in the initial reactions between catalyst components and CO, small scale experiments were conducted in wet and dried methanol to see if there were any differences in pH behaviour when CO was added prior to PdI_2 . If so, this may indicate alternative reactions of the catalyst components. The experimental procedure is described in Section 4.5.2 and the results of the experiments are shown in Figure 6.8.

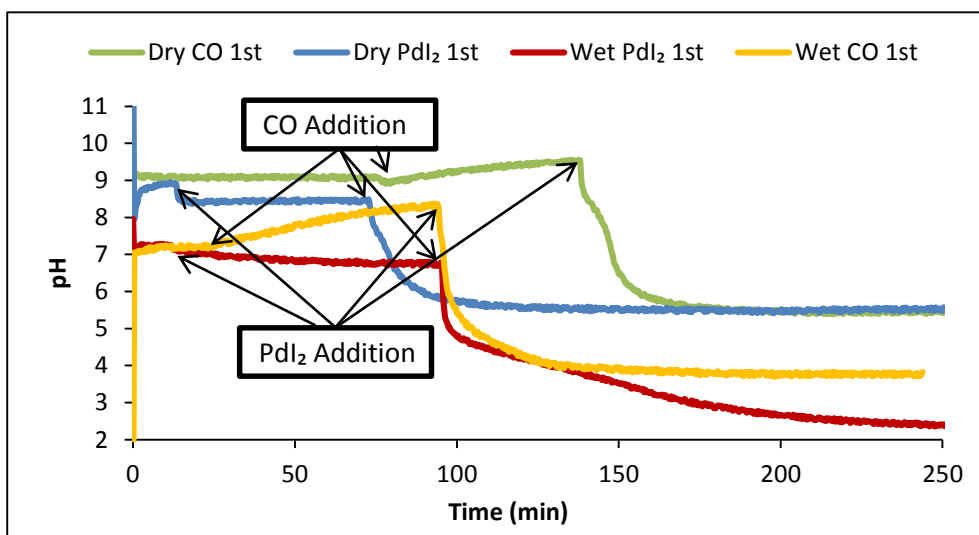


Figure 6.8. Comparison of pH behaviour in the catalytic system when CO is added to wet or dried methanolic KI solution: i) before PdI₂ is added; ii) after PdI₂ is added.

Note that the experiments conducted in dried MeOH had a higher initial starting pH than the experiments conducted in wet MeOH. Figure 6.8 also shows that regardless of whether PdI₂ or CO was added first there was no significant change in the pH behaviour until the other reactant was added. Only then did the pH drop significantly indicating the rapid production of H⁺ via a reaction involving PdI₂ and CO. As discussed in Section 6.2.1, this is likely due to the reaction shown in Equation (6.1).

It is also noticeable from Figure 6.8 that, as in previous experiments, the pH in the wet experiments dropped to a lower value than the pH in the dried experiments. This is likely due to the additional reaction between PdI₂, CO and water given in Equations (6.2) and (6.3).

6.2.3 Filtered Catalyst Solution

The rate of PdI₂ dissolution is very slow. To ensure the initial concentration of PdI₂ was known for all experiments the catalyst solution was prepared in advance and filtered before use as detailed in Section 4.5.3. The PdI₂ concentration was then calculated based on the amount of PdI₂ remaining on the dry filter as follows:

Weight of unused filter = 106 mg

Weight of filter & PdI₂ after rinsing/drying = 122 mg

Weight of filter & PdI₂ after rinsing/drying + 60 min drying = 122 mg

Mass of PdI₂ on filter = 16 mg

Calculated concentration of PdI₂ in catalyst solution = $2.22 \times 10^{-3} \text{ mol dm}^{-3}$

Comparing the results from the baseline experiment with the results from the experiment where extra KI was added (Figure 6.9) shows that the increased KI concentration had little effect on the pH of the solution as the initial values are similar. It also had little effect on the behaviour of the catalyst system when purging with CO. The same initial pH drop occurred and the pH settled to pH 2 in both cases.

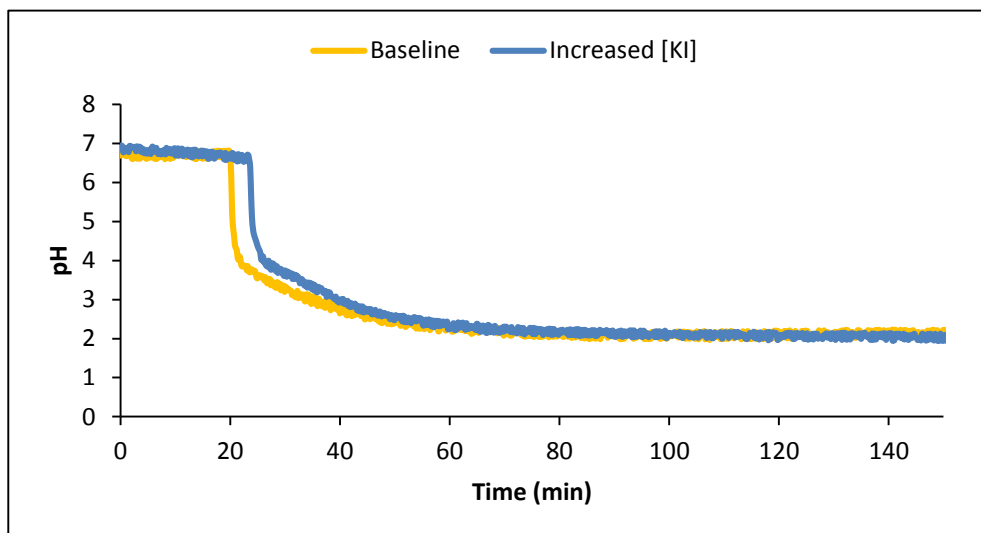


Figure 6.9. The effect of increased [KI] on the pH behaviour of the catalyst solution with CO. It may be that the concentration of CO in the solution is already in such excess that any effect of KI on CO solubility is not affecting the behaviour of the catalyst and therefore is not shown by the pH curve of catalyst solution when [KI] is increased. The effect of diluting the catalyst solution is shown in Figure 6.10.

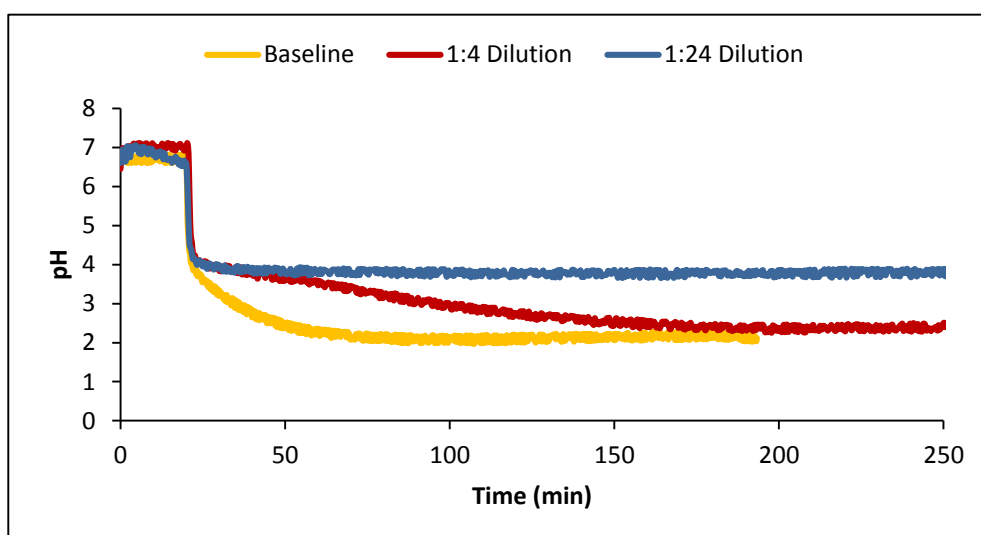


Figure 6.10. Effect of catalyst dilution on pH behaviour when purging with CO. It is apparent from this plot that the initial pH drop on purging with CO is independent of PdI_2 concentration as the pH drops to the same value (pH 4) in the baseline

experiment and the experiments using diluted catalyst solution. It is clear that the second pH fall is dependent on the concentration of PdI_2 : the baseline solution - the most concentrated solution – displayed the fastest second pH fall whereas the least concentrated displayed no fall 225 min after purging with CO began. These results agree with those of the experiments discussed in Section 6.1.4 which used solutions containing different amounts of PdI_2 .

Finally, the effect of increasing the flow of carbon monoxide to the catalyst system was studied. Using a dilute catalyst solution ($[\text{PdI}_2] = 4.44 \times 10^{-4} \text{ mol dm}^{-3}$) the flow of CO was increased by more than 800% from 6 mL min^{-1} to 50 mL min^{-1} . Figure 6.11 shows that the behaviour of the recorded pH is not affected by the increase in the rate of CO addition. This suggests CO flow rate does not affect gas-liquid mass transfer rates under the conditions used in this experiment.

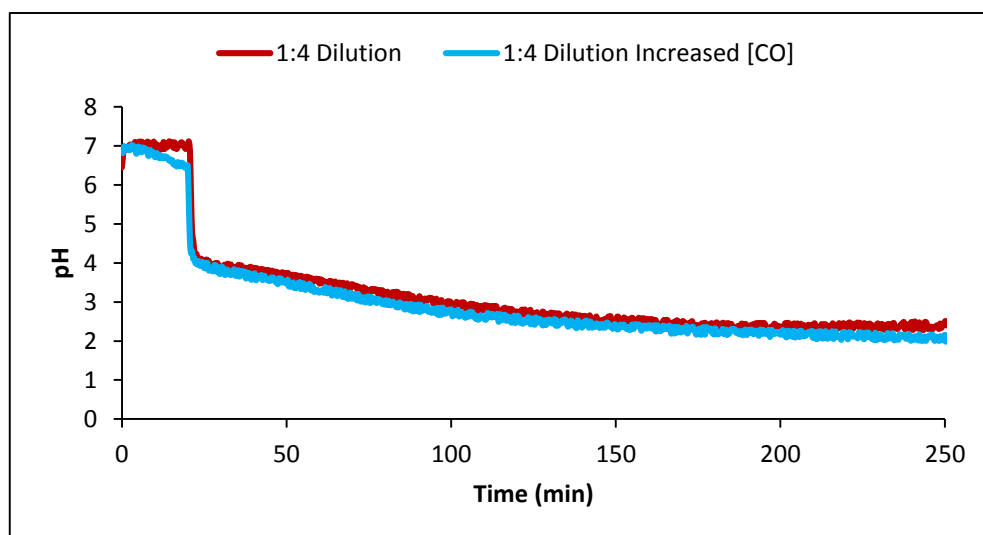


Figure 6.11. Purging dilute catalyst solution, $[\text{PdI}_2] = 4.44 \times 10^{-4} \text{ mol dm}^{-3}$, with CO flows of 6 mL min^{-1} and 50 mL min^{-1} .

6.2.4 Modelling Study

The results of the experiments in Sections 6.1 and 6.2 suggest the existence of reactions between PdI_2 , CO, MeOH and water as well as the formation of $\text{Pd}(0)$. The results of the experiments were used to conduct an initial modelling study.^[138] The models considered the interactions of PdI_2 , CO, MeOH and water using BatchCAD, a kinetic fitting and simulation software package.

The BatchCAD software has two environments, a simulation environment and a kinetic fitting environment.^[147] The simulation environment can model the dynamic heat, reaction kinetics and mass balances of CSTRs, jacketed batch and fed batch

reactors. The kinetic fitting environment can estimate reaction orders, heats of reaction, Arrhenius constants and reaction rate constants from experimental data.

To perform these processes BatchCAD has a choice of 5 integrators: Euler (first order); Adaptive Euler; Runge-Kutta (fourth order); Adaptive Runge-Kutta and Bulirsch-Stoer. The Euler and Runge-Kutta integrators are fixed step integrators. The Euler integrator is used with a step size of 1-10 s whereas the Runge-Kutta integrator uses a larger step size of 10-100 s. The step size is entered by the user and remains constant throughout the simulation. The validity of the step size can be checked by repeating the simulation with a step size half that of the original value. If there is no difference in the two simulations then the larger step size is fine, however if the model differs significantly then a smaller step size is needed. Under these circumstances the process should be repeated using subsequently smaller step sizes until there are no differences between successive simulations.

The Adaptive Euler, Adaptive Runge-Kutta and Bulirsch-Stoer integrators are adaptive step integrators which alter the step size during the kinetic fitting process in order to reduce the estimated error in the solution. This error is called the tolerance. The default tolerances used in BatchCAD for each of the integrators are:

Adaptive Euler: Tolerance= 1×10^{-4}

Adaptive Runge-Kutta: Tolerance= 1×10^{-4}

Bulirsch-Stoer: Tolerance= 1×10^{-8}

As the PCPOC reaction system is oscillatory, with the period of the oscillations varying during the course of the reaction depending on the reaction conditions, the Adaptive Euler and Adaptive Runge-Kutta integrators were used for the modelling studies in this thesis.

How well the model fits the data, the goodness of fit, is determined in BatchCAD using an objective function. This is based on the sum of squares of the errors between the values predicted by the model and the recorded experimental data. For one data set containing n measurements of data y the objective function is described by Equation (6.8).

$$\sum_{i=1}^{n_i} (y_i^{\text{observed}} - y_i^{\text{predicted}})^2 \quad (6.8)$$

The lower the value of the objective function the better the model fits the experimental data. However, this is not infallible so the data must be plotted to visually verify the goodness of fit. The BatchCAD settings used for the models are shown in Table 6.2.

Table 6.2. BatchCAD settings used to model the experimental data from the experiments on the catalyst subsystem of the PCPOC reaction described in Section 4.5.

BatchCAD Model Settings	
Maximum run time (min)	1500
Integrator	Adaptive Euler/Adaptive Runge-Kutta
Step size (s)	100
Maximum step size (s)	unlimited
Tolerance	0.0001
Discontinuity Monitoring	off
Plot frequency	Auto
Number of points	200
Fitting options: Method	Simplex
Maximum resets	Infinite
Maximum iterations	100
Parameter	Isothermal rate constants

Note that the BatchCAD software expresses all rate constants in units of min^{-1} regardless of the kinetic laws. In reality the units differ to reflect the order of the reaction and, for order n , the rate coefficient has units of $\text{mol}^{(1-n)}\text{dm}^{3(n-1)}\text{min}^{-1}$.

Initially, modelling studies were conducted to establish a basic model for the pH behaviour of the catalyst solution when it is purged with CO. The reactions were all assumed to be elementary processes. The initial conditions for the models (listed in Table 6.3) were those used in the small scale experiments described in Section 4.5.

Table 6.3. Initial conditions used in the modelling studies.

Model No	1-2	3	4-12
[PdI ₂] (mol dm^{-3})	2.66×10^{-3}	2.66×10^{-3}	2.22×10^{-3}
[KI] (mol dm^{-3})	0.48	0.48	0.48
[CO] (mol dm^{-3})	9.64×10^{-4}	8.26×10^{-3}	8.26×10^{-3}
Solvent (mL)	25 (H ₂ O)	25 (Dried MeOH)	25 (MeOH)

The solubility of CO in water used in the study was $2.76 \times 10^{-2} \text{ gdm}^{-3}$ ($9.64 \times 10^{-4} \text{ moldm}^{-3}$) at 20°C ^[138] with equilibrium solubility being achieved in 2 min.^[148] The solubility of CO in MeOH was estimated to be $8.26 \times 10^{-3} \text{ moldm}^{-3}$ at 20°C using the software packages DynoChem and BatchCad. This is in good agreement with the $9.24 \times 10^{-3} \text{ moldm}^{-3}$ reported in the literature.^[149] Although the rate of CO solubility in MeOH is reported to be fast, reaching equilibrium solubility in 2 min,^[148] the solubility of CO in MeOH may have a rate limiting effect on the PCPOC reaction.

As the only variable measured in the experiments was pH this needed to be incorporated into the modelling study. This was done by converting pH to hydrogen ion concentration but this has its limitations. In all of the PCPOC experiments reported here pH is measured using a combined pH electrode which removes the need for having separate “measuring” and reference electrodes. However, the definition of pH refers to the measurement in aqueous solution.^[150] In the PCPOC system all measurements are made in methanol. This means that the pH measured cannot be directly related to $[\text{H}^+]$ in the reaction mixture. However, studies have been made into pH measurement and acid-base equilibria in non-aqueous media providing possible solutions to this problem.^[142, 143, 151-153] The simplest solution was to use a pH electrode containing standard KCl/AgCl aqueous filling solution that was calibrated with standard aqueous buffers. Experiments by Porras *et al* have shown that, using such a setup, the equivalent pH in water of an organic solution can be obtained by adjusting the pH measured in experiments by an appropriate amount, δ , which depends on the solvent.^[142] The δ -value for methanol is +2.3. After adjusting pH in this way the adjusted pH value was then used to estimate hydrogen ion concentration using the relationship shown in Equation (6.9).

$$[\text{H}^+] = 10^{-(\text{pH}+2.3)} \quad (6.9)$$

The pH data from Experiment 1, involving the catalyst solution in water, was used to estimate the value of the rate constant for the reaction of Pdl_2 and CO with water in Model 1. The rate constant for the reaction of Pdl_2 and CO with MeOH was estimated in Model 3 using the pH data from Experiment 3. These rate constants were then used as initial values in Models 4-12 to estimate the remaining rate constants.

The CO flow rate was maintained constant throughout the experiments. This was accounted for by adding the first 2 equations for CO (Table 6.4) to each of the

BatchCAD models. The onset of the reaction in the experiments occurred when CO was added. However, to simplify modelling, the onset of reaction in the modelling study was taken to be the addition of PdI₂.

Model 1

The first model focused on the reaction of PdI₂, KI and CO with water as the solvent as discussed in Section 6.2.1. The reactions and rates used in this model are shown in Table 6.4. To achieve an equilibrium CO solubility of $2.76 \times 10^{-2} \text{ gdm}^{-3}$ ($9.64 \times 10^{-4} \text{ moldm}^{-3}$) in 25 mL (55.55 moldm^{-3}) water at 20 °C^[138] in 2 min^[148] required $k_a = 2.47 \text{ min}^{-1}$ and $k_b = 2.4 \times 10^{-3} \text{ moldm}^{-3}\text{min}^{-1}$ in BatchCAD.

Table 6.4. Reactions and reaction rates used in Model 1.

Possible Reactions	Reaction Rate
CO →	$k_a [\text{CO}]$
→ CO	k_b
PdI ₂ + CO + H ₂ O → HPdI + HI + CO ₂	$k_c [\text{PdI}_2][\text{CO}]$
HPdI → HI + Pd	$k_f [\text{HPdI}]$

Malaskevich *et al* and Gorodskii *et al* consider water to play a critical role in the formation of the active catalytic species (which they postulate to be Pd(I)) in the PCPOC reaction.^[4, 5, 9] Model 1 investigated this scenario by including the third reaction in Table 6.4 which assumes the direct synthesis of HPdI. The concentration of water was not included in the rate of reaction as, being the solvent, it was in a large excess and was therefore considered to be constant throughout the reaction. The pH at the end of the reaction was approximately 2.4 (Figure 6.7) which is equivalent to $[\text{H}^+] = 3.98 \times 10^{-3} \text{ moldm}^{-3}$. This value is higher than the PdI₂ concentration used in the reaction indicating the presence of a second process which generates HI. As a black precipitate was formed during the reaction (suggesting the formation of Pd(0)) the decomposition of HPdI, which would account for both of these observations, was postulated as the fourth reaction in the model (Table 6.4). The rate constants were estimated: $k_c = 1.489 \text{ dm}^3\text{mol}^{-1}\text{min}^{-1}$; $k_f = 8.413 \times 10^{-3} \text{ min}^{-1}$. The fitted data are compared with the experimental data in Figure 6.12. The experiment using water as solvent was conducted for 1464 min. This is much longer than the subsequent experiments using MeOH which were conducted for a maximum of 200

min. The experiments in Section 6.1.3 had shown a shorter run time was sufficient to record the changes in pH behaviour in the experiments in MeOH.

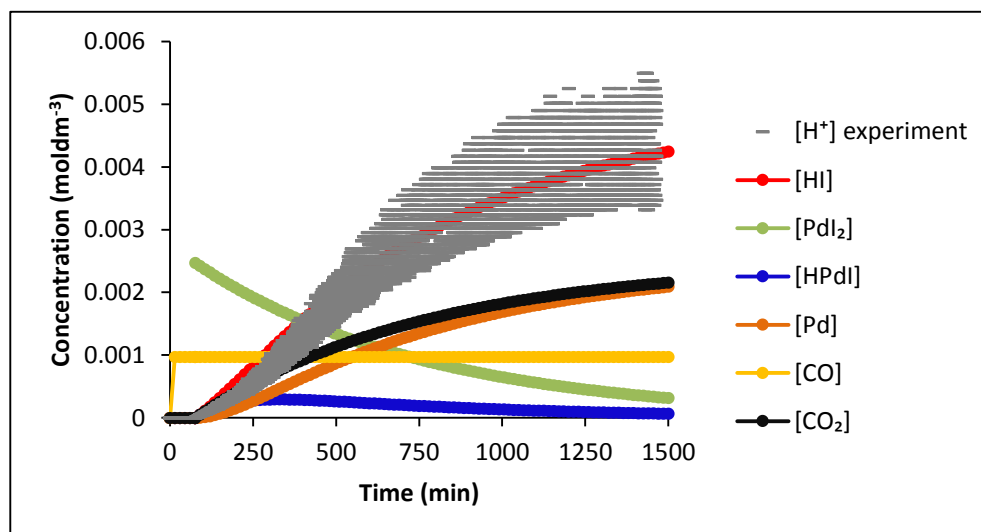


Figure 6.12. Fitted data from Model 1 compared with the calculated $[H^+]$ from the experimental pH data for water shown in Figure 6.7.

There is high dispersion in the data from the experiment which is a characteristic of the experimental setup as it used a magnetic stirrer. This is in contrast to the overhead stirring used in the large scale experiments conducted in the HEL Simular (Section 4.2.2). In spite of this, the model is a good fit to the experimental data with an objective function of 3.479×10^{-5} .

Model 2

The second model considered the alternative, indirect formation of HPdI which is postulated by Chiusoli *et al* and Gabriele *et al* to occur via the formation of an intermediate, IPdCOOH.^[10, 146] The reactions used in this model are given in Table 6.5. As in Model 1, the concentration of water was not included in the rate of reaction for the formation of IPdCOOH as water was the solvent. The water was, therefore, in large excess so its concentration was assumed to be constant throughout the experiment. The values of k_a and k_b were the same as in Model 1 ($k_a = 2.47 \text{ min}^{-1}$ and $k_b = 2.4 \times 10^{-3} \text{ mol dm}^{-3} \text{ min}^{-1}$). The other rate constants were estimated to be $k_d = 1.635 \text{ dm}^3 \text{ mol}^{-1} \text{ min}^{-1}$, $k_e = 1.148 \times 10^{-2} \text{ min}^{-1}$ and $k_f = 7.496 \times 10^{-3} \text{ min}^{-1}$.

Table 6.5. Reactions and reaction rates used in Model 2.

Possible Reactions	Reaction Rate
$\text{CO} \rightarrow$	$k_a[\text{CO}]$
$\rightarrow \text{CO}$	k_b
$\text{PdI}_2 + \text{CO} + \text{H}_2\text{O} \rightarrow \text{IPdCOOH} + \text{HI}$	$k_d[\text{PdI}_2][\text{CO}]$
$\text{IPdCOOH} \rightarrow \text{HPdI} + \text{CO}_2$	$k_e[\text{IPdCOOH}]$
$\text{HPdI} \rightarrow \text{HI} + \text{Pd}$	$k_f[\text{HPdI}]$

The fitted data from Model 2 are compared with the experimental data in Figure 6.13. Model 2 gives a good fit to the experimental data with an objective function of 2.125×10^{-5} . This is similar to the result obtained from Model 1 so all future models assume the direct synthesis of HPdI rather than its formation via the IPdCOOH intermediate.

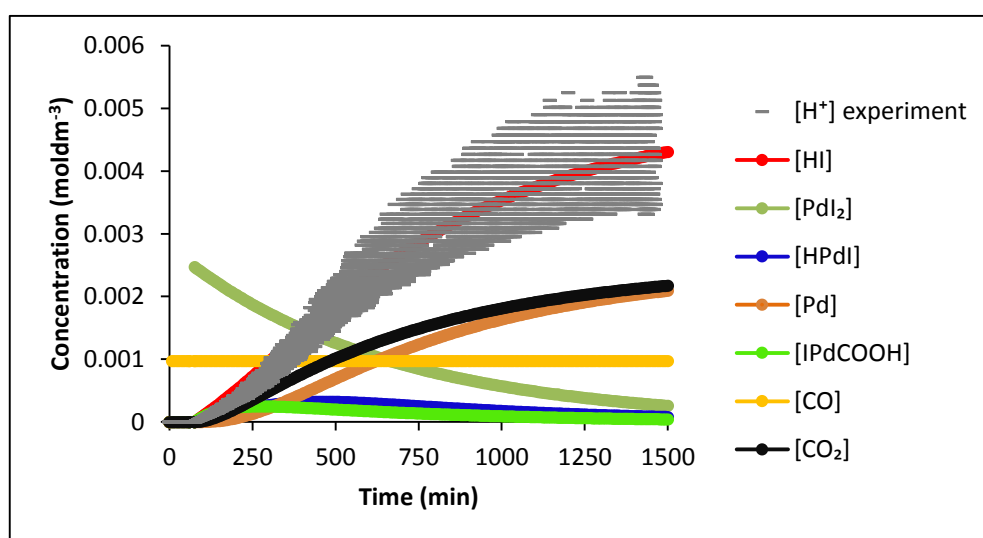


Figure 6.13. Fitted data from Model 2 compared with the calculated $[\text{H}^+]$ from the experimental pH data for water shown in Figure 6.7.

Model 3

Model 3 considered the use of dried MeOH as solvent. The solubility of CO in MeOH was estimated to be $8.26 \times 10^{-3} \text{ mol dm}^{-3}$ at 20°C using BatchCAD and DynoChem. This was achieved in the BatchCAD models by setting $k_a = 1 \text{ min}^{-1}$ and $k_b = 8.26 \times 10^{-3} \text{ mol dm}^{-3} \text{ min}^{-1}$. To test the influence of a decrease in the dissolution rate of CO the equilibrium solubility was set to be achieved in 15 min as opposed to the 2 min used in Models 1 and 2.

The fall in pH recorded when CO was added in the experiment using dried MeOH (Figure 6.7) was lower than that recorded in the experiments using water or wet MeOH and no precipitate was observed. This suggested a small change in $[\text{H}^+]$ when

CO was added (from $10^{-10.86}$ to $10^{-7.82}$ based on adjusted pH). To account for this, the pH fall was limited by including reversibility in the model. The reactions used in Model 3 are shown in Table 6.6.

Table 6.6. Reactions and reaction rates used in Model 3.

Possible Reactions	Reaction Rate
$\text{CO} \rightarrow$	$k_a[\text{CO}]$
$\rightarrow \text{CO}$	k_b
$\text{PdI}_2 + \text{CO} + \text{CH}_3\text{OH} \rightarrow \text{IPdCOOCH}_3 + \text{HI}$	$k_g[\text{PdI}_2][\text{CO}]$
$\text{IPdCOOCH}_3 + \text{HI} \rightarrow \text{PdI}_2 + \text{CO} + \text{CH}_3\text{OH}$	$k_h[\text{IPdCOOCH}_3][\text{HI}]$

Methanol was in large excess in this experiment so the rate of reaction for the reaction involving MeOH does not include $[\text{MeOH}]$ as it was assumed to be constant. The rate constants k_g and k_h were estimated: $k_g = 2.013 \times 10^{-5} \text{ dm}^3\text{mol}^{-1}\text{min}^{-1}$ and $k_h = 1.535 \times 10^6 \text{ dm}^3\text{mol}^{-1}\text{min}^{-1}$. The fitted data from Model 3 are compared with the experimental data in Figure 6.13. The fitted data from Model 3 are a good fit to the experimental data with an objective function of 2.970×10^{-18} .

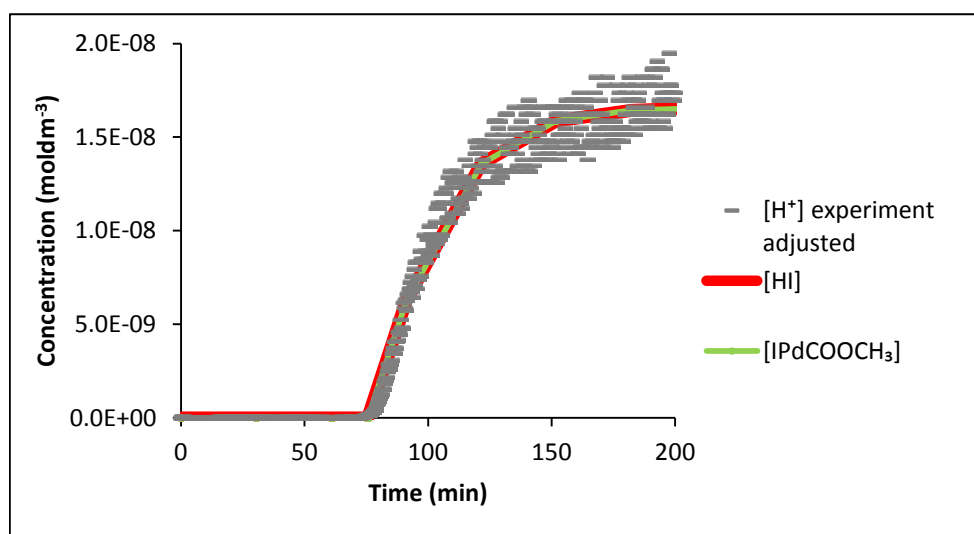


Figure 6.14. Fitted data from Model 3 compared with the calculated $[\text{H}^+]$ from the experimental pH data for dried MeOH shown in Figure 6.7.

Model 4

Model 4 considered the use of the standard HPLC MeOH (wet MeOH) as solvent. It was assumed that the reactions occurring when water was used as solvent would occur along with the reactions occurring in dried MeOH. Hence the reactions used were a combination of Model 1 and Model 3 (Table 6.7).

Table 6.7. Reactions and reaction rates used in Model 4.

Possible Reactions	Reaction Rate
$\text{CO} \rightarrow$	$k_a[\text{CO}]$
$\rightarrow \text{CO}$	k_b
$\text{PdI}_2 + \text{CO} + \text{H}_2\text{O} \rightarrow \text{HPdI} + \text{HI} + \text{CO}_2$	$k_c[\text{PdI}_2][\text{CO}][\text{H}_2\text{O}]$
$\text{HPdI} \rightarrow \text{HI} + \text{Pd}$	$k_f[\text{HPdI}]$
$\text{PdI}_2 + \text{CO} + \text{CH}_3\text{OH} \rightarrow \text{IPdCOOCH}_3 + \text{HI}$	$k_g[\text{PdI}_2][\text{CO}]$
$\text{IPdCOOCH}_3 + \text{HI} \rightarrow \text{PdI}_2 + \text{CO} + \text{CH}_3\text{OH}$	$k_h[\text{IPdCOOCH}_3][\text{HI}]$

However, in this instance the concentration of water could not be assumed to be constant as the water concentration in the HPLC grade MeOH used in the experiments was low ($<0.03\%$, $<1.67 \times 10^{-2} \text{ mol dm}^{-3}$). The water concentration is therefore included in the rate of reaction for the third reaction in Table 6.7. The maximum water concentration is approximately 7.5 times larger than the concentration of PdI_2 used in the experiments. The actual initial concentration of water was not known but plays a significant role in the model, hence a series of values were estimated until a good fit was obtained. The closest fit was achieved using an initial water concentration of $3.4 \times 10^{-4} \text{ mol dm}^{-3}$.

The rate constants k_a and k_b were maintained constant: $k_a = 1 \text{ min}^{-1}$ and $k_b = 8.26 \times 10^{-3} \text{ mol dm}^{-3} \text{ min}^{-1}$, whilst the others were estimated as $k_c = 1.3 \times 10^3 \text{ dm}^6 \text{ mol}^{-2} \text{ min}^{-1}$, $k_f = 8.4 \times 10^{-3} \text{ min}^{-1}$, $k_g = 2 \times 10^{-5} \text{ dm}^3 \text{ mol}^{-1} \text{ min}^{-1}$ and $k_h = 1.5 \times 10^6 \text{ dm}^3 \text{ mol}^{-1} \text{ min}^{-1}$.

To exclude the influence of the rate of PdI_2 dissolution the experimental data used for comparison in this study was from the experiment using the baseline filtered catalyst solution presented in Figure 6.10. The results from Model 4 are compared with the experimental data in Figure 6.15.

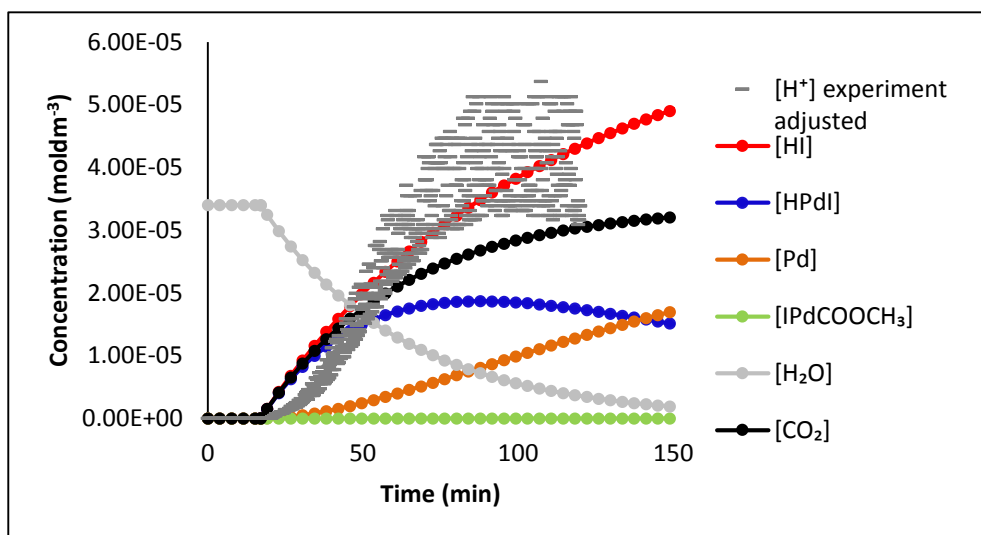


Figure 6.15. Fitted data from Model 4 compared with the calculated $[H^+]$ from the experimental pH data for filtered catalyst solution using wet MeOH shown in Figure 6.10.

Although the model has an objective function of 1.624×10^{-9} it is apparent from Figure 6.15 that Model 4 is not a good fit to the experimental data. It suggests the production of $Pd(0)$ which was not observed during the experiment. Including the reaction which consumes $Pd(0)$ forming Pd_2I_2 would account for this. Figure 6.15 also shows that the concentration of HI in the model during the initial stages of the reaction (20-50 min) disagrees with that found in the experiment. The experimental data shows $[H^+]$ formation was initially slow but rapidly increased. This behaviour suggests an autocatalytic process.

The remaining models focused on the presence of catalysis in the system. The influence of catalysis on the reactions producing HI (the reaction of $PdI_2/CO/H_2O$ and the decomposition of $HPdI$) was investigated. The rate constants used in Models 5-8 are given in Table 6.8.

Table 6.8. Rate constants for Models 5-8 estimated using the BatchCAD kinetic fitting package.

^a Rate constant	Model 5	Model 6	Model 7	Model 8	Model 5	Model 6	Model 7	Model 8
					Additional constraint: [Pd] = 0			
k_a	1	1	1	1	1	1	1	1
k_b	$8.26 \cdot 10^{-3}$	$8.26 \cdot 10^{-3}$	$8.26 \cdot 10^{-3}$	$8.26 \cdot 10^{-3}$	$8.26 \cdot 10^{-3}$	$8.26 \cdot 10^{-3}$	$8.26 \cdot 10^{-3}$	$8.26 \cdot 10^{-3}$
k_c	$3.88 \cdot 10^2$	$1.69 \cdot 10^2$	$2.59 \cdot 10^2$	$6.74 \cdot 10^2$	$4.15 \cdot 10^2$	$1.69 \cdot 10^2$	$2.59 \cdot 10^2$	$6.74 \cdot 10^2$
k_f	$3.95 \cdot 10^{-3}$	$4.16 \cdot 10^{-3}$	$4.81 \cdot 10^{-3}$	$9.18 \cdot 10^{-2}$	$5.14 \cdot 10^{-3}$	$4.16 \cdot 10^{-3}$	$4.81 \cdot 10^{-3}$	$9.18 \cdot 10^{-2}$
k_g	$2.38 \cdot 10^{-6}$	$3.86 \cdot 10^{-6}$	$5.46 \cdot 10^{-10}$	$8.38 \cdot 10^{-16}$	$3.53 \cdot 10^{-7}$	$3.86 \cdot 10^{-6}$	$5.46 \cdot 10^{-10}$	$8.40 \cdot 10^{-16}$
k_h	$5.69 \cdot 10^{-3}$	$8.04 \cdot 10^{-3}$	$6.01 \cdot 10^{-3}$	$1.53 \cdot 10^{-5}$	$3.21 \cdot 10^{-3}$	$8.04 \cdot 10^{-3}$	$6.01 \cdot 10^{-3}$	$1.53 \cdot 10^{-5}$
k_i	$1.52 \cdot 10^{-6}$	$7.63 \cdot 10^{-7}$	$2.22 \cdot 10^{-6}$	$2.00 \cdot 10^1$	$1.00 \cdot 10^2$	$1.00 \cdot 10^2$	$1.00 \cdot 10^2$	$3.97 \cdot 10^1$
k_j	$2.66 \cdot 10^7$				$5.18 \cdot 10^7$			
k_k		$1.39 \cdot 10^6$				$1.39 \cdot 10^6$		
k_l			$1.21 \cdot 10^6$				$1.21 \cdot 10^6$	
k_m				2.63				2.63

^a k_a, k_f have units min^{-1} ; k_b has units $\text{mol dm}^{-3} \text{min}^{-1}$; k_g, k_h, k_i have units $\text{dm}^3 \text{mol}^{-1} \text{min}^{-1}$; k_c, k_j, k_k, k_l, k_m have units $\text{dm}^6 \text{mol}^{-2} \text{min}^{-1}$.

Model 5

Model 5 considered the influence of Pd(0) as a catalyst for the PdI₂/CO/H₂O reaction. The reactions and reaction rates used in the model are shown in Table 6.9.

Table 6.9. Reactions and reaction rates used in Model 5.

Possible Reactions	Reaction Rate
$\text{CO} \rightarrow$	$k_a [\text{CO}]$
$\rightarrow \text{CO}$	k_b
$\text{PdI}_2 + \text{CO} + \text{H}_2\text{O} \rightarrow \text{HPdI} + \text{HI} + \text{CO}_2$	$k_c [\text{PdI}_2][\text{CO}][\text{H}_2\text{O}]$
$\text{HPdI} \rightarrow \text{HI} + \text{Pd}$	$k_f [\text{HPdI}]$
$\text{PdI}_2 + \text{CO} + \text{CH}_3\text{OH} \rightarrow \text{IPdCOOCH}_3 + \text{HI}$	$k_g [\text{PdI}_2][\text{CO}]$
$\text{IPdCOOCH}_3 + \text{HI} \rightarrow \text{PdI}_2 + \text{CO} + \text{CH}_3\text{OH}$	$k_h [\text{IPdCOOCH}_3][\text{HI}]$
$\text{Pd} + \text{PdI}_2 \rightarrow \text{Pd}_2\text{I}_2$	$k_j [\text{Pd}][\text{PdI}_2]$
$\text{PdI}_2 + \text{CO} + \text{H}_2\text{O} \rightarrow \text{HPdI} + \text{HI} + \text{CO}_2$	$k_j [\text{PdI}_2][\text{H}_2\text{O}][\text{Pd}]$

Two scenarios were considered, one in which no constraints were included and one with the constraint that $[\text{Pd}] = 0$. A comparison of the experimental data from the

baseline experiment using filtered catalyst solution and both scenarios of Model 5 is shown in Figure 6.16.

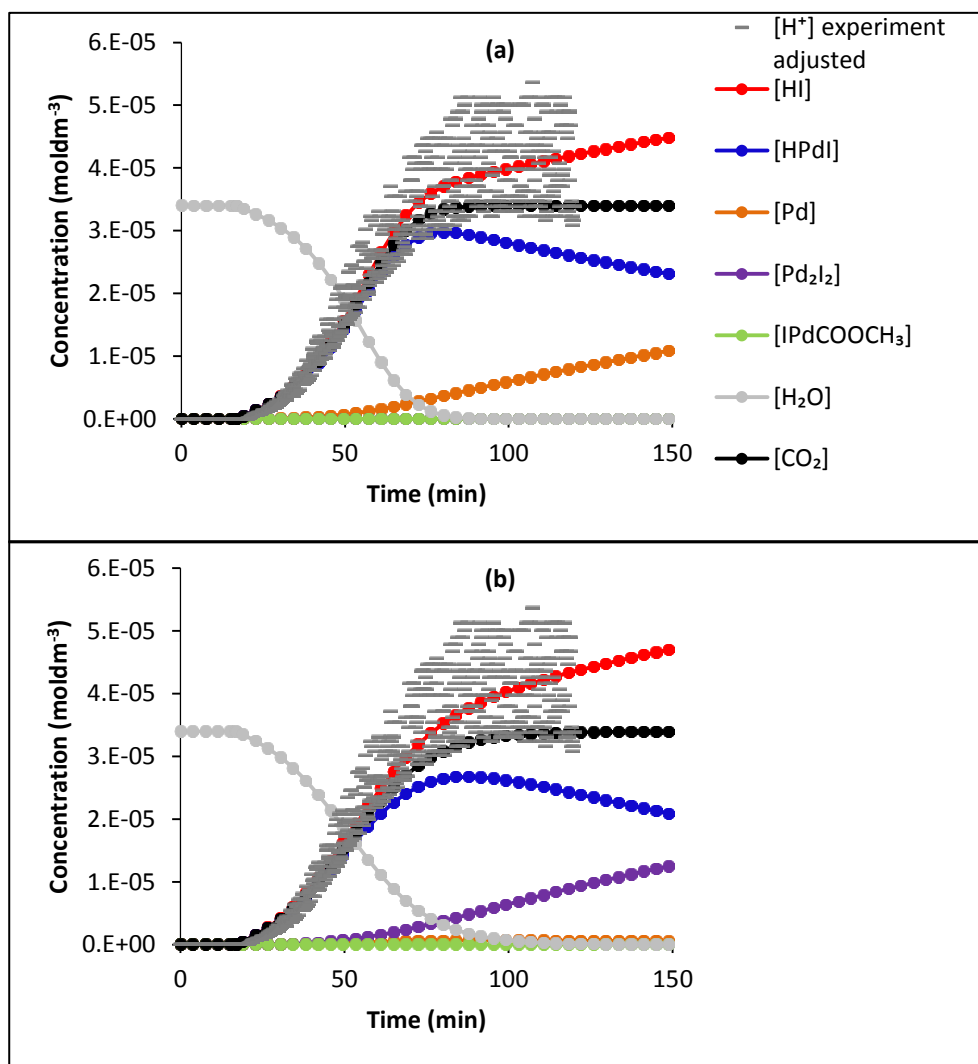


Figure 6.16. Fitted data from Model 5: (a) no constraints; (b) constraint that $[Pd] = 0$; compared with the calculated $[H^+]$ from the experimental pH data for filtered catalyst solution using wet MeOH shown in Figure 6.10.

As Figure 6.16 shows, Model 5 is a good fit to the experimental data in both scenarios: with no constraints the model had an objective function of 9.569×10^{-10} and with the constraint that $[Pd] = 0$ the model had an objective function of 1.009×10^{-9} .

Model 6

Model 6 considered the influence of HI as a catalyst for the $PdI_2/CO/H_2O$ reaction. The reactions and reaction rates used in the model are shown in Table 6.10.

Table 6.10. Reactions and reaction rates used in Model 6.

Possible Reactions	Reaction Rate
$\text{CO} \rightarrow$	$k_a[\text{CO}]$
$\rightarrow \text{CO}$	k_b
$\text{PdI}_2 + \text{CO} + \text{H}_2\text{O} \rightarrow \text{HPdI} + \text{HI} + \text{CO}_2$	$k_c[\text{PdI}_2][\text{CO}][\text{H}_2\text{O}]$
$\text{HPdI} \rightarrow \text{HI} + \text{Pd}$	$k_f[\text{HPdI}]$
$\text{PdI}_2 + \text{CO} + \text{CH}_3\text{OH} \rightarrow \text{IPdCOOCH}_3 + \text{HI}$	$k_g[\text{PdI}_2][\text{CO}]$
$\text{IPdCOOCH}_3 + \text{HI} \rightarrow \text{PdI}_2 + \text{CO} + \text{CH}_3\text{OH}$	$k_h[\text{IPdCOOCH}_3][\text{HI}]$
$\text{Pd} + \text{PdI}_2 \rightarrow \text{Pd}_2\text{I}_2$	$k_i[\text{Pd}][\text{PdI}_2]$
$\text{PdI}_2 + \text{CO} + \text{H}_2\text{O} \rightarrow \text{HPdI} + \text{HI} + \text{CO}_2$	$k_k[\text{PdI}_2][\text{H}_2\text{O}][\text{HI}]$

Again, two scenarios were considered, one in which no constraints were included and one with the constraint that $[\text{Pd}] = 0$. A comparison of the experimental data from the baseline experiment using filtered catalyst solution (Figure 6.10) prepared using wet MeOH and both scenarios of Model 6 is shown in Figure 6.17. As with Model 5, Model 6 is a good fit to the experimental data in both scenarios: with no constraints the objective function was 9.889×10^{-10} and with the constraint that $[\text{Pd}] = 0$ the objective function was 9.893×10^{-10} .

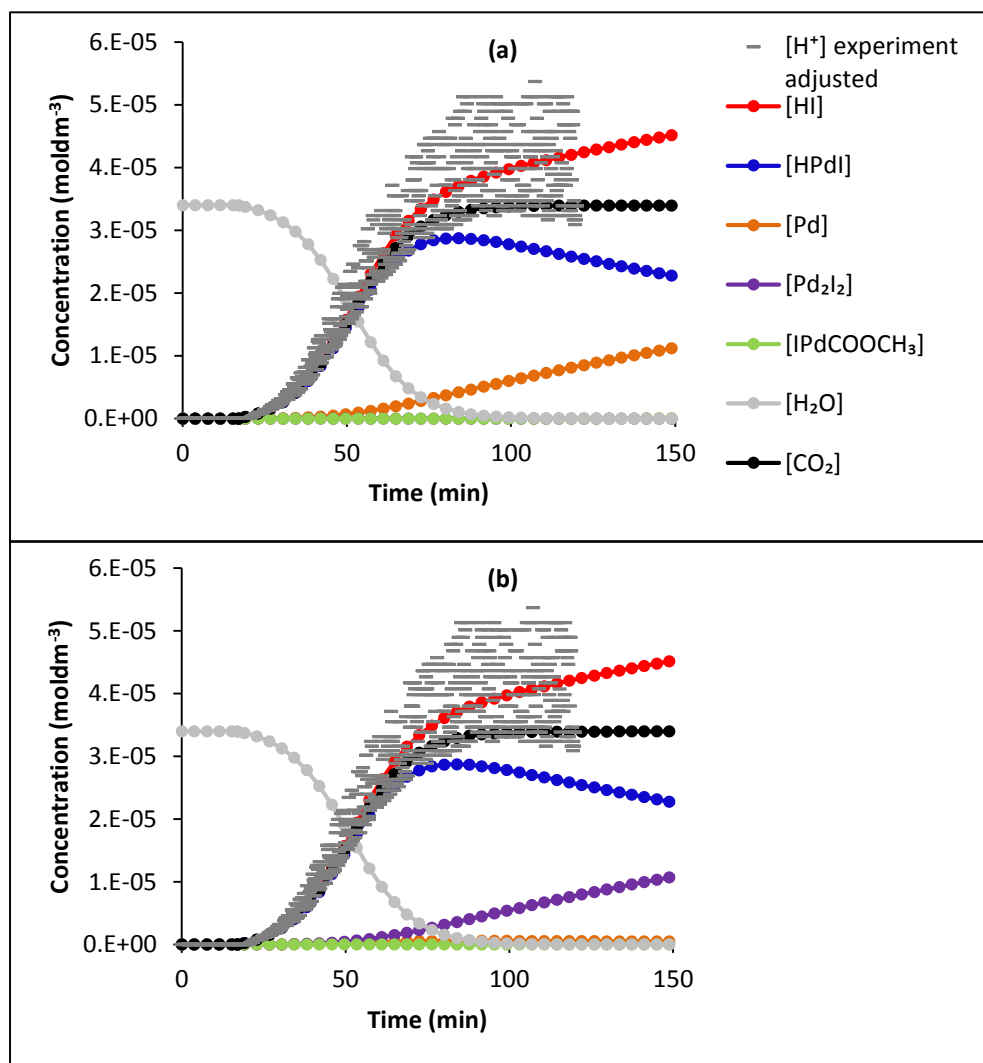


Figure 6.17. Fitted data from Model 6: (a) no constraints; (b) constraint that $[\text{Pd}] = 0$; compared with the calculated $[\text{H}^+]$ from the experimental pH data for filtered catalyst solution using wet MeOH shown in Figure 6.10.

Model 7

Model 7 considered the influence of HPdI as a catalyst. The reactions and reaction rates used in the model are shown in Table 6.11.

As in the previous models, two scenarios were considered, one in which no constraints were included and one with the constraint that $[\text{Pd}] = 0$. A comparison of the experimental data from the baseline experiment using filtered catalyst solution (Figure 6.10) and both scenarios of Model 7 is shown in Figure 6.18.

Table 6.11. Reactions and reaction rates used in Model 7.

Possible Reactions	Reaction Rate
$\text{CO} \rightarrow$	$k_a[\text{CO}]$
$\rightarrow \text{CO}$	k_b
$\text{PdI}_2 + \text{CO} + \text{H}_2\text{O} \rightarrow \text{HPdI} + \text{HI} + \text{CO}_2$	$k_c[\text{PdI}_2][\text{CO}][\text{H}_2\text{O}]$
$\text{HPdI} \rightarrow \text{HI} + \text{Pd}$	$k_f[\text{HPdI}]$
$\text{PdI}_2 + \text{CO} + \text{CH}_3\text{OH} \rightarrow \text{IPdCOOCH}_3 + \text{HI}$	$k_g[\text{PdI}_2][\text{CO}]$
$\text{IPdCOOCH}_3 + \text{HI} \rightarrow \text{PdI}_2 + \text{CO} + \text{CH}_3\text{OH}$	$k_h[\text{IPdCOOCH}_3][\text{HI}]$
$\text{Pd} + \text{PdI}_2 \rightarrow \text{Pd}_2\text{I}_2$	$k_i[\text{Pd}][\text{PdI}_2]$
$\text{PdI}_2 + \text{CO} + \text{H}_2\text{O} \rightarrow \text{HPdI} + \text{HI} + \text{CO}_2$	$k_l[\text{PdI}_2][\text{H}_2\text{O}][\text{HPdI}]$

As shown in Figure 6.18, Model 7, which uses HPdI as catalyst for the $\text{PdI}_2/\text{CO}/\text{H}_2\text{O}$ reaction, is also a good fit to the data. With no constraints the objective function was 1.054×10^{-9} and with the constraint that $[\text{Pd}] = 0$ the objective function was 1.055×10^{-9} .

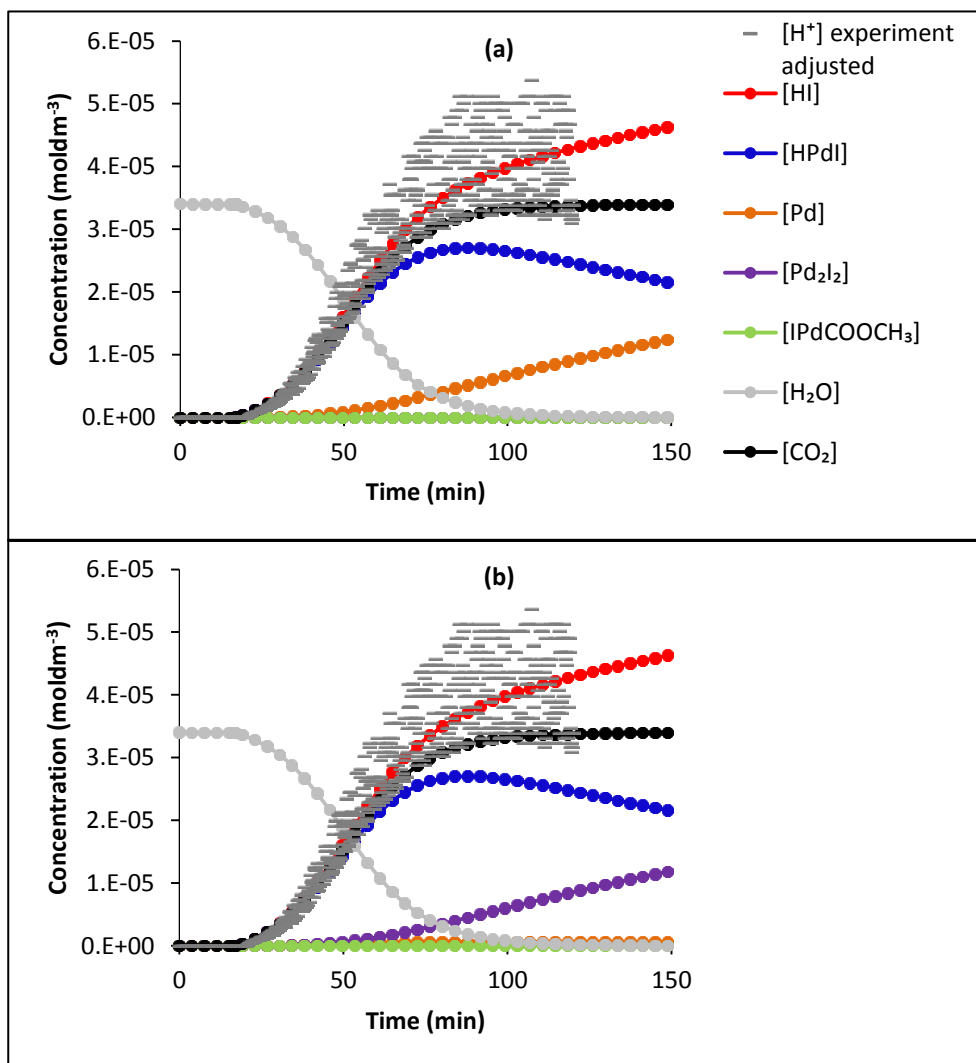


Figure 6.18. Fitted data from Model 7: (a) no constraints; (b) constraint that $[Pd] = 0$; compared with the calculated $[H^+]$ from the experimental pH data for filtered catalyst solution using wet MeOH shown in Figure 6.10.

Model 8

Model 8 considered the influence of Pd_2I_2 as a catalyst for the $PdI_2/CO/H_2O$ reaction. The reactions and reaction rates used in the model are shown in Table 6.12.

Table 6.12. Reactions and reaction rates used in Model 8.

Possible Reactions	Reaction Rate
$\text{CO} \rightarrow$	$k_a[\text{CO}]$
$\rightarrow \text{CO}$	k_b
$\text{PdI}_2 + \text{CO} + \text{H}_2\text{O} \rightarrow \text{HPdI} + \text{HI} + \text{CO}_2$	$k_c[\text{PdI}_2][\text{CO}][\text{H}_2\text{O}]$
$\text{HPdI} \rightarrow \text{HI} + \text{Pd}$	$k_f[\text{HPdI}]$
$\text{PdI}_2 + \text{CO} + \text{CH}_3\text{OH} \rightarrow \text{IPdCOOCH}_3 + \text{HI}$	$k_g[\text{PdI}_2][\text{CO}]$
$\text{IPdCOOCH}_3 + \text{HI} \rightarrow \text{PdI}_2 + \text{CO} + \text{CH}_3\text{OH}$	$k_h[\text{IPdCOOCH}_3][\text{HI}]$
$\text{Pd} + \text{PdI}_2 \rightarrow \text{Pd}_2\text{I}_2$	$k_i[\text{Pd}][\text{PdI}_2]$
$\text{PdI}_2 + \text{CO} + \text{H}_2\text{O} \rightarrow \text{HPdI} + \text{HI} + \text{CO}_2$	$k_m[\text{PdI}_2][\text{H}_2\text{O}][\text{Pd}_2\text{I}_2]$

As in the previous models, two scenarios were considered, one in which no constraints were included and one with the constraint that $[\text{Pd}] = 0$. A comparison of the experimental data from the baseline experiment using filtered catalyst solution (Figure 6.10) and both scenarios of Model 8 is shown in Figure 6.19. With no constraints the objective function was 1.406×10^{-9} and with the constraint that $[\text{Pd}] = 0$ the objective function was 1.407×10^{-9} . As shown in Figure 6.19, Model 8 does not fit the experimental data as well as Models 5-7 during the early stages of the reaction.

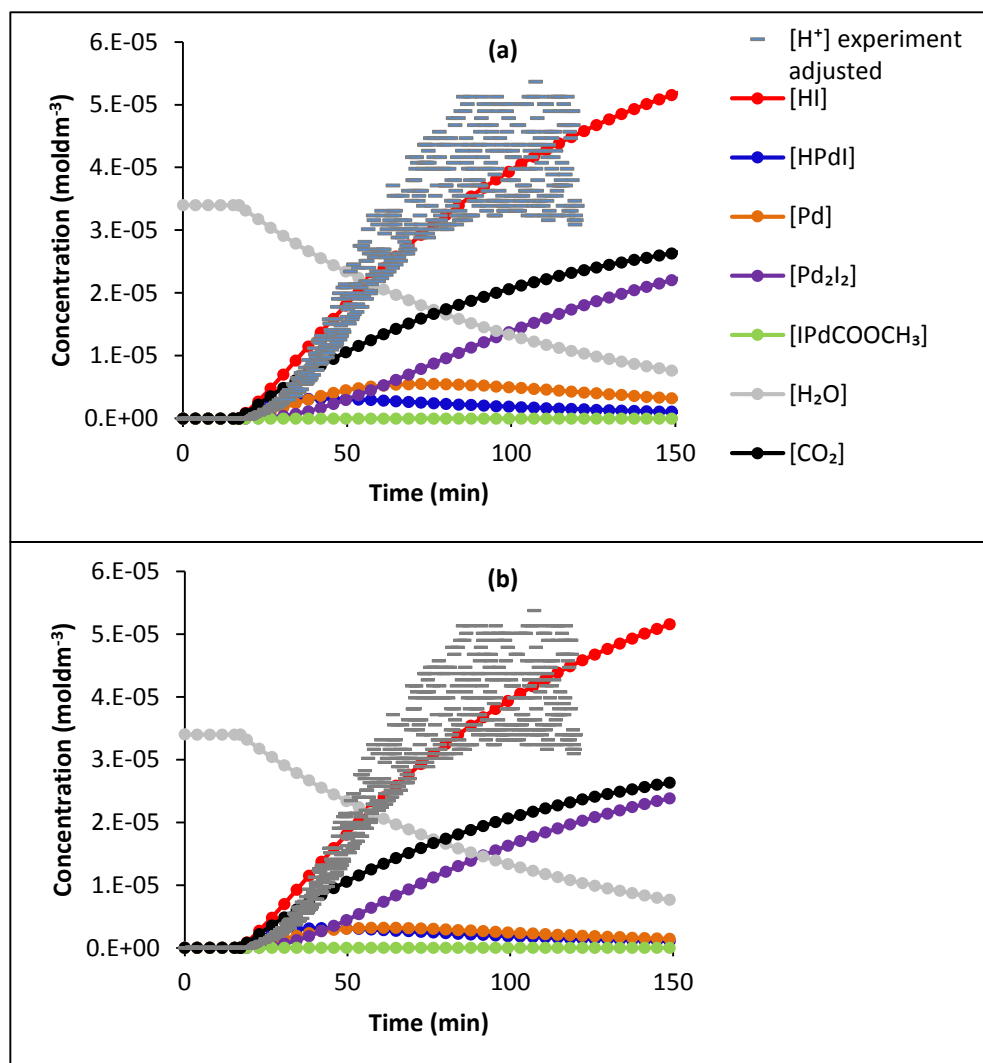


Figure 6.19. Fitted data from Model 8: (a) no constraints; (b) constraint that $[Pd] = 0$; compared with the calculated $[H^+]$ from the experimental pH data for filtered catalyst solution using wet MeOH shown in Figure 6.10.

Models 9-12

Models 9-12 considered catalysis of the decomposition of HPdI using Pd (Model 9), HI (Model 10), HPdI (Model 11) and Pd_2I_2 (Model 12) as catalysts with no constraints and under the same conditions but with the constraint that $[Pd] = 0$. The reactions and reaction rates for each of the models are given in Table 6.13-Table 6.16.

Table 6.13. Reactions and reaction rates used in Model 9.

Possible Reactions	Reaction Rate
$\text{CO} \rightarrow$	$k_a[\text{CO}]$
$\rightarrow \text{CO}$	k_b
$\text{PdI}_2 + \text{CO} + \text{H}_2\text{O} \rightarrow \text{HPdI} + \text{HI} + \text{CO}_2$	$k_c[\text{PdI}_2][\text{CO}][\text{H}_2\text{O}]$
$\text{HPdI} \rightarrow \text{HI} + \text{Pd}$	$k_f[\text{HPdI}]$
$\text{PdI}_2 + \text{CO} + \text{CH}_3\text{OH} \rightarrow \text{IPdCOOCH}_3 + \text{HI}$	$k_g[\text{PdI}_2][\text{CO}]$
$\text{IPdCOOCH}_3 + \text{HI} \rightarrow \text{PdI}_2 + \text{CO} + \text{CH}_3\text{OH}$	$k_h[\text{IPdCOOCH}_3][\text{HI}]$
$\text{Pd} + \text{PdI}_2 \rightarrow \text{Pd}_2\text{I}_2$	$k_i[\text{Pd}][\text{PdI}_2]$
$\text{HPdI} \rightarrow \text{HI} + \text{Pd}$	$k_n[\text{HPdI}][\text{Pd}]$

Table 6.14. Reactions and reaction rates used in Model 10.

Possible Reactions	Reaction Rate
$\text{CO} \rightarrow$	$k_a[\text{CO}]$
$\rightarrow \text{CO}$	k_b
$\text{PdI}_2 + \text{CO} + \text{H}_2\text{O} \rightarrow \text{HPdI} + \text{HI} + \text{CO}_2$	$k_c[\text{PdI}_2][\text{CO}][\text{H}_2\text{O}]$
$\text{HPdI} \rightarrow \text{HI} + \text{Pd}$	$k_f[\text{HPdI}]$
$\text{PdI}_2 + \text{CO} + \text{CH}_3\text{OH} \rightarrow \text{IPdCOOCH}_3 + \text{HI}$	$k_g[\text{PdI}_2][\text{CO}]$
$\text{IPdCOOCH}_3 + \text{HI} \rightarrow \text{PdI}_2 + \text{CO} + \text{CH}_3\text{OH}$	$k_h[\text{IPdCOOCH}_3][\text{HI}]$
$\text{Pd} + \text{PdI}_2 \rightarrow \text{Pd}_2\text{I}_2$	$k_i[\text{Pd}][\text{PdI}_2]$
$\text{HPdI} \rightarrow \text{HI} + \text{Pd}$	$k_o[\text{HPdI}][\text{HI}]$

Table 6.15. Reactions and reaction rates used in Model 11.

Possible Reactions	Reaction Rate
$\text{CO} \rightarrow$	$k_a[\text{CO}]$
$\rightarrow \text{CO}$	k_b
$\text{PdI}_2 + \text{CO} + \text{H}_2\text{O} \rightarrow \text{HPdI} + \text{HI} + \text{CO}_2$	$k_c[\text{PdI}_2][\text{CO}][\text{H}_2\text{O}]$
$\text{HPdI} \rightarrow \text{HI} + \text{Pd}$	$k_f[\text{HPdI}]$
$\text{PdI}_2 + \text{CO} + \text{CH}_3\text{OH} \rightarrow \text{IPdCOOCH}_3 + \text{HI}$	$k_g[\text{PdI}_2][\text{CO}]$
$\text{IPdCOOCH}_3 + \text{HI} \rightarrow \text{PdI}_2 + \text{CO} + \text{CH}_3\text{OH}$	$k_h[\text{IPdCOOCH}_3][\text{HI}]$
$\text{Pd} + \text{PdI}_2 \rightarrow \text{Pd}_2\text{I}_2$	$k_i[\text{Pd}][\text{PdI}_2]$
$\text{HPdI} \rightarrow \text{HI} + \text{Pd}$	$k_p[\text{HPdI}]^2$

Table 6.16. Reactions and reaction rates used in Model 12.

Possible Reactions	Reaction Rate
$\text{CO} \rightarrow$	$k_a[\text{CO}]$
$\rightarrow \text{CO}$	k_b
$\text{PdI}_2 + \text{CO} + \text{H}_2\text{O} \rightarrow \text{HPdI} + \text{HI} + \text{CO}_2$	$k_c[\text{PdI}_2][\text{CO}][\text{H}_2\text{O}]$
$\text{HPdI} \rightarrow \text{HI} + \text{Pd}$	$k_f[\text{HPdI}]$
$\text{PdI}_2 + \text{CO} + \text{CH}_3\text{OH} \rightarrow \text{IPdCOOCH}_3 + \text{HI}$	$k_g[\text{PdI}_2][\text{CO}]$
$\text{IPdCOOCH}_3 + \text{HI} \rightarrow \text{PdI}_2 + \text{CO} + \text{CH}_3\text{OH}$	$k_h[\text{IPdCOOCH}_3][\text{HI}]$
$\text{Pd} + \text{PdI}_2 \rightarrow \text{Pd}_2\text{I}_2$	$k_i[\text{Pd}][\text{PdI}_2]$
$\text{HPdI} \rightarrow \text{HI} + \text{Pd}$	$k_q[\text{HPdI}][\text{Pd}_2\text{I}_2]$

In all cases the fit achieved was poor and similar to the one achieved using Model 4 (Figure 6.15). There was a pronounced disagreement between the estimated concentration of HI and the experimentally measured and adjusted hydrogen ion concentration during the initial stages of the reaction.

6.2.5 Summary

The experiments on the reaction of the catalyst subsystem, consisting of $\text{PdI}_2/\text{KI}/\text{solvent}$ (where the solvent was water or MeOH (wet or dried)), with CO identified a number of possible reactions responsible for the observed pH behaviour. These reactions have been summarised in Table 6.17.

Table 6.17. Reactions and reaction rates used in the modelling study of the catalyst subsystem.

Reaction No.	Possible Reactions	Reaction Rate
1	$\text{CO} \rightarrow$	$k_a[\text{CO}]$
2	$\rightarrow \text{CO}$	k_b
3	$\text{PdI}_2 + \text{CO} + \text{H}_2\text{O} \rightarrow \text{HPdI} + \text{HI} + \text{CO}_2$	$k_c[\text{PdI}_2][\text{CO}][\text{H}_2\text{O}]$
4	$\text{PdI}_2 + \text{CO} + \text{H}_2\text{O} \rightarrow \text{IPdCOOH} + \text{HI}$	$k_d[\text{PdI}_2][\text{CO}][\text{H}_2\text{O}]$
5	$\text{IPdCOOH} \rightarrow \text{HPdI} + \text{CO}_2$	$k_e[\text{IPdCOOH}]$
6	$\text{HPdI} \rightarrow \text{HI} + \text{Pd}$	$k_f[\text{HPdI}]$
7	$\text{PdI}_2 + \text{CO} + \text{CH}_3\text{OH} \rightarrow \text{IPdCOOCH}_3 + \text{HI}$	$k_g[\text{PdI}_2][\text{CO}]$
8	$\text{IPdCOOCH}_3 + \text{HI} \rightarrow \text{PdI}_2 + \text{CO} + \text{CH}_3\text{OH}$	$k_h[\text{IPdCOOCH}_3][\text{HI}]$
9	$\text{Pd} + \text{PdI}_2 \rightarrow \text{Pd}_2\text{I}_2$	$k_i[\text{Pd}][\text{PdI}_2]$
10	$\text{PdI}_2 + \text{CO} + \text{H}_2\text{O} \rightarrow \text{HPdI} + \text{HI} + \text{CO}_2$	$k_j[\text{PdI}_2][\text{H}_2\text{O}][\text{Pd}]$
11	$\text{PdI}_2 + \text{CO} + \text{H}_2\text{O} \rightarrow \text{HPdI} + \text{HI} + \text{CO}_2$	$k_k[\text{PdI}_2][\text{H}_2\text{O}][\text{HI}]$
12	$\text{PdI}_2 + \text{CO} + \text{H}_2\text{O} \rightarrow \text{HPdI} + \text{HI} + \text{CO}_2$	$k_l[\text{PdI}_2][\text{H}_2\text{O}][\text{HPdI}]$
13	$\text{PdI}_2 + \text{CO} + \text{H}_2\text{O} \rightarrow \text{HPdI} + \text{HI} + \text{CO}_2$	$k_m[\text{PdI}_2][\text{H}_2\text{O}][\text{Pd}_2\text{I}_2]$
14	$\text{HPdI} \rightarrow \text{HI} + \text{Pd}$	$k_n[\text{HPdI}][\text{Pd}]$
15	$\text{HPdI} \rightarrow \text{HI} + \text{Pd}$	$k_o[\text{HPdI}][\text{HI}]$
16	$\text{HPdI} \rightarrow \text{HI} + \text{Pd}$	$k_p[\text{HPdI}]^2$
17	$\text{HPdI} \rightarrow \text{HI} + \text{Pd}$	$k_q[\text{HPdI}][\text{Pd}_2\text{I}_2]$

The experiments and subsequent modelling study found that:

- pH drops when water is the solvent suggesting a reaction between $\text{PdI}_2/\text{KI}/\text{H}_2\text{O}$ and CO (Reaction 3 or 4, Table 6.17);
- pH drops when dried MeOH is the solvent suggesting a reaction between $\text{PdI}_2/\text{KI}/\text{MeOH}$ and CO (Reaction 7, Table 6.17);
- the pH drops to a lower value when wet MeOH is the solvent compared to that observed using dried MeOH. This is likely due to the occurrence of two reactions, $\text{PdI}_2/\text{KI}/\text{CO}/\text{H}_2\text{O}$ (via Reaction 3 or 4, Table 6.17) and $\text{PdI}_2/\text{KI}/\text{CO}/\text{MeOH}$ (via Reaction 7, Table 6.17);
- the presence of a black precipitate suggests the formation of Pd(0) which can be accounted for by the decomposition of HPdI (Reaction 6, Table 6.17);
- the shape of the pH curves in each experiment suggests the presence of autocatalysis;

- based on the modelling study, the reaction of $\text{PdI}_2/\text{KI}/\text{H}_2\text{O}$ with CO catalysed by HI (Reaction 11, Table 6.17) gives the best fit to the experimental data.

6.3 Study of the Phenylacetylene/KI/MeOH/CO/Air Subsystem

The experiments in Sections 6.1 and 6.2 have established that there is a pH drop when PdI_2 in methanolic KI solution is purged with CO, but without PdI_2 there is no drop in pH. This indicates that the pH drop is the result of a reaction involving PdI_2 . To see if any change in the pH behaviour of methanolic KI is caused by the addition of PhAc an experiment was conducted in which 0.0182 mol PhAc was added to a $0.693 \text{ mol dm}^{-3}$ KI/MeOH solution purged with CO and air (Section 4.6). The results are shown in Figure 6.20.

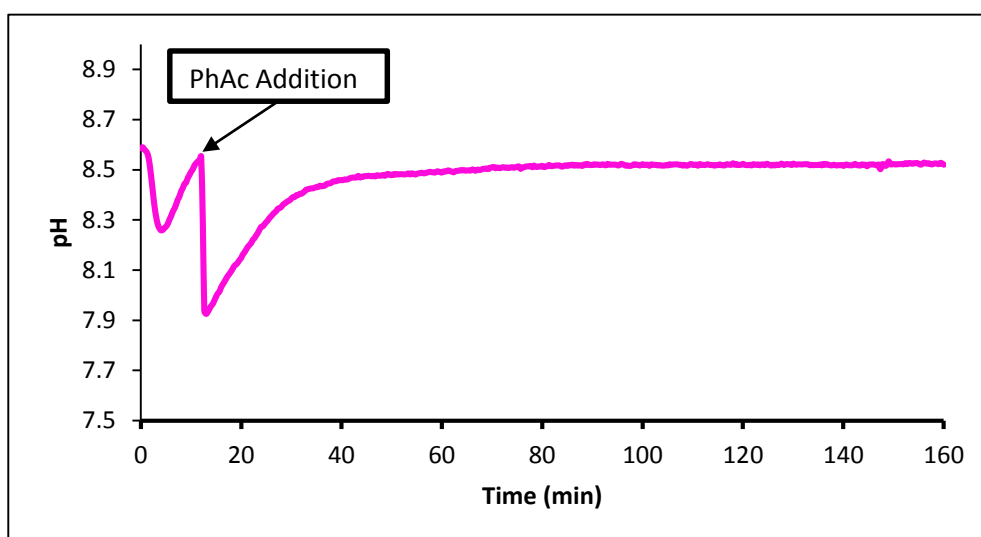


Figure 6.20. The pH behaviour on the addition of PhAc (2 mL) to a $0.693 \text{ mol dm}^{-3}$ solution of KI in MeOH purged with CO = 50 mL min^{-1} and air = 50 mL min^{-1} .

As Figure 6.20 shows, there was a small drop in pH (8.5 to 7.9) when PhAc was added to methanol/KI solution but the pH very quickly recovered to 8.4. This suggests that there are no reactions occurring generating HI unless PdI_2 is present.

6.4 Study of the Phenylacetylene/Catalyst/CO Subsystem

6.4.1 Changing the Order of Reactant Addition in Wet and Dried Methanol^{[154]§§}

The experiments discussed in Section 6.2 focused on understanding the reaction network responsible for the initial reactions of the catalyst during the PCPOC reaction.^[138] The experiments in this section studied the catalyst system further with

^{§§}Reprinted and adapted with permission from Parker, J. and Novakovic, K. (2013) 'Influence of Water and the Reactant Addition Sequence on Palladium(II) Iodide-Catalyzed Phenylacetylene Carbonylation', *Industrial & Engineering Chemistry Research*, 52(7), 2520-2527. Copyright 2013 American Chemical Society.

the inclusion of another variable: phenylacetylene (PhAc), whilst also further investigating the effect of water. The system studied, therefore, consisted of MeOH (both reactant and solvent), PdI_2 , KI, CO and PhAc using standard MeOH (HPLC grade methanol used without further manipulation) and dried MeOH (stock catalyst solution in methanol was dried over 3 Å molecular sieves before use). The reaction conditions that produced the oscillations shown in Figure 2.13 used 2% of PdI_2 relative to the amount of PhAc added and also a stream of air (oxygen) was brought to the system to allow for catalyst recycling. A low level of catalyst results in low reaction rates producing small changes in the concentrations of species with time which are hard to follow. This makes it difficult to understand the pathway to product formation and to make unambiguous connections between oscillations in pH and Q_r , and the dynamics of reactant and product conversions. To overcome this, the amount of catalyst was increased significantly to 64% relative to PhAc concentration, while oxygen was not included in the reaction system. The aim was to have a stoichiometric process rather than a catalytic system, i.e. have one cycle of PdI_2 activity in this system. Working under such extreme conditions, while excluding recycling of the catalyst, was also intended to allow the concentration profile of reaction intermediates to be recorded.

Four experiments were conducted following the procedure described in Section 4.7.1. Two experiments were conducted using catalyst solution that had been dried prior to use and two experiments were conducted using catalyst solution that had not been dried. In each case, one of the solutions was purged with CO before PhAc was added and the other solution had PhAc added to it before purging with CO began.

The concentrations of PhAc and relevant products (Figure 5.1) were measured using the GCMS method described in Section 4.2.5. The products detected were: methyl (E)-cinnamate, (MeCin), (**1**); methyl atropate, (MeAt), (**2**); dimethyl (2Z)-2-phenyl-2-butenedioate, (Z-isomer), (**3**); dimethyl (2E)-2-phenyl-2-butenedioate, (E-isomer), (**4**), 5,5-dimethoxy-3-phenyl-2(5H)-furanone, (DMO), (**5**); and phenylmaleic anhydride, (PhMAAn), (**6**) or phenylmaleic acid, (PhMAc), (**7**). Analysis of standard samples showed the phenylmaleic acid (**7**) was dehydrated to the anhydride (**6**) in the injector of the GCMS making it impossible to distinguish between them. It was confirmed using HPLC that both of these products are present however, due to the limitations of the equipment, it was not possible to determine the product ratio satisfactorily. For

that reason, the formation of products **6** and **7** is referred to as the mixture **6/7** (PhMAn or PhMAc) in the discussion that follows.

All of the products mentioned have previously been reported by various researchers studying the carbonylation of alkynes. Table 6.18 summarises reactant and product conversions at the end of Experiments 1-4.

Table 6.18. Reactant and product conversion in Experiments 1-4.

Reactant and Products (%)	Experiments			
	1	2	3	4
PhAc Conversion	79.96	49.56	78.67	52.32
1	0	0	0	0
2	0	0	trace	trace
3	31.05	16.36	22.4	5.79
4	6.2	2.7	5.7	2.2
5	0	0	10.79	3.51
6/7 mixture	38.96	26.82	2.41	0.16
Total Products (%)	76.21	45.88	40.79	11.66
End Time (min)	372	418	316	409

When PhAc was added prior to CO (Experiment 1 and 3), the conversion achieved was approximately 80%. On the other hand, when the stock solution was purged with carbon monoxide prior to PhAc addition a significantly lower conversion of PhAc was obtained (50 to 52%). Based on this, it may be presumed that conversion of PhAc is determined by the reactant addition sequence rather than the presence of water in the system.

The initial amount of Pdl_2 present in the system was $6.46 \times 10^{-3} \text{ moldm}^{-3}$, i.e. 64.6% relative to the amount of PhAc initially added. As up to 80% PhAc conversion was achieved in Experiments 1 and 3 (Table 6.18), it suggests that approximately 15% of catalyst was recycled and reused. However, when CO was added first, the conversion of PhAc was only 50-52% suggesting that approximately 12-14% of catalyst became ineffective. These differences from initial catalyst concentration are similar and equate to approximately $1 \times 10^{-3} \text{ moldm}^{-3}$ of catalyst. This suggests two different reactions involving Pdl_2 catalyst: one where it is recycled and the other where it is involved in a secondary process. Both of these require the presence of an

oxidant e.g. O₂ or I₂ dissolved in the system.^[155] Thus, when PhAc is added first the carbonylation reaction catalysed by PdI₂ occurs unhindered by other processes potentially due to it having a faster reaction rate compared to the competing reactions. In this case the oxidant present in the system serves as an oxidising agent for the Pd(0) formed in the process. However, when CO is added first a number of reactions with the catalytic system take place^[138] including, for example, the unwanted oxidation of CO^[155] which is catalysed by PdI₂, thereby reducing the amount of PdI₂ available to catalyse PhAc carbonylation.

The results in Table 6.18 reveal significant and comparable discrepancies in Experiments 3 and 4 (dry solution) between the conversion of PhAc and the total amount of products formed (discrepancy of 38% Experiment 3, 41% Experiment 4) which do not occur in Experiments 1 and 2. A parallel reaction between PhAc and catalyst forming a species that does not react further in the absence of water and is not detected by GC could account for this. This could be similar to the intermediate Pd complex proposed by Bruk *et al* that requires water to form maleic anhydride.^[156] Alternatively, in the carbonylation of methanol, Tonde *et al* proposed a mechanism proceeding via a [PdI₄(CO)(R)]⁻ species which reacts with water to form the product.^[157]

pH

The pH recorded in Experiments 1-4 and the hydrogen ion concentrations calculated according to the method described in Section 6.2.4 are presented in Figure 6.21.

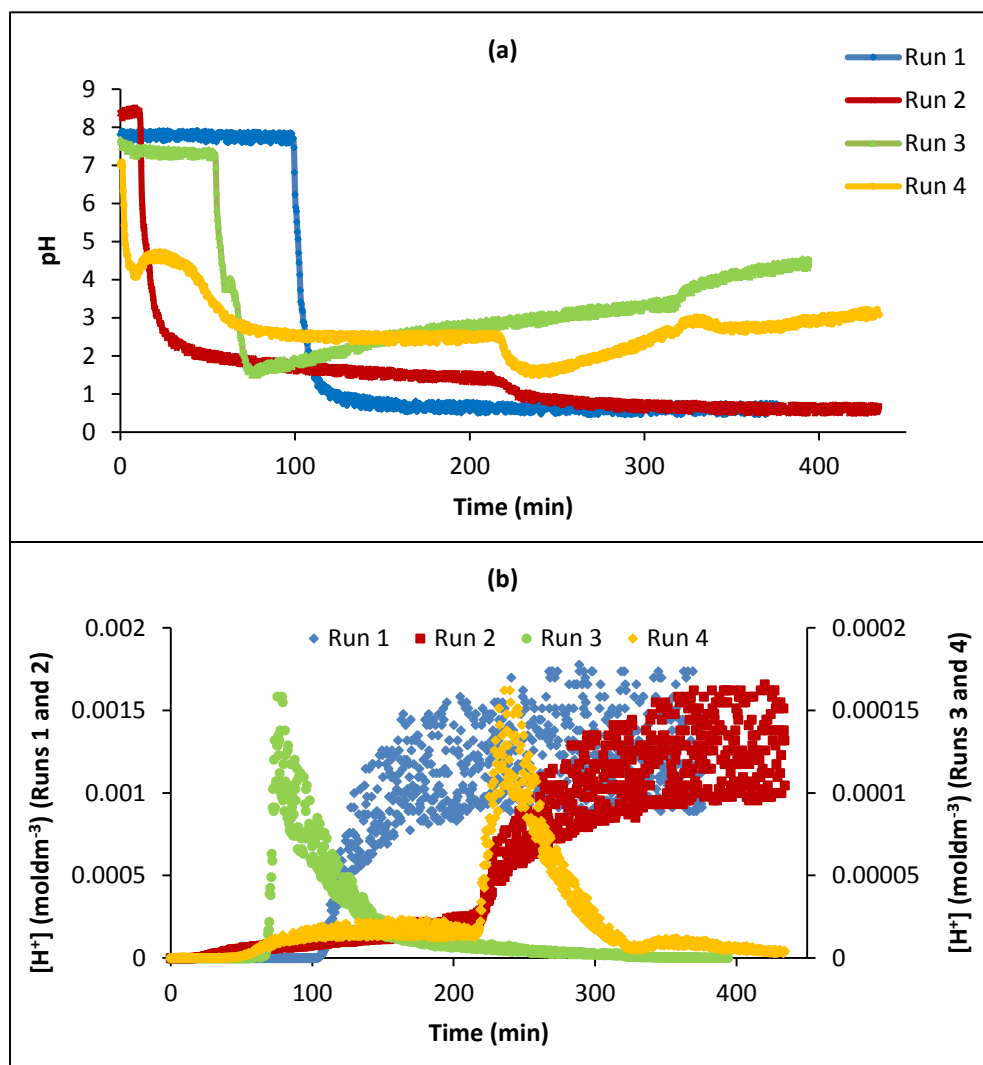


Figure 6.21. (a) pH recorded in Experiments 1-4 and (b) hydrogen ion concentrations calculated from adjusted pH.

A number of observations can be made from Figure 6.21. Experiments 1 and 2 revealed significant overall drops in pH (from 7.8 (Experiment 1) and 8.4 (Experiment 2) to 0.6) which correspond to sharp increases in hydrogen ion concentration to maximum values of $1.8 \times 10^{-3} \text{ mol dm}^{-3}$ (Experiment 1) and $1.6 \times 10^{-3} \text{ mol dm}^{-3}$ (Experiment 2). The initial pH drops were triggered by carbon monoxide addition in both experiments. However, as PhAc was added prior to CO in Experiment 1, it is not possible to differentiate the effect of carbonylation of the catalytic system from the carbonylation reaction of PhAc. On the other hand, the initial pH drop in Experiment 2 (from 8.4 to 1.5) can be attributed to reactions between CO and the catalytic system and credited to the reaction network presented in our previous studies.^[138] The second pH drop in Experiment 2 was recorded following PhAc addition and can be attributed to the PhAc carbonylation reaction. Experiments 3 and 4 were performed with dried catalyst solution and, in both experiments, smaller pH drops were noted

compared to Experiments 1 and 2, which were not dried. The pH drop in Experiment 3 is attributed to carbonylation of both the catalytic system and PhAc. In Experiment 4, the initial pH fall from 7.6 to 4 followed by a further drop to 2.5 can be attributed to carbon monoxide reactions with the catalytic system. Following PhAc addition a further pH drop from approximately 2.5 to 1.5 was recorded. The maximum pH drop achieved in both dry experiments was approximately the same (7.8 to 1.5) after which the pH began to increase. This corresponds in both cases to a sharp increase in hydrogen ion concentration to a maximum value of $1.6 \times 10^{-4} \text{ mol dm}^{-3}$, which subsequently decreased (Figure 6.21b). Note that in Experiments 1 and 2 the maximum concentrations of hydrogen ions were ten times higher than those recorded in Experiments 3 and 4.

Concentration Profiles

The concentration profiles of PhAc, product **1** and products **3-7** are presented in Figure 6.22. Product **2** was only detected in trace amounts in dry catalyst solution so is not included.

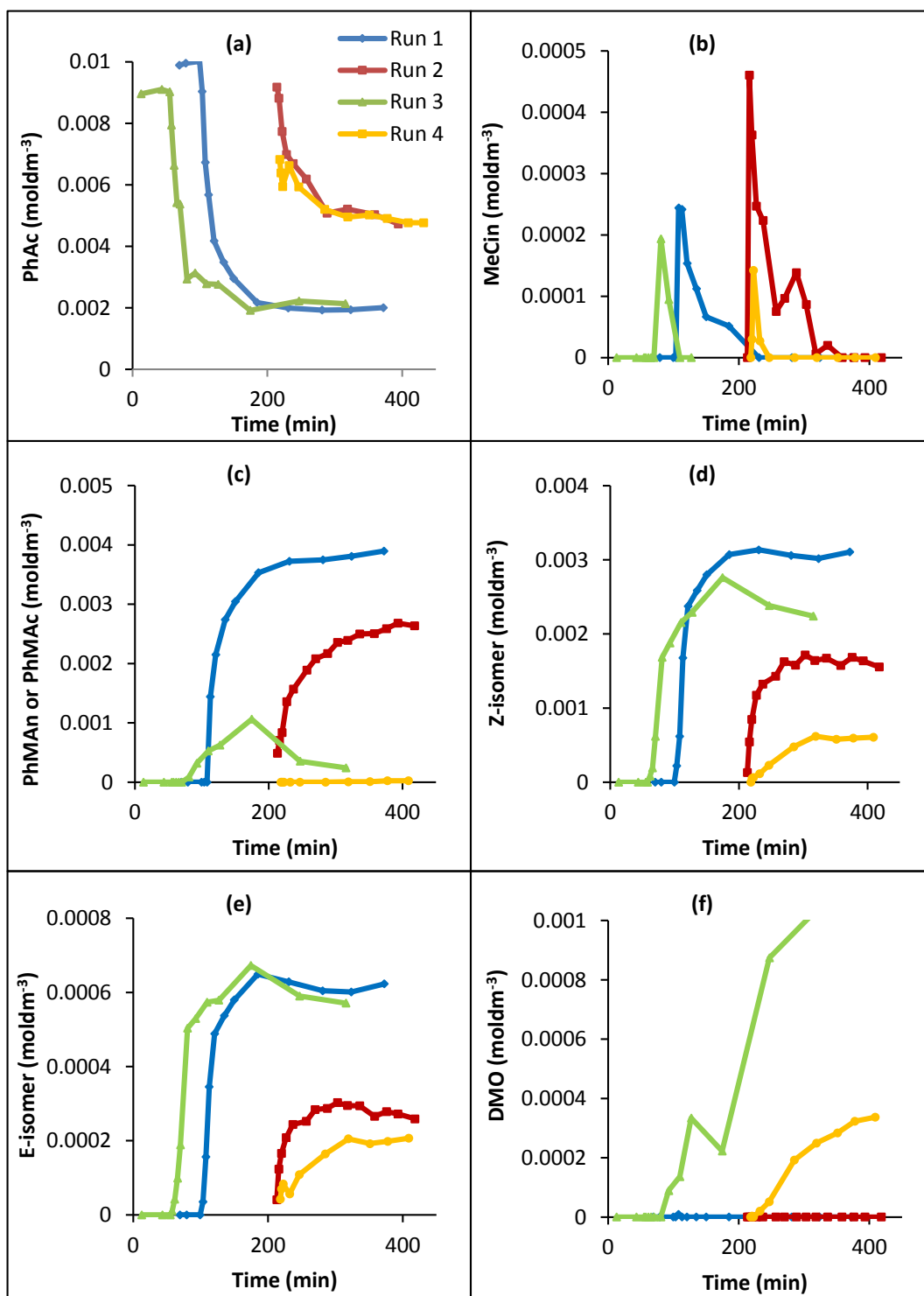


Figure 6.22. Concentration profiles of phenylacetylene and products in Experiments 1-4: (a) Phenylacetylene (PhAc); (b) Methyl (E)-cinnamate, (MeCin), (**1**); (c) Phenylmaleic anhydride/Phenylmaleic acid, (PhMAN or PhMAc) (**6/7**); (d) Dimethyl (2Z)-2-phenyl-2-butenedioate, (Z-isomer), (**3**); (e) Dimethyl (2E)-2-phenyl-2-butenedioate, (E-isomer), (**4**); (f) 5,5-Dimethoxy-3-phenyl-2(5H)-furanone, (DMO), (**5**). Phenylacetylene added first in Experiments 1 and 3; CO added first in Experiments 2 and 4.

As illustrated in Table 6.18, the extent of phenylacetylene conversion appears to be dependent on the reactant addition sequence. Also, while Experiment 1 shows a

steady fall in phenylacetylene concentration, Experiments 2, 3 and 4 show some fluctuations. In some cases these fluctuations mirror those seen in pH, for example, in Experiment 3 (Figure 6.23a).

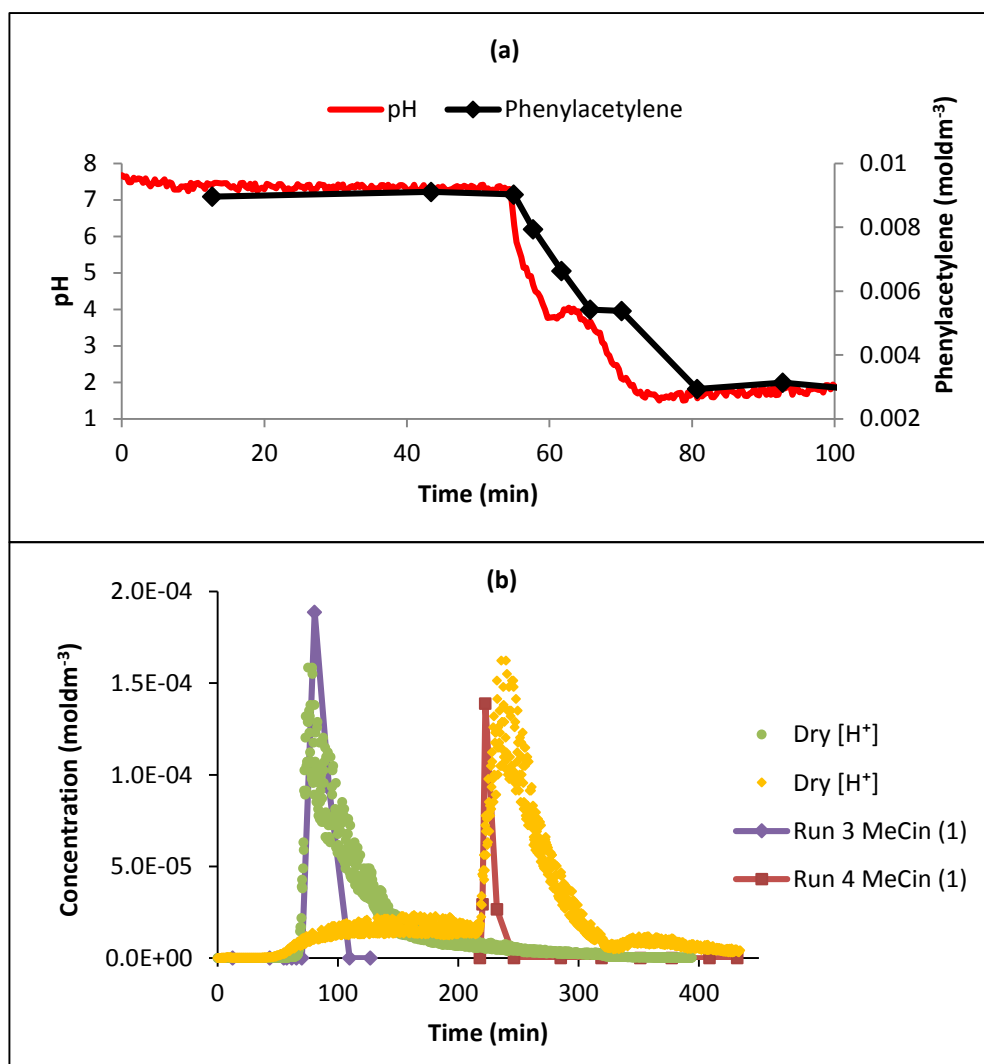


Figure 6.23. (a) pH and phenylacetylene measured in Experiment 3, (b) comparison of product **1** and H⁺ concentration in Experiments 3 and 4.

As shown in Figure 6.22b, product **1** (MeCin) appears to be an intermediate. It is formed in the presence of carbon monoxide and phenylacetylene and is later consumed. Although there are peak values in the concentration of **1** in Figure 6.22b and Figure 6.23b they may be misleading as the actual peaks could have been missed when sampling. However, in all four experiments a sudden increase in **1** was followed by a decrease. At the same time Experiment 1 and, in particular, Experiment 2 exhibited fluctuations in the fall of product **1** concentration. In addition, there is a correlation between the formation/consumption of **1** and [H⁺] in Experiments 3 and 4 (Figure 6.23b) with both being of the order 10⁻⁴. The same correlation is not apparent

in Experiments 1 and 2, however it may still be present. It could be that the correlation is masked by the much higher hydrogen ion concentration in these experiments.

The maximum in product **1** concentration in Experiment 3 coincides with a local minimum in PhAc concentration (Figure 6.22a and Figure 6.23b). A similar trend also occurred in Experiment 4. In both cases, once the concentration of **1** starts to decrease PhAc consumption slows.

In Experiments 1 and 2, i.e. when the catalyst solution was not dried, the major product was **6/7** (Figure 6.22c). This may be accounted for if the species formed in the parallel reaction mentioned previously, between phenylacetylene and catalyst, only reacts to form **6/7** in the presence of water. This agrees with mechanisms proposed by Bruk *et al* as well as Gabriele *et al* for the formation of maleic acids and anhydrides from the carbonylation of alkynes.^[119, 156] In Experiment 3 product **6/7** appears to act as an intermediate, being formed although at low concentrations and then consumed, while it was not detected in Experiment 4. To clarify the reasons for this behaviour, the role of product **6/7** in dry conditions requires further study. Note from Figure 6.22d that the formation of product **3** was lower using dry catalyst solution compared to the equivalent experiment when the catalyst solution was not dried. Note also that product **5** was only detected when using dry catalyst solution (Figure 6.22e). The amount of product **5** formed may account for the reduction in product **3** formation. As product **2** was detected in trace amounts in dry catalyst solution (Experiments 3 and 4) it may be postulated that it acts as intermediate. In addition, product **4** was formed in all experiments (Figure 6.22f).

The results of the validation experiments (Experiments 5 and 6) are presented in Figure 6.24.

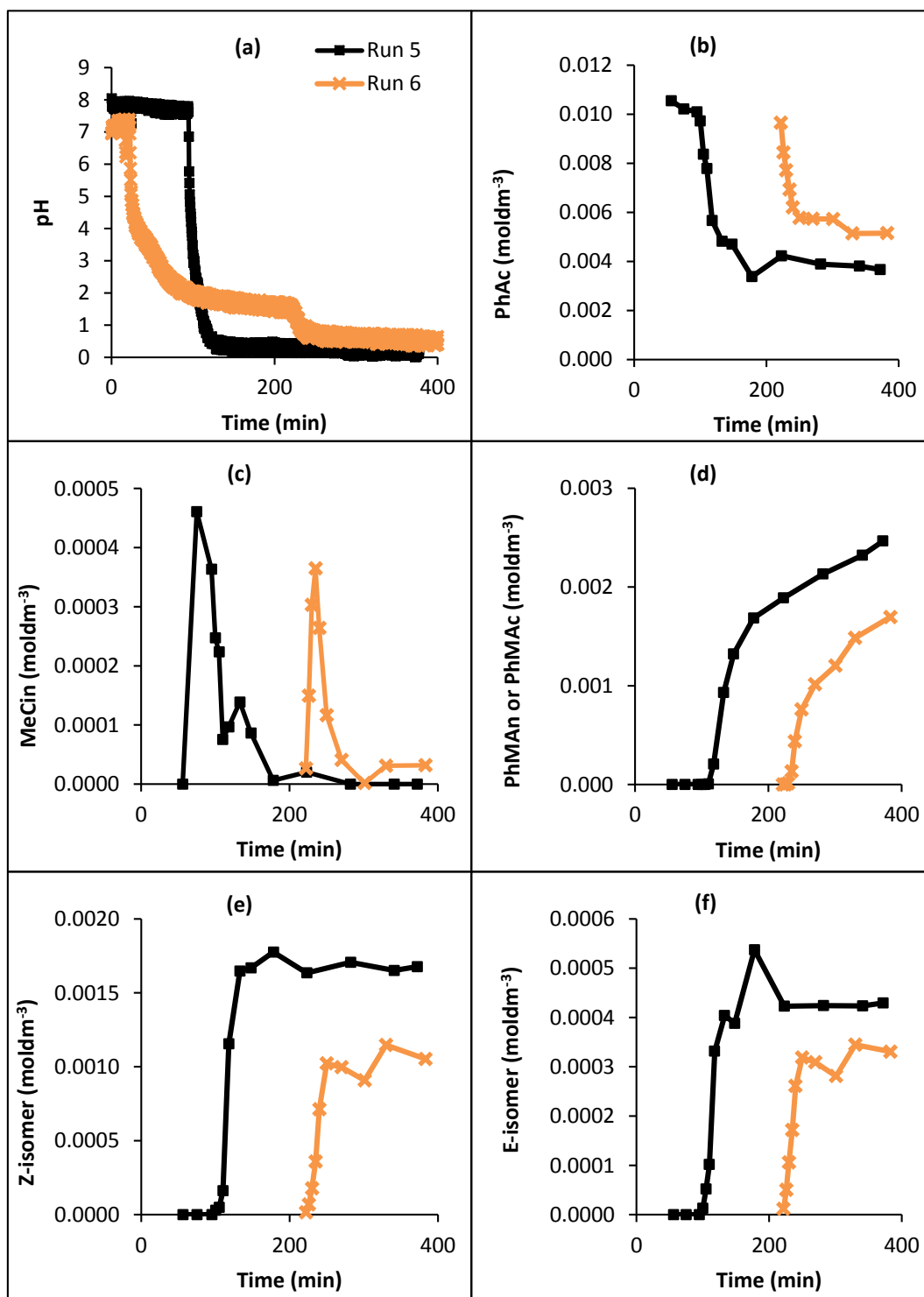


Figure 6.24. pH and concentration profiles of phenylacetylene and products in experiments 5-6: (a) pH; (b) Phenylacetylene, (PhAc); (c) Methyl (E)-cinnamate, (MeCin), (**1**); (d) Phenylmaleic anhydride/Phenylmaleic acid, (PhMAN or PhMAc), (**6/7**); (e) Dimethyl (2Z)-2-phenyl-2-butenedioate, (Z-isomer), (**3**); (f) Dimethyl (2E)-2-phenyl-2-butenedioate, (E-isomer), (**4**). Phenylacetylene added first in Experiment 5; CO added first in Experiment 6.

The results confirmed the trends in Experiments 1 and 2 that used catalyst solution that was not dried. Both pH behaviour on phenylacetylene addition and the trend in PhAc conversions were comparable. At the same time, product **1** was formed and

consumed as seen in the previous experiments. In addition products **3**, **4** and **6/7** were observed and product **5** was not detected. While all trends are in agreement some differences in actual concentrations measured are due to the inability to accurately reproduce the amount of water present in the HPLC grade methanol.

Modelling

The goal of the modelling study was to uncover the key steps in the process rather than precisely describe the reaction mechanism, which would require a more substantial model. A simplified model that consists of a minimal number of steps required to describe the main experimental trends discussed previously is given in Table 6.19. In developing the model it was assumed that: as methanol is present in excess its concentration is constant; as carbon monoxide is brought to the system continuously it is also present in excess and its concentration is constant. Note that the reactions are not balanced and only species considered to be rate relevant are taken into account. The software used for the modelling study was BatchCAD.

Table 6.19. Model used in the simulation study in BatchCAD.

Reactions		Reaction Rates	Rate Constants ^a	
			Wet	Dry
R1	$\text{PdI}_2 \rightarrow \text{Inactive species}$	$k_{R1}[\text{PdI}_2]$	1.4×10^{-3}	1.4×10^{-3}
R2	$\text{PhAc} + \text{PdI}_2 \rightarrow \text{Undetected species}$	$k_{R2}[\text{PhAc}][\text{PdI}_2]$	5	5
R3	$\text{PhAc} + \text{PdI}_2 \rightarrow \text{Intermediate 1} + \text{HI}$	$k_{R3}[\text{PhAc}][\text{PdI}_2]$	3.5	3.5
R4	$\text{Intermediate 1} + \text{HI} \rightarrow \mathbf{3}$	$k_{R4}[\text{Int1}][\text{HI}]$	2×10^2	2×10^2
R5	$\mathbf{3} \rightarrow \mathbf{5}$	$k_{R5}[\mathbf{3}]$	3×10^{-2}	3×10^{-2}
R6	$\mathbf{5} \rightarrow \mathbf{3}$	$k_{R6}[\mathbf{5}]$	1.5×10^{-1}	1.5×10^{-1}
R7	$\text{Undetected species} + \text{H}_2\text{O} \rightarrow \mathbf{6} + \mathbf{7} + \text{HI}$	$k_{R7}[\text{Undet.sp}][\text{H}_2\text{O}]$	1×10^2	0
R8	$\text{PhAc} + \text{PdI}_2 \rightarrow \text{Intermediate 2} + \text{HI}$	$k_{R8}[\text{PhAc}][\text{PdI}_2]$	0	7×10^{-1}
R9	$\text{Intermediate 2} + \text{HI} \rightarrow \mathbf{4}$	$k_{R9}[\text{Int2}][\text{HI}]$	0	1×10^3

^a k_{R1} , k_{R5} , k_{R6} have units min^{-1} ; k_{R2} , k_{R3} , k_{R4} , k_{R7} , k_{R8} , k_{R9} have units $\text{dm}^3\text{mol}^{-1}\text{min}^{-1}$.

The model uses the terms “intermediate **1**” and “intermediate **2**”, while the data used to extract the rate constants in the modelling study are those recorded for product **1** and product **2** from Experiments 1-4. This is because the data (time-concentration profile) for product **1** suggests that it behaves as an intermediate (Figure 6.22). However, presently there is no plausible reaction mechanism able to account for the direct conversion of product **1** into product **3** under PdI_2/KI -catalysed oxidative carbonylation conditions. It may be the case that product **1** is detected as a result of the decomposition of the actual reaction intermediate in the injector of the GCMS, or as a result of a series of reactions that are kinetically fast and, therefore, superfluous for this model. Since product **2** is an isomer of product **1**, it is postulated that it behaves in a similar manner.

In the model (Table 6.19):

- the amount of PdI_2 available for reaction is acknowledged to be changing (R1);
- product **1** is recognised as an intermediate which is formed from PhAc (R3);
- the correlation between **1** and hydrogen ion formation, as seen in Figure 6.23b, is acknowledged (R3, R4);
- product **3** reacts further to form product **5** (R5);^[1]
- a consideration of the stable concentrations of **3** and **5** recorded at the end of the experiments (Figure 6.22d and Figure 6.22f) is attributed to an equilibrium (R6);
- formation of products **6/7**, accompanied by hydrogen ion formation, is accredited to a reaction in the presence of water (R7);
- it is postulated that **6/7** is produced via an undetected species (R2);
- product **2** is detected in trace amounts when the solution is dry (R8) and is given the role of an intermediate;
- the correlation between product **2** and hydrogen ion formation is postulated (R8, R9).

The simulations produced from the model are presented in Figure 6.25.

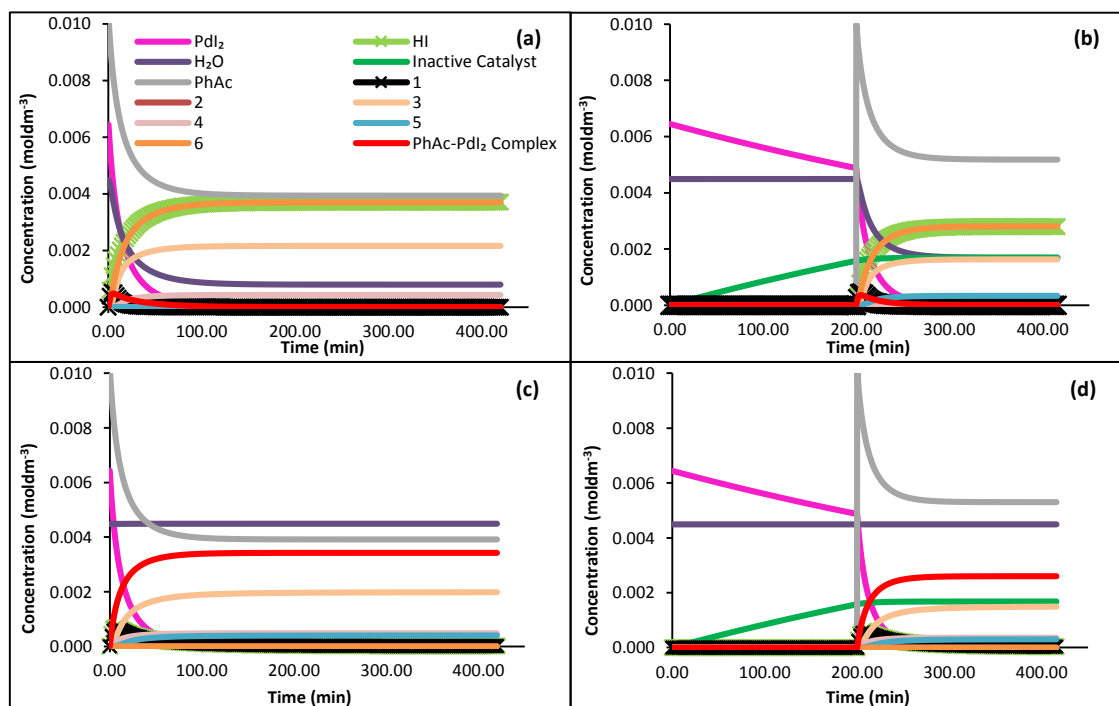


Figure 6.25. Simulation of the trends observed in Experiments 1-4: $[\text{PhAc}] = 0.01 \text{ mol dm}^{-3}$, $\text{CO} = 10 \text{ mL min}^{-1}$, (a) Run 1 – PhAc added first, not dried; (b) Run 2 – CO added first, not dried; (c) Run 3 – PhAc added first, dried (d) Run 4 – CO added first, dried.

The model captures a number of experimentally observed trends e.g. formation and consumption of product **1**, formation of products **3**, **4** and **6/7**, trends in hydrogen ion concentration, formation and consumption of product **2** in dry conditions and the formation of product **5** in dry conditions.

6.4.2 CO Purging Time

The experiments in wet and dried methanol when the order of addition of PhAc and CO were changed (Section 4.7.1) highlighted some unusual behaviour in the conversion of PhAc. The results of those experiments showed that when the Pdl_2 catalyst solution was purged with CO prior to PhAc addition, PhAc conversion stopped at around 50%. In those experiments the catalyst solution was purged for 200 min prior to PhAc addition. In order to see if there was a relationship between the length of time the catalyst solution was purged (CO purging time) and the extent of PhAc conversion, a set of experiments were conducted in which the PhAc concentration was measured with time when the solution was purged with CO for 0, 4, 60, 120 and 200 min prior to PhAc addition. Figure 6.26 shows PhAc conversion of 80% was achieved when the purging time was 0 min with the conversion dropping to 68% when the purging time was 4 min. For CO purging times of 60-200 min PhAc conversion was reduced further to around 50 %. These results suggest that CO is

deactivating the PdI_2 catalyst. Additional data showing the results are repeatable is given in Appendix C.

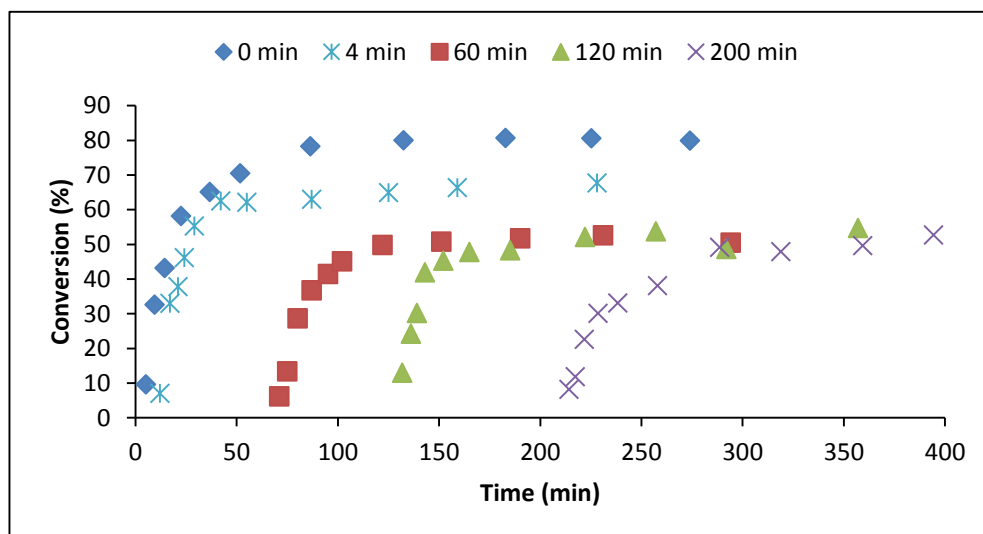


Figure 6.26. PhAc conversion in catalyst solutions that were purged with CO for 0-200 min prior to PhAc addition.

6.4.3 Varying CO Flow Rate

All experiments so far have been conducted with a constant CO flow rate for the duration of the experiments, the CO flow rate only being altered to suit the scale of the experiments. The experiments in this section investigated the effect on pH and PhAc conversion with different CO flow rates in the absence of air. The flow rates used were 5, 10 and 15 mLmin^{-1} as small scale (50 mL) experiments were conducted. The experiments were conducted following the procedure described in Section 4.7.3 using the 6 channel parallel reaction equipment (Section 4.2.4). The pH behaviour (Figure 6.27) was similar for all experiments suggesting that changing the CO flow rate had little effect on the reaction. This implies that CO flow rate has no effect on gas-liquid mass transfer rates under these conditions.

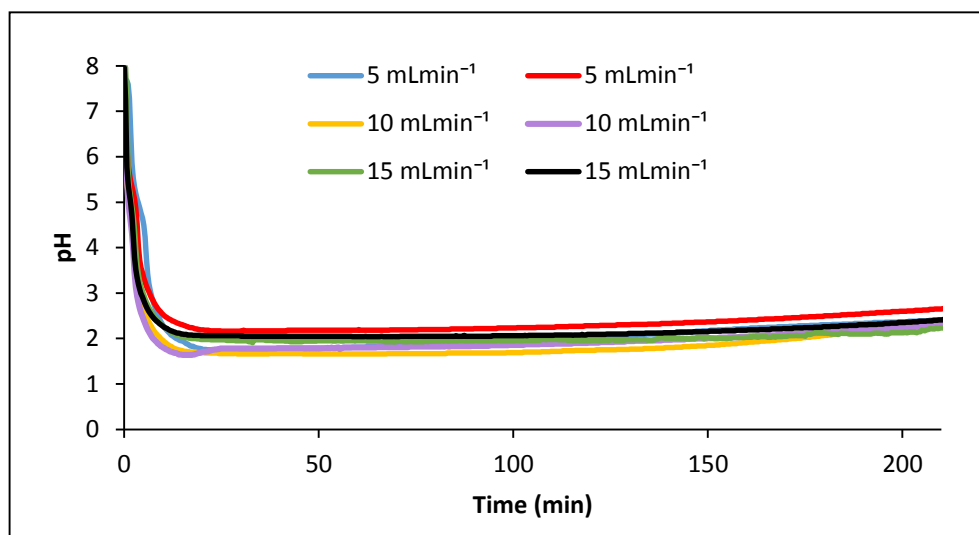


Figure 6.27. pH during the reaction of the catalyst system with PhAc at CO flow rates of 5, 10 and 15 mLmin⁻¹ in the absence of air.

The concentration of PhAc remaining in each of the reactors after 30 min of purging at flow rates of 5, 10 and 15 mLmin⁻¹ were determined by GCMS analysis. The results are shown in Figure 6.28. It appears from Figure 6.28 that the highest conversions were achieved with a CO flow rate of 5 mLmin⁻¹. PhAc conversion when the CO flow rate was 10 mLmin⁻¹ was the same as that obtained using a CO flow rate of 15 mLmin⁻¹. This suggests that CO flow rate has no effect on gas-liquid mass transfer rates under these conditions.

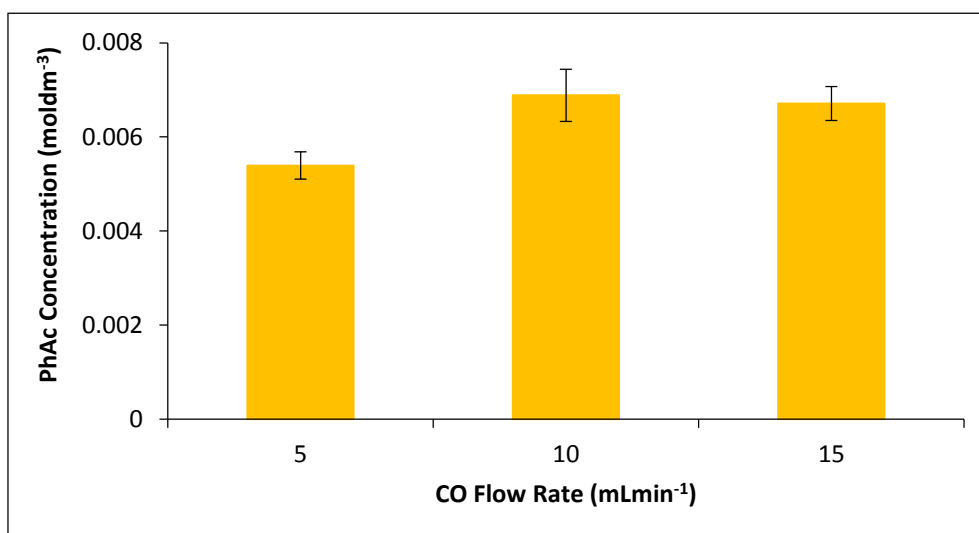


Figure 6.28. Concentration of PhAc after 30 min of purging with CO at flow rates of 5, 10 and 15 mLmin⁻¹.

6.4.4 Gas-Liquid Mass Transfer

In order to further assess the gas-liquid mass transfer limitations an experiment was conducted in the Automate high pressure reactor (Section 4.2.3) using a PdI₂

concentration of $6.46 \times 10^{-3} \text{ mol dm}^{-3}$ as used in the experiments discussed in Section 6.4.1. The experiments were conducted following the procedure in Section 4.7.1 at slow (188 rpm) and high (1036 rpm) stirring speeds. The concentration of PhAc was monitored with time by GCMS analysis. The results are presented in Figure 6.29.

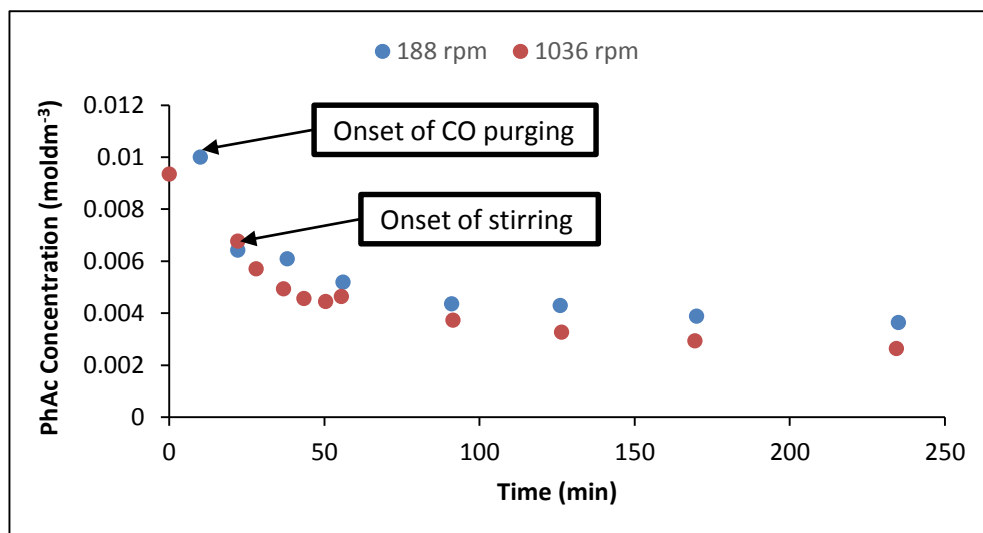


Figure 6.29. Comparing the effect of increased stirring rate on the reaction of PhAc with PdI₂/KI/CO in the absence of air.

As shown by Figure 6.29, approximately 30% of the PhAc reacted while the reactor was being purged with CO even though there was no stirring taking place. Once stirring started, it appears that the reaction was slightly faster with the increased stirring rate. However, the reaction vessel has no temperature control at room temperature so the reactor temperature gradually increased during the course of the reaction due to the action of stirring. At 188 rpm the temperature gradually increased from 16.9 °C to 19.6 °C whereas, at 1036 rpm, the temperature increase was from 18.1 °C to 25.6 °C. The increased reaction temperature may account for the increased reaction rate, rather than the increase in the agitation rate.

Chapter 7. Conclusions and Recommendations for Future Work

Understanding the reaction network behind the oscillatory behaviour in the PCPOC reaction is a challenging task. The experimental study in this work has gone some way to achieving this goal.

Initially, studies on the full PCPOC reaction system were conducted. The first study expanded on the work by Novakovic *et al*^[134] by extending the investigation on the effect of reaction temperature on the pH oscillations to cover the temperature range of 0-40 °C. It also studied the effect of temperature on PhAc conversion and product distribution.

Novakovic and colleagues found that the period and amplitude of pH oscillations increase as reaction temperature decreases, and the rate of reaction increases when oscillations start.^[134] The experiments described in Section 5.1 found that these trends continue down to 0 °C. The duration of the oscillations also increases as the temperature decreases with sustained oscillations in batch being observed for more than 266 hr at 0 °C. Sets of oscillations were observed at temperatures of 0 and 10 °C whereas at 20-40 °C one main set of oscillations was observed. It was also found that lower temperatures produced changes in the shape of the waveform near the end of the oscillatory region. The relaxation waves which predominate become more sinusoidal. The addition of MeOH to the reaction increased the period and amplitude of the pH oscillations. As MeOH is already in excess this suggests water (present in trace amounts in the MeOH) is involved in the oscillatory processes.

Oscillations in turbidity were also observed. At 30 °C the turbidity oscillations were in phase with the pH oscillations, at 20 °C the turbidity oscillations were out of phase with the pH oscillations. At 10 °C no turbidity oscillations were observed and at 0 °C no regular turbidity oscillations were observed but large drops in turbidity occurred at the same time as the large final pH drop in each set of pH oscillations. Turbidity is a measure of the cloudiness of a liquid caused by the presence of particulates. It is, therefore, used to measure crystal formation but as the turbidity probe used in these experiments is a reflectance probe it can be affected by changes in colour. The probe shines red light across a gap to a reflector, the intensity of the reflected light is measured and the difference is calculated as the turbidity measurement. If the reaction mixture changes colour so that it absorbs more light then this will be seen as

a change in turbidity. If crystals form then the light is scattered and so less light is reflected back to be detected. This also results in a change in turbidity. The changes in turbidity are likely to be linked to changes in the oxidation state of the palladium which may be in the form of crystal formation.

The previous work by Novakovic and colleagues^[134] did not consider the effect of temperature on the product distribution of the oscillatory PCPOC reaction. This work found that reaction temperature has a significant impact on product distribution in the reaction. At 40 °C, the main product is Z-isomer but the proportion of this decreases as the temperature decreases. The reaction favours DMO formation at 0 and 10 °C with approximately equal proportions of DMO and Z-isomer at 20 °C. This is in contrast to the work of Gabriele *et al* who, although observing a reduction from 42% Z-isomer at 40 °C to 36% Z-isomer at 25 °C, found that DMO production changed little with 44% DMO at 40 °C and 45% DMO at 25 °C. This suggests that product distribution is affected by both temperature and the presence of oscillatory behaviour. In agreement with Novakovic and colleagues the rate of reaction increases when oscillations start.^[3] PhAc conversions of 80-90% were achieved at 20 and 30 °C, as well as at 0 °C although the reaction was very slow taking 16000 min to reach this point.

The second study on the full PCPOC reaction system investigated the effect of increasing the concentration of water in the system (from 0-40%) on the pH oscillations and also on the product distribution during the reaction. The experiments were conducted at 30 °C. The study found that adding water to the PCPOC reaction system reduced the induction period to the onset of oscillations from 2421 min, when no water was added, to 845 min when the H₂O:MeOH solvent volume ratio was 5:95 at 30 °C. Although, as the amount of water in the system increased the onset of oscillations was increasingly delayed. However, the oscillations still occurred earlier (at 2387 min) when a H₂O:MeOH solvent volume ratio of 30:70 was used compared to the 2421 min with 100% MeOH. It was also found that when 100% MeOH was used as the solvent, oscillations did not start until after the pH had dropped to 1.5, following the addition of PhAc, and was rising again. In contrast, when the water content of the system was increased, even to only 5%, the onset of oscillations occurred while the pH was falling following PhAc addition. At a H₂O:MeOH solvent volume ratio of 5:95 pH oscillations still had a similar shape to those that occurred in

100% MeOH, however, this changed to stepwise pH behaviour when a H₂O:MeOH solvent volume ratio of 20:80 was used. Oscillations were barely discernible at a H₂O:MeOH solvent volume ratio of 40:60. The period of oscillations was fairly constant but in 5% water the oscillations suddenly changed from small oscillations to large period and amplitude oscillations. This requires more investigation to see if it may be evidence of birhythmicity.

In terms of product formation, increasing the concentration of water in the system almost completely stopped the formation of DMO. It also led to the increased formation of PhMAn or PhMAc although this decreased as the water content was increased. The formation of monocarbonylation products MeAt and MeCin also increased. The formation of E-isomer decreased with increasing water concentration along with the formation of Z-isomer although Z-isomer was still the major product.

To gain an understanding of the reaction network behind the observations on the full PCPOC system a series of experiments on the subsystems of the reaction were conducted. Initial experiments established the baseline behaviour of the catalyst components KI and PdI₂ and MeOH. It was found that the solubility of PdI₂ in methanolic KI was dependent on the length of time the solution was stirred and on the concentration of KI. The maximum solubility appeared to occur with KI concentrations of 0.602 mol dm⁻³ and equilibrium solubility took several weeks to be achieved. It is, therefore, challenging to achieve consistency between experiments. To ensure consistency and to enable comparisons between experiments a stock solution of catalyst should be prepared and filtered before each set of experiments to determine the initial PdI₂ concentration used. Also experiments that are to be compared should be performed using the same initial stock solution. It was also shown that water plays a significant role in the PCPOC reaction even though it may only be present in trace amounts.

The experiments on the catalyst system i.e. MeOH, PdI₂, KI (added to dissolve PdI₂) and CO showed that the addition of CO to MeOH/PdI₂/KI causes pH to drop initially, indicating a reaction forming H⁺ ions. Any subsequent pH drop requires the presence of water in the system and is dependent on the concentration of PdI₂ in the solution. As water plays an important role in the mechanism of this reaction it cannot be ruled out of any reaction scheme. Water appears to react with PdI₂ and CO generating H⁺ ions which accompany the H⁺ ions generated by the reaction of MeOH, CO and PdI₂.

The observations from the experiments on the catalyst subsystem were incorporated into an initial modelling study conducted using BatchCAD software. To account for the experimental observations, reaction networks consisting of up to eight reactions were proposed and validated in the modelling study. The reactions for the models that fit the data well are shown in Table 7.1.

Table 7.1. Reactions and rates used to produce models that gave a good fit to the observed pH behaviour of the catalyst system; [cat] = HI, Pd(0), HPdI or Pd₂I₂.

No.	Possible Reactions	Reaction Rate
1	CO →	$k_a[\text{CO}]$
2	→ CO	k_b
3	$\text{PdI}_2 + \text{CO} + \text{H}_2\text{O} \rightarrow \text{HPdI} + \text{HI} + \text{CO}_2$	$k_c[\text{PdI}_2][\text{CO}][\text{H}_2\text{O}]$
4	$\text{HPdI} \rightarrow \text{HI} + \text{Pd}$	$k_r[\text{HPdI}]$
5	$\text{PdI}_2 + \text{CO} + \text{CH}_3\text{OH} \rightarrow \text{IPdCOOCH}_3 + \text{HI}$	$k_g[\text{PdI}_2][\text{CO}]$
6	$\text{IPdCOOCH}_3 + \text{HI} \rightarrow \text{PdI}_2 + \text{CO} + \text{CH}_3\text{OH}$	$k_h[\text{IPdCOOCH}_3][\text{HI}]$
7	$\text{Pd} + \text{PdI}_2 \rightarrow \text{Pd}_2\text{I}_2$	$k_i[\text{Pd}][\text{PdI}_2]$
8	$\text{PdI}_2 + \text{CO} + \text{H}_2\text{O} \rightarrow \text{HPdI} + \text{HI} + \text{CO}_2$	$k_j[\text{PdI}_2][\text{H}_2\text{O}][\text{cat}]$

The modelling study found that the reaction between PdI₂, CO and H₂O generating HI appeared to be catalytic with HI, Pd(0) or HPdI or Pd₂I₂ being suitable as catalysts of the reaction. The best fit was obtained with HI as catalyst.

When PhAc was added to the catalyst system in wet and dry conditions and the order of addition was changed so that CO or PhAc was added first it was found that:

1. the amount of PdI₂ available for reaction was changing;
2. product **1** appeared to be an intermediate which is formed from PhAc;
3. there is a correlation between **1** and hydrogen ion formation;
4. formation of products **6/7**, accompanied by hydrogen ion formation, only occurred in the presence of water;
5. product **2** was detected in trace amounts when the solution was dry;

As MeCin appeared to be an intermediate, the formation of which was correlated with hydrogen ion formation it was postulated that MeAt may also be an intermediate, the formation of which is also correlated with hydrogen ion formation. A second

modelling study which took account of these observations was conducted and a model that gave a good fit to the data was produced.

7.1 Summary

The aim of this thesis was to understand the reaction network responsible for the oscillatory behaviour of the PCPOC reaction. This was a challenging task due to the number of reactants involved in the process, reaction intermediates being unknown and the system involving 2 gases. Without being able to identify the catalytic species and intermediates in the reaction it is difficult to postulate a reaction mechanism to describe the observed pH behaviour. GCMS analysis did not show any species other than reaction products. As a result, reactions had to be postulated based on the observed pH behaviour during the experiment and general observations made during the course of the experiments such as the formation of precipitates.

This study has found that:

1. The increase in the period and amplitude of pH oscillations in the PCPOC reaction as reaction temperature is decreased continues down to 0 °C.
2. The PCPOC reaction can produce pH oscillations for over 11 days in batch without the need for additional reactant due to the slow reaction rate.
3. Turbidity oscillations accompany pH oscillations and can be in-phase or out of phase depending on reaction temperature. These oscillations in turbidity likely signify the change in oxidation state of the palladium in solution and may be linked to oscillations in colour which are difficult to see due to the deep red-brown colour of the reaction mixture.
4. The reduction in reaction temperature from 40 °C to 0 °C changes the product distribution of the reaction from favouring Z-isomer formation above 10 °C to favouring DMO at 0 °C.
5. When the water content of the PCPOC reaction is increased by replacing 5-30% of the MeOH with water
 - a. the induction period prior to the onset of pH oscillations decreases.
 - b. The oscillations change to stepwise behaviour with solvent volume ratios of H₂O:MeOH of 20:80 and 30:70.
6. Oscillations in pH stop when the solvent volume ratio of H₂O:MeOH is 40:60.
7. DMO formation is suppressed when the solvent volume ratio of H₂O:MeOH is 5:95 and above.

8. PhMAN or PhMAc formation occurs when the solvent volume ratio of H₂O:MeOH is between 5:95 and 30:70. It does not form in 100% MeOH.
9. Oscillations in pH occur when pH is falling following PhAc addition when the solvent volume ratio of H₂O:MeOH is between 5:95 and 30:70.
10. Several unknown products are formed when the water concentration of the oscillatory PCPOC reaction is increased.
11. Two models have been produced: one is a good fit to the behaviour of the catalyst system and suggests HI is the autocatalyst, the second describes the pH behaviour and observed product formation.
12. A correlation between MeCin formation and peaks in [H⁺] have been found.

7.2 Future Work

Although significant insights into the processes responsible for the oscillatory behaviour in the PCPOC reaction have been gained by this work there remain a number of unanswered questions. These include:

Is PhMAN or PhMAc produced in this reaction? GCMS analysis of PhMAN and PhMAc showed that they have the same retention time and produce the same mass spectra under the analysis conditions used in this study. This is likely due to decomposition of the PhMAc in the injector of the GC at 150 °C. Reducing the injection temperature was not a viable option. It is therefore necessary to clarify which product is formed in this reaction under the reaction conditions used in this study. Reversed-phase HPLC may be able to answer this question and quantify the product. This will help to gain a better understanding of the reaction mechanism.

What is the palladium species that is the catalyst of this reaction? It may be possible to gain insight to this by using UV-Vis to look for absorbance peaks related to palladium species, for example PdI₄²⁻ gives characteristic absorbances at 316 nm, 408 nm and 485 nm.

Which iodine species are involved in the reaction? Oscillatory behaviour has been found in the carbonylation of PhAc in the absence of oxygen suggesting the presence of another oxidant in the system.^[158] This may be iodine. It may be possible to identify this using UV-Vis.

What reaction conditions are required to produce oscillations with filtered catalyst solution? The oscillatory reactions studied in this work were all conducted by adding

each of the reagents in turn to the reactor. As Pdl_2 is not readily soluble the exact concentration of Pdl_2 in solution is unknown. A study is required to determine the catalyst/PhAc concentrations (parameter space) that generate oscillations. This will improve the accuracy of mathematical models of the reaction.

What is the link between oscillatory turbidity and the mechanism of the reaction? Oscillatory turbidity may be evidence of oscillatory precipitation in this reaction or it may be evidence of oscillatory changes in the oxidation state of palladium. By combining UV-VIS analysis with turbidity measurements it may be possible to determine the relationship between oscillatory turbidity and the change in oxidation state of the palladium and hence gain more information on the reaction mechanism.

Is there oscillatory behaviour in product formation? Some of the results from this work suggest that product formation is oscillatory but the changes are small. Looking more closely at product formation during individual oscillations will confirm this behaviour and shed more light on the mechanism of the reaction.

Does the oscillatory PCPOC reaction exhibit spatiotemporal phenomena? Other oscillating processes for example the BZ reaction have been known to produce a wide range of spatiotemporal phenomena;^[159] so far these phenomena have not been reported in the PCPOC reaction. It would be challenging to investigate this due to the reaction requiring the presence of 2 gases however any pattern formation would also give insights into the reaction mechanism.

Does the oscillatory PCPOC reaction exhibit bistability? Much of the recent work on oscillatory reactions has been conducted in CSTRs. This has led to the discovery of a wide range of non-linear behaviour such as bistability, bifurcations and chaos.^[160] Although bistability is generally associated with open systems (CSTR) there has been evidence of bistability occurring in batch conditions.^[32] As the non-linear properties of the PCPOC reaction are not understood this requires further investigation.

What is the relationship between waveform and the reaction mechanism? This work has demonstrated the presence of a number of different waveforms in the PCPOC depending on the reaction conditions. How these link to the reaction mechanism is unknown.

Is the PCPOC reaction a “pH oscillator”?^[101] Orban and colleagues define a pH oscillator as a system in which H⁺ plays the most important kinetic role in bringing about oscillatory behaviour. Although the PCPOC reaction exhibits oscillations in pH does it fit this definition? Conducting the oscillatory PCPOC reaction in fully buffered conditions will answer this question. If the PCPOC is an actual pH oscillator the oscillations will be suppressed.^[101]

How does light affect the oscillatory behaviour of the PCPOC reaction? Light has been shown to quench oscillations^[161] and also cause the isomerisation of organic compounds.^[162] As unpublished exploratory work on this reaction (not included in this work) showed that light can affect the pH oscillations the experiments in this study were, as far as was possible, conducted in the same manner/lighting conditions. A study of the effect of light on this reaction is therefore worth investigating.

What are the applications of the oscillatory behaviour in this reaction? Oscillatory reactions have found an application in the field of smart polymers as a stimulus of polymers that can respond to changes in their environment.^[163, 164] These smart polymers have the potential to be used as pulsatile drug delivery systems. Developing a smart polymer that can pulse autonomously is difficult but the results of this study have already been making inroads to this field. The first oscillatory reaction that has a polymeric substrate has been designed by grafting the alkyne functionality onto a PEG backbone and using it instead of PhAc in the carbonylation reaction.^[165] A greater understanding of the oscillatory mechanism of the PCPOC reaction can further the work towards creating the first fully autonomous pulsatile smart material. Oscillatory reactions have also been used for analysis and if the reaction mechanism is better understood then there is scope for using this reaction in, for example, carbon monoxide monitoring.^[166-168] Inducing oscillations in a CSTR has been found to increase conversion. Combining this with the already oscillatory behaviour of the PCPOC reaction may improve selectivity in the PCPOC reaction and have application to other carbonylation processes.

Appendix A - Additional Temperature Experiments

Initial Experiments on the Effect of Temperature on the PCPOC Reaction

Following the procedure set out by Novakovic *et al.*^[134] initial experiments were conducted at 10 and 20 °C. Methanol (400 mL) was added to the HEL Simular reactor and heated to the required reaction temperature (10 or 20 °C) while stirring at 250 rpm after which the palladium(II) iodide (434 mg) was added. After stirring for 35 min from PdI₂ addition, 113 mg of NaOAc and 37.392 g of KI were added along with 50 mL of methanol to wash down any solid remaining on the reactor walls. The stirrer speed was increased to 350 rpm to aid the dissolution of the KI. After stirring for a further 15 min purging with CO (50 mLmin⁻¹) and air (50 mLmin⁻¹) commenced. Twenty minutes after purging began, 6.2 mL of phenylacetylene was added and the stirrer speed was returned to 250 rpm. Temperature and pH were monitored throughout. Additional MeOH was added as required to compensate for evaporative loss of the solvent (52 mL MeOH after 2889 min to the experiment conducted at 20 °C). An initial sample was taken 2-3 min after PhAc was added and further samples were taken periodically throughout the reaction. All samples were filtered over silica (see Section 4.2.6) then 200 µL of the filtered sample was added to 200 µL of 0.02M Np solution in methanol (used as an internal standard for GCMS analysis^[6]) and 1600 µL MeOH in a 4 mL vial. The vial was capped and then well shaken to ensure the contents were well mixed. The diluted sample was transferred to a 2 mL GC vial and analysed by GCMS using the method specified in Section 4.2.5. The oscillations in pH, heater power and turbidity were observed as shown Figure A1.

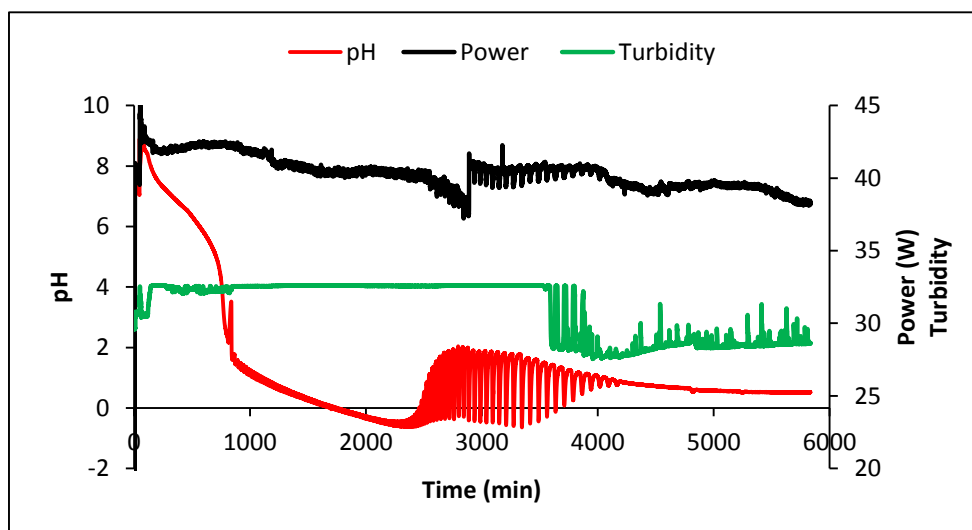


Figure A1. Oscillations in pH, heater power and turbidity observed in the PCPOC reaction at 20 °C without Np in the reactor.

Naphthalene as Internal Standard

To test the suitability of naphthalene as a standard to be used inside the reactor during the PCPOC reaction a small scale experiment was conducted. Methanol (100 mL) was transferred to a 150 mL conical flask along with a stirbar. The flask was placed on a magnetic stirrer - setting 3 - and the MeOH was stirred whilst monitoring pH at room temperature for approximately 5 min. Palladium(II) iodide (96 mg) was transferred to the reaction flask. After approximately 35 min NaOAc (25 mg) was added along with 8.307 g of KI. The solution was stirred for 15 min. Naphthalene (0.257 g) was added and the solution was stirred for 5 min before purging with CO (15 mLmin⁻¹) and air (15 mLmin⁻¹) 20 min. Phenylacetylene (1.380 mL) was added using a 100-1000 µL pipette in 2 portions of 690 µL. The first sample was taken approximately 5 min after phenylacetylene addition. Samples were taken periodically. All samples were filtered through silica using filters as in Figure 4.10 and diluted for analysis (200 µL sample, 1800 µL MeOH) before being analysed by GCMS. Oscillations in pH were recorded at room temperature indicating the presence of Np in the reactor does not prevent oscillatory behaviour. The general shape of the oscillatory pH behaviour (Figure A2) is similar to that observed in Figure A1 although it is not exactly the same. This is most likely because the reaction temperature was not controlled as accurately. This experiment was also conducted on a smaller scale.

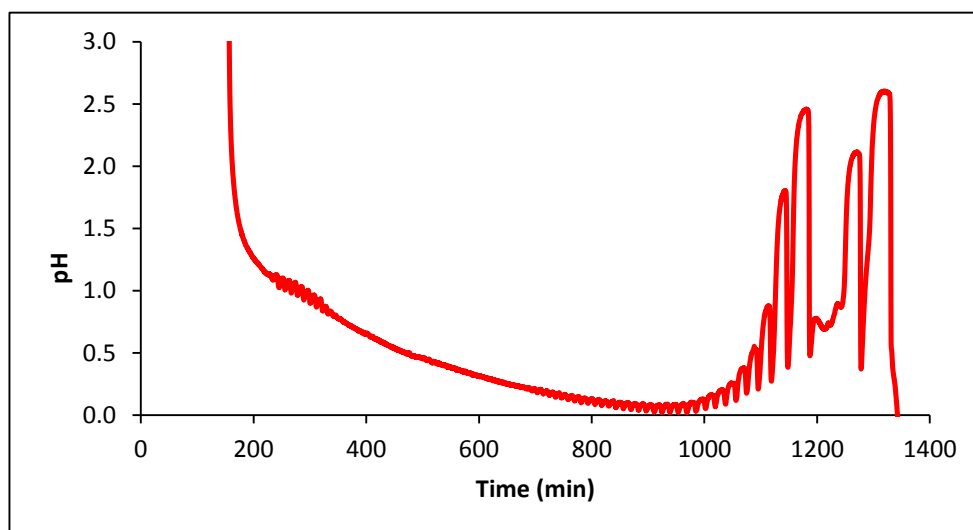


Figure A2. Oscillations in pH during the PCPOC reaction with Np in the reactor.

The GC results from this experiment were compared to those from a previous experiment in which naphthalene was added as an internal standard to each sample after filtration but prior to GC analysis. As additional products were not detected the naphthalene was determined to be suitable to be used in the reactor without interfering with the PCPOC reaction. The products with and without Np were the same Figure A3.

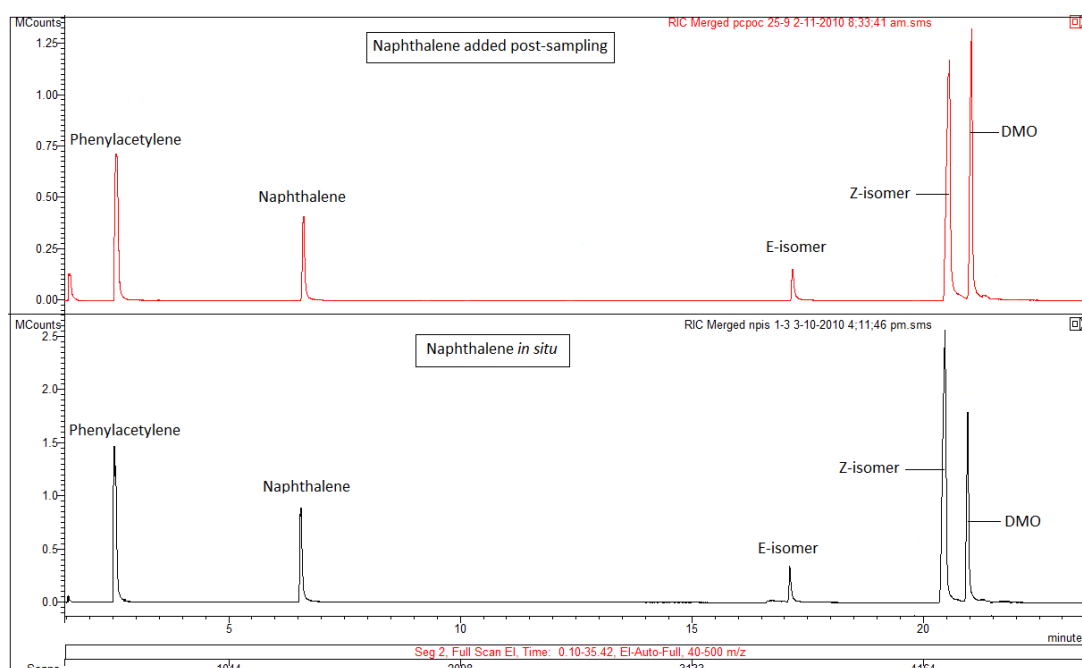


Figure A3. A comparison of products during the PCPOC reaction with and without Naphthalene in the reactor.

Appendix B – GCMS Calibration

Calibration Using Relative Response Factors

Samples of known concentration were prepared and then analysed by GCMS using the analysis method described in Section 4.2.5.

Response factors were calculated as follows:

$$RRF = \frac{Peak\ Area_{Analyte}}{Peak\ Area_{Standard}} \times \frac{[Standard]}{[Analyte]} \quad (B1)$$

The internal standard was naphthalene with $[Np] = 0.01\text{ mol dm}^{-3}$ in the GCMS sample vial.

A stock solution of each analyte of interest was prepared and then analytical samples were made up in 2 mL GC vials by combining 100 μL Np solution, 100 μL analyte solution and 800 μL MeOH. The analytes and sample concentrations are shown in Table B1.

Table B1. Concentration of analyte stock solutions and RRF values calculated from Equation (B1) used to calculate product and reactant concentrations in the experiments in Section 5.1. ^aRRF for DMO calculated from the last sample in the experiment at 0 °C where $[DMO] = [PhAc]_0 - [\text{unreacted PhAc}] - [\text{Z-isomer}] - [\text{E-isomer}]$; [E-isomer] calculated using the calibration curve shown in Figure B2.

Analyte	Stock Concentration (M)	RRF
Z-isomer	0.05	2.67
DMO	0.0477	2.236 ^a
MeCin	0.1	1.05
MeAt	0.1	1.075
PhAc	0.1	0.7
Lactone	0.0125	0.3

Calibration Using Calibration Curves

Calibration curves were produced where possible by preparing a range of calibration samples with concentrations ranging from 0.015 mol dm^{-3} to as low as could be detected for PhAc and each of the products. Naphthalene was added to all samples as an internal standard. Examples of the calibration curves produced are shown in Figure B1-Figure B5.

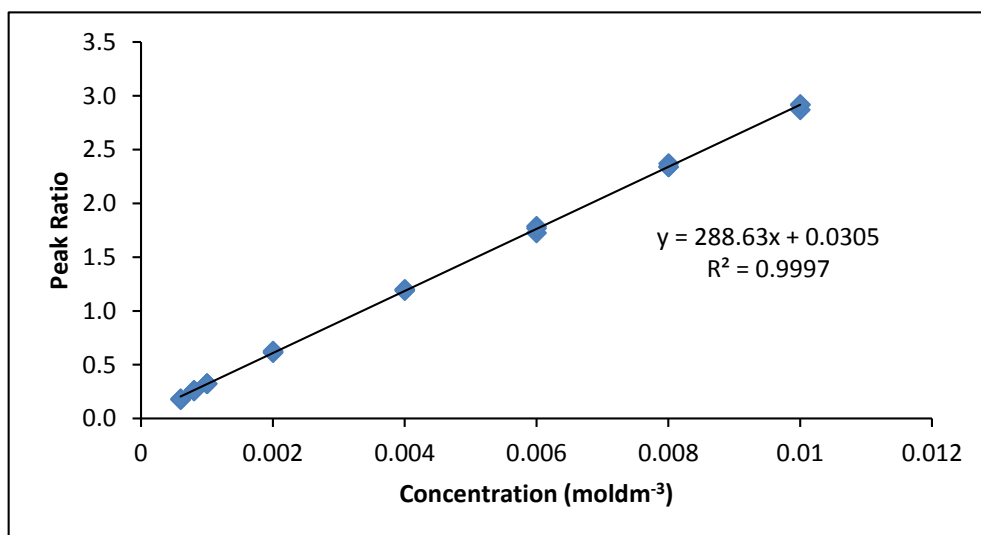


Figure B1. Calibration curve used to calculate [PhAc].

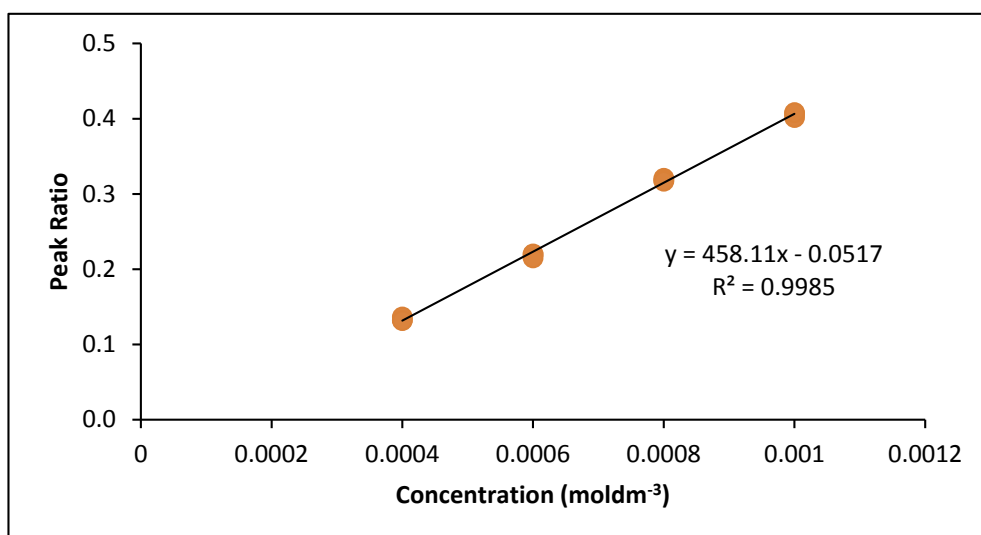


Figure B2. Calibration curve used to calculate [E-isomer].

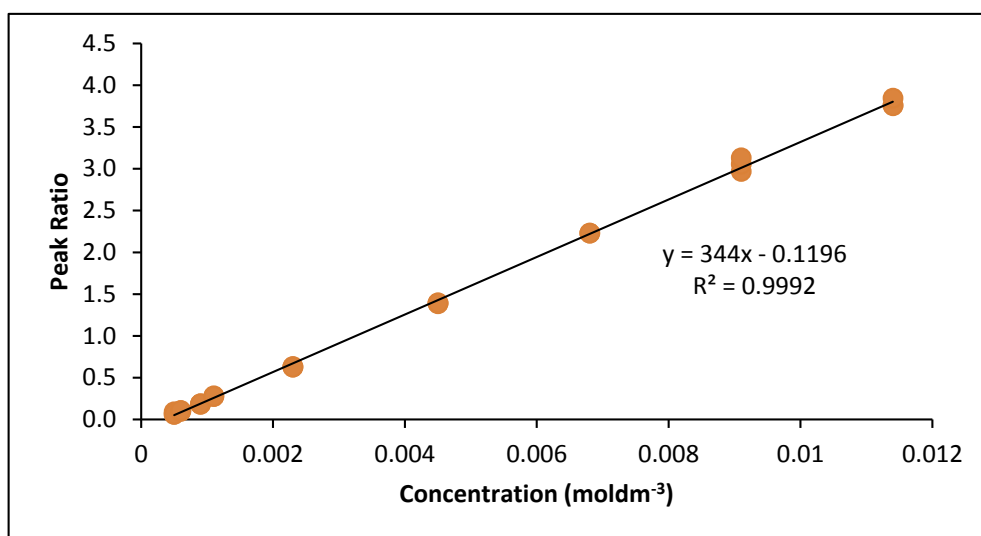


Figure B3. Calibration curve used to calculate [Z-isomer].

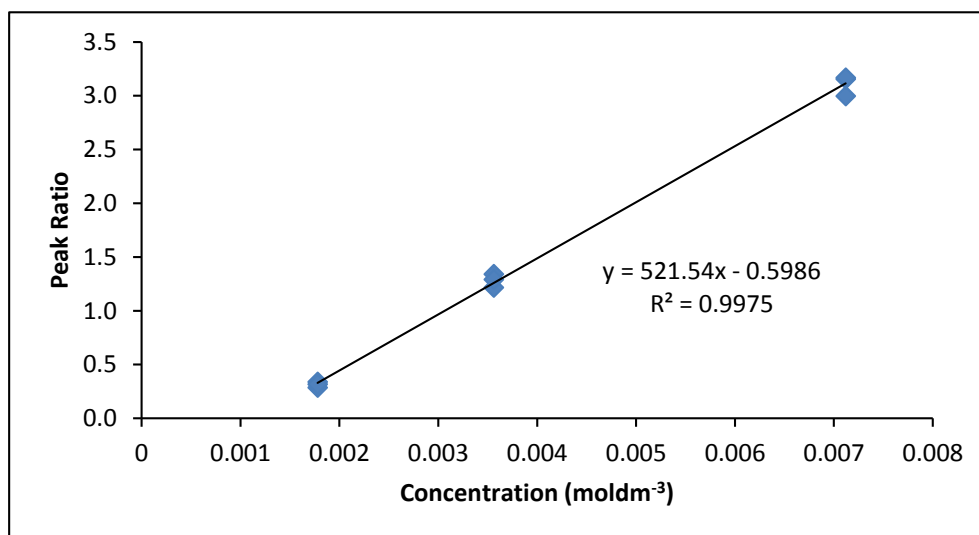


Figure B4. Calibration curve used to calculate [PhMAN or PhMAc].

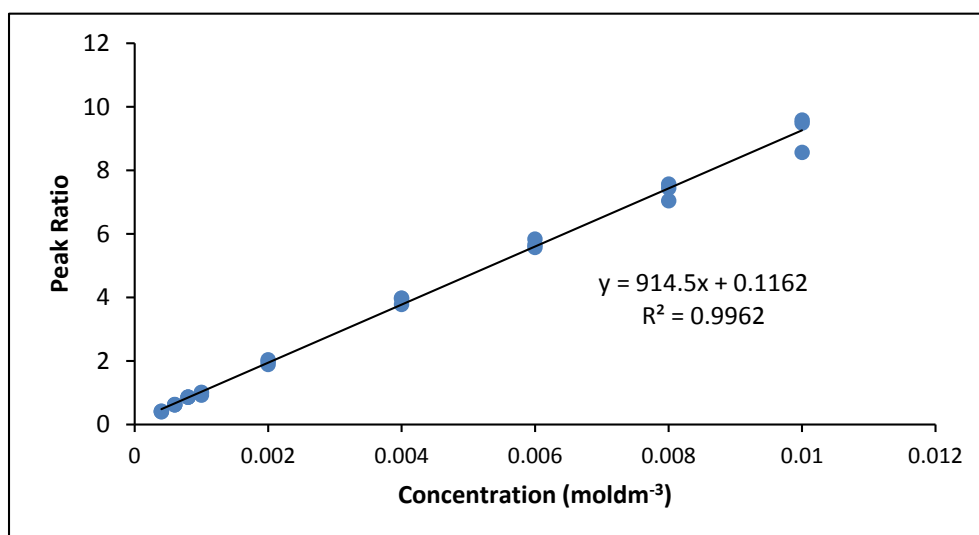


Figure B5. Calibration curve used to calculate [MeCin].

Appendix C - Additional Data for the CO Purging Time Experiments

Repeat runs of the experiments designed to determine the relationship between the length of time the catalyst solution was purged with CO prior to PhAc addition and PhAc conversion were conducted. The results in Figure C1-Figure C3 show the experiments are repeatable and that PhAc conversions of around 50% are achieved with CO purging times of 60-200 min.

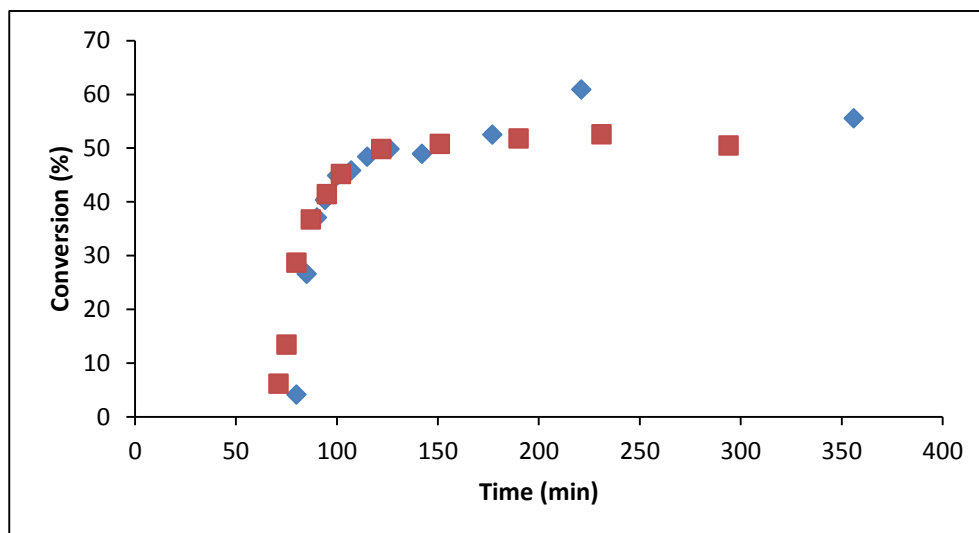


Figure C1. PhAc conversion when catalyst solution was purged with CO for 60 min prior to PhAc addition.

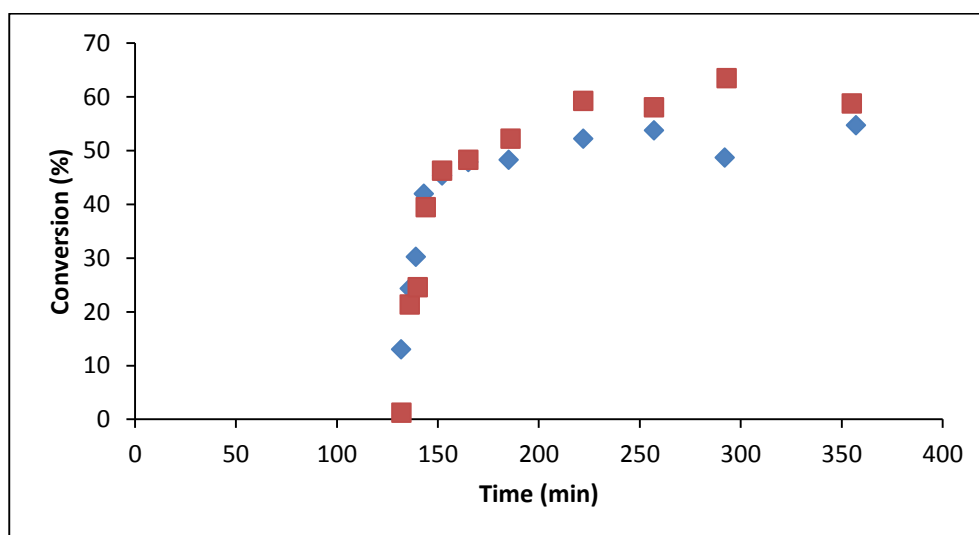


Figure C2. PhAc conversion when catalyst solution was purged with CO for 120 min prior to PhAc addition.

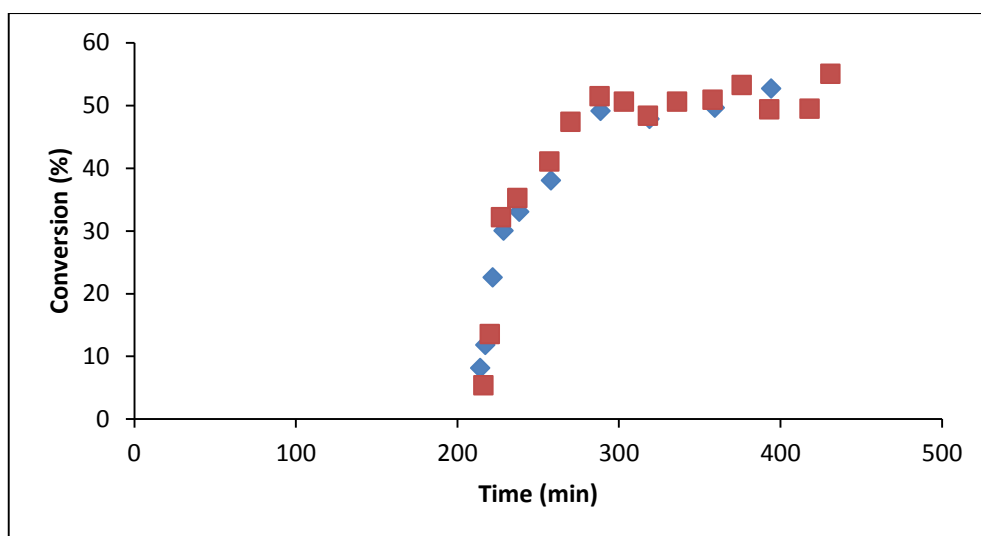


Figure C3. PhAc conversion when catalyst solution was purged with CO for 200 min prior to PhAc addition.

References

1. Gabriele, B., et al., *Recent developments in the synthesis of heterocyclic derivatives by PdI₂-catalyzed oxidative carbonylation reactions*. Journal of Organometallic Chemistry, 2003. **687**(2): p. 219-228.
2. Novakovic, K., et al., *The influence of oscillations on product selectivity during the palladium-catalysed phenylacetylene carbonylation reaction*. Phys. Chem. Chem. Phys., 2008: p. 749-753.
3. Novakovic, K., et al., *Achieving pH and Qr oscillations in a palladium-catalysed phenylacetylene oxidative carbonylation reaction using an automated reactor system*. Chemical Physics Letters, 2007. **435**(1-3): p. 142-147.
4. Gorodskii, S.N., et al., *Oxidative carbonylation of alkynes in self-oscillating mode. Effect of the nature of substrates on the dynamic behavior of reaction system*. Russian Chemical Bulletin, 2003. **52**(7): p. 1534-1543.
5. Malashkevich, A.V., L.G. Bruk, and O.N. Temkin, *New oscillating reaction in catalysis by metal complexes: a mechanism of alkyne oxidative carbonylation*. The Journal of Physical Chemistry A, 1997. **101**(51): p. 9825-9827.
6. Grosjean, C., et al., *Product identification and distribution from the oscillatory versus non-oscillatory palladium(II) iodide-catalysed oxidative carbonylation of phenylacetylene*. Journal of Molecular Catalysis A: Chemical, 2008. **284**(1-2): p. 33-39.
7. Bruk, L.G., et al., *Mechanism of oxidative carbonylation of phenylacetylene and methylacetylene. Generation and experimental discrimination of hypotheses*. Russian Chemical Bulletin, 1999. **48**(5): p. 873-880.
8. Bruk, L.G., et al., *Oxidative carbonylation of phenylacetylene catalyzed by Pd(II) and Cu(I): experimental tests of forty-one computer-generated mechanistic hypotheses*. Journal of Molecular Catalysis A: Chemical, 1998. **130**(1-2): p. 29-40.
9. Gorodskii, S.N., et al., *Oxidative carbonylation of alkynes in an oscillation mode: I. Concentration limits for oscillations in the course of phenylacetylene carbonylation and possible mechanisms of the process*. Kinetics and Catalysis, 2001. **42**(2): p. 251-263.

10. Gabriele, B., et al., *Combined oxidative and reductive carbonylation of terminal alkynes with palladium iodide-thiourea catalysts*. Journal of Organometallic Chemistry, 1995. **503**(1): p. 21-28.
11. Harvey, E.N., ed. *A history of luminescence from the earliest times until 1900*. 1957, American Philosophical Society, Philadelphia.
12. Nicolis, G. and J. Portnow, *Chemical oscillations*. Chemical Reviews, 1973. **73**(4): p. 365-384.
13. Lotka, A.J., *Contribution to the theory of periodic reactions*. The Journal of Physical Chemistry, 1910. **14**(3): p. 271-274.
14. Lotka, A.J., *Undamped oscillations derived from the law of mass action*. Journal of the American Chemical Society, 1920. **42**(8): p. 1595-1599.
15. Volterra, V., *Fluctuations in the abundance of a species considered mathematically*. Nature, 1926. **118**: p. 558-560.
16. Bray, W.C., *A periodic reaction in homogeneous solution and its relation to catalysis*. Journal of the American Chemical Society, 1921. **43**(6): p. 1262-1267.
17. Rice, F.O. and O.M. Reiff, *The thermal decomposition of hydrogen peroxide*. The Journal of Physical Chemistry, 1927. **31**(9): p. 1352-1356.
18. Bray, W.C. and H.A. Liebhafsky, *Reactions involving hydrogen peroxide, iodine and iodate ion. I. Introduction*. Journal of the American Chemical Society, 1931. **53**(1): p. 38-44.
19. Bray, W.C. and A.L. Caulkins, *Reactions involving hydrogen peroxide, iodine and iodate ion. II. The preparation of iodic acid. Preliminary rate measurements*. Journal of the American Chemical Society, 1931. **53**(1): p. 44-48.
20. Liebhafsky, H.A., *Reactions involving hydrogen peroxide, iodine and iodate ion. IV. The oxidation of iodine to iodate ion by hydrogen peroxide*. Journal of the American Chemical Society, 1931. **53**(6): p. 2074-2090.
21. Liebhafsky, H.A., *Reactions involving hydrogen peroxide, iodine and iodate ion. III. The reduction of iodate ion by hydrogen peroxide*. Journal of the American Chemical Society, 1931. **53**(3): p. 896-911.
22. Liebhafsky, H.A., *The catalytic decomposition of hydrogen peroxide by the iodine—iodide couple. IV. The approach to the steady state*. Journal of the American Chemical Society, 1934. **56**(11): p. 2369-2372.

23. Liebhafsky, H.A., *The catalytic decomposition of hydrogen peroxide by the iodine-iodide couple. II and III. The rate of oxidation in neutral, and in acid, solution of hydrogen peroxide by iodine.* Journal of the American Chemical Society, 1932. **54**(9): p. 3499-3508.
24. Liebhafsky, H.A., *The catalytic decomposition of hydrogen peroxide by the iodine-iodide couple at 25°.* Journal of the American Chemical Society, 1932. **54**(5): p. 1792-1806.
25. Liebhafsky, H.A. and L.S. Wu, *Reactions involving hydrogen peroxide, iodine, and iodate ion. V. Introduction to the oscillatory decomposition of hydrogen peroxide.* Journal of the American Chemical Society, 1974. **96**(23): p. 7180-7187.
26. Epstein, I.R. and J.A. Pojman, *An introduction to nonlinear chemical dynamics: oscillations, waves, patterns and chaos.* Topics in Physical Chemistry, ed. D.G. Truhlar. 1998: Oxford University Press.
27. Kasperek, G.J. and T.C. Bruice, *Oscillating reaction. Reaction of potassium bromate, ceric sulfate, and a dicarboxylic acid.* Inorganic Chemistry, 1971. **10**(2): p. 382-386.
28. Field, R.J., E. Körös, and R.M. Noyes, *Oscillations in chemical systems. II. Thorough analysis of temporal oscillation in the bromate-cerium-malonic acid system.* Journal of the American Chemical Society, 1972. **94**(25): p. 8649-8664.
29. Blandamer, M.J. and D.L. Roberts, *Analysis of the dependence on temperature of the frequency of oscillation of the Belousov-Zhabotinskii reaction.* Journal of the Chemical Society, Faraday Transactions 1: Physical Chemistry in Condensed Phases, 1977. **73**: p. 1056-1065.
30. Bánsági, T., et al., *High-frequency oscillations in the Belousov-Zhabotinsky reaction.* The Journal of Physical Chemistry A, 2009. **113**(19): p. 5644-5648.
31. Taylor, A.F., *Mechanism and phenomenology of an oscillating chemical reaction.* Progress in Reaction Kinetics and Mechanism, 2002. **27**: p. 247-325.
32. Ruoff, P. and R.M. Noyes, *Chemical oscillations and instabilities. Part 61. Temporary bistability and unusual oscillatory behavior in a closed Belousov-Zhabotinskii reaction system.* The Journal of Physical Chemistry, 1985. **89**(8): p. 1339-1341.

33. Winfree, A.T., *The prehistory of the Belousov-Zhabotinsky oscillator*. Journal of Chemical Education, 1984. **61**(8): p. 661-663.
34. Zhabotinsky, A.M., *A history of chemical oscillations and waves*. Chaos: An Interdisciplinary Journal of Nonlinear Science, 1991. **1**(4): p. 379-386.
35. Field, R.J., *A reaction periodic in time and space. A lecture demonstration*. Journal of Chemical Education, 1972. **49**(5): p. 308-311.
36. Briggs, T.S. and W.C. Rauscher, *An oscillating iodine clock*. Journal of Chemical Education, 1973. **50**(7): p. 496.
37. Bowers, P.G., K.E. Caldwell, and D.F. Prendergast, *Kinetic oscillations in the oxidation of 2,4-pentanedione by bromate ion, catalyzed by manganese(II)*. The Journal of Physical Chemistry, 1972. **76**(15): p. 2185-2186.
38. Rinker, R.G., et al., *Kinetics and mechanism of thermal decomposition of sodium dithionite in aqueous solution*. Industrial & Engineering Chemistry Fundamentals, 1965. **4**(3): p. 282-288.
39. Jensen, J.H., *New type of oscillating reaction: air oxidation of benzaldehyde*. Journal of the American Chemical Society, 1983. **105**(9): p. 2639-2641.
40. Zaikin, A.N. and A.M. Zhabotinsky, *Concentration wave propagation in two-dimensional liquid-phase self-oscillating system*. Nature, 1970. **225**(5232): p. 535-537.
41. Matsuzaki, I., J.H. Woodson, and H.A. Liebhafsky, *pH and temperature pulses during the periodic decomposition of hydrogen peroxide*. Bulletin of the Chemical Society of Japan, 1970. **43**(10): p. 3317-3317.
42. Graziani, K.R., J.L. Hudson, and R.A. Schmitz, *The Belousov—Zhabotinskii reaction in a continuous flow reactor*. The Chemical Engineering Journal, 1976. **12**(1): p. 9-21.
43. Pacault, A., et al., *Phenomena in homogeneous chemical systems far from equilibrium*. Accounts of Chemical Research, 1976. **9**(12): p. 438-445.
44. Degn, H., *Bistability caused by substrate inhibition of peroxidase in an open reaction system*. Nature, 1968. **217**(5133): p. 1047-1050.
45. Papsin, G.A., A. Hanna, and K. Showalter, *Bistability in the iodate oxidation of arsenous acid*. The Journal of Physical Chemistry, 1981. **85**(17): p. 2575-2582.

46. Boissonade, J. and P. De Kepper, *Transitions from bistability to limit cycle oscillations. Theoretical analysis and experimental evidence in an open chemical system*. The Journal of Physical Chemistry, 1980. **84**(5): p. 501-506.
47. Orban, M., et al., *Systematic design of chemical oscillators. 11. Chlorite oscillators: new experimental examples, tristability, and preliminary classification*. Journal of the American Chemical Society, 1982. **104**(22): p. 5911-5918.
48. Maselko, J. and I.R. Epstein, *Systematic design of chemical oscillators. Part 22. Dynamical behavior of coupled chemical oscillators: chlorite-thiosulfate-iodide-iodine*. The Journal of Physical Chemistry, 1984. **88**(22): p. 5305-5308.
49. Alamgir, M. and I.R. Epstein, *Systematic design of chemical oscillators. 17. Birhythmicity and compound oscillation in coupled chemical oscillators: chlorite-bromate-iodide system*. Journal of the American Chemical Society, 1983. **105**(8): p. 2500-2502.
50. Nagy, A. and L. Treindl, *A novel, non-halogen-based chemical oscillator*. Nature, 1986. **320**(6060): p. 344-345.
51. Orbán, M. and I.R. Epstein, *Systematic design of chemical oscillators. 59. Minimal permanganate oscillator: the Guyard reaction in a CSTR*. Journal of the American Chemical Society, 1989. **111**(22): p. 8543-8544.
52. Doona, C.J., et al., *Systematic design of chemical oscillators. 74. Newly designed permanganate-reductant chemical oscillators*. Journal of the American Chemical Society, 1991. **113**(20): p. 7484-7489.
53. Tóthová, M., A. Nagy, and L. Treindl, *Oscillations in the reduction of permanganate by hydrogen peroxide or by ninhydrin in a batch reactor and mixed-mode oscillations in a continuous-flow stirred tank reactor*. Chemical Physics Letters, 1999. **299**(2): p. 243-246.
54. Silva, L.C. and R.B. Faria, *Complex dynamic behavior in the bromate-oxalic acid-acetone-Mn(II) oscillating reaction in a continuous stirred tank reactor (CSTR)*. Chemical Physics Letters, 2007. **440**(1-3): p. 79-82.
55. Busse, H.G., *Spatial periodic homogeneous chemical reaction*. The Journal of Physical Chemistry, 1969. **73**(3): p. 750-750.
56. Winfree, A.T., *Spiral waves of chemical activity*. Science, 1972. **175**(4022): p. 634-636.

57. Winfree, A.T., *Scroll-shaped waves of chemical activity in three dimensions*. Science, 1973. **181**(4103): p. 937-939.
58. Winfree, A.T., *Two kinds of wave in an oscillating chemical solution*. Faraday Symposia of the Chemical Society, 1974. **9**(0): p. 38-46.
59. Winfree, A.T. and S.H. Strogatz, *Singular filaments organize chemical waves in three dimensions: I. Geometrically simple waves*. Physica D: Nonlinear Phenomena, 1983. **8**(1–2): p. 35-49.
60. Winfree, A.T. and S.H. Strogatz, *Singular filaments organize chemical waves in three dimensions: II. Twisted waves*. Physica D: Nonlinear Phenomena, 1983. **9**(1–2): p. 65-80.
61. Winfree, A.T. and S.H. Strogatz, *Singular filaments organize chemical waves in three dimensions: III. Knotted waves*. Physica D: Nonlinear Phenomena, 1983. **9**(3): p. 333-345.
62. Winfree, A.T. and S.H. Strogatz, *Singular filaments organize chemical waves in three dimensions: IV. Wave taxonomy*. Physica D: Nonlinear Phenomena, 1984. **13**(1–2): p. 221-233.
63. Winfree, A.T. and S.H. Strogatz, *Organizing centres for three-dimensional chemical waves*. Nature, 1984. **311**(5987): p. 611-615.
64. Winfree, A.T. and W. Jahnke, *Three-dimensional scroll ring dynamics in the Belousov-Zhabotinskii reagent and in the two-variable Oregonator model*. The Journal of Physical Chemistry, 1989. **93**(7): p. 2823-2832.
65. Nagy-Ungvarai, Z., et al., *Experimental study of spiral waves in the cerium-catalyzed Belousov-Zhabotinskii reaction*. The Journal of Physical Chemistry, 1990. **94**(24): p. 8677-8682.
66. Mihaliuk, E., et al., *Experimental and theoretical studies of feedback stabilization of propagating wave segments*. Faraday Discussions, 2002. **120**(0): p. 383-394.
67. Zhabotinsky, A.M. and A.N. Zaikin, *Autowave processes in a distributed chemical system*. Journal of Theoretical Biology, 1973. **40**(1): p. 45-61.
68. Turing, A.M., *The chemical basis of morphogenesis*. Philosophical Transactions of the Royal Society of London. Series B, Biological Sciences, 1952. **237**(641): p. 37-72.
69. Mair, T., C. Warnke, and S.C. Müller, *Spatio-temporal dynamics in glycolysis*. Faraday Discussions, 2002. **120**(0): p. 249-259.

70. Field, R.J. and R.M. Noyes, *Explanation of spatial band propagation in the Belousov reaction*. *Nature*, 1972. **237**(5355): p. 390-392.
71. Toth, A., V. Gaspar, and K. Showalter, *Signal transmission in chemical systems: propagation of chemical waves through capillary tubes*. *The Journal of Physical Chemistry*, 1994. **98**(2): p. 522-531.
72. Agladze, K., et al., *Propagation of chemical waves at the boundary of excitable and inhibitory fields*. *The Journal of Physical Chemistry A*, 2000. **104**(29): p. 6677-6680.
73. Zhang, D., W.R. Peltier, and R.L. Armstrong, *Buoyant convection in the Belousov–Zhabotinsky reaction. I. Thermally driven convection and distortion of chemical waves*. *The Journal of Chemical Physics*, 1995. **103**(10): p. 4069-4077.
74. Zhang, D., W.R. Peltier, and R.L. Armstrong, *Buoyant convection in the Belousov–Zhabotinsky reaction. II. Chemically driven convection and instability of the wave structure*. *The Journal of Chemical Physics*, 1995. **103**(10): p. 4078-4089.
75. Pojman, J.A. and I.R. Epstein, *Convective effects on chemical waves. 1. Mechanisms and stability criteria*. *The Journal of Physical Chemistry*, 1990. **94**(12): p. 4966-4972.
76. Pojman, J.A., et al., *Convective effects on chemical waves. 2. Simple convection in the iodate-arsenous acid system*. *The Journal of Physical Chemistry*, 1991. **95**(3): p. 1299-1306.
77. Pojman, J.A., I.P. Nagy, and I.R. Epstein, *Convective effects on chemical waves. 3. Multicomponent convection in the iron(II)-nitric acid system*. *The Journal of Physical Chemistry*, 1991. **95**(3): p. 1306-1311.
78. Molnár, I. and I. Szalai, *Pattern formation in the bromate–sulfite–ferrocyanide reaction*. *The Journal of Physical Chemistry A*, 2015. **119**(39): p. 9954-9961.
79. Orbán, M., *Chemical oscillation during the uncatalyzed reaction of aromatic compounds with bromates. 4. Stationary and moving structures in uncatalyzed oscillatory chemical reactions*. *Journal of the American Chemical Society*, 1980. **102**(13): p. 4311-4314.
80. Wood, P.M. and J. Ross, *A quantitative study of chemical waves in the Belousov–Zhabotinsky reaction*. *The Journal of Chemical Physics*, 1985. **82**(4): p. 1924-1936.

81. Orbán, M., et al., *A new chemical system for studying pattern formation: bromate-hypophosphite-acetone-dual catalyst*. Faraday Discussions, 2002. **120**(0): p. 11-19.
82. De Kepper, P., et al., *Systematic design of chemical oscillators. Part 8. Batch oscillations and spatial wave patterns in chlorite oscillating systems*. The Journal of Physical Chemistry, 1982. **86**(2): p. 170-171.
83. Castets, V., et al., *Experimental evidence of a sustained standing Turing-type nonequilibrium chemical pattern*. Physical Review Letters, 1990. **64**(24): p. 2953-2956.
84. Ouyang, Q., Z. Noszticzius, and H.L. Swinney, *Spatial bistability of two-dimensional Turing patterns in a reaction-diffusion system*. The Journal of Physical Chemistry, 1992. **96**(16): p. 6773-6776.
85. Kurin-Csörgei, K., et al., *Bromate-1,4-cyclohexanedione-ferroin gas-free oscillating reaction. 1. Basic features and crossing wave patterns in a reaction-diffusion system without gel*. The Journal of Physical Chemistry, 1996. **100**(13): p. 5393-5397.
86. Orbán, M., et al., *Pattern formation during polymerization of acrylamide in the presence of sulfide ions*. The Journal of Physical Chemistry B, 1999. **103**(1): p. 36-40.
87. Ouyang, Q., et al., *Bubble-free Belousov-Zhabotinskii-type reactions*. The Journal of Physical Chemistry, 1987. **91**(8): p. 2181-2184.
88. Agladze, K., E. Dulos, and P. De Kepper, *Turing patterns in confined gel and gel-free media*. The Journal of Physical Chemistry, 1992. **96**(6): p. 2400-2403.
89. Blanchedeau, P., J. Boissonade, and P. De Kepper, *Theoretical and experimental studies of spatial bistability in the chlorine-dioxide-iodide reaction*. Physica D: Nonlinear Phenomena, 2000. **147**(3-4): p. 283-299.
90. Liu, H., et al., *Pattern formation in the iodate-sulfite-thiosulfate reaction-diffusion system*. Physical Chemistry Chemical Physics, 2012. **14**(1): p. 131-137.
91. Horvath, D. and A. Toth, *Turing patterns in a single-step autocatalytic reaction*. Journal of the Chemical Society, Faraday Transactions, 1997. **93**(24): p. 4301-4303.
92. Horváth, J., I. Szalai, and P. De Kepper, *An experimental design method leading to chemical Turing patterns*. Science, 2009. **324**(5928): p. 772-775.

93. Prigogine, I. and R. Lefever, *Symmetry breaking instabilities in dissipative systems. II.* The Journal of Chemical Physics, 1968. **48**(4): p. 1695-1700.
94. Tyson, J.J., *Some further studies of nonlinear oscillations in chemical systems.* The Journal of Chemical Physics, 1973. **58**(9): p. 3919-3930.
95. Noyes, R.M., R. Field, and E. Körös, *Oscillations in chemical systems. I. Detailed mechanism in a system showing temporal oscillations.* Journal of the American Chemical Society, 1972. **94**(4): p. 1394-1395.
96. Field, R.J. and R.M. Noyes, *Oscillations in chemical systems. 4. Limit cycle behavior in a model of a real chemical reaction.* Journal of Chemical Physics, 1974. **60**(5): p. 1877-1884.
97. Noyes, R.M., *Mechanisms of some chemical oscillators.* Journal of Physical Chemistry, 1990. **94**(11): p. 4404-4412.
98. Showalter, K., R.M. Noyes, and K. Bar-Eli, *A modified Oregonator model exhibiting complicated limit cycle behavior in a flow system.* The Journal of Chemical Physics, 1978. **69**(6): p. 2514-2524.
99. Schmitz, R.A., K.R. Graziani, and J.L. Hudson, *Experimental evidence of chaotic states in the Belousov–Zhabotinskii reaction.* The Journal of Chemical Physics, 1977. **67**(7): p. 3040-3044.
100. Nagy-Ungvarai, Z., J.J. Tyson, and B. Hess, *Experimental study of the chemical waves in the cerium-catalyzed Belousov-Zhabotinskii reaction. 1. Velocity of trigger waves.* The Journal of Physical Chemistry, 1989. **93**(2): p. 707-713.
101. Orbán, M., K. Kurin-Csörgei, and I.R. Epstein, *pH-regulated chemical oscillators.* Accounts of Chemical Research, 2015. **48**(3): p. 593-601.
102. Pullela, S.R., et al., *Temperature dependence of the Oregonator model for the Belousov-Zhabotinsky reaction.* Physical Chemistry Chemical Physics, 2009. **11**(21): p. 4236-4243.
103. Gray, P. and S.K. Scott, *Autocatalytic reactions in the isothermal, continuous stirred tank reactor: Isolates and other forms of multistability.* Chemical Engineering Science, 1983. **38**(1): p. 29-43.
104. Gray, P. and S.K. Scott, *Autocatalytic reactions in the isothermal, continuous stirred tank reactor: Oscillations and instabilities in the system $A + 2B \rightarrow 3B$; $B \rightarrow C$.* Chemical Engineering Science, 1984. **39**(6): p. 1087-1097.

105. Gray, P. and S.K. Scott, *Sustained oscillations and other exotic patterns of behavior in isothermal reactions*. The Journal of Physical Chemistry, 1985. **89**(1): p. 22-32.
106. Scott, S.K., *Isolas, mushrooms and oscillations in isothermal, autocatalytic reaction-diffusion equations*. Chemical Engineering Science, 1987. **42**(2): p. 307-315.
107. Scott, S.K. and K. Showalter, *Simple and complex propagating reaction-diffusion fronts*. The Journal of Physical Chemistry, 1992. **96**(22): p. 8702-8711.
108. De Kepper, P., I.R. Epstein, and K. Kustin, *A systematically designed homogeneous oscillating reaction: the arsenite-iodate-chlorite system*. Journal of the American Chemical Society, 1981. **103**(8): p. 2133-2134.
109. De Kepper, P., I.R. Epstein, and K. Kustin, *Bistability in the oxidation of arsenite by iodate in a stirred flow reactor*. Journal of the American Chemical Society, 1981. **103**(20): p. 6121-6127.
110. Orbán, M. and I.R. Epstein, *Systematic design of chemical oscillators. 26. A new halogen-free chemical oscillator: the reaction between sulfide ion and hydrogen peroxide in a CSTR*. Journal of the American Chemical Society, 1985. **107**(8): p. 2302-2305.
111. Frerichs, G.A., et al., *A new pH oscillator: the chlorite-sulfite-sulfuric acid system in a CSTR*. The Journal of Physical Chemistry A, 2001. **105**(5): p. 829-837.
112. Tsukada, M., *Belousov-Zhabotinskii oscillating reaction without strong acid such as sulfuric acid*. Chemistry Letters, 1987. **16**(9): p. 1707-1710.
113. Rábai, G., M. Orbán, and I.R. Epstein, *Systematic design of chemical oscillators. 64. Design of pH-regulated oscillators*. Accounts of Chemical Research, 1990. **23**(8): p. 258-263.
114. Edblom, E.C., M. Orban, and I.R. Epstein, *A new iodate oscillator: the Landolt reaction with ferrocyanide in a CSTR*. Journal of the American Chemical Society, 1986. **108**(11): p. 2826-2830.
115. Rábai, G. and I.R. Epstein, *Oxidation of hydroxylamine by periodate in a continuous-flow stirred tank reactor: a new pH oscillator*. The Journal of Physical Chemistry, 1989. **93**(22): p. 7556-7559.

116. Poros, E., et al., *Generation of pH-oscillations in closed chemical systems: method and applications*. Journal of the American Chemical Society, 2011. **133**(18): p. 7174-7179.
117. Edblom, E.C., et al., *Systematic design of chemical oscillators. 45. Kinetics and mechanism of the oscillatory bromate-sulfite-ferrocyanide reaction*. The Journal of Physical Chemistry, 1989. **93**(7): p. 2722-2727.
118. Okazaki, N., G. Rábai, and I. Hanazaki, *Discovery of novel bromate-sulfite pH oscillators with Mn^{2+} or MnO_4^- as a negative-feedback species*. The Journal of Physical Chemistry A, 1999. **103**(50): p. 10915-10920.
119. Gabriele, B., et al., *Synthesis of maleic anhydrides and maleic acids by Pd-catalyzed oxidative dicarbonylation of alk-1-ynes*. Eur. J. Org. Chem., 2003(9): p. 1722-1728.
120. Schoenberg, A., I. Bartoletti, and R.F. Heck, *Palladium-catalyzed carboalkoxylation of aryl, benzyl, and vinylic halides*. The Journal of Organic Chemistry, 1974. **39**(23): p. 3318-3326.
121. Schoenberg, A. and R.F. Heck, *Palladium-catalyzed amidation of aryl, heterocyclic, and vinylic halides*. Journal of Organic Chemistry, 1974. **39**(23): p. 3327-3331.
122. Schoenberg, A. and R.F. Heck, *Palladium-catalyzed formylation of aryl, heterocyclic, and vinylic halides*. Journal of the American Chemical Society, 1974. **96**(25): p. 7761-7764.
123. Barnard, C.F.J., *Palladium-catalyzed carbonylation - a reaction come of age*. Organometallics, 2008. **27**(21): p. 5402-5422.
124. Beller, M., et al., *Progress in hydroformylation and carbonylation*. Journal of Molecular Catalysis A: Chemical, 1995. **104**(1): p. 17-85.
125. Chiusoli, G.P., et al., *Palladium-catalyzed carbonylation of alkynes. II. Aspects of additive, oxidative, and reductive carbonylation*. Gazzetta Chimica Italiana, 1985. **115**: p. 691-696.
126. Tsuji, J., M. Takahashi, and T. Takahashi, *Facile synthesis of acetylenecarboxylates by the oxidative carbonylation of terminal acetylenes catalyzed by $PdCl_2$ under mild conditions*. Tetrahedron Letters, 1980. **21**(9): p. 849-850.

127. Bettucci, L., et al., *Chemoselective methoxycarbonylation of terminal alkynes catalyzed by Pd(II)-TROPP complexes*. Dalton Transactions, 2010. **39**(28): p. 6509-6517.
128. Drent, E., P. Arnoldy, and P.H.M. Budzelaar, *Efficient palladium catalysts for the carbonylation of alkynes*. Journal of Organometallic Chemistry, 1993. **455**(1-2): p. 247-253.
129. Suleiman, R., J. Tijani, and B. El Ali, *Palladium(II)-catalyzed catalytic aminocarbonylation and alkoxycarbonylation of terminal alkynes: regioselectivity controlled by the nucleophiles*. Applied Organometallic Chemistry, 2010. **24**(1): p. 38-46.
130. Gabriele, B., et al., *An efficient and selective palladium-catalysed oxidative dicarbonylation of alkynes to alkyl- or aryl-maleic esters*. J. Chem. Soc. Perkin Trans. 1 1994: p. 83-87.
131. Zargarian, D. and H. Alper, *Palladium chloride catalyzed dicarbonylation of terminal alkynes*. Organometallics, 1991. **10**(8): p. 2914-2921.
132. Hartstock, F.W., L.B. McMahon, and I.P. Tell, *Indirect electrochemical carbonylation of alkynes with a palladium catalyst*. Tetrahedron Letters, 1993. **34**(50): p. 8067-8070.
133. Chiarotto, I. and I. Carelli, *Palladium-catalyzed electrochemical carbonylation of alkynes under very mild conditions*. Synthetic Communications: An International Journal for Rapid Communication of Synthetic Organic Chemistry, 2002. **32**(6): p. 881 - 886.
134. Novakovic, K., et al., *The influence of reaction temperature on the oscillatory behaviour in the palladium-catalysed phenylacetylene oxidative carbonylation reaction*. Phys. Chem. Chem. Phys., 2009: p. 9044-9049.
135. Mukherjee, A., *Analysis and control of oscillations and chaos in reactions*. 2009, Newcastle University.
136. Larson, R.G. and H. Hunt, *Molecular forces and solvent power*. The Journal of Physical Chemistry, 1939. **43**(4): p. 417-423.
137. Ruckenstein, E. and I. Shulgin, *Salting-out or -in by fluctuation theory*. Industrial & Engineering Chemistry Research, 2002. **41**(18): p. 4674-4680.
138. Novakovic, K. and J. Parker, *Catalyst initiation in the oscillatory carbonylation reaction*. International Journal of Chemical Engineering, 2011.

139. Parker, J. and K. Novakovic, *Autonomous reorganization of the oscillatory phase in the PdI₂ catalyzed phenylacetylene carbonylation reaction*. Reaction Kinetics, Mechanisms and Catalysis, 2016: p. 1-13.
140. Barron, J.J., C. Ashton, and L. Geary, *The effects of temperature on pH measurement* 2006, Reagecon Diagnostics Ltd, Shannon Free Zone, County Clare, Ireland.
141. Parker, J. and K. Novakovic. *The influence of reaction temperature on the dynamics of product formation during the oscillatory mode of the phenylacetylene oxidative carbonylation reaction*. in *19th International Congress of Chemical and Process Engineering*. 2010. Prague, Czech Republic.
142. Porras, S.P. and E. Kenndler, *Capillary zone electrophoresis in non-aqueous solutions: pH of the background electrolyte*. Journal of Chromatography A, 2004. **1037**(1-2): p. 455-465.
143. Rosés, M., *Determination of the pH of binary mobile phases for reversed-phase liquid chromatography*. Journal of Chromatography A, 2004. **1037**(1-2): p. 283-298.
144. Karlberg, B., *Response-time properties of some hydrogen ion-selective glass electrodes in non-aqueous solutions*. Analytica Chimica Acta, 1973. **66**(1): p. 93-103.
145. Elding, L.I. and L.F. Olsson, *Kinetics, mechanism, and equilibrium for formation/cleavage of a dinuclear iodide-bridged complex of palladium(II)*. Inorganic Chemistry, 1977. **16**(11): p. 2789-2794.
146. Chiusoli, G.P., et al., *Carbon dioxide effect on palladium-catalyzed sequential reactions with carbon monoxide, acetylenic compounds and water*. Journal of Molecular Catalysis A: Chemical, 2003. **204-205**: p. 133-142.
147. GSE Systems Inc., *BatchCAD 7.1: User Manual*. 2000, Baltimore, MD: Author.
148. Tonner, S.P., et al., *Solubility of carbon monoxide in alcohols*. Journal of Chemical & Engineering Data, 1983. **28**(1): p. 59-61.
149. Colquhoun, H.M., D. J. Thompson, and M.V. Twigg, *Carbonylation: direct synthesis of carbonyl compounds*. 1991, New York: Plenum Press.
150. Feldman, I., *Use and abuse of pH measurements*. Analytical Chemistry, 1956. **28**(12): p. 1859-1866.

151. Castells, C.B., et al., *Effect of temperature on pH measurements and acid-base equilibria in methanol-water mixtures*. Journal of Chromatography A, 2003. **1002**(1-2): p. 41-53.
152. Mussini, T., et al., *Determination of standard pH values for potassium hydrogen phthalate reference buffer solutions in 10, 20, 50, 64 and 84.2 wt per cent methanol/water mixed solvents at temperatures from 283.15 to 313.15 K*. Electrochimica Acta, 1983. **28**(11): p. 1593-1598.
153. Rived, F., et al., *Acidity in methanol-water*. Analytica Chimica Acta, 2001. **439**(2): p. 315-333.
154. Parker, J. and K. Novakovic, *Influence of Water and the Reactant Addition Sequence on Palladium(II) Iodide-Catalyzed Phenylacetylene Carbonylation*. Industrial & Engineering Chemistry Research, 2013. **52**(7): p. 2520-2527.
155. Gabriele, B., G. Salerno, and M. Costa, *Oxidative carbonylations*, in *Catalytic Carbonylation Reactions*, M. Beller, Editor. 2006, Springer Berlin / Heidelberg. p. 239-272.
156. Bruk, L.G., et al., *Mechanistic study of acetylene carbonylation to anhydrides of dicarboxylic acids in solutions of palladium complexes*. Journal of Molecular Catalysis. A, Chemical, 1995. **104**(1): p. 9-16.
157. Tonde, S.S., et al., *Isolation and characterization of an iodide-bridged dimeric palladium complex in carbonylation of methanol*. Journal of Organometallic Chemistry, 2005. **690**(6): p. 1677-1681.
158. Donlon, L., J. Parker, and K. Novakovic, *Oscillatory carbonylation of phenylacetylene in the absence of externally supplied oxidant*. Reaction Kinetics, Mechanisms and Catalysis, 2014. **112**(1): p. 1-13.
159. Epstein, I.R. and K. Showalter, *Nonlinear Chemical Dynamics: Oscillations, Patterns, and Chaos*. The Journal of Physical Chemistry, 1996. **100**(31): p. 13132-13147.
160. Field, R.J. and F.W. Schneider, *Oscillating chemical reactions and nonlinear dynamics*. Journal of Chemical Education, 1989. **66**(3): p. 195.
161. Sørensen, P.G., T. Lorenzen, and F. Hynne, *Quenching of chemical oscillations with light*. The Journal of Physical Chemistry, 1996. **100**(49): p. 19192-19196.
162. Xu, J. and D.J. Burton, *Highly stereoselective synthesis of (E)- and (Z)- α -fluoro- α,β -unsaturated esters and (E)- and (Z)- α -fluoro- α,β -unsaturated*

- amides from 1-bromo-1-fluoroalkenes via palladium-catalyzed carbonylation reactions*. The Journal of Organic Chemistry, 2005. **70**(11): p. 4346-4353.
163. Yoshida, R., et al., *Aspects of the Belousov–Zhabotinsky reaction in polymer gels*. The Journal of Physical Chemistry A, 1999. **103**(43): p. 8573-8578.
164. Yoshida, R., *Self-oscillating gels driven by the Belousov–Zhabotinsky reaction as novel smart materials*. Advanced Materials, 2010. **22**(31): p. 3463-3483.
165. Donlon, L. and K. Novakovic, *Oscillatory carbonylation using alkyne-functionalised poly(ethylene glycol)*. Chemical Communications, 2014. **50**(98): p. 15506-15508.
166. Jiménez-Prieto, R., M. Silva, and D. Pérez-Bendito, *Critical review. Approaching the use of oscillating reactions for analytical monitoring*. Analyst, 1998. **123**(2): p. 1R-8R.
167. Gao, J.Z., et al., *Determination of L-valine based on an oscillating chemical reaction*. Electroanalysis, 2002. **14**(17): p. 1191-1196.
168. Ren, J., et al., *The application of oscillating chemical reactions to analytical determinations*. Central European Journal of Chemistry, 2013. **11**(7): p. 1023-1031.